Charged-Current Quasi-elastic Double-Differential Antineutrino Scattering Cross Section at MINERvA

Cheryl Patrick, Northwestern University (now at University College London)

Fermilab Wine And Cheese Seminar, June 17, 2016

How to make an oscillation experiment

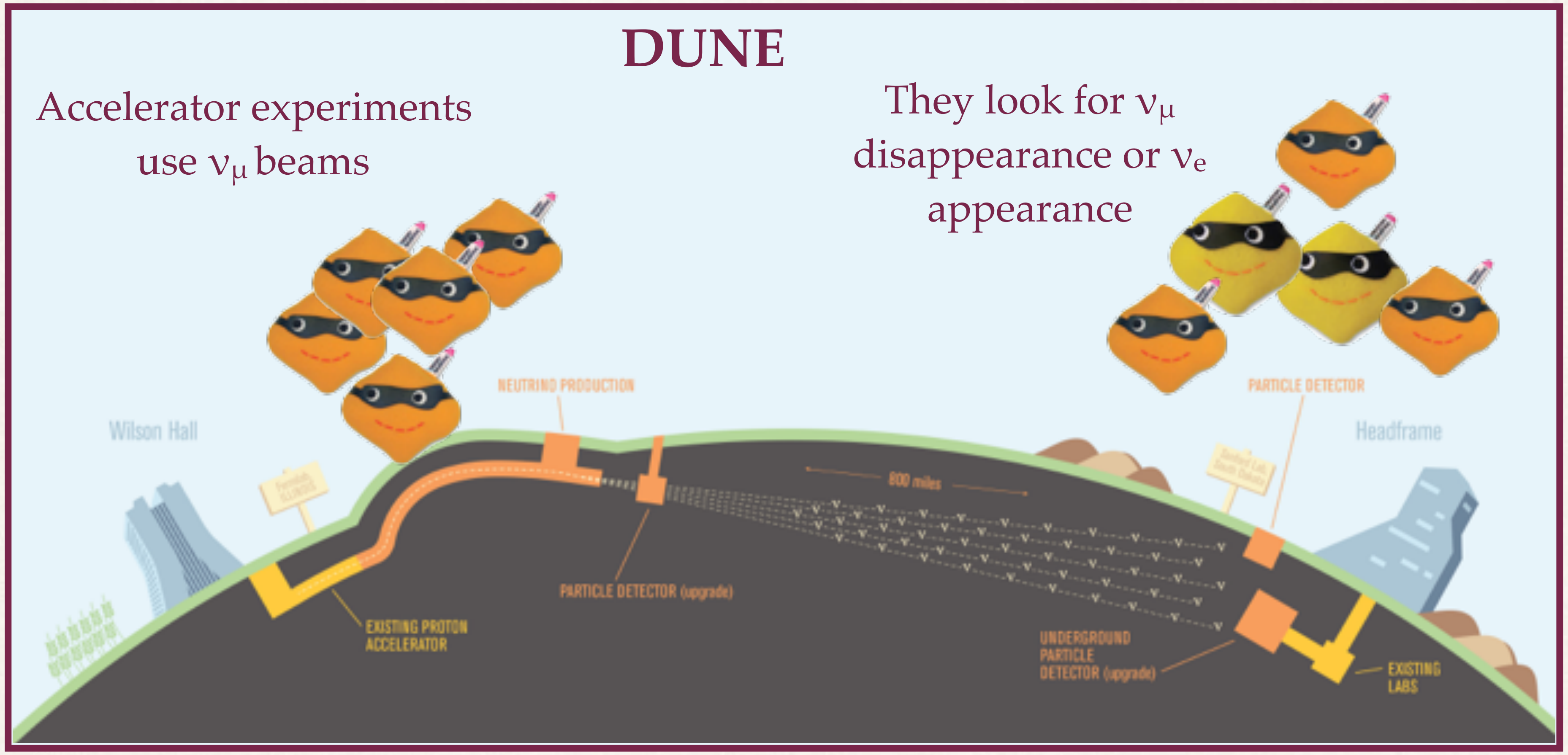

Image: symmetry Adorable cuddly neutrinos: Particle zoo

To discover parameters such as the CP-violating angle and the mass hierarchy, experiments compare the energy spectrum of neutrinos detected in the far detector with models' predictions

Two reasons cross sections matter

$$P(\nu_\alpha \rightarrow \nu_\beta) \approx 1 - \sin^2 2\theta \sin^2\left(\frac{\Delta m^2 L}{E_\nu}\right)$$

To convert this predicted neutrino flux to an expected number of events, we must know the probability that a given neutrino will interact; i.e. the **cross section** on the detector's material

As the prediction depends on **neutrino energy**, E_ν, we must be able to **reconstruct** this accurately

Cross section is one of the largest systematic uncertainties for oscillation experiments like T2K.

TABLE IV. Percentage change in the number of one-ring μ-like events before the oscillation fit from 1σ systematic parameter variations, assuming the oscillation parameters listed in Table III and that the antineutrino and neutrino oscillation parameters are identical.

Source of uncertainty (number of parameters)	$\delta n_{\mathrm{SK}}^{\mathrm{exp}} / n_{\mathrm{SK}}^{\mathrm{exp}}$ (%)
ND280-unconstrained cross section (6)	10.0
Flux and ND280-constrained cross section (31)	3.4
Super-Kamiokande detector systematics (6)	3.8
Pion FSI and reinteractions (6)	2.1
Total (49)	11.6

T2K's uncertainties, from PRL 116, 181801 (2016)

We must understand cross sections at oscillation experiments' energies. For CP-violation measurements, antineutrinos are important.

Three kinds of interactions

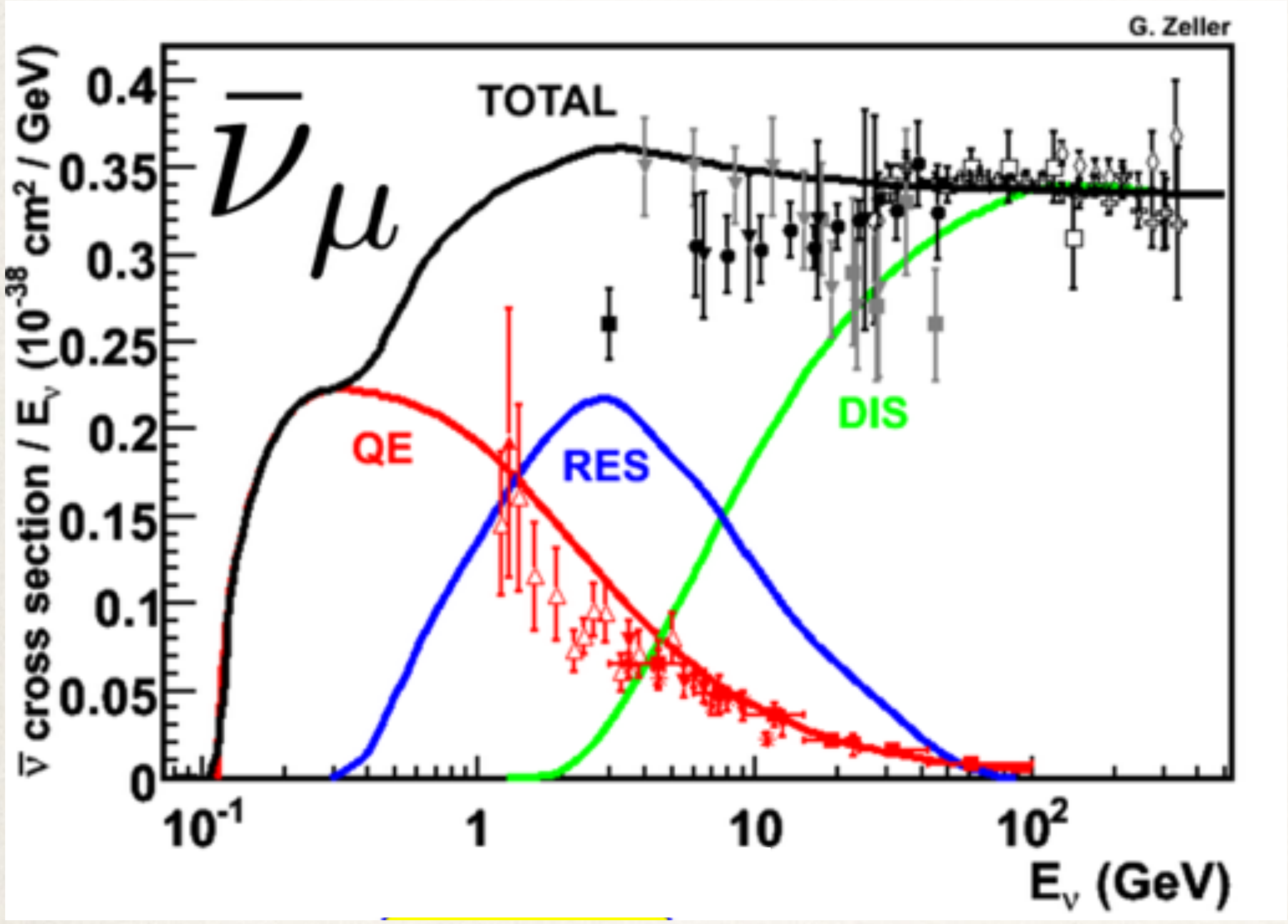

J.A. Formaggio and G.P. Zeller, Rev. Mod. Phys. 84, 1307-1341, 2012

Three kinds of interactions

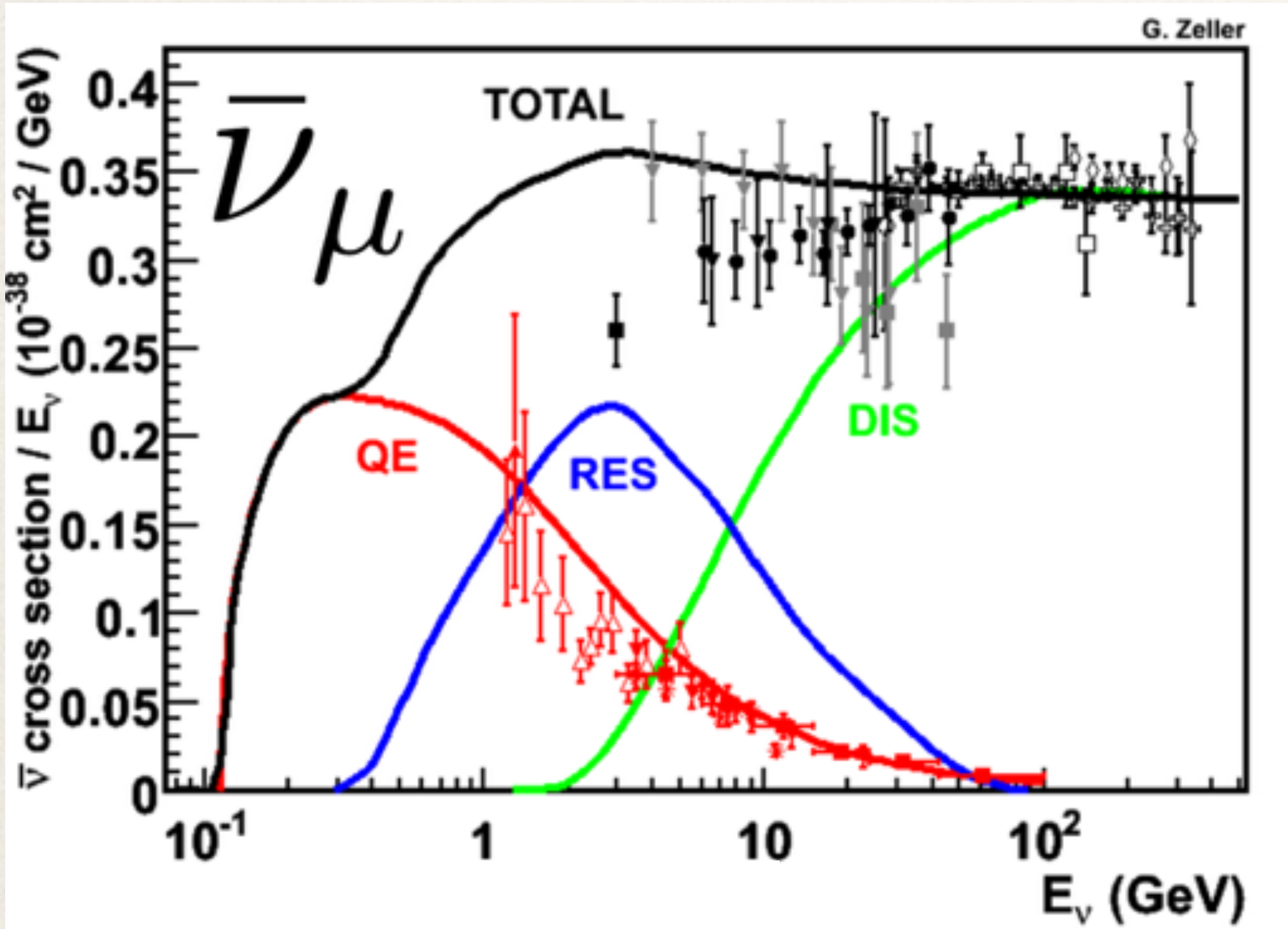

J.A. Formaggio and G.P. Zeller, Rev. Mod. Phys. 84, 1307-1341, 2012

Quasi-elastic scattering

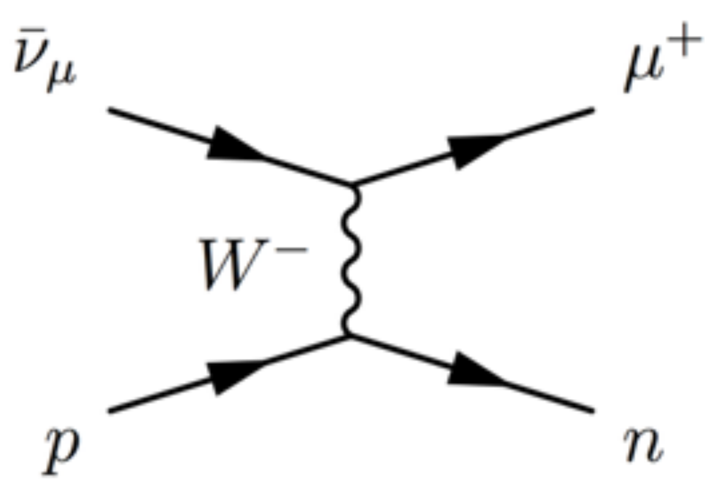

Three kinds of interactions

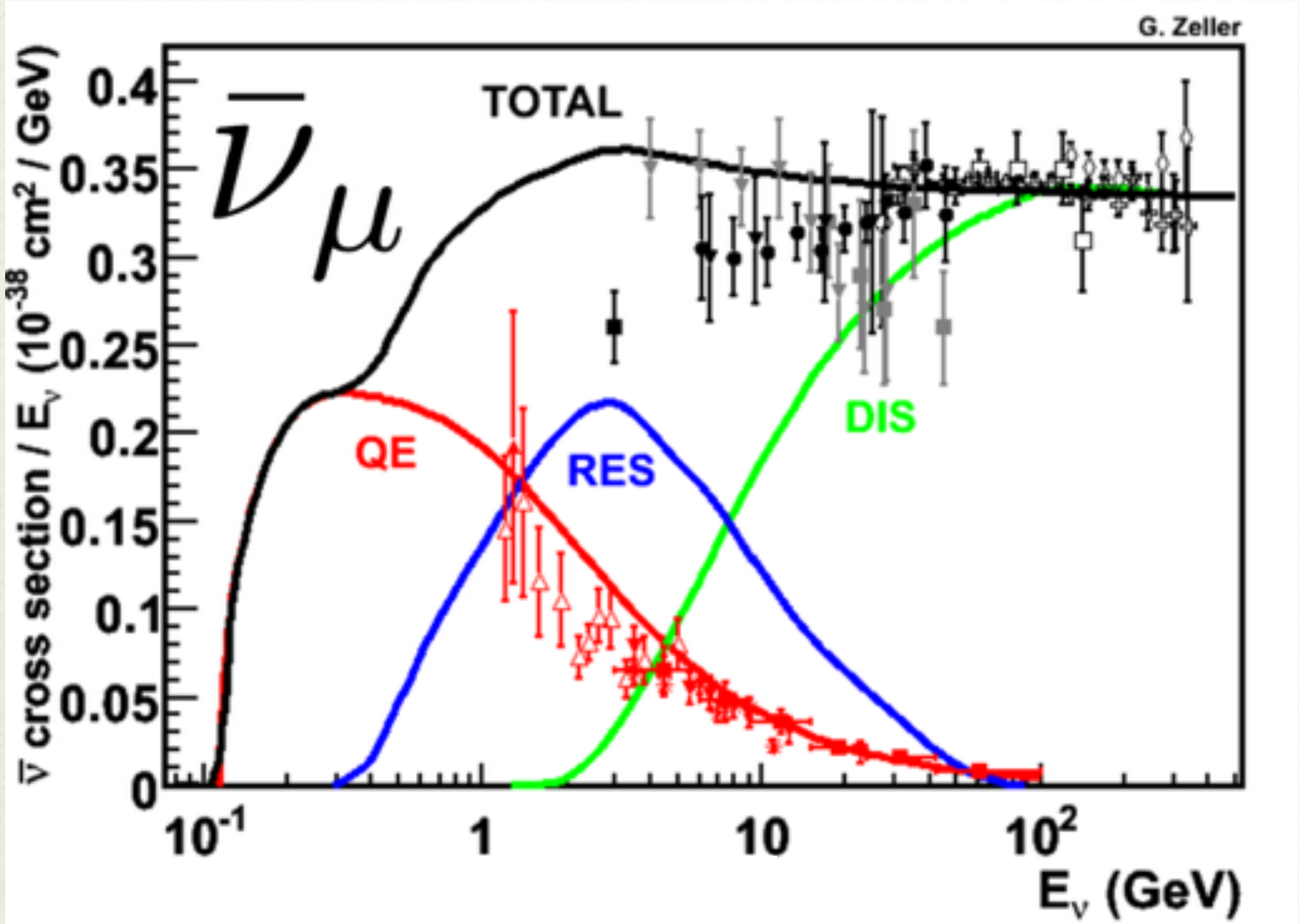

J.A. Formaggio and G.P. Zeller, Rev. Mod. Phys. 84, 1307-1341, 2012

Quasi-elastic scattering

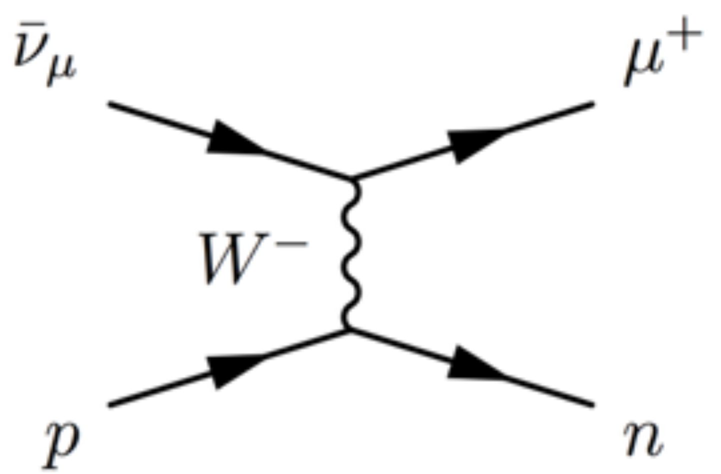

Resonant pion production

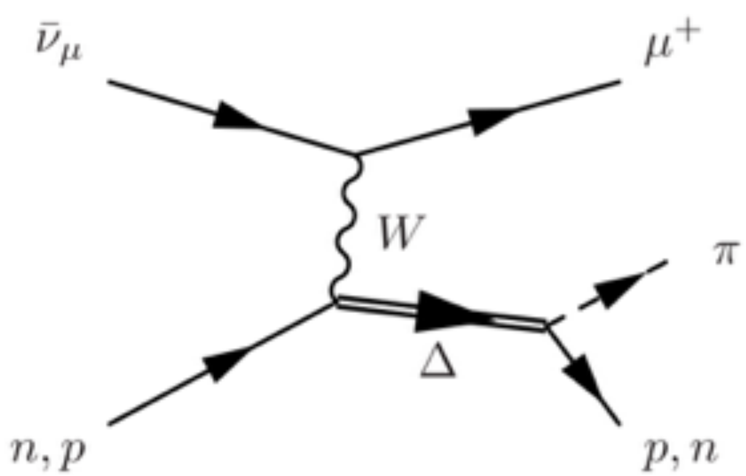

Three kinds of interactions

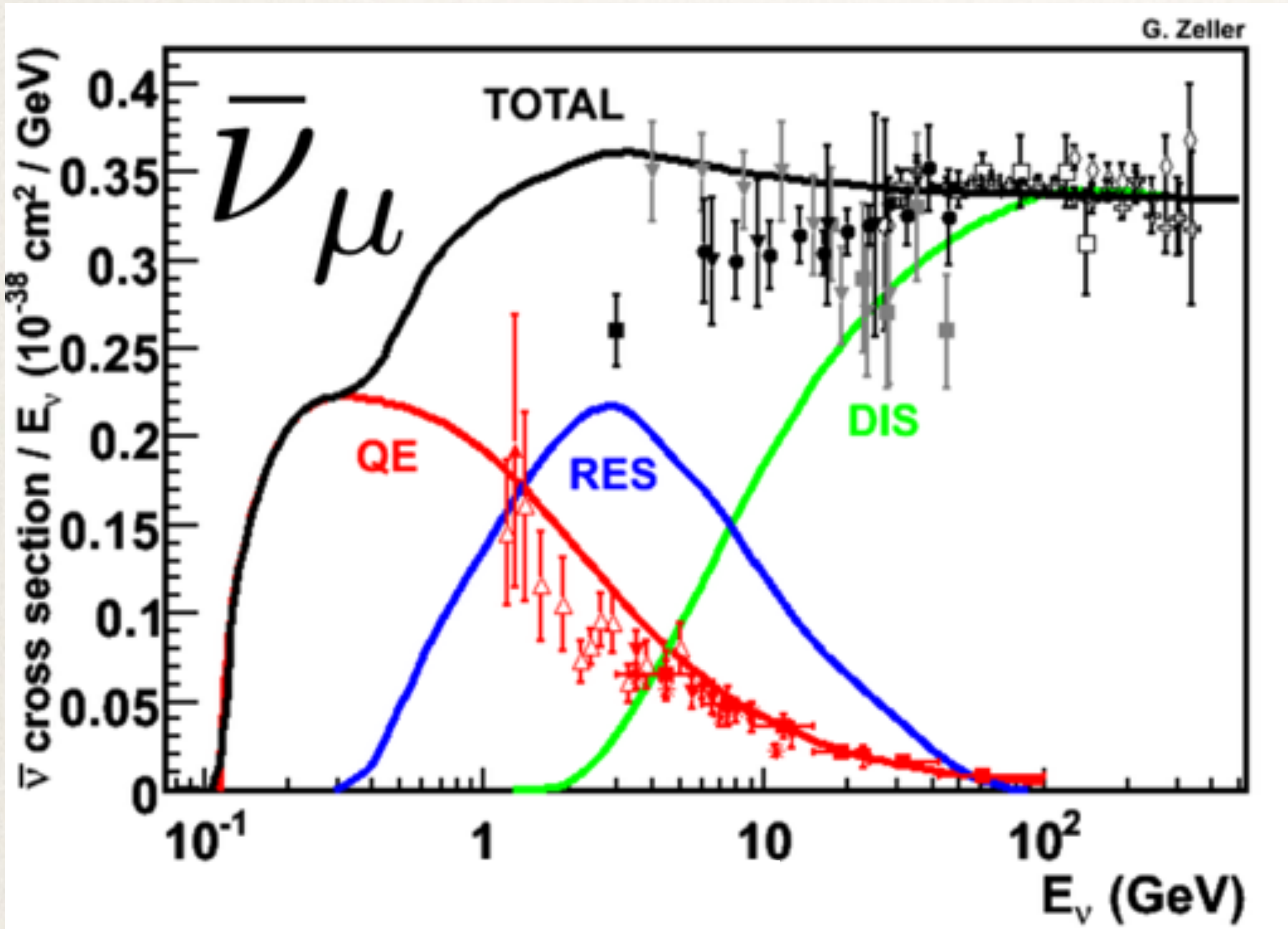

J.A. Formaggio and G.P. Zeller, Rev. Mod. Phys. 84, 1307-1341, 2012

Quasi-elastic scattering

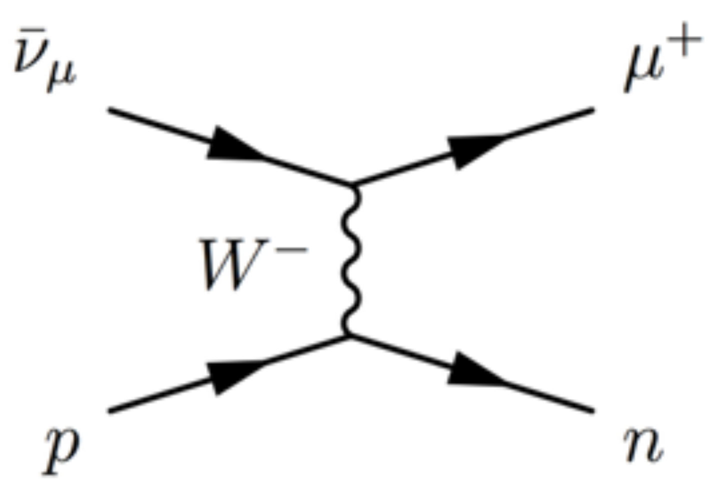

Resonant pion production

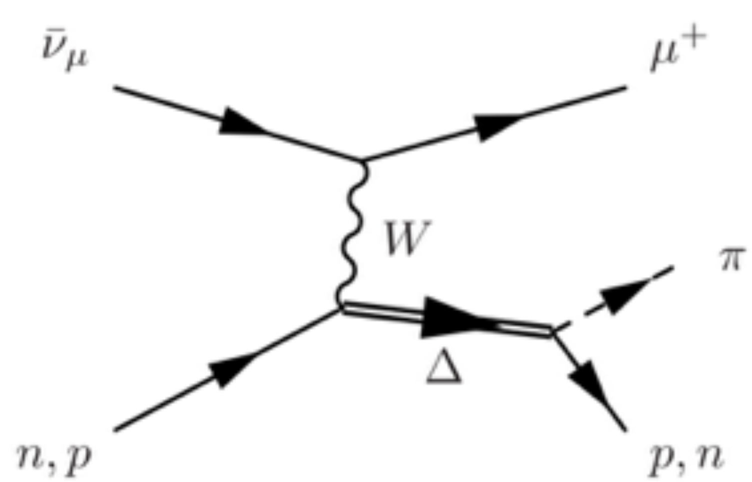

Deep inelastic scattering

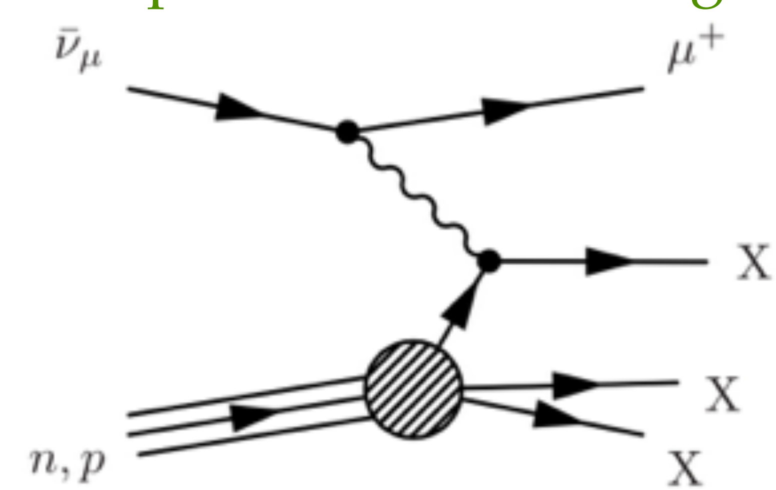

Three kinds of interactions

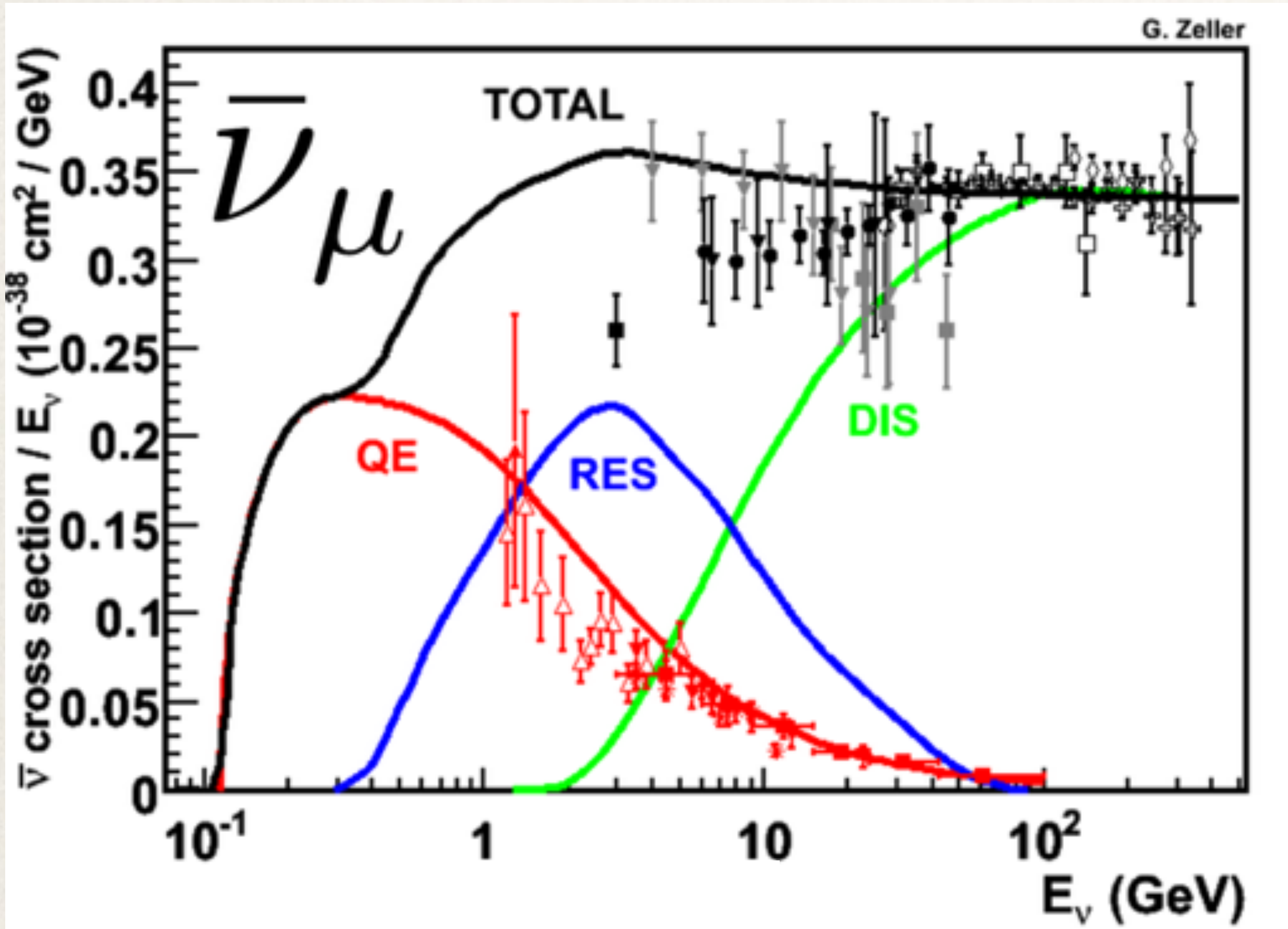

J.A. Formaggio and G.P. Zeller, Rev. Mod. Phys. 84, 1307-1341, 2012

I'll be focusing on quasi-elastic (CCQE) scattering

Quasi-elastic scattering

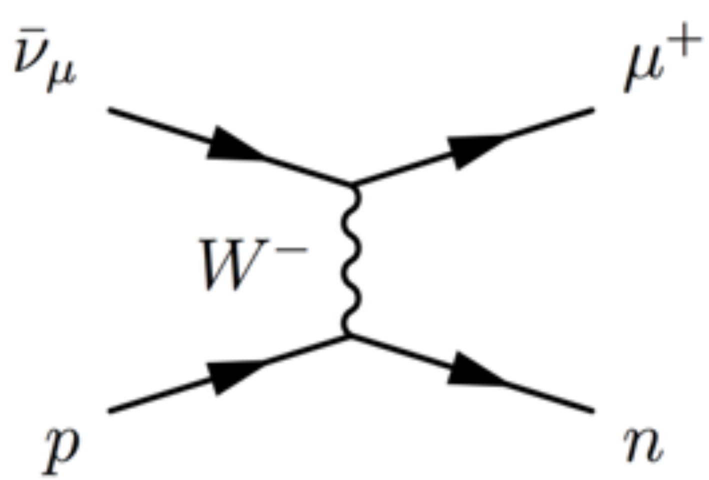

Resonant pion production

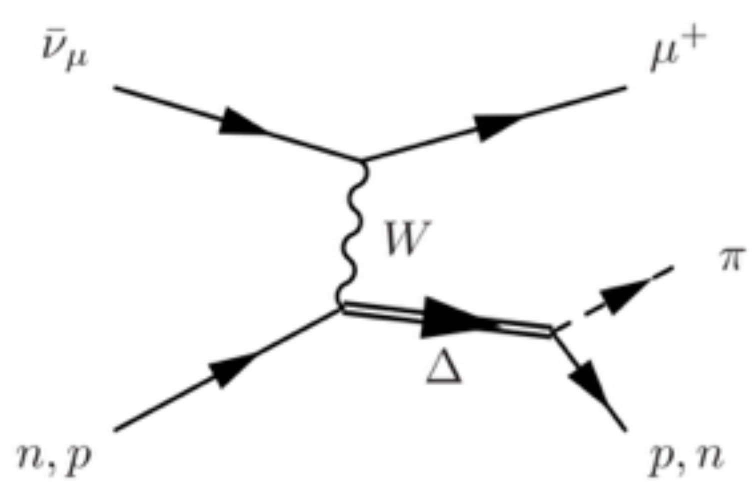

Deep inelastic scattering

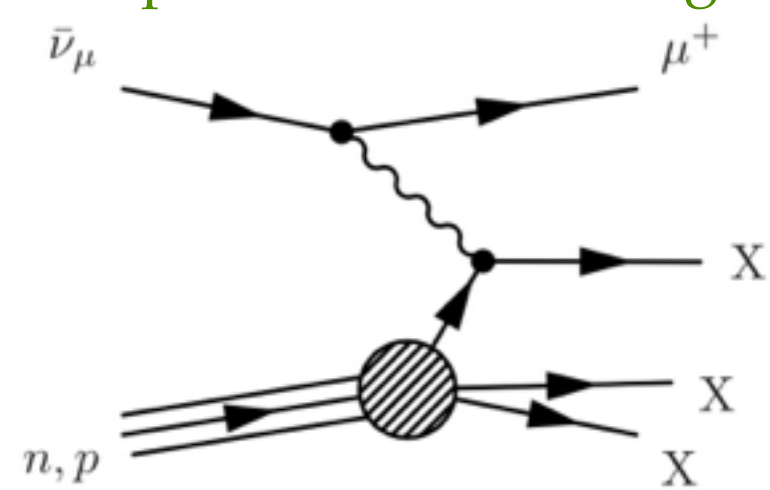

Three kinds of interactions

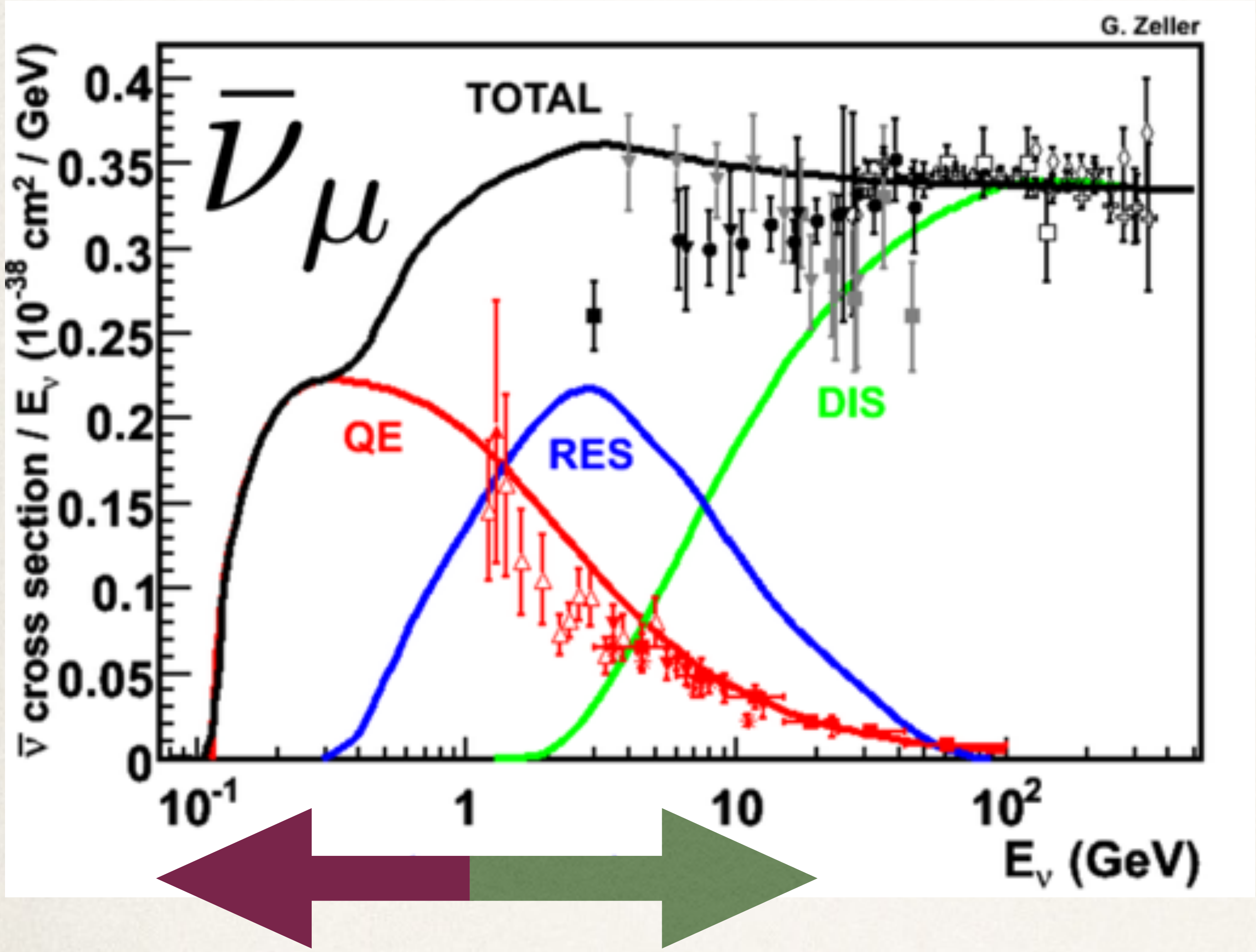

J.A. Formaggio and G.P. Zeller, Rev. Mod. Phys. 84, 1307-1341, 2012

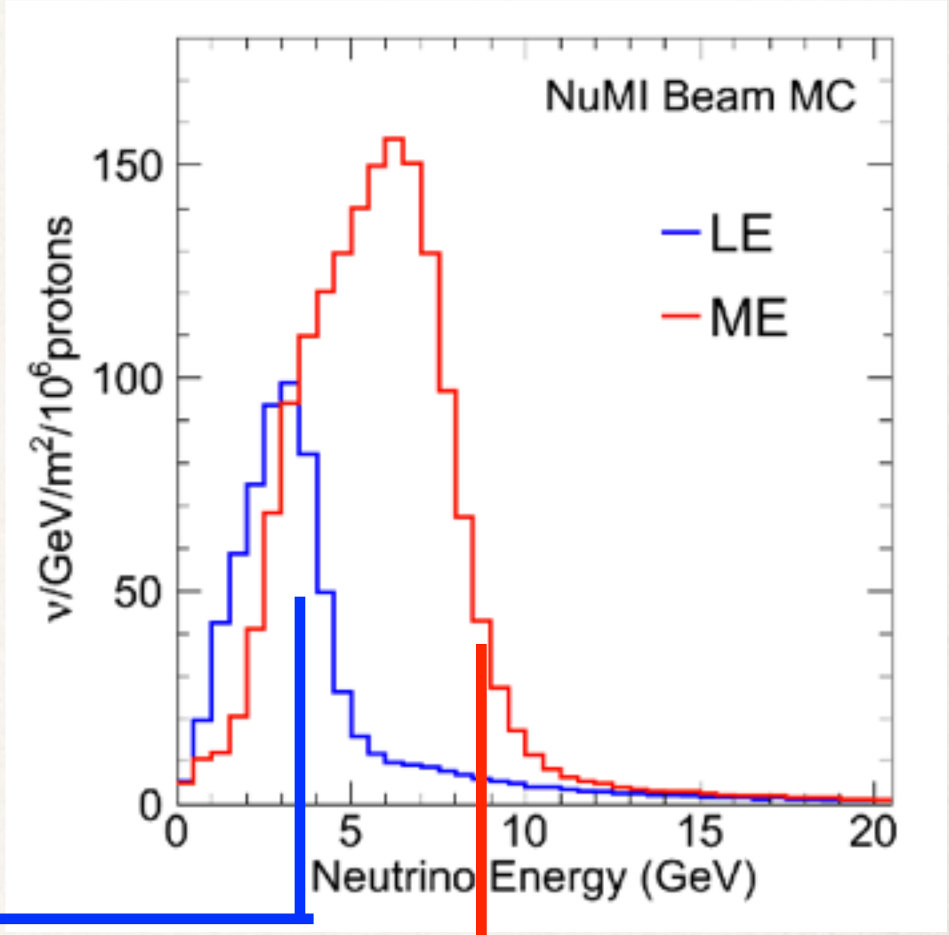

BooNE experiments, T2K

MINERνA, DUNE, NOνA, MINOS

Low-energy run, 2010-2012
~3.x10^{20} POT (ν)
~1x10^{20} POT ($\bar{\nu}$)

Medium-energy run, 2013-
ν mode only so far

MINERνA is ideally placed to measure cross sections in DUNE's energy range

I'll be talking about:

The charged-current quasi-elastic interaction and why it's important

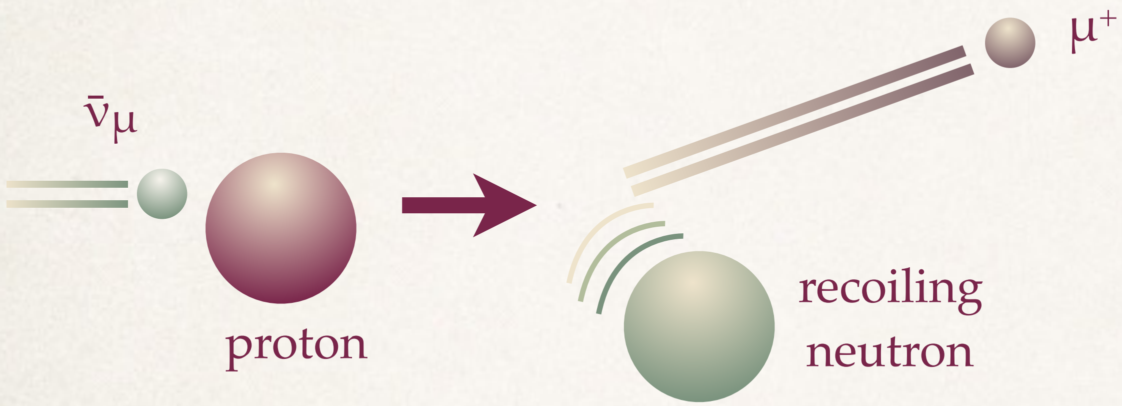

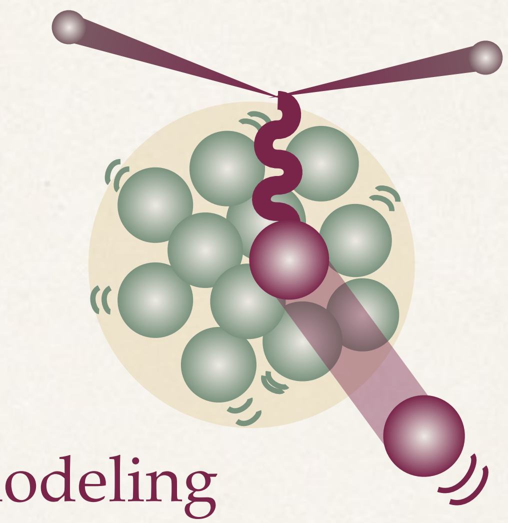

The challenges of modeling quasi-elastic scattering on heavy nuclei

The cross sections oscillation experiments need and how MINERvA can measure them

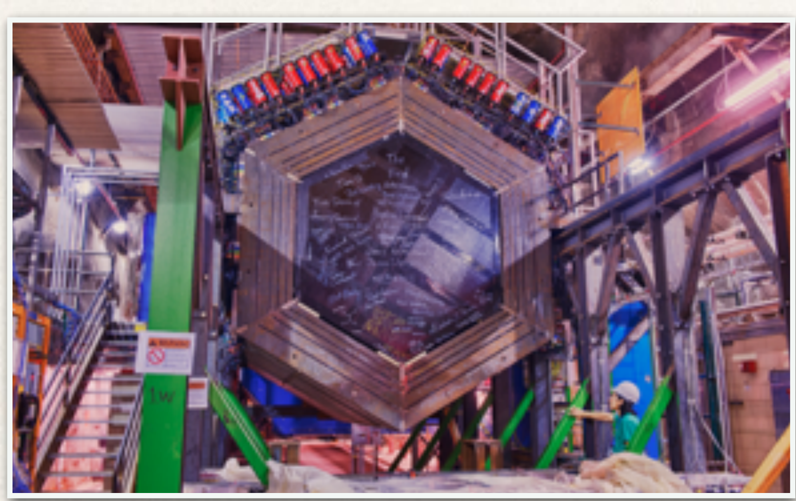

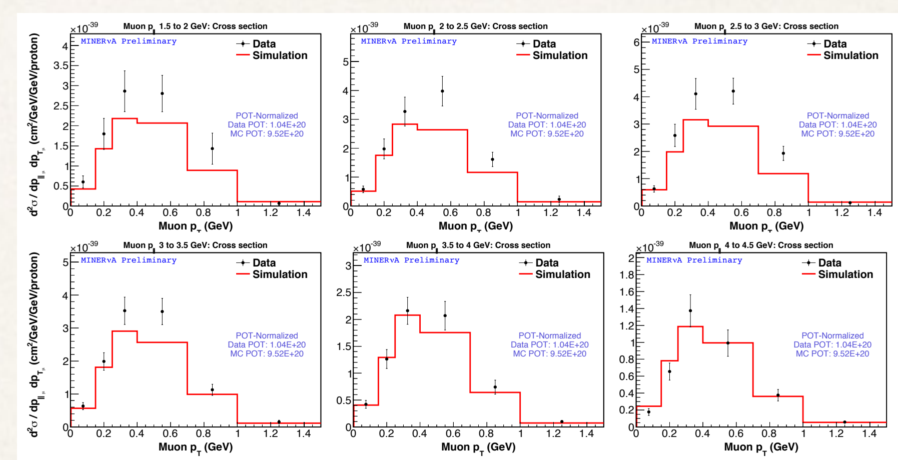

A new double-differential analysis that expands upon the 2013 antineutrino CCQE result

Quasi-elastic scattering from nucleons

- A relatively "simple" interaction process
- There is a **single charged muon** in the final state, plus the **recoil nucleon** (no pions etc)
- Oscillation experiments **reconstruct the neutrino energy and 4-momentum transfer** Q^2 from just the **muon kinematics**

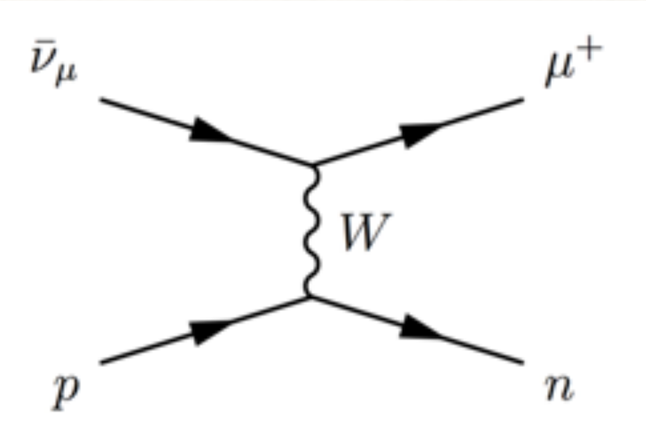

$$Q^2_{QE} = 2E_\nu^{QE}(E_\mu - p_\mu \cos\theta_\mu) - m_\mu^2$$

$$E_\nu^{QE} = \frac{m_n^2 - (m_p - E_b)^2 - m_\mu^2 + 2(m_p - E_b)E_\mu}{2(m_p - E_b - E_\mu + p_\mu \cos\theta_\mu)}$$

Antineutrinos turn **protons** into **neutrons**

Neutrinos turn **neutrons** into **protons**

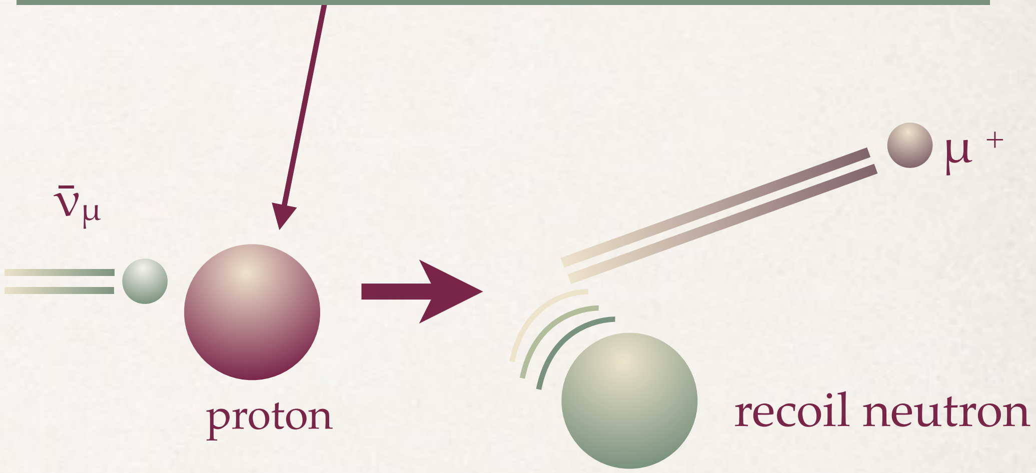

- But this assumes scattering from a free, stationary nucleon
- Once we know Q^2, there is a reliable cross-section model for free-nucleon scattering

Llewellyn-Smith formula

$$\frac{\mathrm{d}\sigma}{\mathrm{d}Q^2}_{QE}\begin{pmatrix}\nu_l n \to l^- p \\ \bar{\nu}_l p \to l^+ n\end{pmatrix} = \frac{M^2 G_F^2 \cos^2\theta_C}{8\pi E_\nu^2}\left\{A(Q^2) \mp B(Q^2)\frac{s-u}{M^2} + C(Q^2)\frac{(s-u)^2}{M^4}\right\}$$

$$\begin{aligned}A(Q^2) = \frac{m_l^2+Q^2}{M^2}\Bigg\{&\left(1+\frac{Q^2}{4M^2}\right)|F_A|^2 - (1-\frac{Q^2}{4M^2})F_1^2 \\ &+ \frac{Q^2}{4M^2}(1-\frac{Q^2}{4M^2})(\xi F_2)^2 + \frac{Q^2}{M^2}Re(F_1^*\xi F_2) - \frac{Q^2}{M^2}(1+\frac{Q^2}{4M^2})(F_A^3)^2 \\ &- \frac{m_\mu^2}{4M^2}\left[|F_1+\xi F_2|^2 + |F_A+2F_P|^2 - 4(1+\frac{Q^2}{4M^2})((F_V^3)^2+F_P^2)\right]\Bigg\}\end{aligned}$$

$$B(Q^2) = \frac{Q^2}{M^2}Re\left[F_A^*(F_1+\xi F_2)\right] - \frac{m_l^2}{M^2}Re\left[(F_1-\tau\xi F_2)F_V^{3*} - (F_A^* - \frac{Q^2}{2M^2}F_P)F_A^3)\right]$$

$$C(Q^2) = \frac{1}{4}\left\{F_A^2 + F_1^2 + \tau(\xi F_2)^2 + \frac{Q^2}{M^2}(F_A^3)^2\right\}$$

C.H. Llewellyn Smith, Phys. Rept. 3C, 261 (1972)

… a simple interaction process?

Llewellyn-Smith formula

$$\frac{d\sigma}{dQ^2}_{QE}\begin{pmatrix}\nu_l n \to l^- p \\ \bar{\nu}_l p \to l^+ n\end{pmatrix} = \frac{M^2 G_F^2 \cos^2\theta_C}{8\pi E_\nu^2}\left\{A(Q^2) \mp B(Q^2)\frac{s-u}{M^2} + C(Q^2)\frac{(s-u)^2}{M^4}\right\}$$

$$\begin{aligned} A(Q^2) = \frac{m_l^2+Q^2}{M^2}\Bigg\{&\left(1+\frac{Q^2}{4M^2}\right)|F_A|^2 - \left(1-\frac{Q^2}{4M^2}\right)\boxed{F_1^2} \\ &+ \frac{Q^2}{4M^2}\left(1-\frac{Q^2}{4M^2}\right)\boxed{\xi F_2}^2 + \frac{Q^2}{M^2}Re\,\boxed{F_1^*\xi F_2} - \frac{Q^2}{M^2}\left(1+\frac{Q^2}{4M^2}\right)(F_A^3)^2 \\ &- \frac{m_\mu^2}{4M^2}\left[\boxed{|F_1+\xi F_2|^2} + |F_A+2F_P|^2 - 4\left(1+\frac{Q^2}{4M^2}\right)\left((F_V^3)^2+F_P^2\right)\right]\Bigg\} \end{aligned}$$

$$B(Q^2) = \frac{Q^2}{M^2}Re\left[F_A^*\boxed{(F_1+\xi F_2)}\right] + \frac{m_l^2}{M^2}Re\left[(F_1-\tau\xi F_2)F_V^{3*} - \left(F_A^* - \frac{Q^2}{2M^2}F_P\right)F_A^3\right]$$

$$C(Q^2) = \frac{1}{4}\left\{F_A^2 + \boxed{F_1^2+\tau(\xi F_2)^2} + \frac{Q^2}{M^2}(F_A^3)^2\right\}$$

C.H. Llewellyn Smith, Phys. Rept. 3C, 261 (1972)

- F_1, F_2 are vector (electromagnetic) form-factors, based on the electric and magnetic form factors of the nucleons. Electron scattering can measure those.

$$F_1(Q^2) = \frac{G_E+\tau G_M}{1+\tau} \qquad \xi F_2(Q^2) = \frac{G_M-G_E}{1+\tau}$$

$$\tau = \frac{Q^2}{4M^2}$$

Llewellyn-Smith formula

$$\frac{\mathrm{d}\sigma}{\mathrm{d}Q^2}_{QE}\begin{pmatrix}\nu_l n \to l^- p \\ \bar{\nu}_l p \to l^+ n\end{pmatrix} = \frac{M^2 G_F^2 \cos^2\theta_C}{8\pi E_\nu^2}\left\{A(Q^2) \mp B(Q^2)\frac{s-u}{M^2} + C(Q^2)\frac{(s-u)^2}{M^4}\right\}$$

$$\begin{aligned}A(Q^2) = \frac{m_l^2+Q^2}{M^2}\Bigg\{&\left(1+\frac{Q^2}{4M^2}\right)|F_A|^2 - \left(1-\frac{Q^2}{4M^2}\right)F_1^2 \\ &+ \frac{Q^2}{4M^2}\left(1-\frac{Q^2}{4M^2}\right)(\xi F_2)^2 + \frac{Q^2}{M^2}Re(F_1^*\xi F_2) - \frac{Q^2}{M^2}\left(1+\frac{Q^2}{4M^2}\right)\boxed{(F_A^3)}^2 \\ &- \frac{m_\mu^2}{4M^2}\left[|F_1+\xi F_2|^2 + |F_A + 2\boxed{F_P}|^2 - 4\left(1+\frac{Q^2}{4M^2}\right)\left(\boxed{(F_V^3)}^2 + \boxed{F_P^2}\right)\right]\Bigg\}\end{aligned}$$

$$B(Q^2) = \frac{Q^2}{M^2}Re\left[F_A^*(F_1+\xi F_2)\right] - \frac{m_l^2}{M^2}Re\left[(F_1-\tau\xi F_2)F_V^{3*} - \left(F_A^* - \frac{Q^2}{2M^2}\boxed{F_P}\right)\boxed{F_A^3)}\right]$$

$$C(Q^2) = \frac{1}{4}\left\{F_A^2 + F_1^2 + \tau(\xi F_2)^2 + \frac{Q^2}{M^2}\boxed{(F_A^3)}\right\}$$

C.H. Llewellyn Smith, Phys. Rept. 3C, 261 (1972)

- F_3 terms are second-class currents and can be taken to be zero
- F_P corresponds to non-tree-level corrections involving pions, and can be related to F_A using PCAC

Llewellyn-Smith formula

$$\frac{d\sigma}{dQ^2}_{QE}\begin{pmatrix}\nu_l n \to l^- p\\ \bar{\nu}_l p \to l^+ n\end{pmatrix} = \frac{M^2 G_F^2 \cos^2\theta_C}{8\pi E_\nu^2}\left\{A(Q^2) \mp B(Q^2)\frac{s-u}{M^2} + C(Q^2)\frac{(s-u)^2}{M^4}\right\}$$

$$\begin{aligned}
A(Q^2) = \frac{m_l^2+Q^2}{M^2}\Bigg\{&\left(1+\frac{Q^2}{4M^2}\right)\boxed{|F_A|}^2 - \left(1-\frac{Q^2}{4M^2}\right)F_1^2 \\
&+ \frac{Q^2}{4M^2}\left(1-\frac{Q^2}{4M^2}\right)(\xi F_2)^2 + \frac{Q^2}{M^2}Re(F_1^*\xi F_2) - \frac{Q^2}{M^2}\left(1+\frac{Q^2}{4M^2}\right)(F_A^3)^2 \\
&- \frac{m_\mu^2}{4M^2}\left[|F_1+\xi F_2|^2 + |\boxed{F_A} + 2F_P|^2 - 4\left(1+\frac{Q^2}{4M^2}\right)\left((F_V^3)^2 + F_P^2\right)\right]\Bigg\}
\end{aligned}$$

$$B(Q^2) = \frac{Q^2}{M^2}Re[\boxed{F_A^*}(F_1+\xi F_2)] - \frac{m_l^2}{M^2}Re\left[(F_1-\tau\xi F_2)F_V^{3*} - (\boxed{F_A^*} - \frac{Q^2}{2M^2}F_P)F_A^3)\right]$$

$$C(Q^2) = \frac{1}{4}\left\{\boxed{F_A^2} + F_1^2 + \tau(\xi F_2)^2 + \frac{Q^2}{M^2}(F_A^3)^2\right\}$$

C.H. Llewellyn Smith, Phys. Rept. 3C, 261 (1972)

- F_A, the axial form factor, is not well constrained by electromagnetic electron scattering. We typically model the axial form factor as a dipole:

$$F_A(Q^2) = -\frac{g_A}{\left(1+\frac{Q^2}{M_A^2}\right)^2}$$

Axial mass, M_A, is the only free parameter

Neutrino bubble chamber experiments measure $M_A \approx 1.0$ GeV

Nucleons in the nucleus: RFG model

- In a heavy nucleus, nucleons are **not stationary**
- They interact with the other nucleons
- A commonly-used simulation of this is the **Relativistic Fermi Gas model**
  - Treat nucleons as independent particles, but in a **mean field** generated by the rest of the nucleus
  - Initial-state momenta are **Fermi distributed**
  - Pauli blocking
- Cross-sections can be modeled by a multiplier to the Llewellyn Smith cross-section

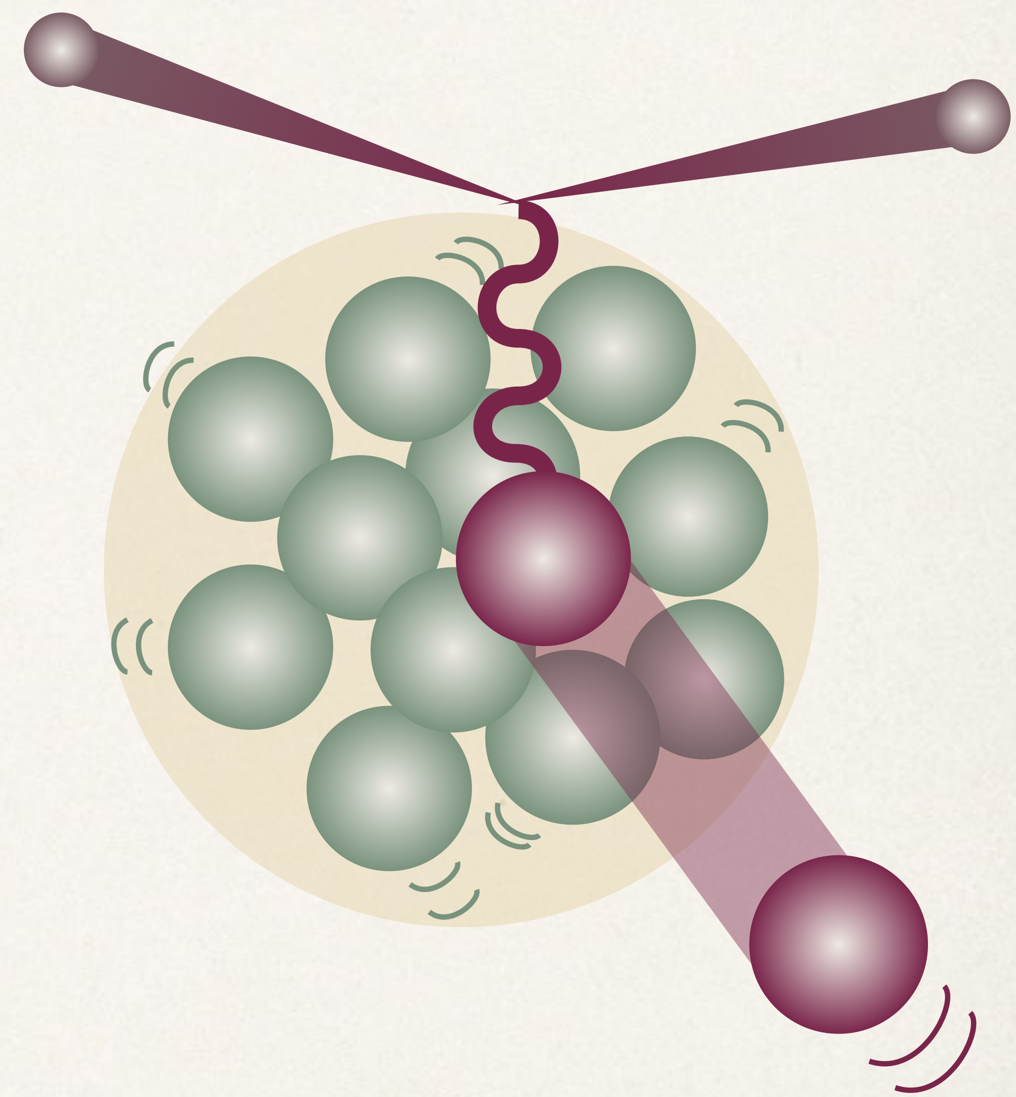

R. Smith and E. Moniz, Nucl.Phys. B43, 605 (1972); Bodek, S. Avvakumov, R. Bradford, and H. S. Budd, J.Phys.Conf.Ser. 110, 082004 (2008);

CCQE $\bar{\nu}$ Scattering at MINERvA, 2013 edition

In 2013, the **MINERvA** collaboration published cross sections, $d\sigma/dQ^2$, for charged-current quasi-elastic $\bar{\nu}_\mu$ scattering on scintillator, at DUNE energies

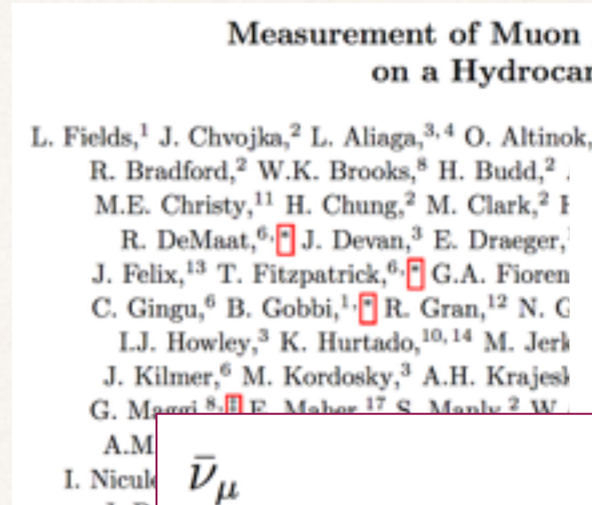
Measurement of Muon Antineutrino Quasi-Elastic Scattering on a Hydrocarbon Target at $E_\nu \sim 3.5$ GeV

L. Fields,[1] J. Chvojka,[2] L. Aliaga,[3,4] O. Altinok,[5] B. Baldin,[6] A. Baumbaugh,[6] A. Bodek,[2] D. Boehnlein,[6] S. Boyd,[7] R. Bradford,[2] W.K. Brooks,[8] H. Budd,[2] M.E. Christy,[11] H. Chung,[2] M. Clark,[2] R. DeMaat,[6] J. Devan,[3] E. Draeger, J. Felix,[13] T. Fitzpatrick,[6] G.A. Fioren C. Gingu,[6] B. Gobbi,[1] R. Gran,[12] N. G I.J. Howley,[3] K. Hurtado,[10,14] M. Jerk J. Kilmer,[6] M. Kordosky,[3] A.H. Krajesk

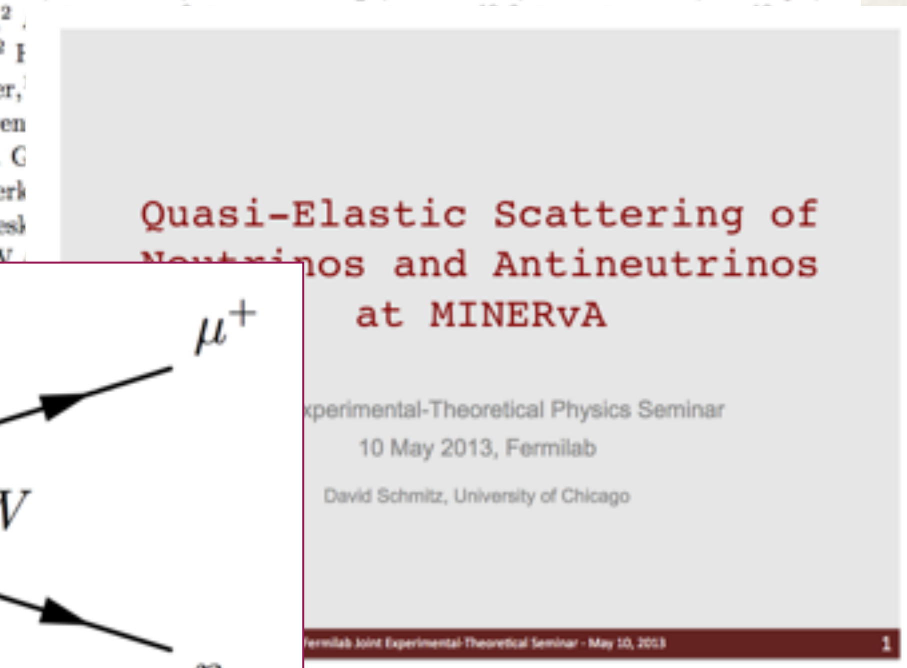

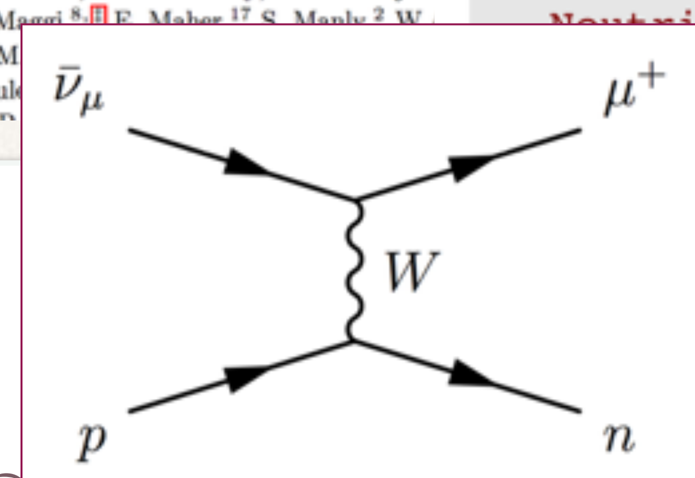

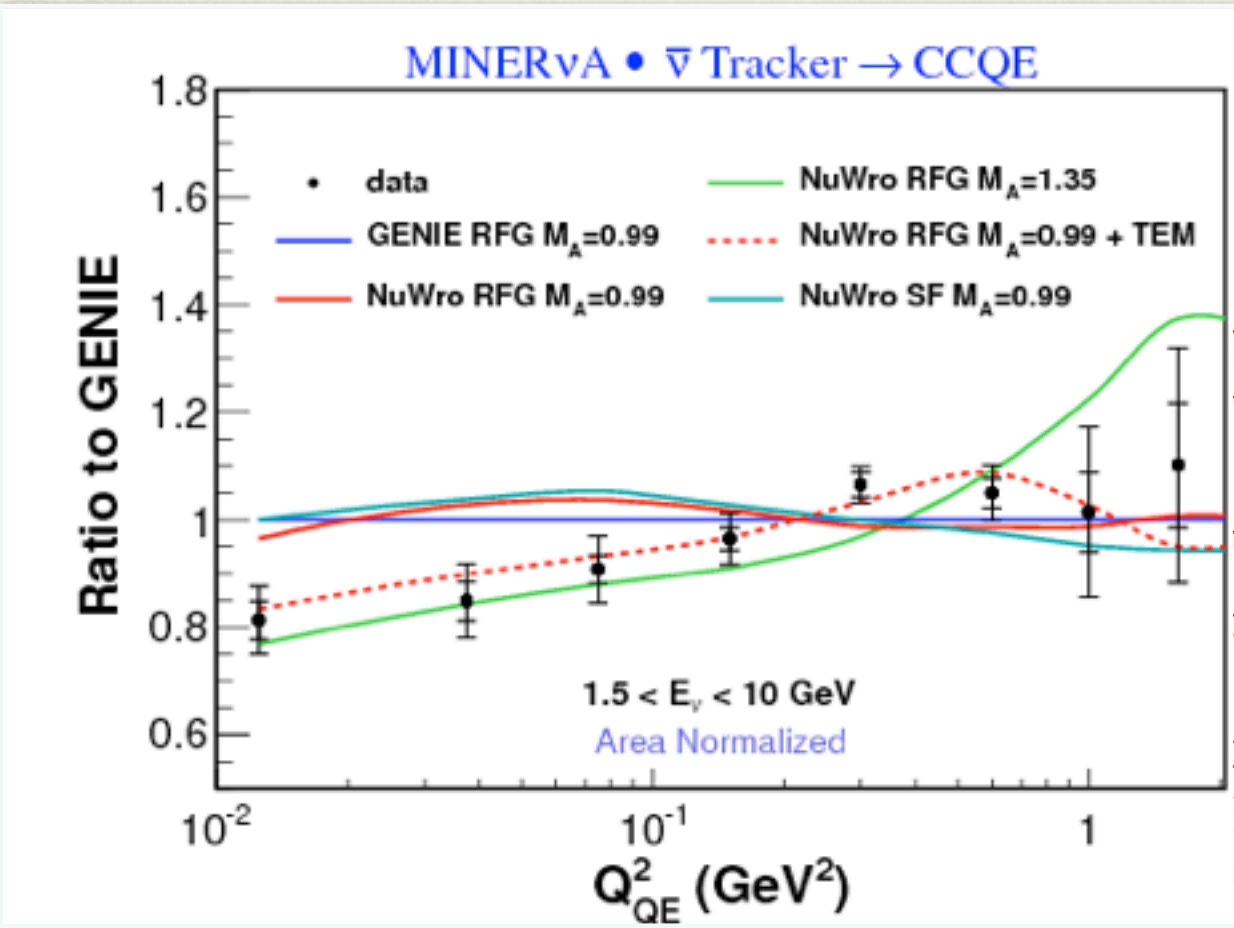

L. Fields, J. Chvojka et al. Phys. Rev. Lett. 111, 022501 (2013)

Our measurement showed tension with the Relativistic Fermi Gas model (shown in blue), and hinted at the possibility of **further nuclear effects** such as those parametrized by the transverse enhancement model.

Our double-differential measurement will expand on this

Antineutrino scattering at MiniBooNE

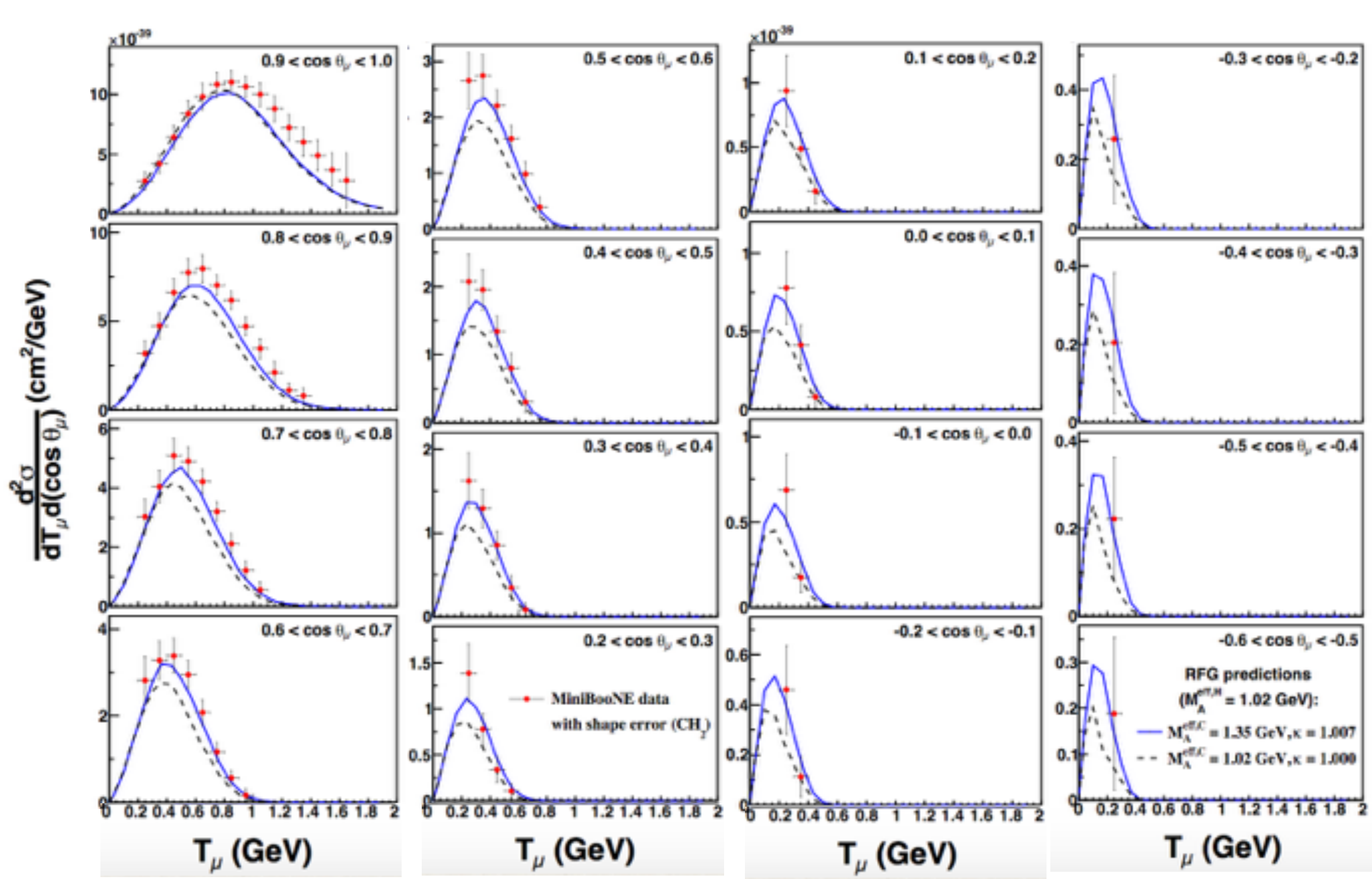

A.A. Aguilar-Arevalo et al. Phys.Rev. D88 (2013) no.3, 032001 (2013)

MiniBooNE's double-differential cross section measurement (red points) also showed poor agreement with the Fermi Gas model with M_A ~1GeV (dashed line)

Two experiments at **different energy ranges**, and **different detector technologies**, both see this evidence of nuclear effects beyond the Relativistic Fermi Gas model.

Effects beyond the Fermi Gas model

Electron-scattering experiments found that, approximately 20% of the time, electrons scattered from **correlated pairs** of nucleons instead of single nucleons.

They saw that 90% of these pairs consisted of a proton and a neutron.

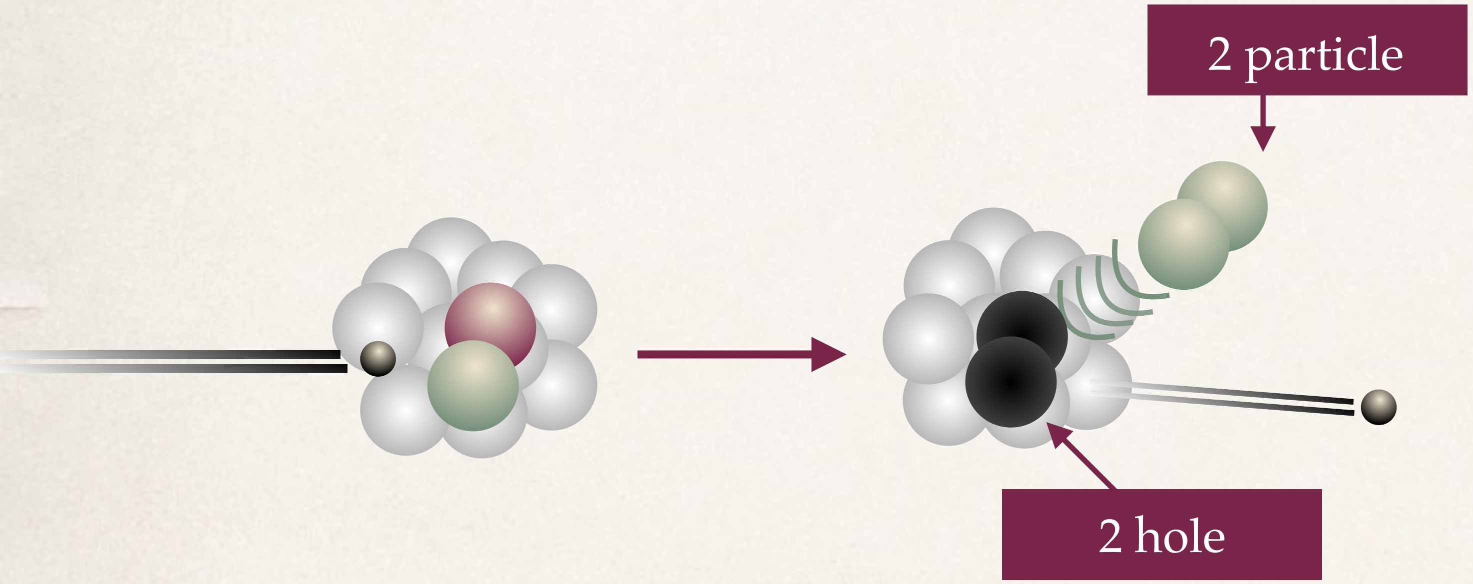

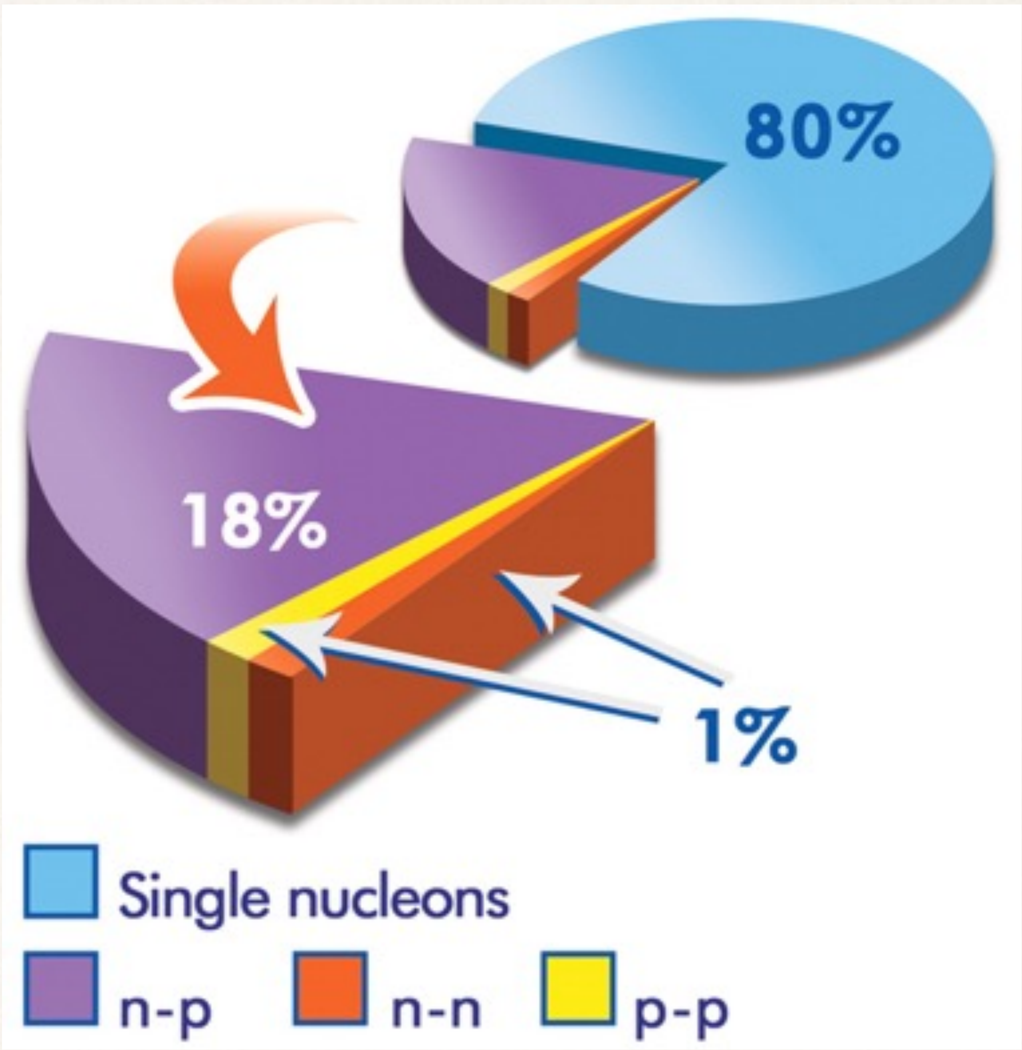

R. Subedi et al. Science, 320(5882):1476–1478, 2008

- The CCQE hypothesis reconstructs E_ν incorrectly if scattering from correlated pairs
- The final state may change as the partner nucleon is ejected (“2 particle, 2 hole”)

Correlation effects

Correlations can be **short range**…

- Bodek-Ritchie tail to RFG
- Spectral functions

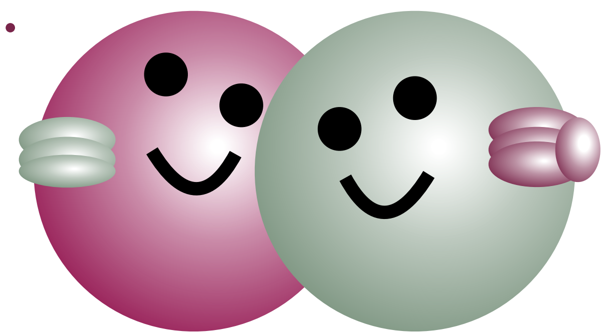

… **medium range**…

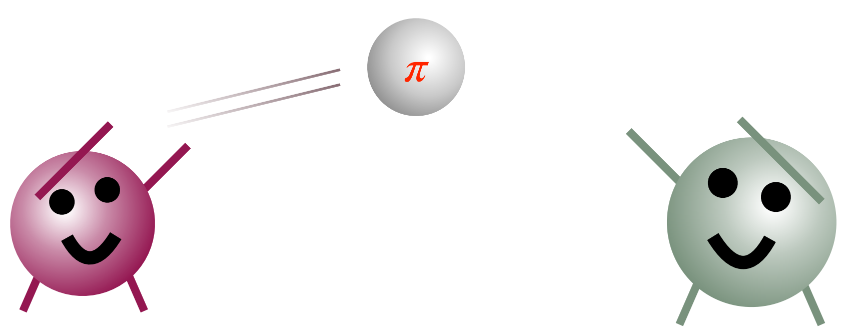

- Meson exchange currents
- Transverse enhancement model

… **or long range**…

Random phase approximation

Some correlation models

Meson exchange currents

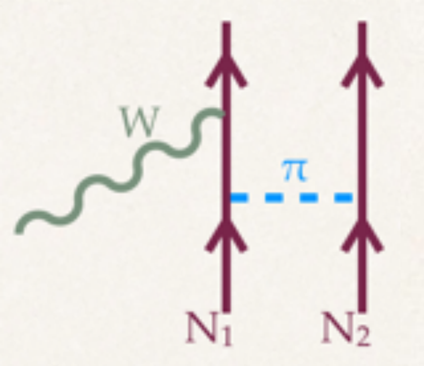

J. Nieves et al. Phys. Rev. C 83 (2011) 045501

- Diagrams such as this correlation have been calculated
- These can represent both short- and long-range correlation effects, including 2p2h

Random phase approximation

- Polarization of the nucleus screens electroweak coupling of the W boson
- Not a 2p2h effect
- Suppresses cross section at low four-momentum transfer Q^2

PRC 70, 055503 (2004)

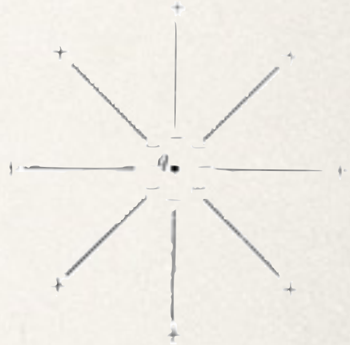

Griffiths, Introduction to Electrodynamics

Transverse Enhancement Model (TEM)

- Parametrizes correlation effect seen in electromagnetic electron scattering by modifying nucleon magnetic form factor *A. Bodek, H. Budd, and M. Christy, Eur.Phys.J. C71, 1726 (2011)*
- We don't know how it extends to axial current
- Parametrizes both MEC and RPA effects

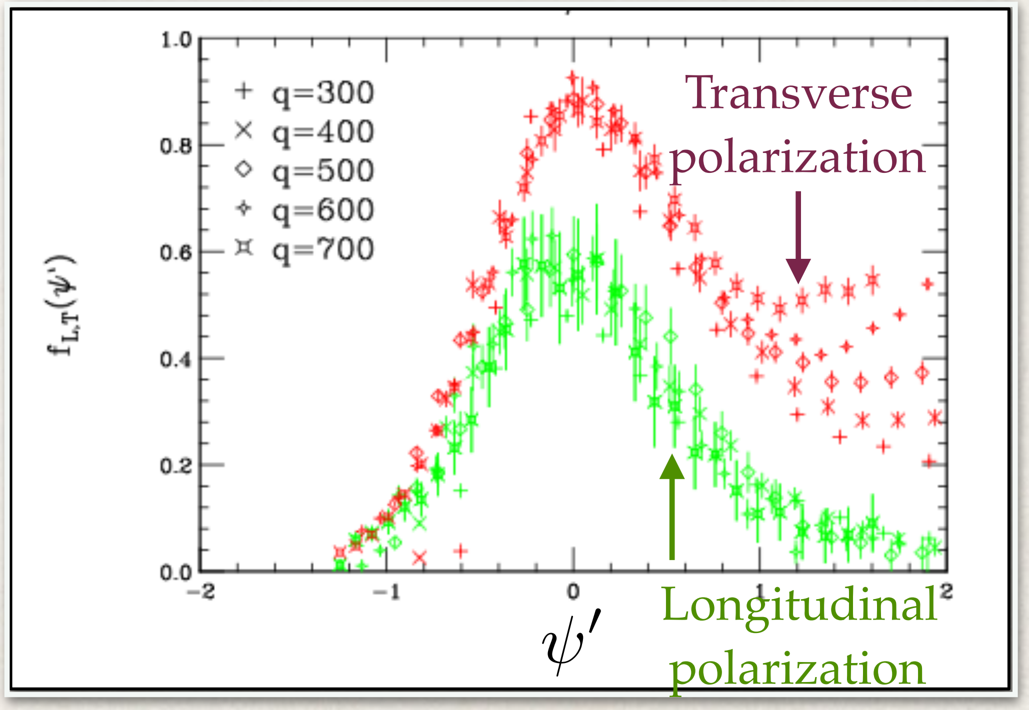

J. Carlson et al, PRC 65, 024002 (2002)

Final-state interactions

- Hadrons produced in a scattering interaction may re-interact with other nucleons before they escape the nucleus: we call these final-state interactions
- Thus the particles that exit the nucleus may be different, both in type and in energy, from those generated in the initial interaction

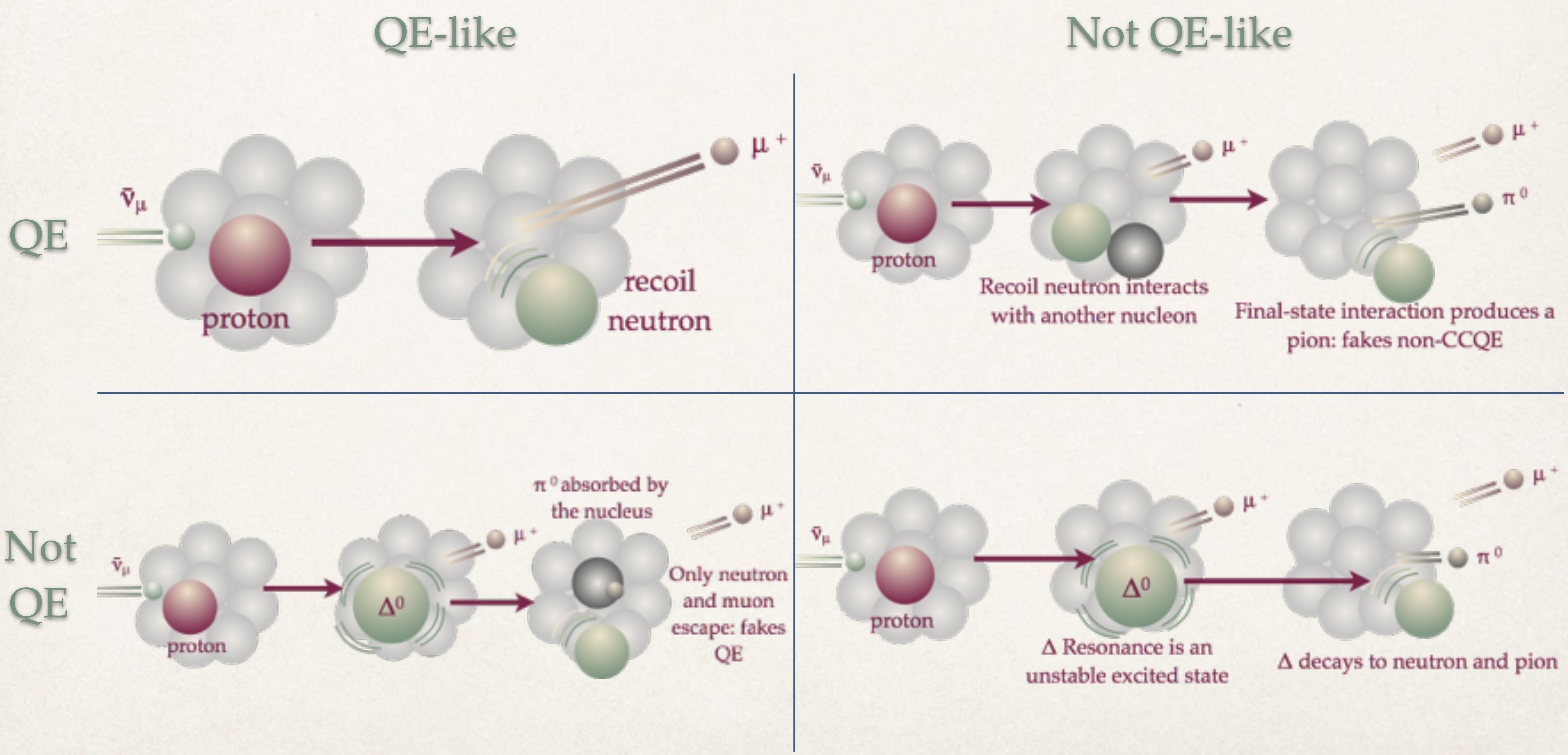

Final-state interactions

- Hadrons produced in a scattering interaction may re-interact with other nucleons before they escape the nucleus: we call these final-state interactions
- Thus the particles that exit the nucleus may be different, both in type and in energy, from those generated in the initial interaction

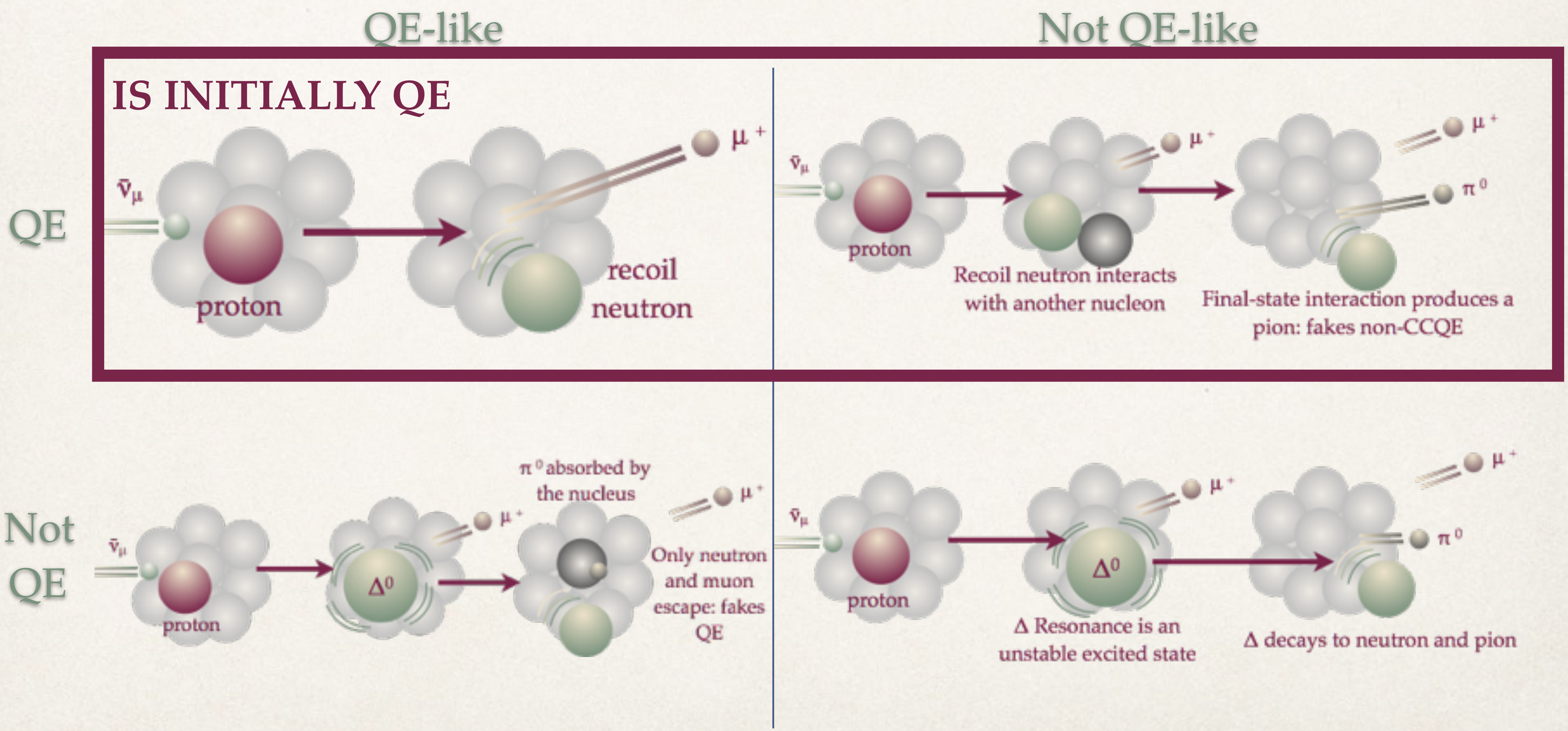

Final-state interactions

- Hadrons produced in a scattering interaction may re-interact with other nucleons before they escape the nucleus: we call these final-state interactions
- Thus the particles that exit the nucleus may be different, both in type and in energy, from those generated in the initial interaction

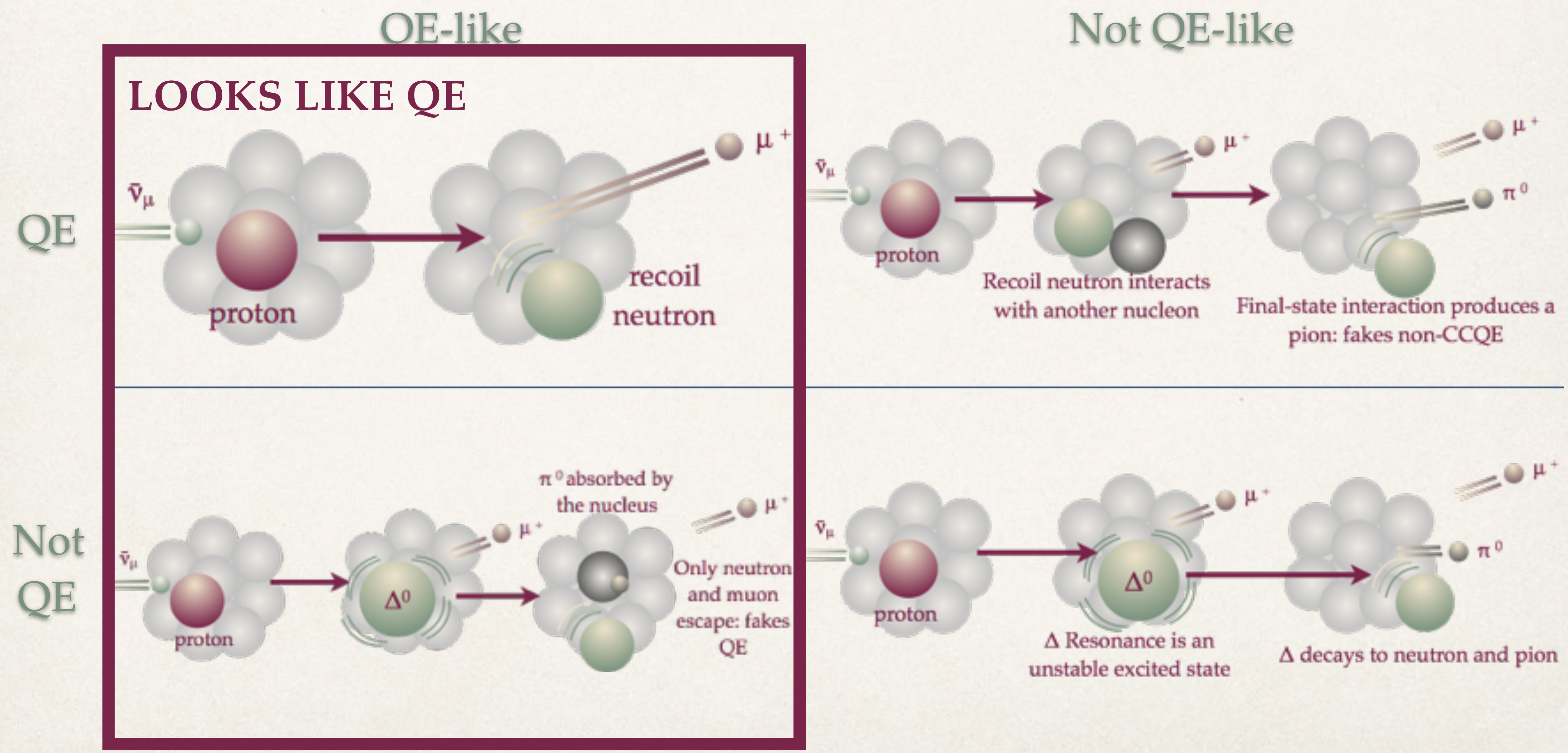

So what counts as a quasi-elastic?

Resonant events that fake CCQE?

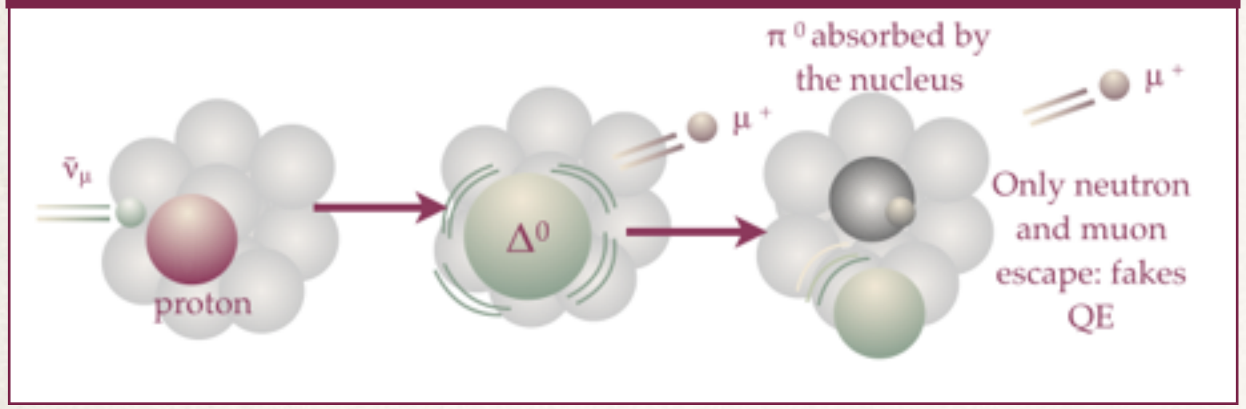

"Quasi-elastic" 2p2h scattering?

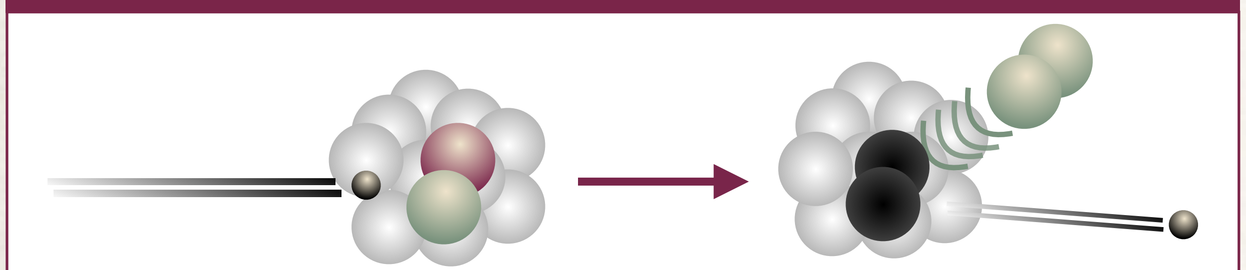

Initially QE events with final-state pions?

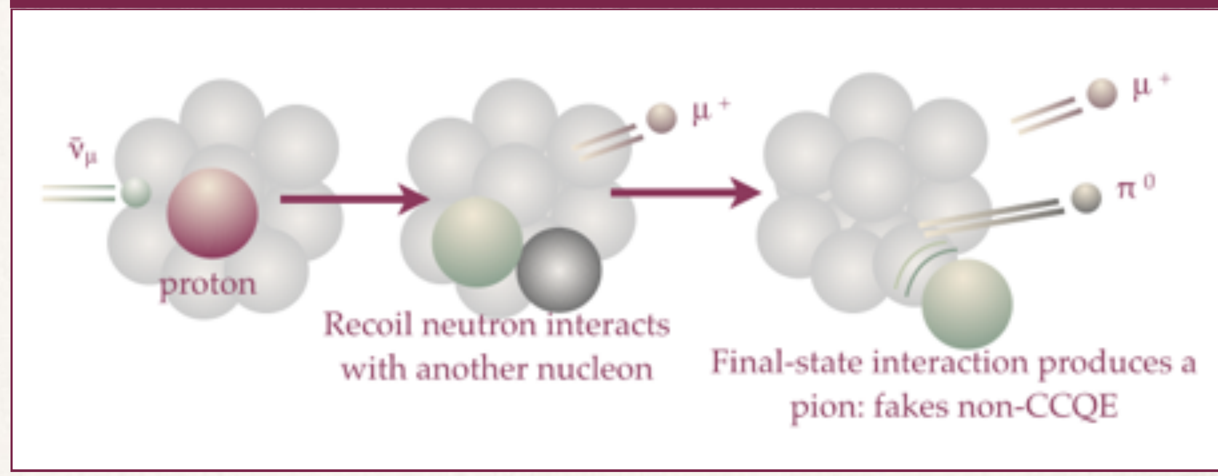

We looked at two "similar" analyses from MINERvA and MiniBooNE… but in fact they used **different definitions** for what counted as CCQE. What should we use?

Remember that we are trying to help **oscillation experiments.** To decide how to define a quasi-elastic, we should think about them: what are their **detectors** like? What **energies** do they operate at? **How do CCQE events look** in them?

Quasi-elastics at T2K and MiniBooNE

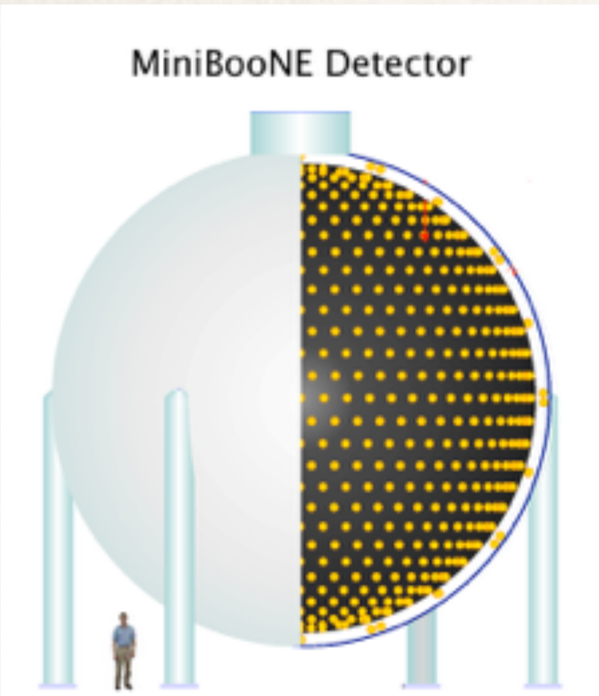

MiniBooNE used a mineral oil Cherenkov detector

T2K's far detector, Super Kamiokande, is water Cherenkov

- Muons and electrons travel through the large detectors to produce characteristic Cherenkov rings
- Most **pions** can also be detected
- Most **nucleons are invisible,** so a CCQE event presents as a muon ring

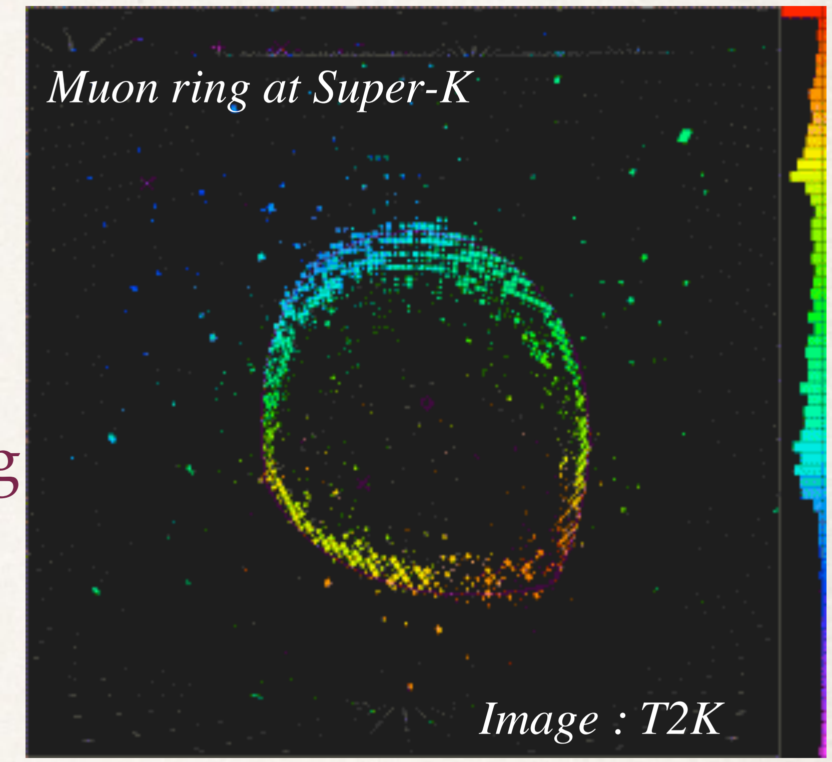

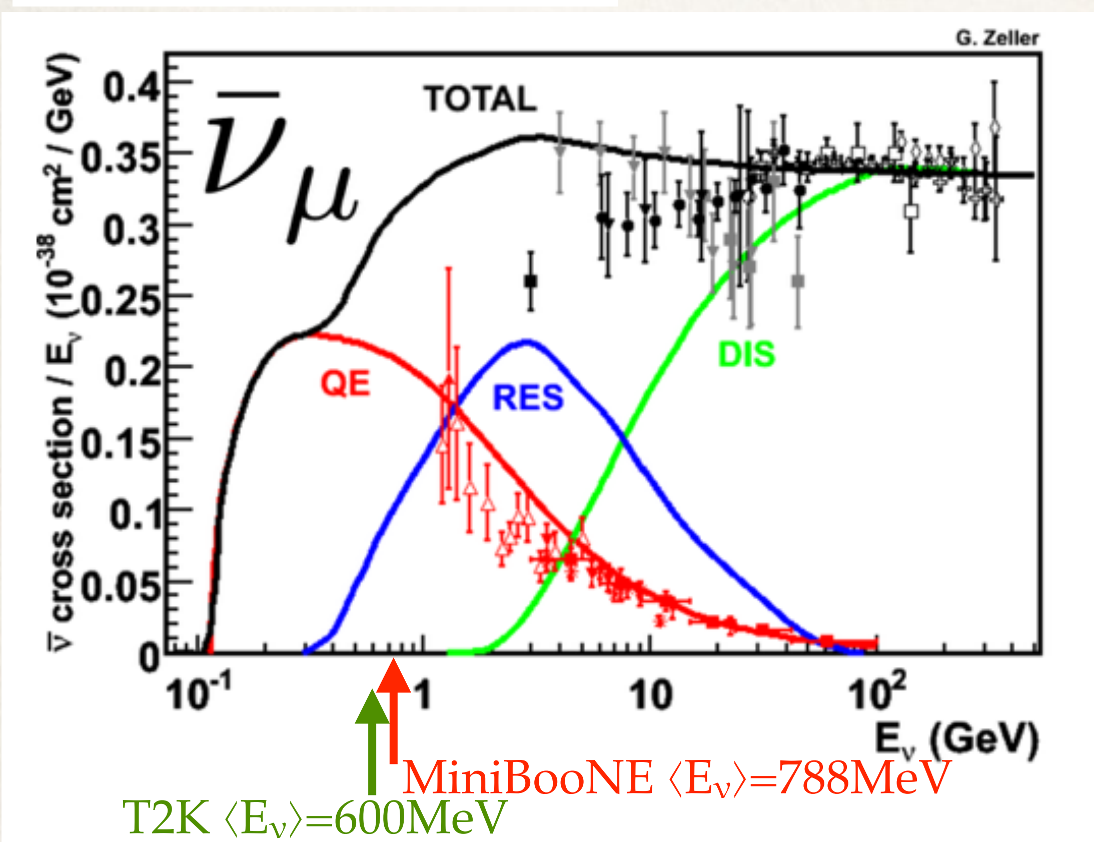

- Both experiments have mean energies **below 1GeV**, where **quasi-elastics dominate** and resonant contamination is small
- T2K and MiniBooNE have both published CCQE results were the signal is defined as events with a muon and **no pions in the final state (CC0π)**
- As these **look like** quasi-elastics, we call them **quasi-elastic-like**

Quasi-elastics at NOvA and DUNE

NOvA's segmented liquid scintillator detector can see protons

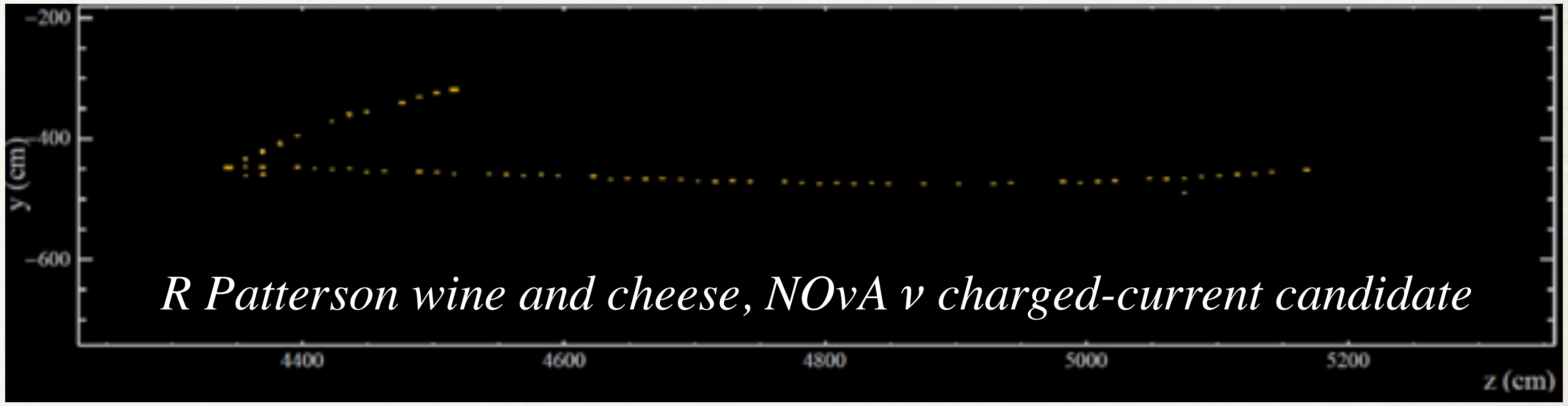

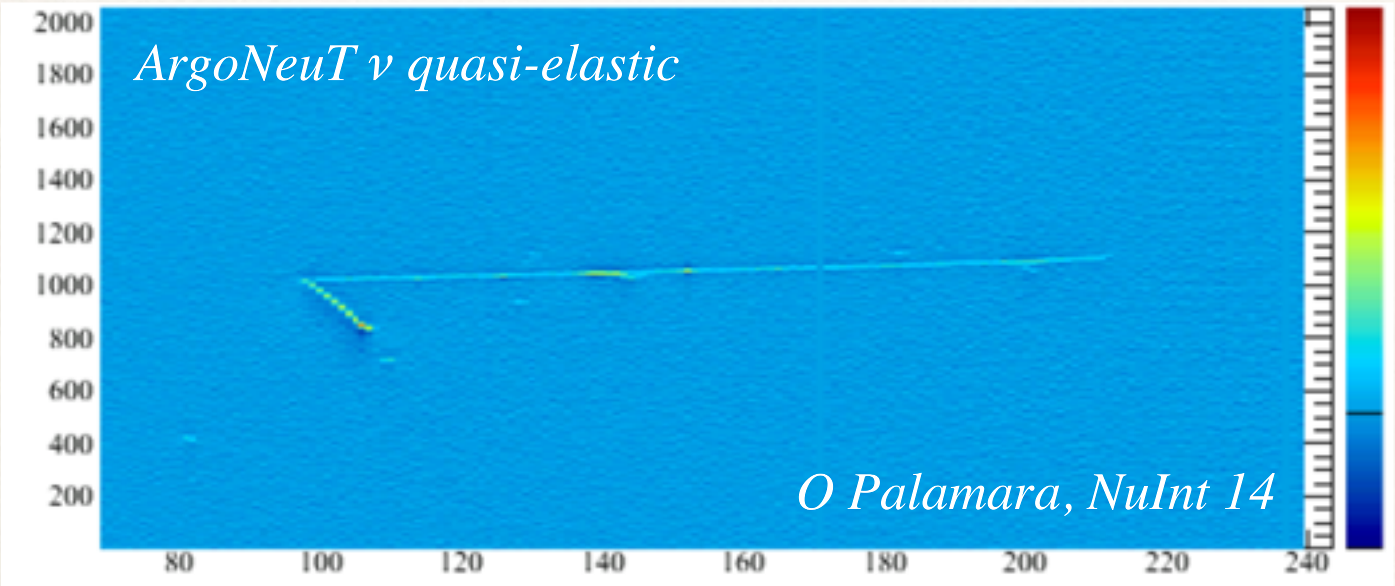

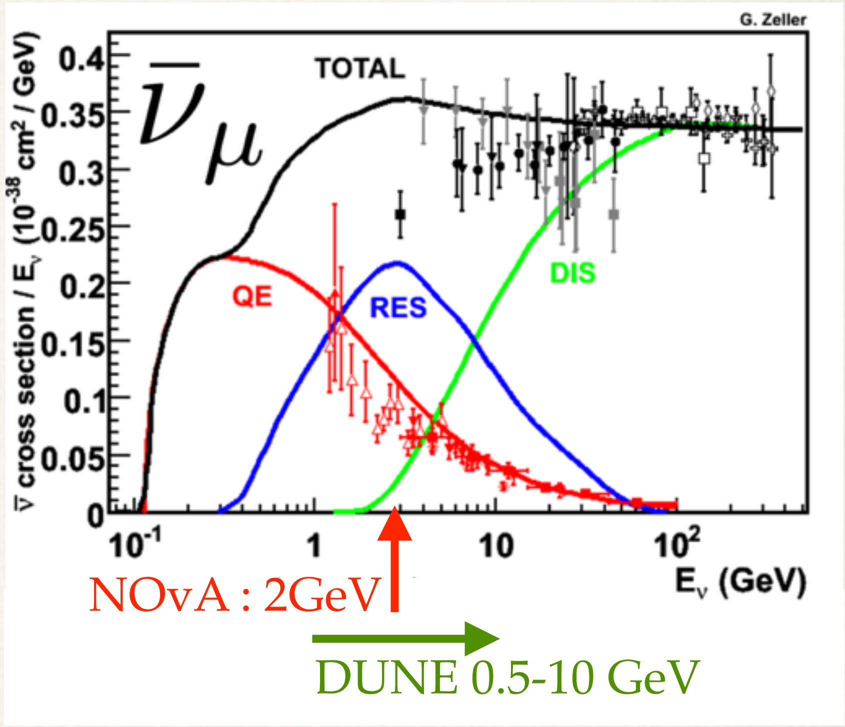

- Liquid argon detectors like DUNE, MicroBooNE and ArgoNeuT (above) have excellent charged particle resolution
- CC0π makes less sense now we have **more information** on the final state

To reconstruct the energy, we must understand the final state

True CCQE signal definition

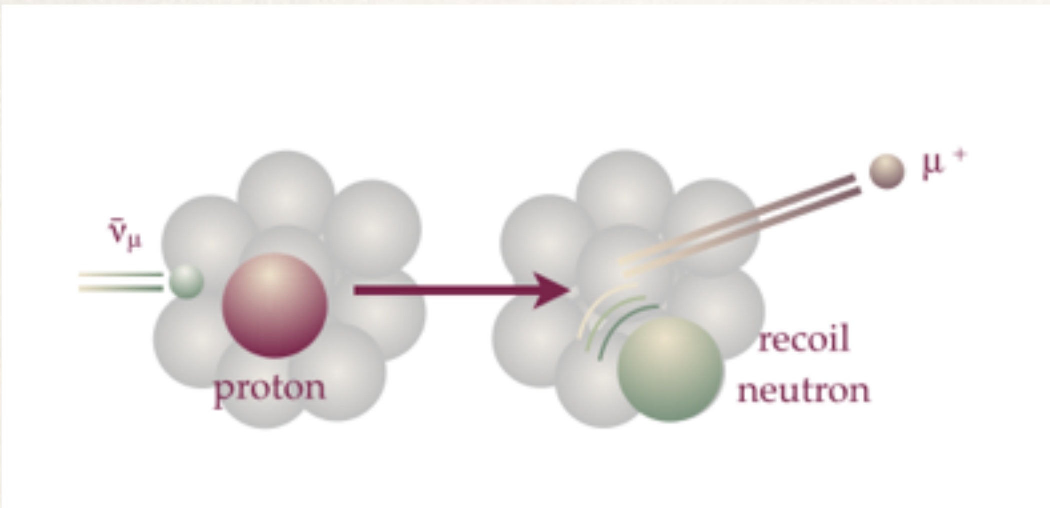

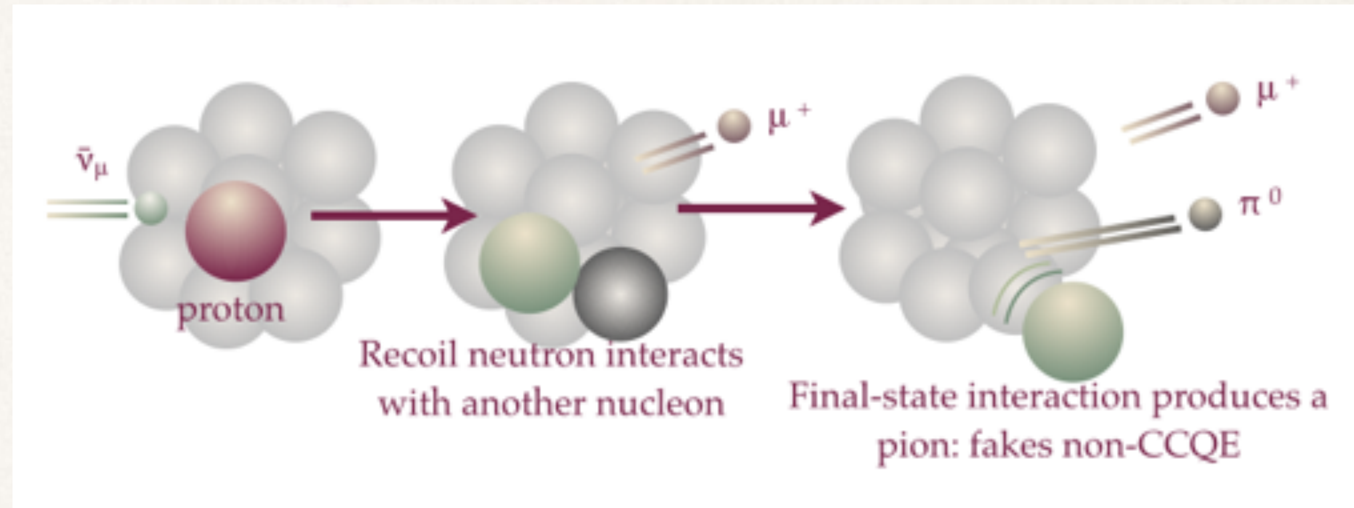

- **Previous MINERvA** $\bar{\nu}$ analysis defined signal as **true CCQE**, regardless of final state
- We corrected our data based on our simulation's model of CCQE cross sections

Pros:	**Cons**:
- Signal only depends on **one interaction type** - comparing with models doesn't involve the FSI model, resonant processes etc	- This signal definition is based on the initial interaction, rather than the final state that we observe in our detector - What is a CCQE anyway? Does it include correlation effects? - Complicates comparisons with other experiments that use different definitions

CC0π quasi-elastic-like signal definition

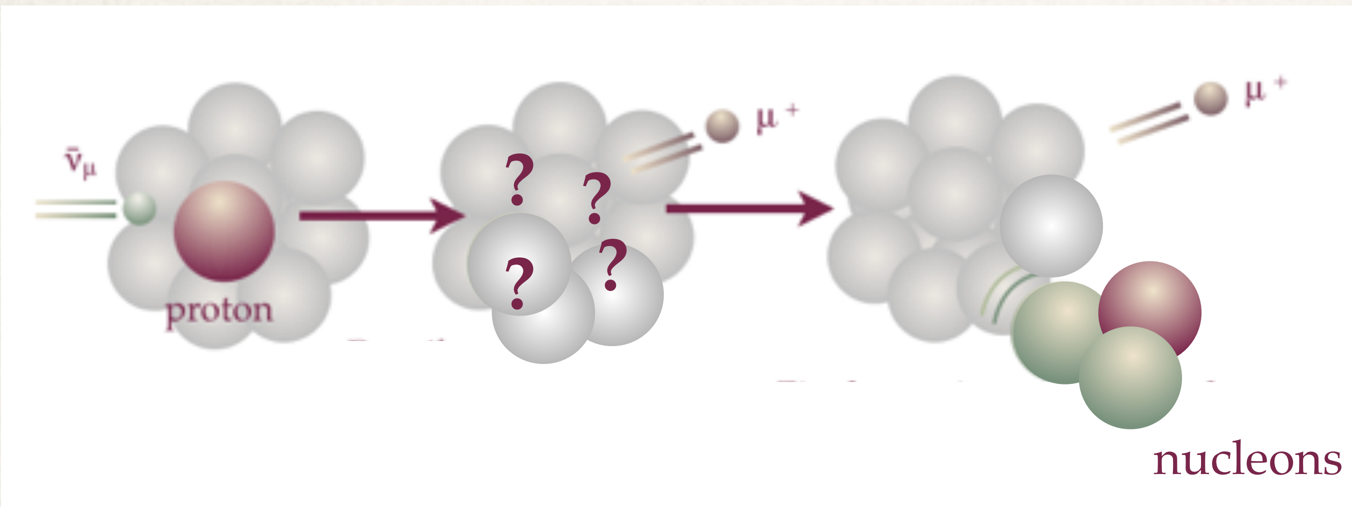

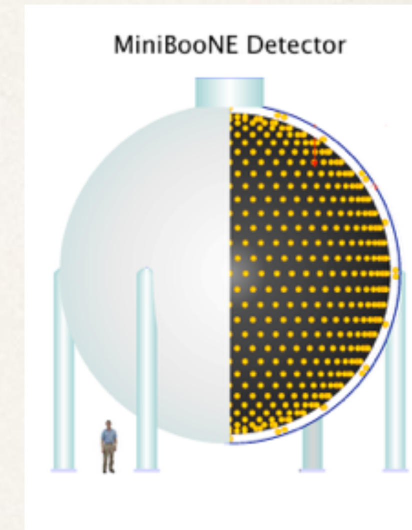

- **MiniBooNE** and **T2K** define a CCQE-like signal as only the **μ^+** and **nucleons** in the final state (**zero pions**, photons, other hadrons). These may be resonant + FSI.
- These events all have the same signature (muon ring) in MiniBooNE and Super-K

Pros:	**Cons**:
- Signal depends on **final-state observable** - Cherenkov-detector friendly	- Simulating this depends on several models: CCQE, resonant, FSI… - "Any number of nucleons" is not so easy to identify in MINERvA, where **a proton and neutron look very different**

MINERvA detector

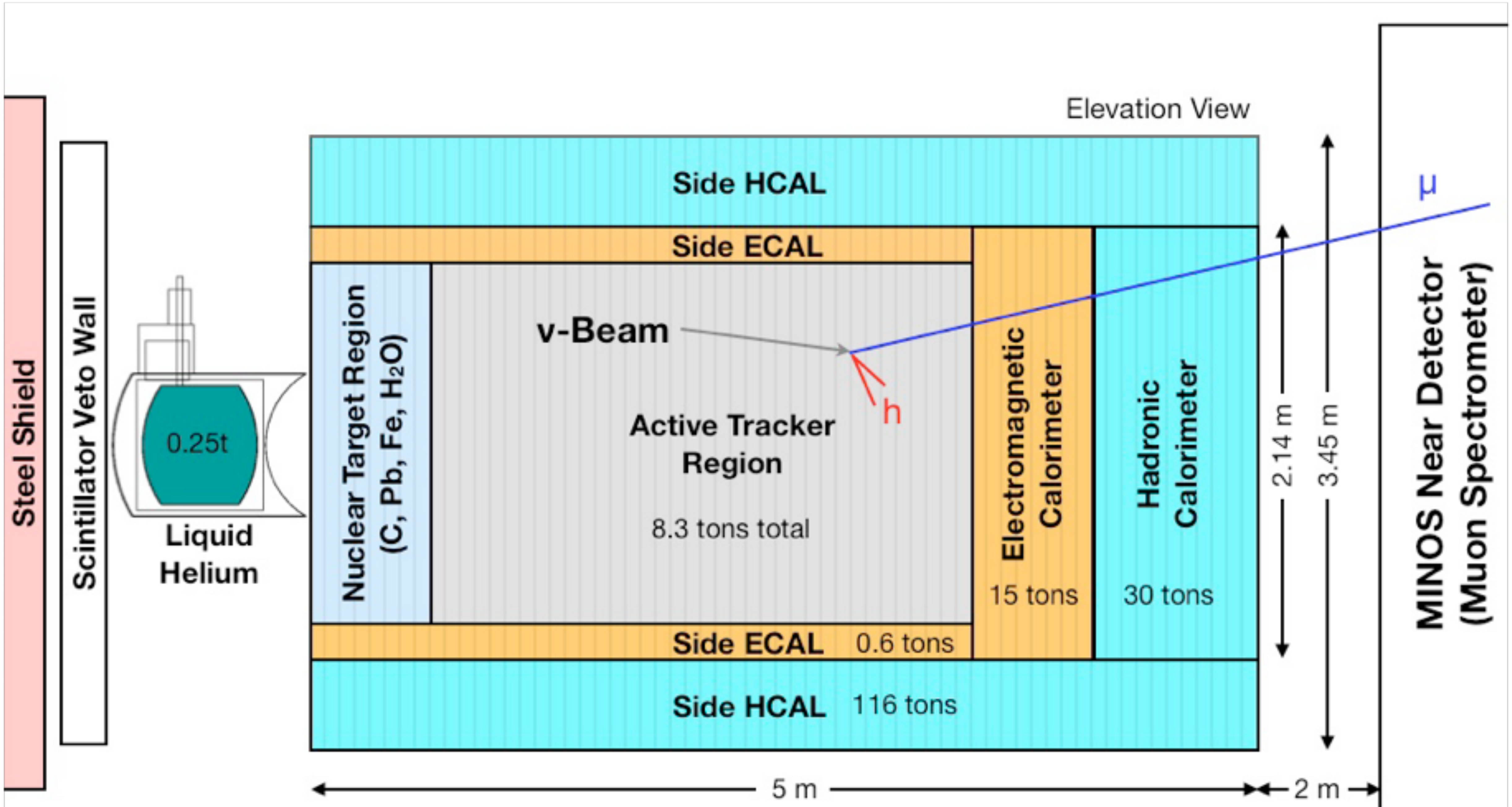

Nucl. Inst. and Meth. A743 (2014) 130
arXiv:1305.5199

All photographs: Reidar Hahn, Fermilab visual media services

MINERvA detector

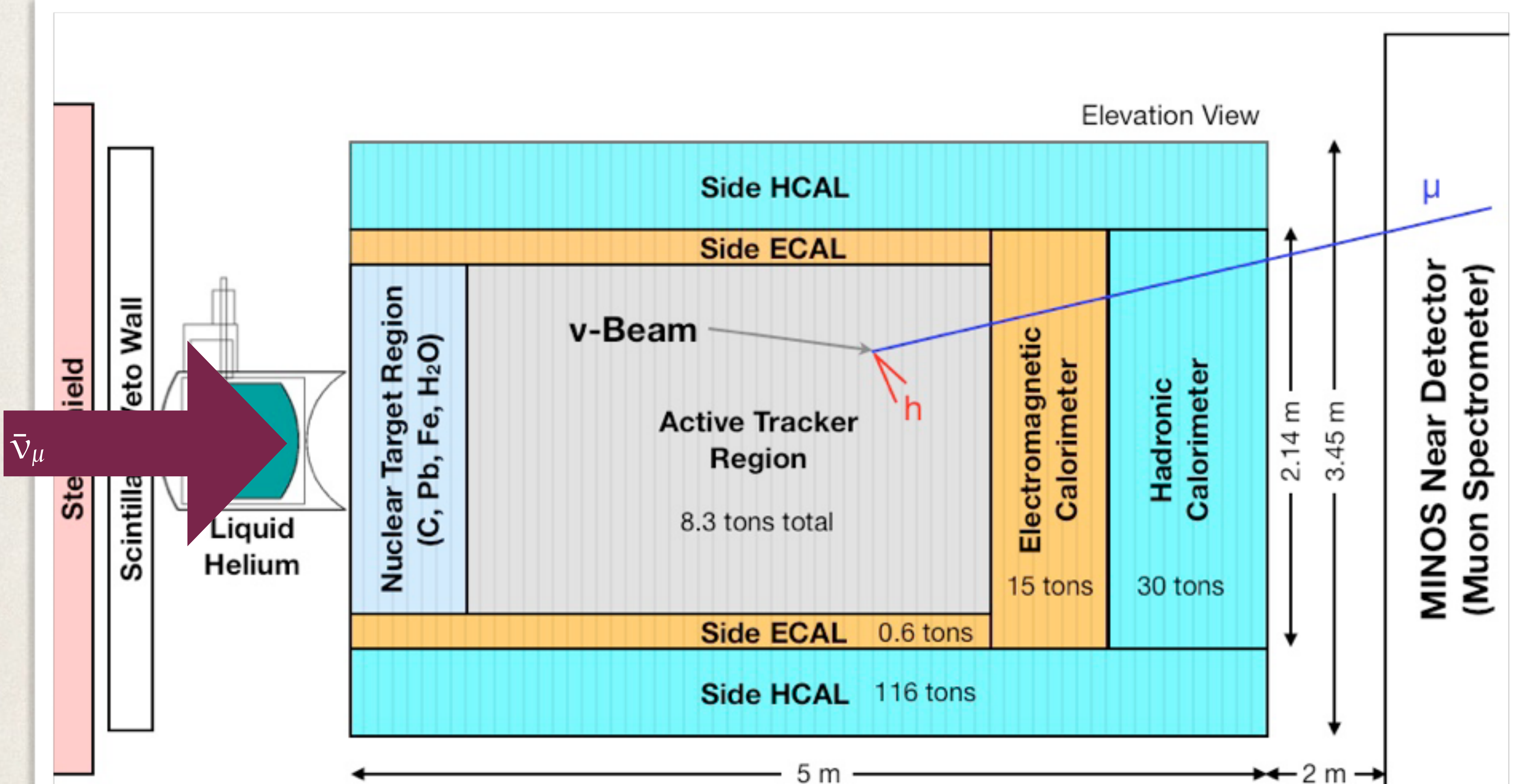

Nucl. Inst. and Meth. A743 (2014) 130
arXiv:1305.5199

All photographs: Reidar Hahn, Fermilab visual media services

MINERvA detector

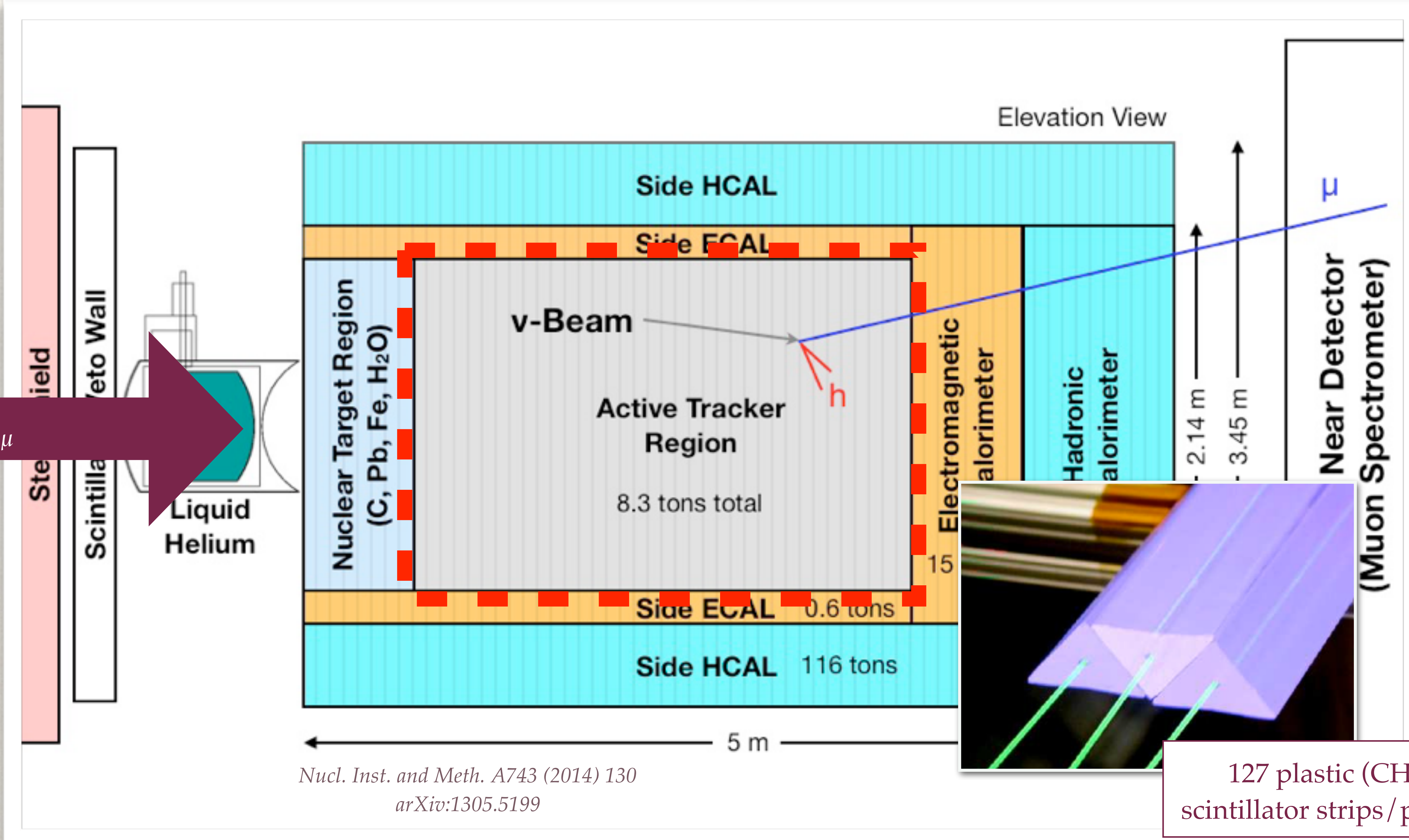

Nucl. Inst. and Meth. A743 (2014) 130
arXiv:1305.5199

127 plastic (CH) scintillator strips/plane

All photographs: Reidar Hahn, Fermilab visual media services

MINERvA detector

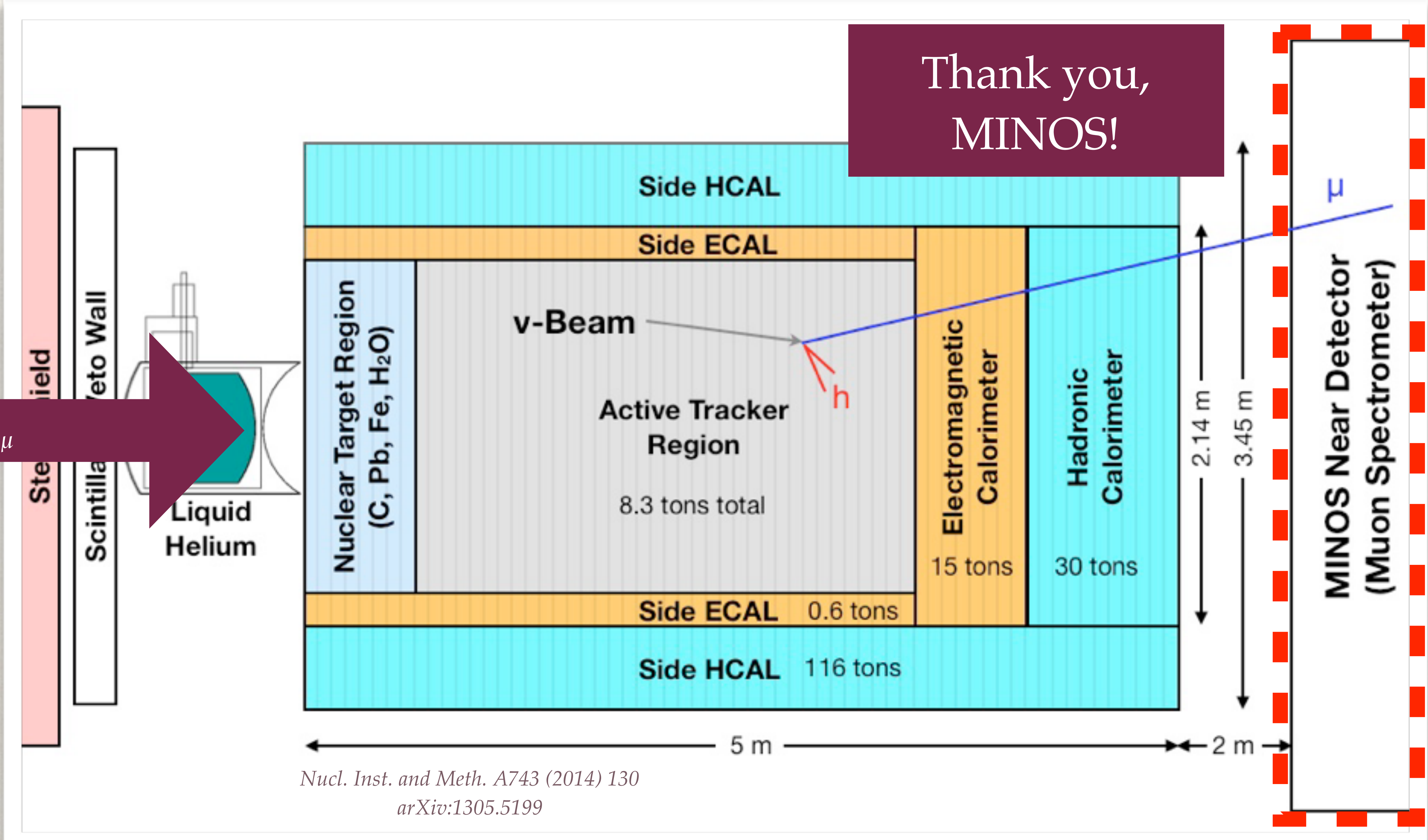

Nucl. Inst. and Meth. A743 (2014) 130
arXiv:1305.5199

All photographs: Reidar Hahn, Fermilab visual media services

Our generator, GENIE

- For this analysis, we use a tweaked GENIE 2.8.4 as our Monte Carlo generator
- Quasi-elastic scattering from nuclei is simulated using
  - Relativistic Fermi Gas model with Bodek-Ritchie tail
  - Axial mass M_A=0.99 GeV
  - Fermi momentum k_F=221MeV
  - BBBA05 model for vector form factors
  - RPA and 2p2h effects are not modeled
- We scale down the cross section for non-resonant pion production by 57% to match fits to bubble chamber data as detailed in arXiv:1601.01888
- We also re-scaled some of the standard uncertainties

WE TUNE GENIE TO MATCH OUR DATA

Thank you, GENIE developers!

CC0π in MINERvA antineutrinos

1) In our simulation, around 90% of CC0π events are true CCQE with no FSI, and they look like this

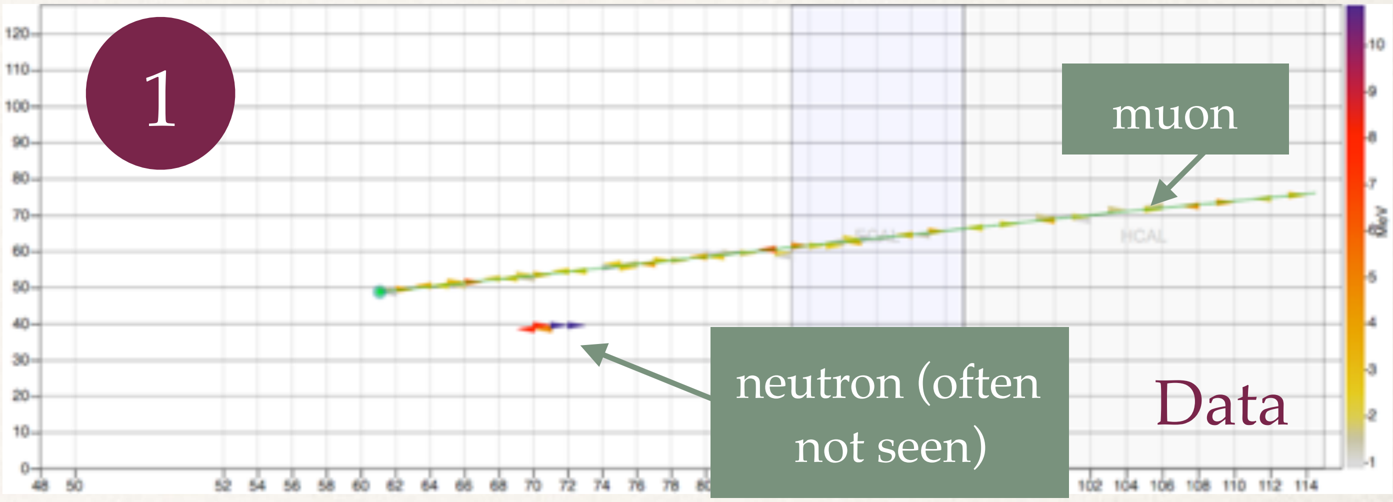

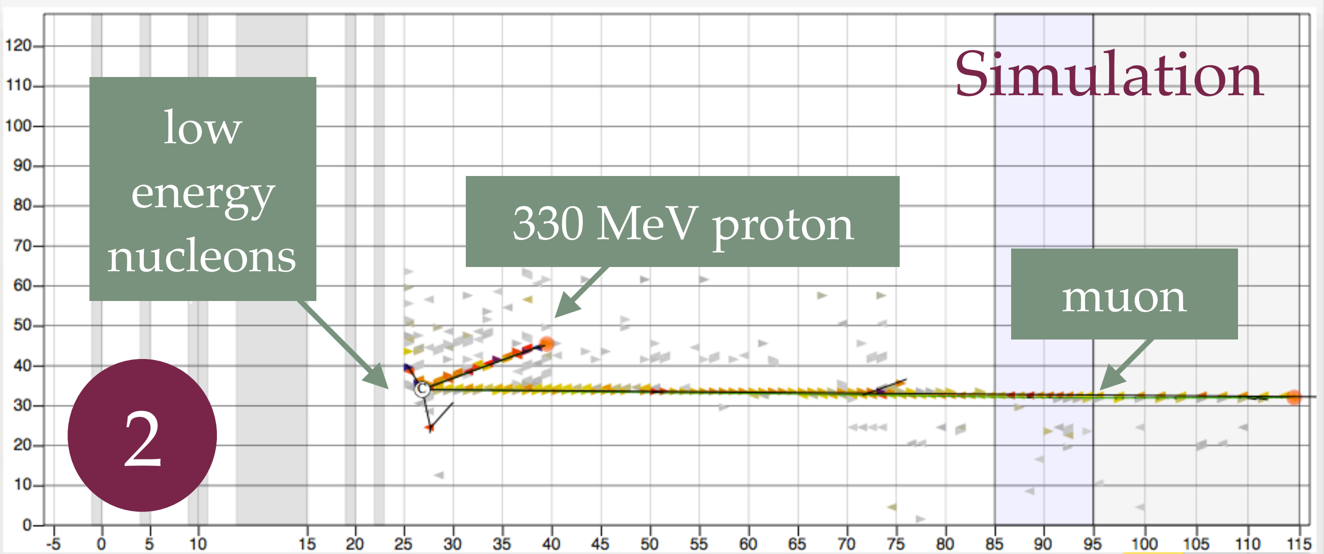

2) This resonant event with 2 neutrons and 4 protons in the final state is also CC0π, but the proton track makes it look very different

Reconstructions that can identify events like 1) with high purity have very poor efficiency when identifying events like 2)

Given what our detector can see, we must make choices about what to measure

Quasi-elastic-like for MINERvA $\bar{\nu}$

Bearing in mind MINERvA's capabilities, we define our QE-like final state signal to be:

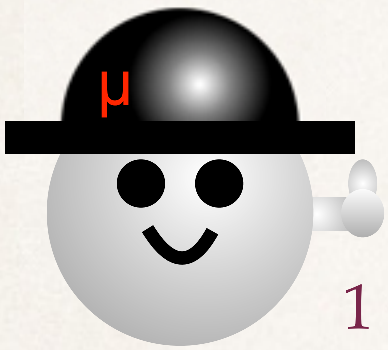

1 positive **muon**

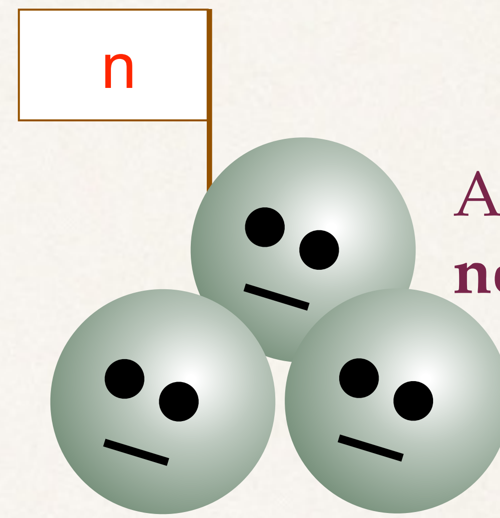

Any number of **neutrons**

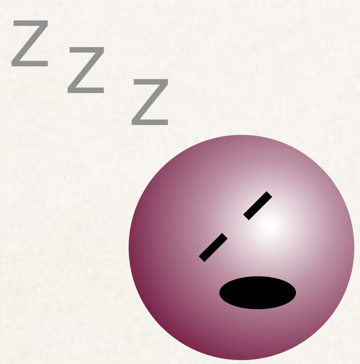

Only **low-energy protons** (below 120 MeV kinetic energy)

Additionally, we look only at events where the **muon's angle is less than 20°**; we have no acceptance at higher angles due to our reliance on the MINOS detector for muon charge and momentum measurement.

Event selection: tracks

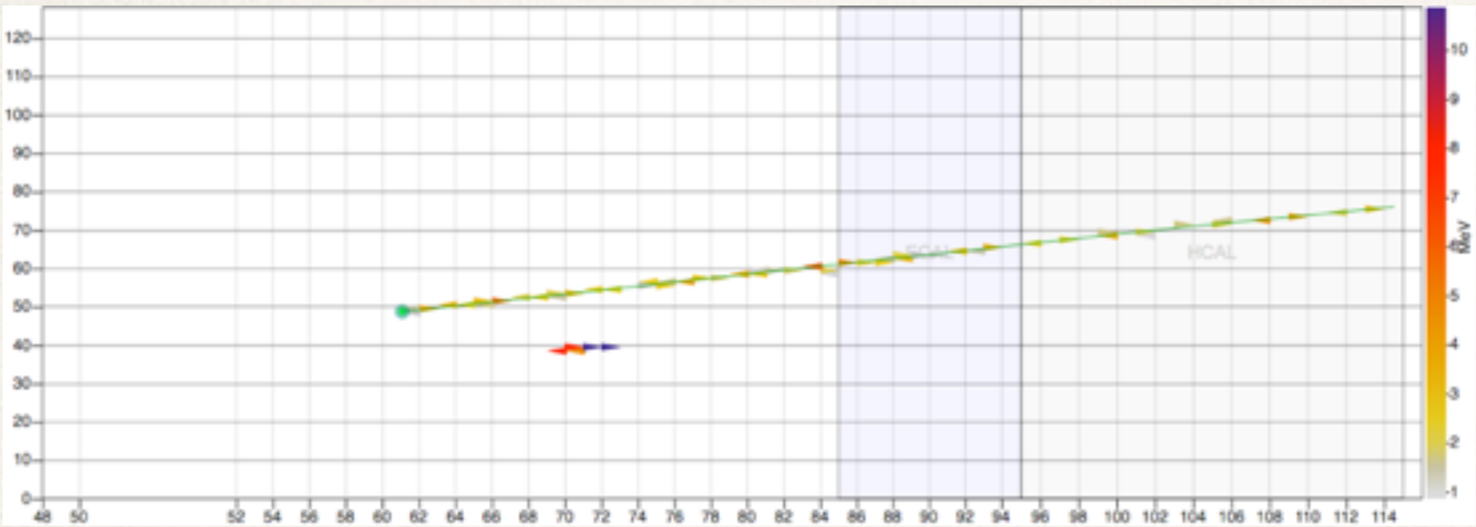

$$\bar{\nu}_\mu + p \to \mu^+ + n$$

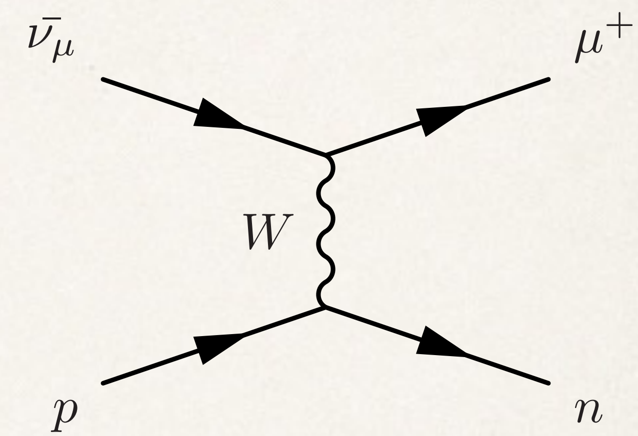

- Muon track charge matched in MINOS as a μ^+
- **No additional tracks from the vertex**
- The ejected neutron may scatter, leaving an energy deposit, but it does not make a track from the vertex
- Low-energy protons are allowed, but are below tracking threshold

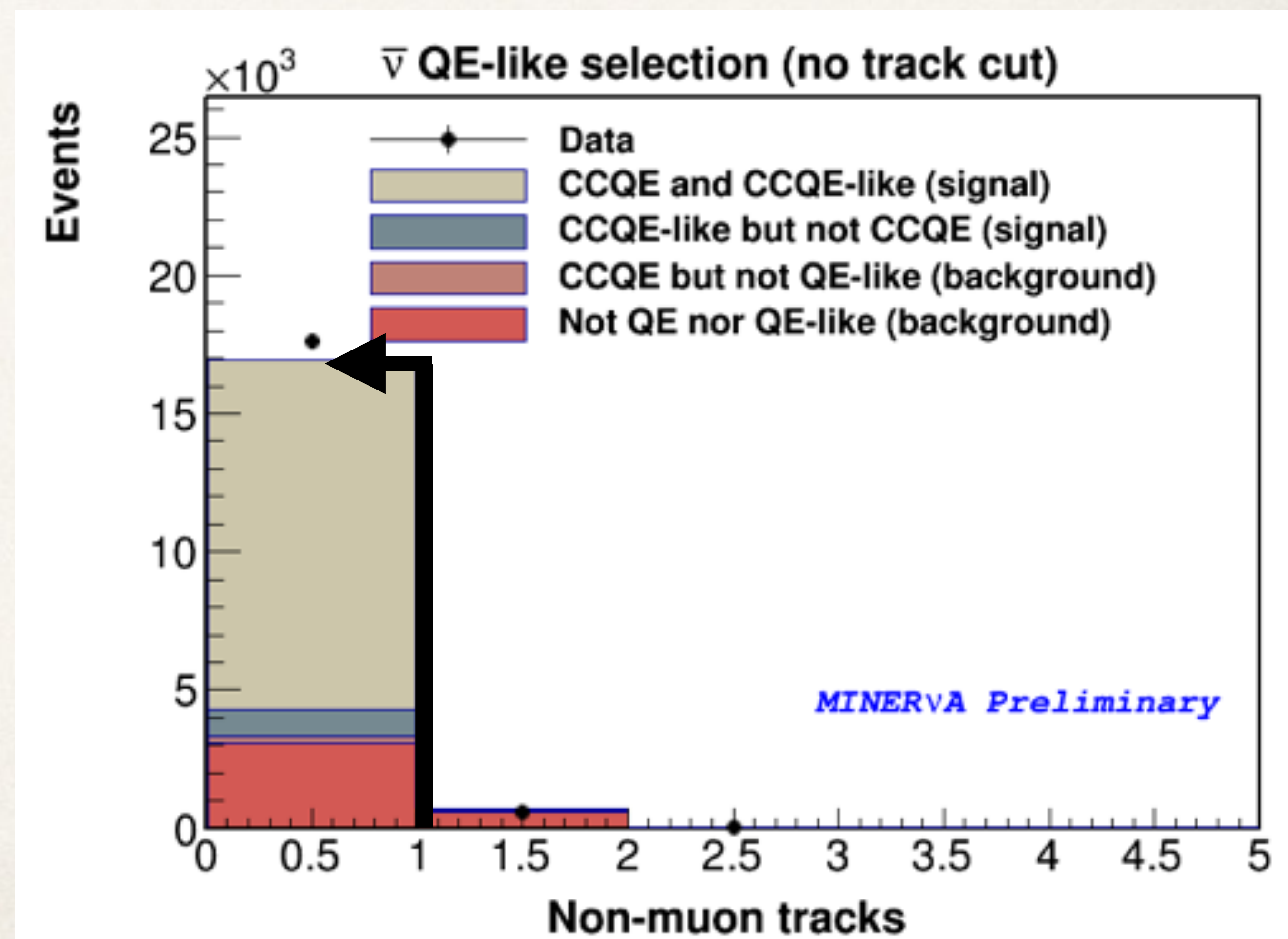

Event selection: recoil energy

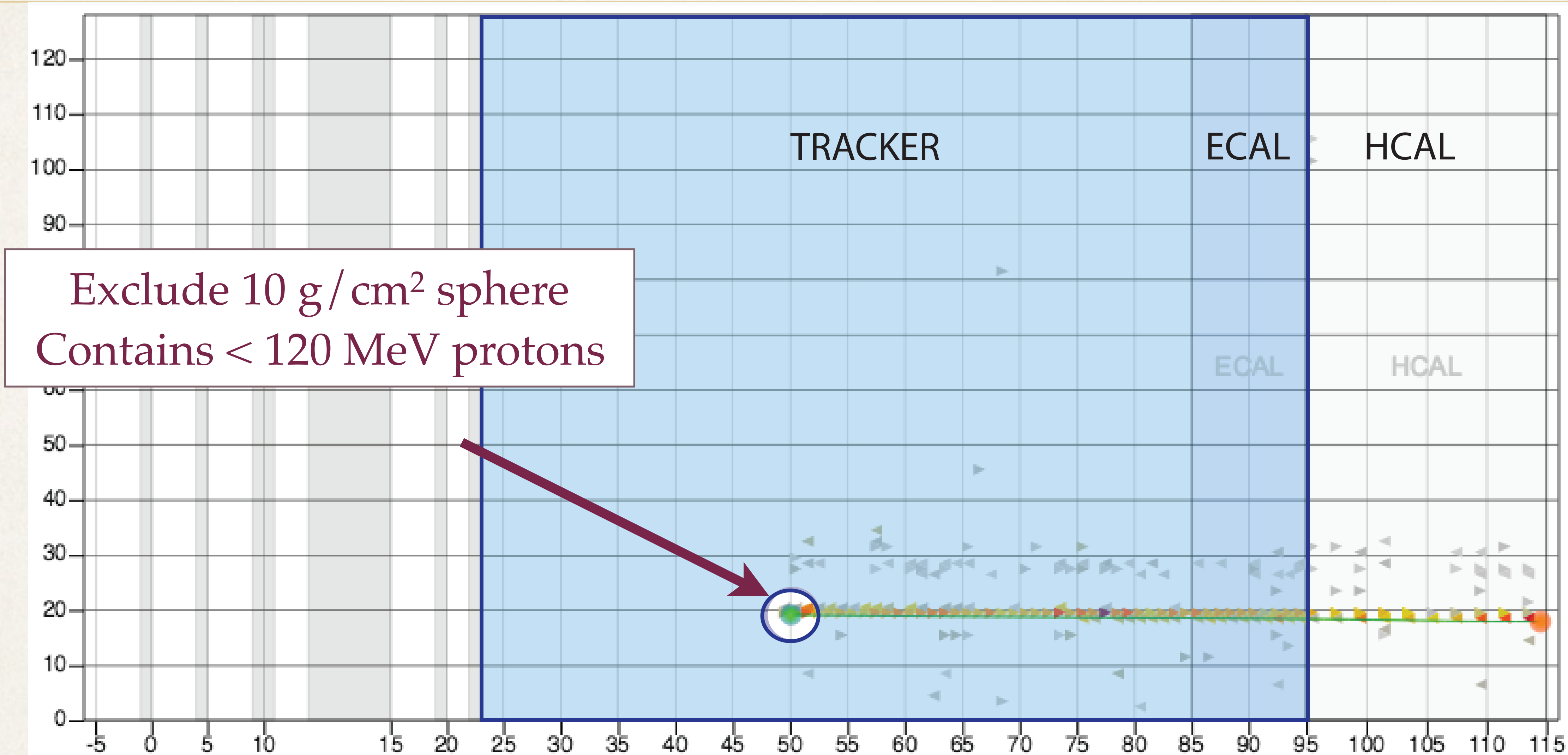

- Sum energy deposited in the recoil region (mostly from pions or protons)
- Exclude the **vertex region** where **extra low-energy nucleons** could come from CCQE scattering from correlated pairs
- We cannot track protons below this energy due to detector reconstruction limitations
- Signal and background distributions depend on Q^2: make a Q^2_{QE}-dependent recoil cut

Event selection: recoil energy

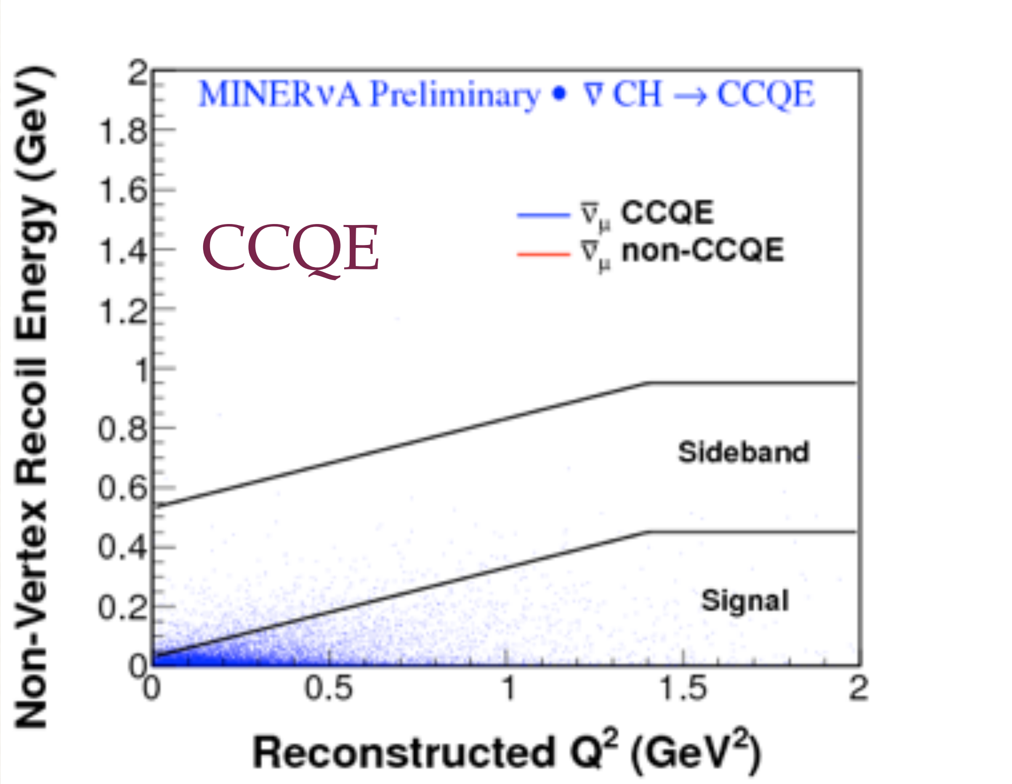

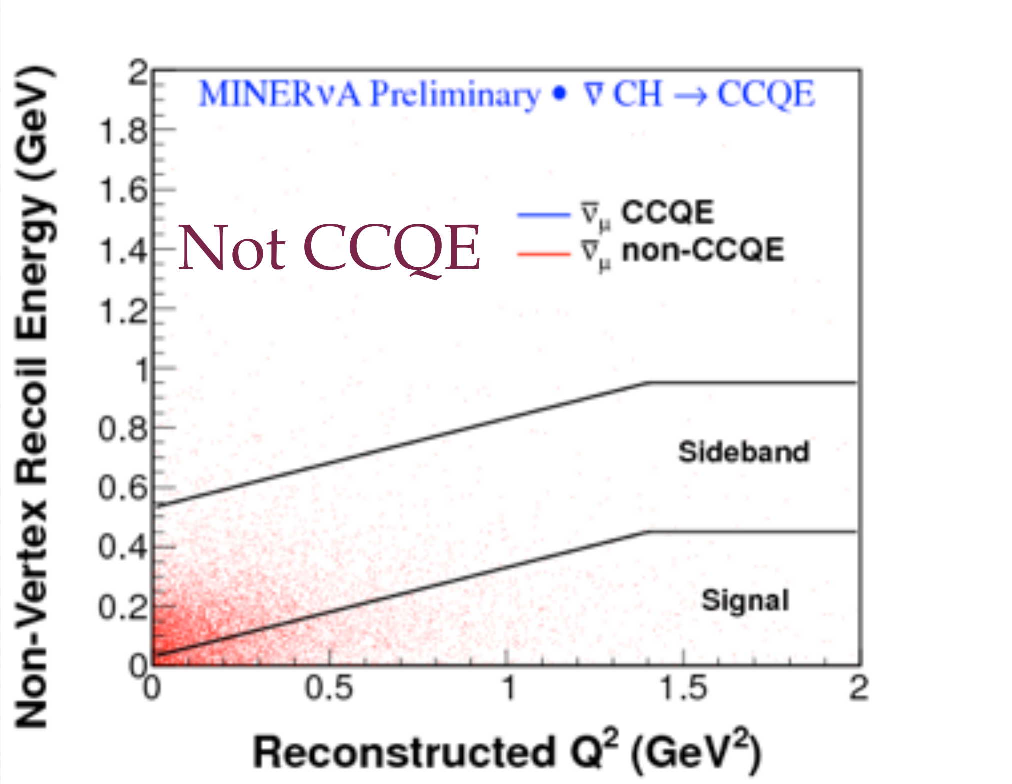

- This cut optimizes efficiency times purity for true CCQE events
- But it does a poor job (17% efficiency) of accepting CC0π events that are not CCQE
- We can improve efficiency by relaxing the cut at low Q^2, but will sacrifice purity

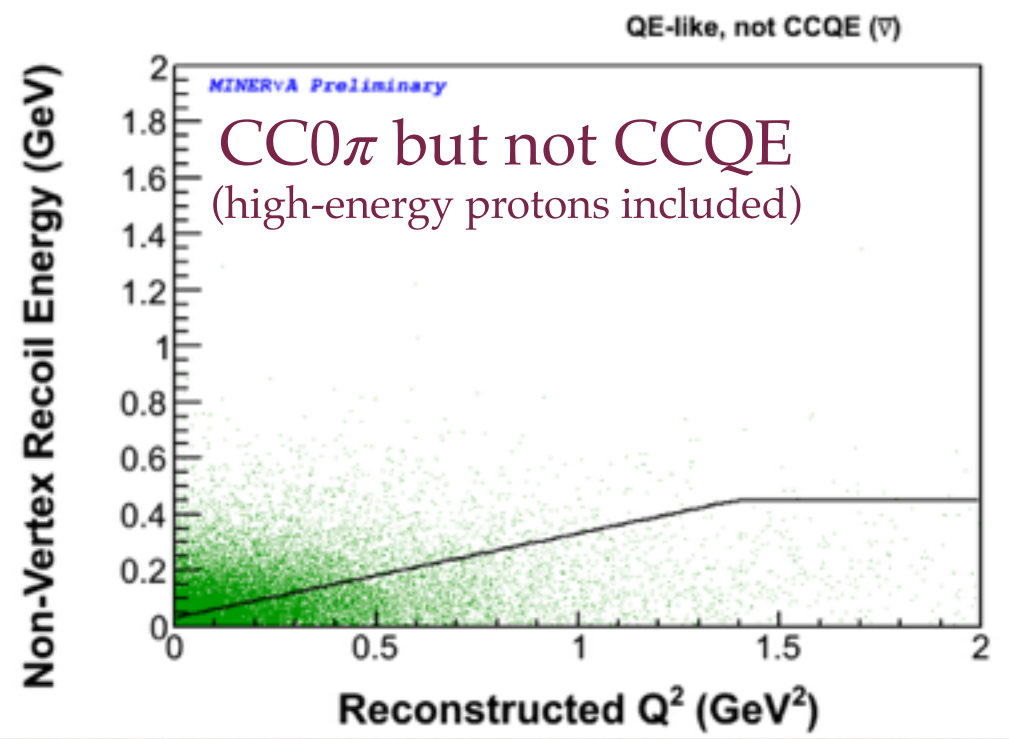

Event selection: recoil energy

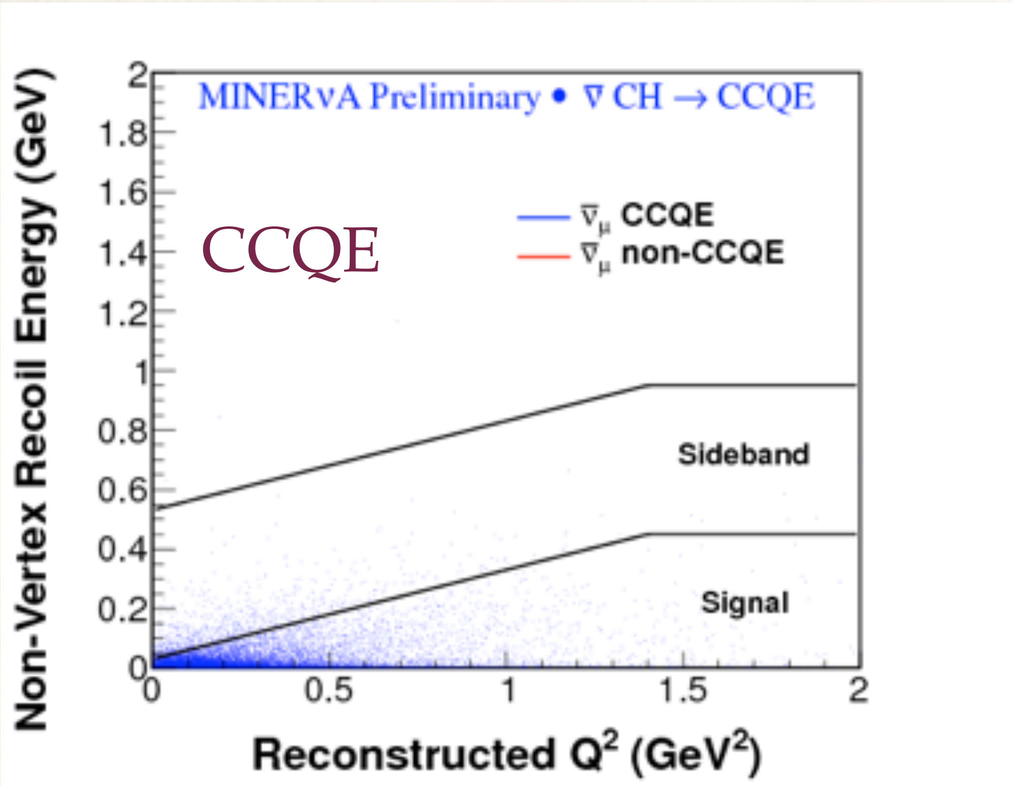

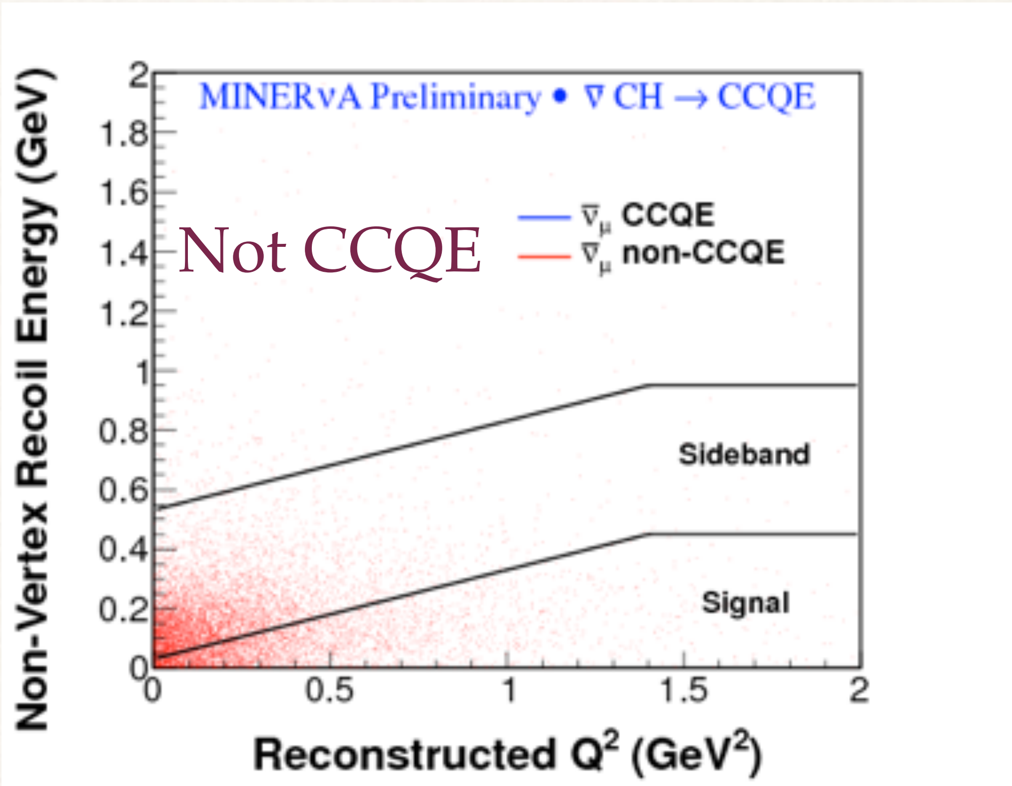

- This cut optimizes efficiency times purity for true CCQE events
- But it does a poor job (17% efficiency) of accepting CC0π events that are not CCQE
- We can improve efficiency by relaxing the cut at low Q^2, but will sacrifice purity

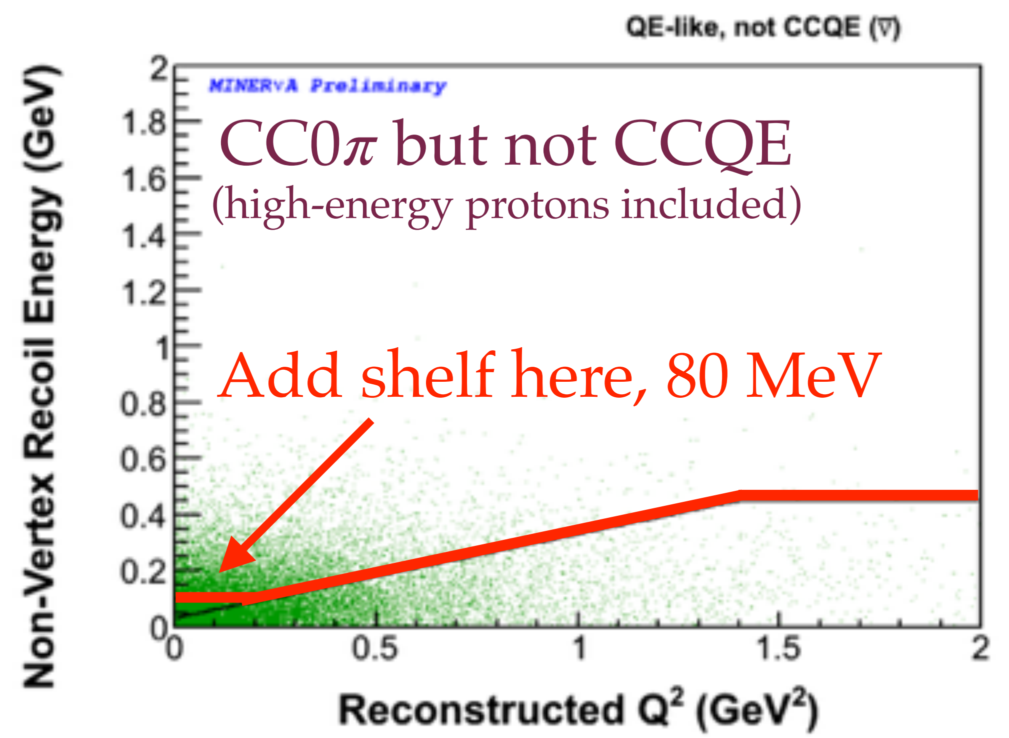

A double differential cross section

We measure a **double differential** cross section, to see how the interaction probability varies in two dimensions. We look at two pairs of variables:

Muon transverse/longitudinal momentum

- Muon p_T and $p_\parallel$ are measurable quantities
- Good phase space coverage

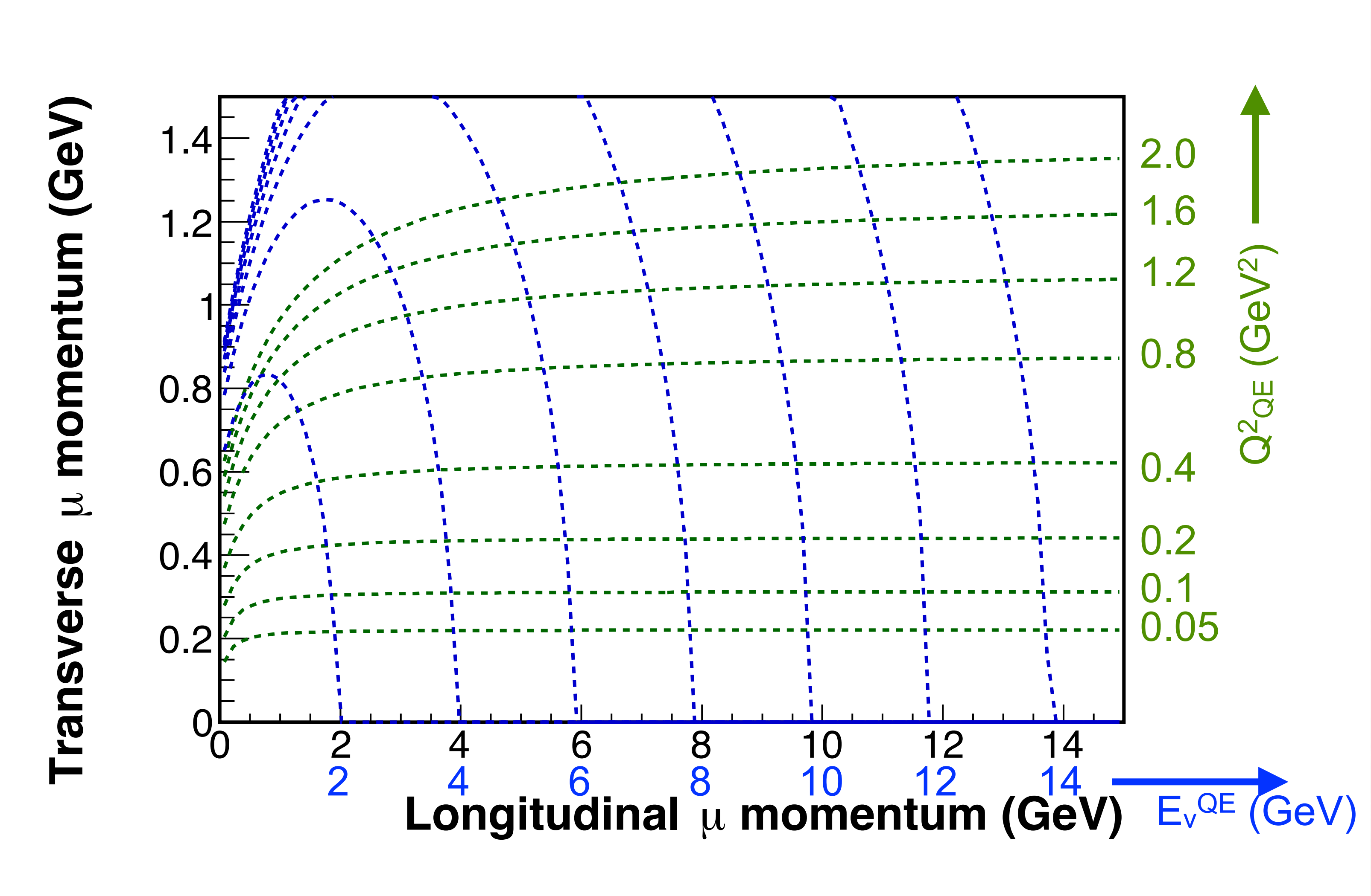

Q^2_{QE} vs. E_ν^{QE}

- Reconstruct from muon kinematics
- Many nuclear effects' strengths depend on squared four-momentum transfer Q^2
- As our neutrino flux is energy-dependent, we can use this to plot flux-weighted cross section vs energy (with caveats)

$$Q^2_{QE} = 2E_\nu^{QE}(E_\mu - p_\mu \cos\theta_\mu) - m_\mu^2$$

$$E_\nu^{QE} = \frac{m_n^2 - (m_p - E_b)^2 - m_\mu^2 + 2(m_p - E_b)E_\mu}{2(m_p - E_b - E_\mu + p_\mu \cos\theta_\mu)}$$

$Q^2_{QE} \sim p_T$

$E_\nu \sim p_\parallel$

Calculating the cross section

To generate a double differential cross section d²σ/dx dy in true bins *(i,j)*, from a reconstructed event count distribution in bins *(α,β)*:

$$\left(\frac{d^2\sigma}{dx\,dy}\right)_{ij} = \frac{\sum_{\alpha\beta} U_{\alpha\beta ij}(N_{\mathrm{data},\alpha\beta} - N^{bkgd}_{\mathrm{data},\alpha\beta})}{\epsilon_{ij}(\Phi T)(\Delta x_i)(\Delta y_j)}$$

Calculating the cross section

To generate a double differential cross section $d^2\sigma/dx\,dy$ in true bins *(i,j)*, from a reconstructed event count distribution in bins *(α,β)*:

$$\left(\frac{d^2\sigma}{dx\,dy}\right)_{ij} = \frac{\sum_{\alpha\beta} U_{\alpha\beta ij}(N_{\mathrm{data},\alpha\beta} - N^{bkgd}_{\mathrm{data},\alpha\beta})}{\epsilon_{ij}(\Phi T)(\Delta x_i)(\Delta y_j)}$$

1. Plot the **reconstructed event distribution** with selection cuts

Calculating the cross section

To generate a double differential cross section $d^2\sigma/dx\,dy$ in true bins *(i,j)*, from a reconstructed event count distribution in bins *(α,β)*:

$$\left(\frac{d^2\sigma}{dx\,dy}\right)_{ij} = \frac{\sum_{\alpha\beta} U_{\alpha\beta ij}(N_{\mathrm{data},\alpha\beta} - N^{bkgd}_{\mathrm{data},\alpha\beta})}{\epsilon_{ij}(\Phi T)(\Delta x_i)(\Delta y_j)}$$

1. Plot the **reconstructed event distribution** with selection cuts
2. Subtract **backgrounds**

Calculating the cross section

To generate a double differential cross section $d^2\sigma/dx\,dy$ in true bins *(i,j)*, from a reconstructed event count distribution in bins *(α,β)*:

$$\left(\frac{d^2\sigma}{dx\,dy}\right)_{ij} = \frac{\sum_{\alpha\beta} U_{\alpha\beta ij}(N_{\text{data},\alpha\beta} - N^{bkgd}_{\text{data},\alpha\beta})}{\epsilon_{ij}(\Phi T)(\Delta x_i)(\Delta y_j)}$$

1. Plot the **reconstructed event distribution** with selection cuts
2. Subtract **backgrounds**
3. **Unfold** data to move events from reconstructed to true bins

Calculating the cross section

To generate a double differential cross section $d^2\sigma/dx\,dy$ in true bins *(i,j)*, from a reconstructed event count distribution in bins *(α,β)*:

$$\left(\frac{d^2\sigma}{dx\,dy}\right)_{ij} = \frac{\sum_{\alpha\beta} U_{\alpha\beta ij}(N_{\text{data},\alpha\beta} - N^{bkgd}_{\text{data},\alpha\beta})}{\epsilon_{ij}(\Phi T)(\Delta x_i)(\Delta y_j)}$$

1. Plot the **reconstructed event distribution** with selection cuts
2. Subtract **backgrounds**
3. **Unfold** data to move events from reconstructed to true bins
4. Correct for **efficiency** and acceptance

Calculating the cross section

To generate a double differential cross section $d^2\sigma/dx\,dy$ in true bins *(i,j)*, from a reconstructed event count distribution in bins *(α,β)*:

$$\left(\frac{d^2\sigma}{dx\,dy}\right)_{ij} = \frac{\sum_{\alpha\beta} U_{\alpha\beta ij}(N_{\text{data},\alpha\beta} - N^{bkgd}_{\text{data},\alpha\beta})}{\epsilon_{ij}(\Phi T)(\Delta x_i)(\Delta y_j)}$$

1. Plot the **reconstructed event distribution** with selection cuts
2. Subtract **backgrounds**
3. **Unfold** data to move events from reconstructed to true bins
4. Correct for **efficiency** and acceptance
5. Divide by neutrino **flux** and number of **targets**

Calculating the cross section

To generate a double differential cross section $d^2\sigma/dx\,dy$ in true bins *(i,j)*, from a reconstructed event count distribution in bins *(α,β)*:

$$\left(\frac{d^2\sigma}{dx\,dy}\right)_{ij} = \frac{\sum_{\alpha\beta} U_{\alpha\beta ij}(N_{\text{data},\alpha\beta} - N^{bkgd}_{\text{data},\alpha\beta})}{\epsilon_{ij}(\Phi T)(\Delta x_i)(\Delta y_j)}$$

1. Plot the **reconstructed event distribution** with selection cuts
2. Subtract **backgrounds**
3. **Unfold** data to move events from reconstructed to true bins
4. Correct for **efficiency** and acceptance
5. Divide by neutrino **flux** and number of **targets**
6. Present **bin-width normalized**

Signal and backgrounds after cuts

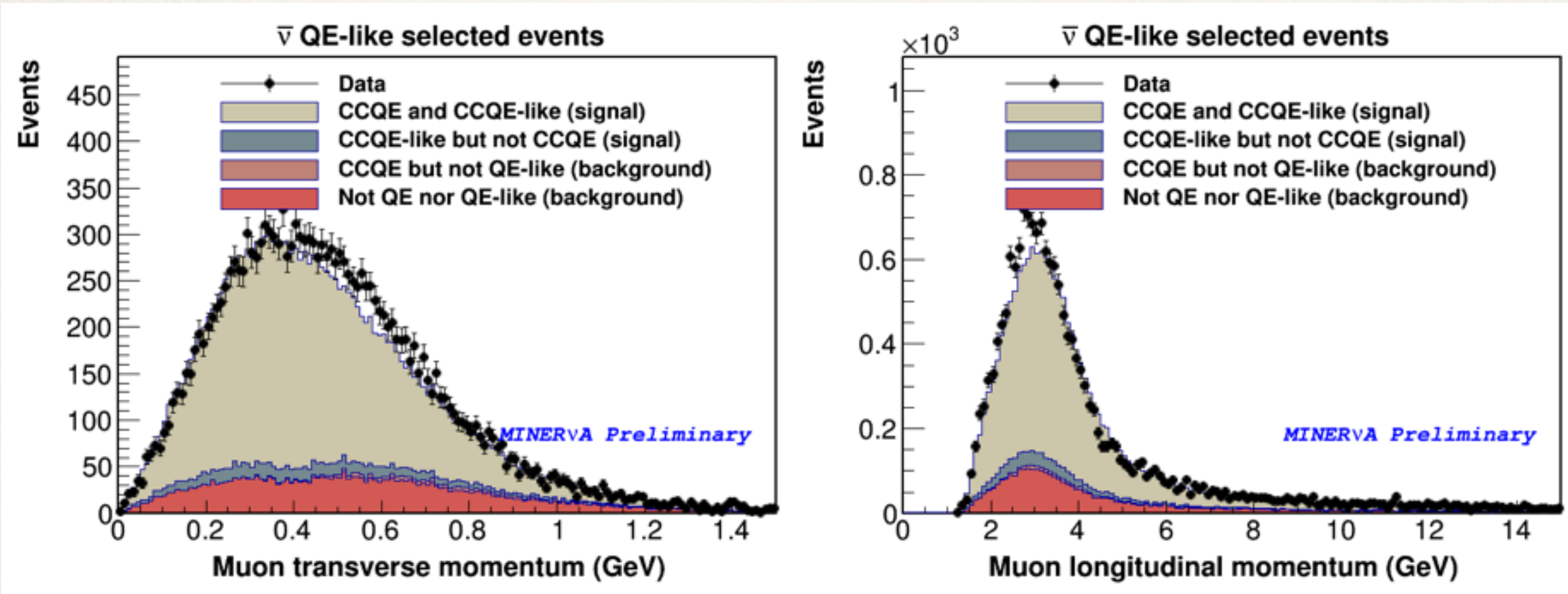

- QE-like signal events include
  - CCQE events with a quasi-elastic-like signature
  - CCQE-like events that originated as resonant or DIS, with an absorbed pion
- Residual backgrounds include
  - CCQE events with pions in the final state
  - Resonant and DIS background

Next step: background subtraction

Fitting our backgrounds

$$\left(\frac{d^2\sigma}{dx\,dy}\right)_{ij} = \frac{\sum_{\alpha\beta} U_{\alpha\beta ij}(N_{\text{data},\alpha\beta} - N^{bkgd}_{\text{data},\alpha\beta})}{\epsilon_{ij}(\Phi T)(\Delta x_i)(\Delta y_j)}$$

We use data to estimate our backgrounds by performing a **fraction fit** of simulated signal and background **recoil energy distribution shapes** from our Monte Carlo, in each of 5 larger $p_T/p_\parallel$ bins

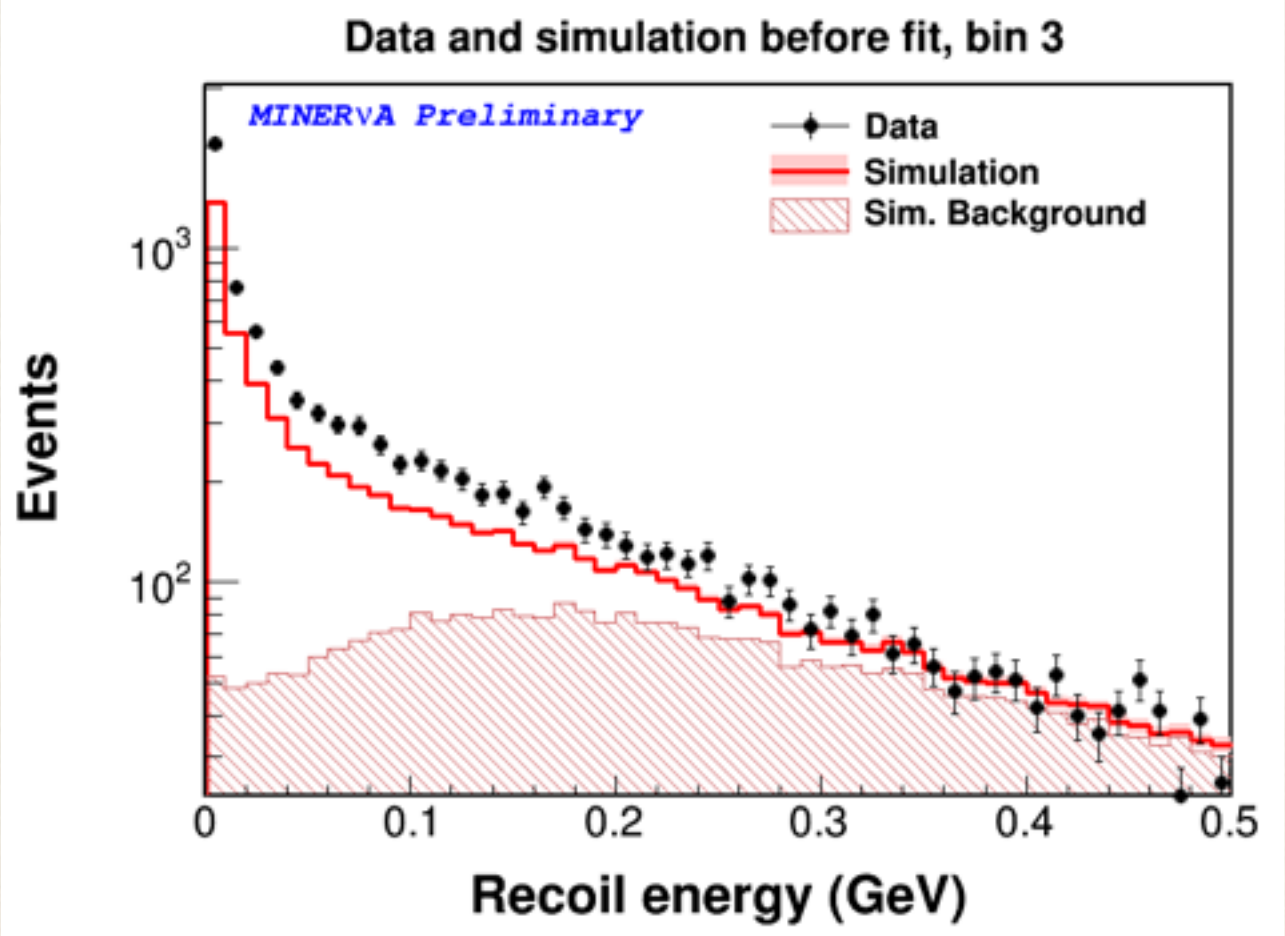

Recoil distribution in one bin before…

Fitting our backgrounds

$$\left(\frac{d^2\sigma}{dx\,dy}\right)_{ij} = \frac{\sum_{\alpha\beta} U_{\alpha\beta ij}(N_{\text{data},\alpha\beta} - N^{bkgd}_{\text{data},\alpha\beta})}{\epsilon_{ij}(\Phi T)(\Delta x_i)(\Delta y_j)}$$

We use data to estimate our backgrounds by performing a **fraction fit** of simulated signal and background **recoil energy distribution shapes** from our Monte Carlo, in each of 5 larger $p_T/p_{\parallel}$ bins

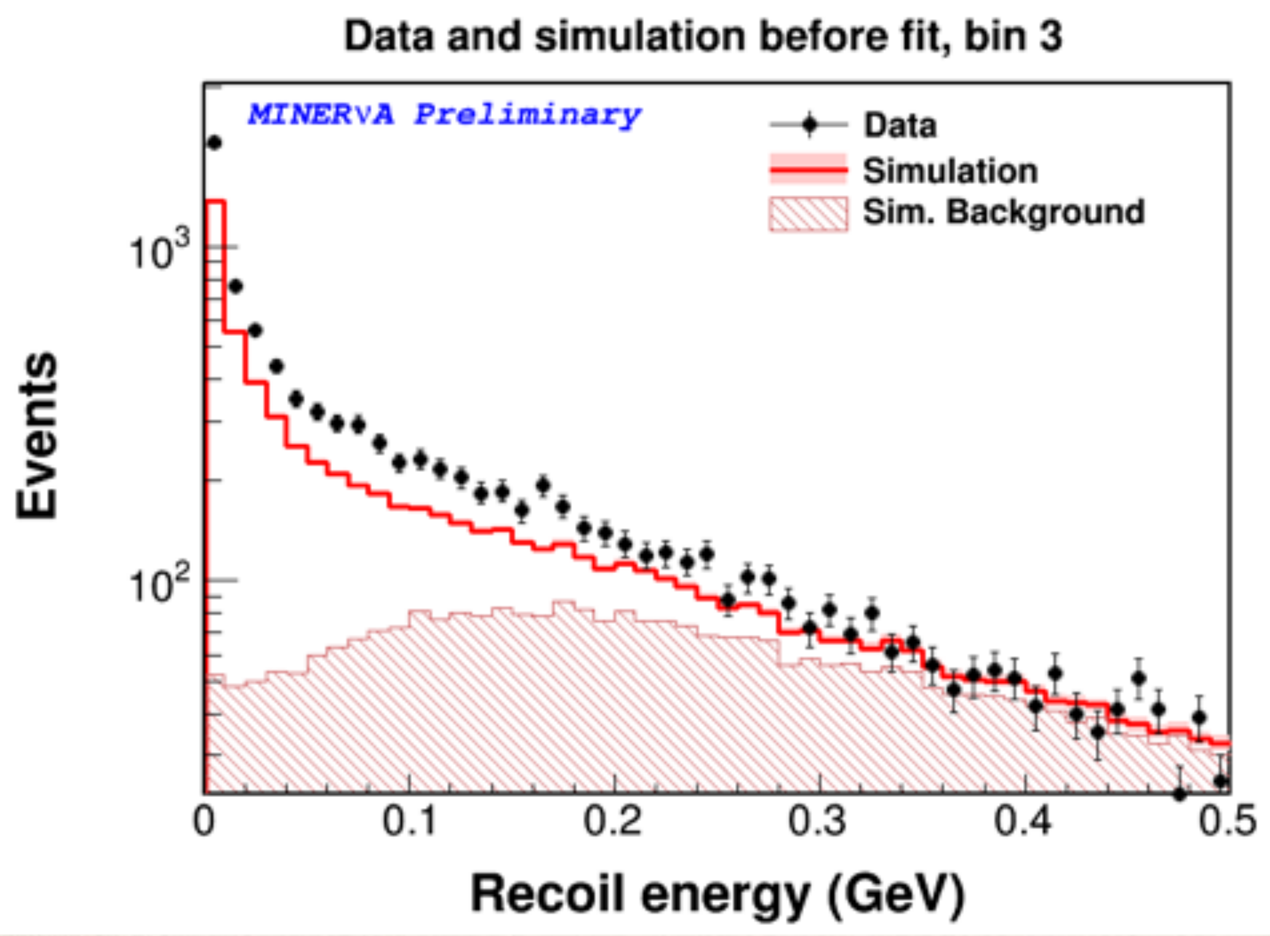

Recoil distribution in one bin before…

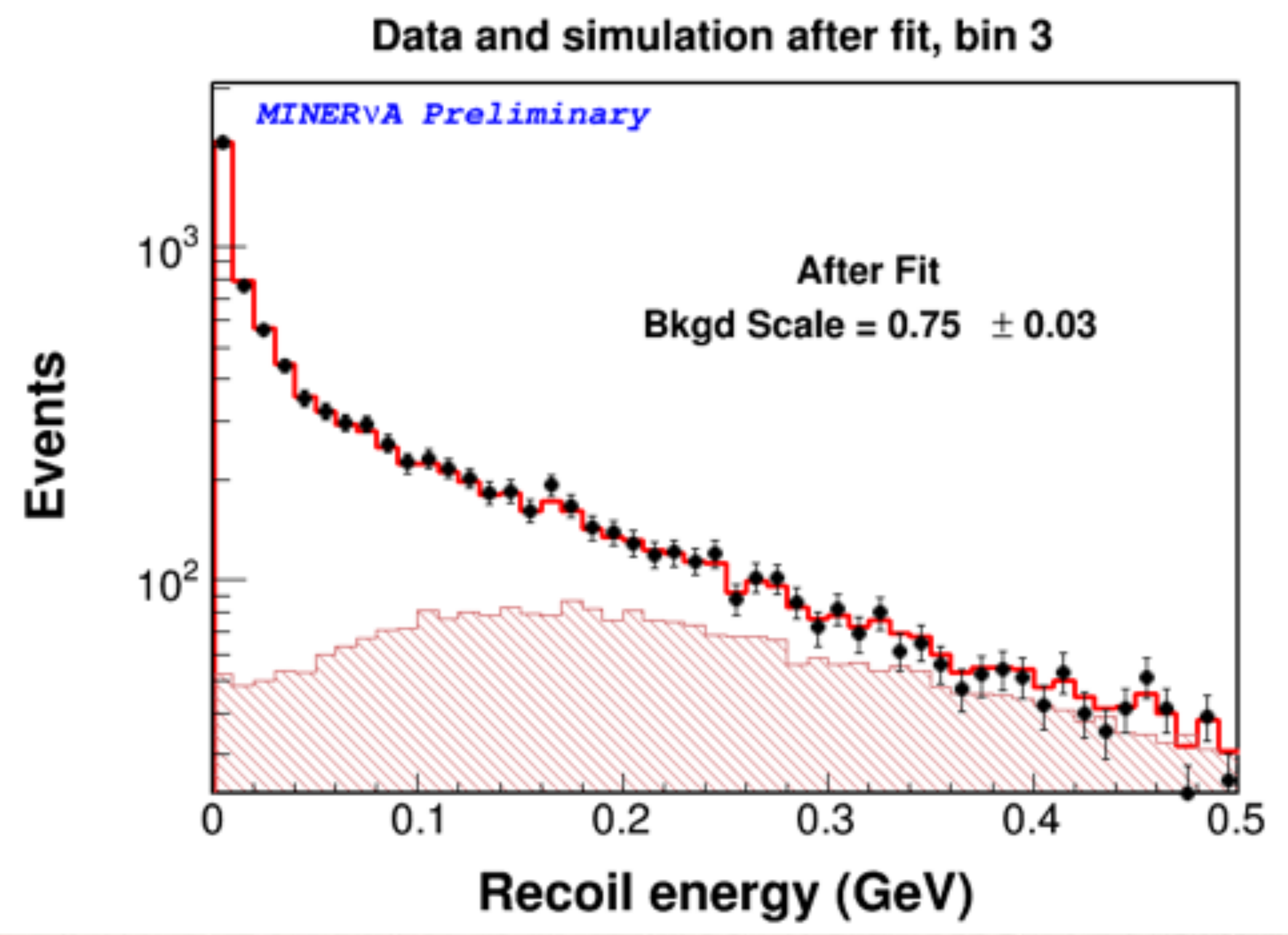

…and after fitting signal and background fractions

Fitting our backgrounds

$$\left(\frac{d^2\sigma}{dx\,dy}\right)_{ij} = \frac{\sum_{\alpha\beta} U_{\alpha\beta ij}\left(N_{\text{data},\alpha\beta} - N^{bkgd}_{\text{data},\alpha\beta}\right)}{\epsilon_{ij}(\Phi T)(\Delta x_i)(\Delta y_j)}$$

When we subtract our backgrounds, we subtract the background fraction extracted from the signal region of the simulation, scaled by the parameter extracted from the fit

This scale shows what the background fraction was multiplied by to get the best fit to data

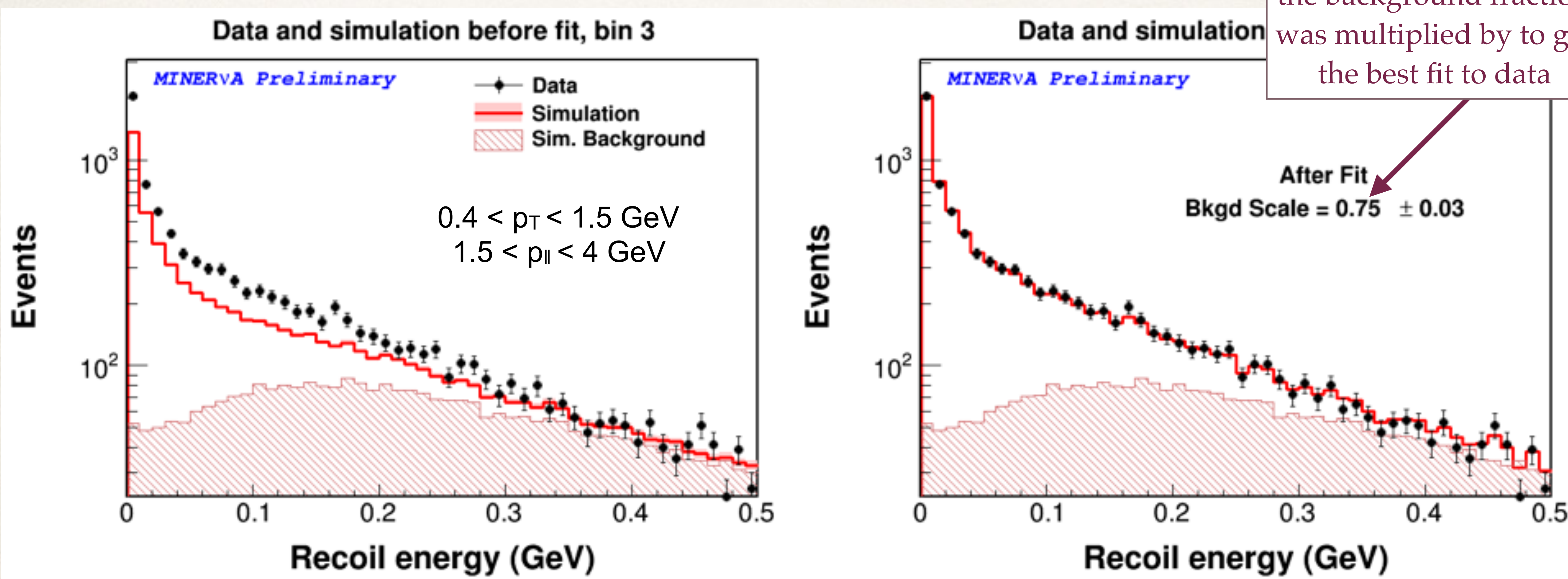

Recoil distribution in one bin before…

…and after fitting signal and background fractions

Fitting our backgrounds

$$\left(\frac{d^2\sigma}{dx\,dy}\right)_{ij} = \frac{\sum_{\alpha\beta} U_{\alpha\beta ij}\left(N_{\mathrm{data},\alpha\beta} - N^{bkgd}_{\mathrm{data},\alpha\beta}\right)}{\epsilon_{ij}(\Phi T)(\Delta x_i)(\Delta y_j)}$$

When we subtract our backgrounds, we subtract the background fraction extracted from the signal region of the simulation, scaled by the parameter extracted from the fit

This scale shows what the background fraction was multiplied by to get the best fit to data

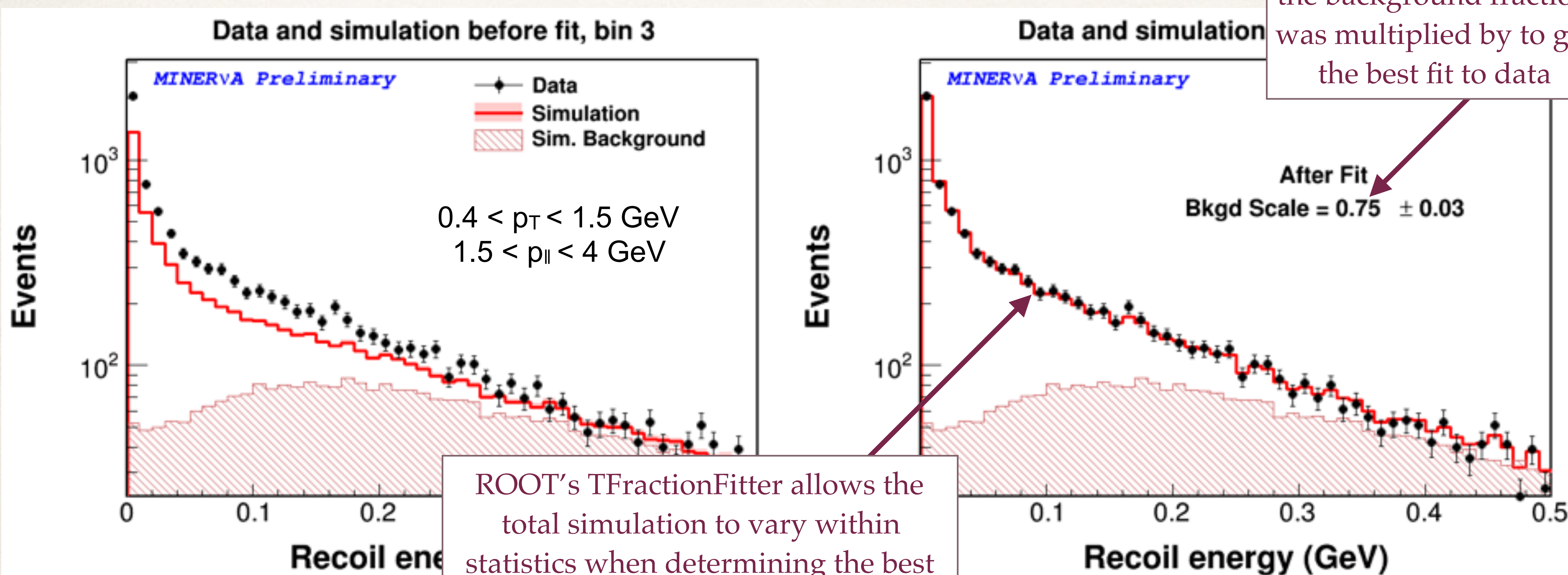

ROOT's TFractionFitter allows the total simulation to vary within statistics when determining the best fit. This makes the fitted simulation appear to be a closer fit to data than the best-fit scaled signal and background would generate

Recoil distribution in one ... and after fitting signal and ...ckground fractions

Background scales

$$\left(\frac{d^2\sigma}{dx\,dy}\right)_{ij} = \frac{\sum_{\alpha\beta} U_{\alpha\beta ij}(N_{\text{data},\alpha\beta} - N^{bkgd}_{\text{data},\alpha\beta})}{\epsilon_{ij}(\Phi T)(\Delta x_i)(\Delta y_j)}$$

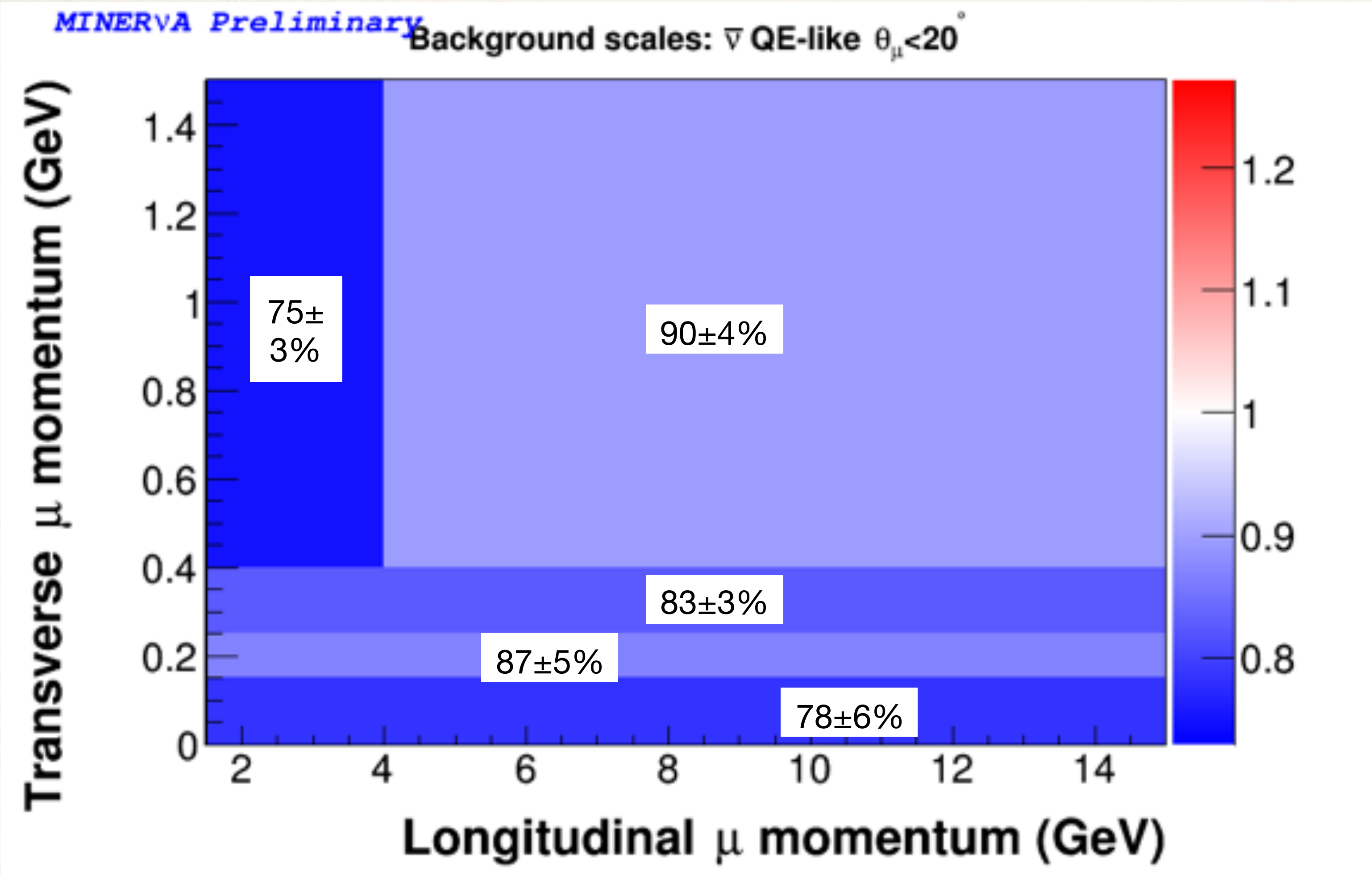

When we subtract our backgrounds, we **subtract the background fraction** extracted from the simulated signal region of recoil, where the background fraction is **scaled** by these extracted scale factors

As seen in other MINERvA studies, GENIE **over-predicts** the (mostly resonant) background by about 10%

Next step: unfolding

Unfolding

$$\left(\frac{d^2\sigma}{dx\,dy}\right)_{ij} = \frac{\sum_{\alpha\beta} U_{\alpha\beta ij}(N_{\mathrm{data},\alpha\beta} - N^{bkgd}_{\mathrm{data},\alpha\beta})}{\epsilon_{ij}(\Phi T)(\Delta x_i)(\Delta y_j)}$$

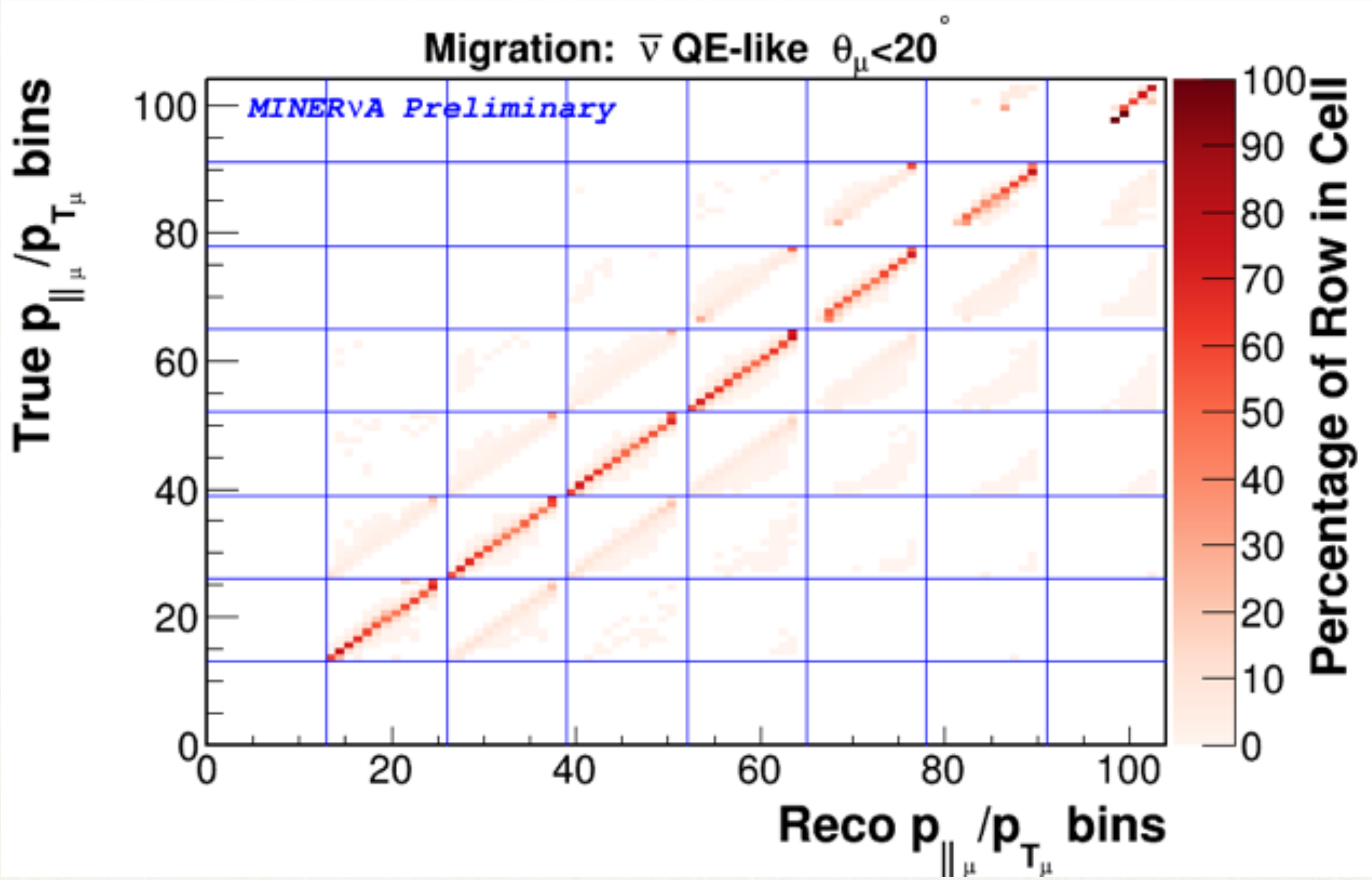

Next step: efficiency correction

Unfolding

$$\left(\frac{d^2\sigma}{dx\,dy}\right)_{ij} = \frac{\sum_{\alpha\beta} U_{\alpha\beta ij}(N_{\mathrm{data},\alpha\beta} - N^{bkgd}_{\mathrm{data},\alpha\beta})}{\epsilon_{ij}(\Phi T)(\Delta x_i)(\Delta y_j)}$$

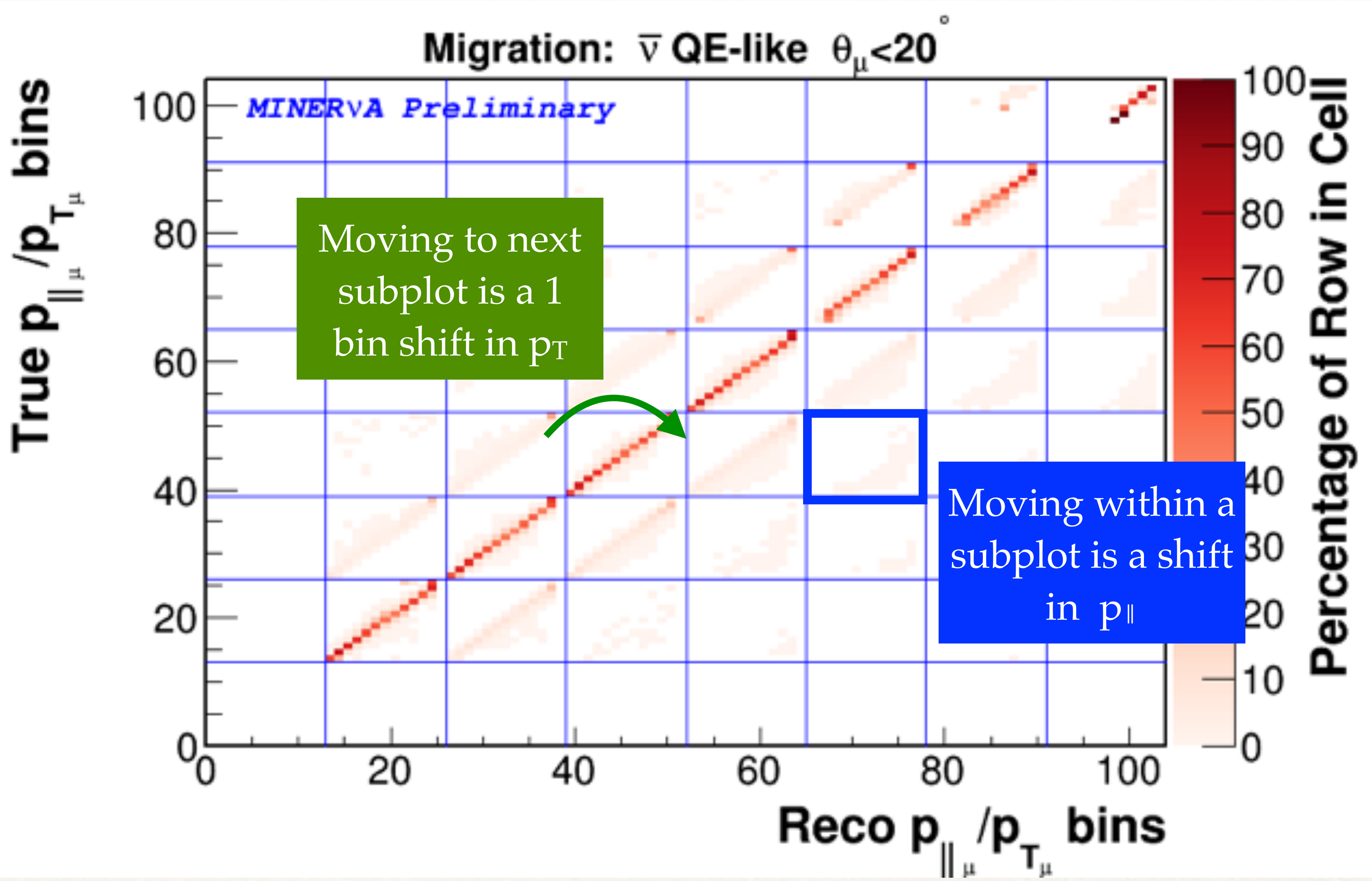

Next step: efficiency correction

Unfolding

$$\left(\frac{d^2\sigma}{dx\,dy}\right)_{ij} = \frac{\sum_{\alpha\beta} U_{\alpha\beta ij}(N_{\text{data},\alpha\beta} - N^{bkgd}_{\text{data},\alpha\beta})}{\epsilon_{ij}(\Phi T)(\Delta x_i)(\Delta y_j)}$$

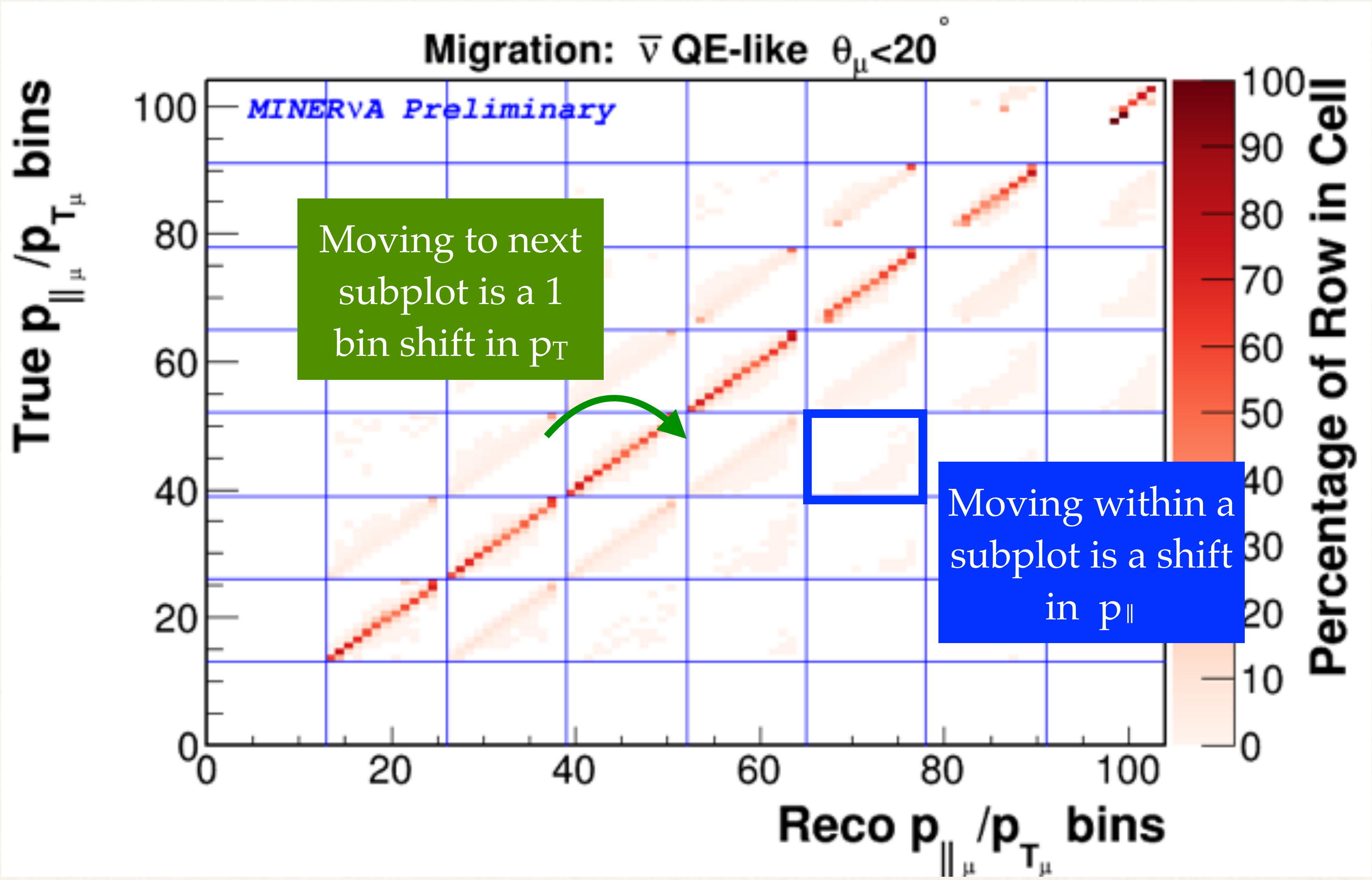

- We use four iterations of a Bayesian unfolding method to correct for events reconstructed in the wrong bin
- Note: our true Q^2_{QE} and E_ν^{QE} refer to Q^2 and E_ν as constructed from true muon kinematics in the CCQE hypothesis, NOT to the actual 4-momentum transfer squared and neutrino energy

Next step: efficiency correction

Efficiency & acceptance

$$\left(\frac{d^2\sigma}{dx\,dy}\right)_{ij} = \frac{\sum_{\alpha\beta} U_{\alpha\beta ij}(N_{\mathrm{data},\alpha\beta} - N^{bkgd}_{\mathrm{data},\alpha\beta})}{\epsilon_{ij}(\Phi T)(\Delta x_i)(\Delta y_j)}$$

MINOS match requirement limits acceptance at high angles

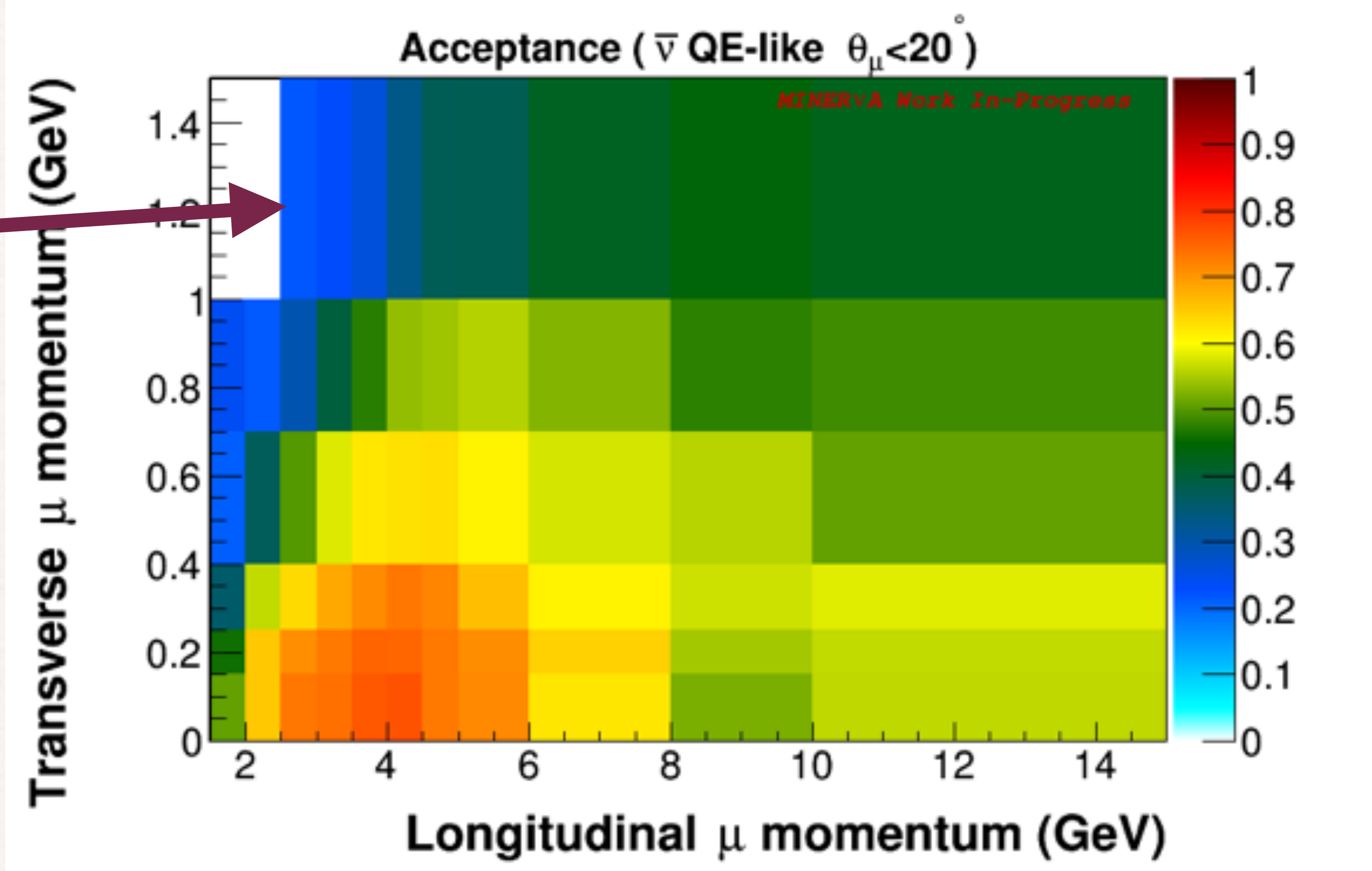

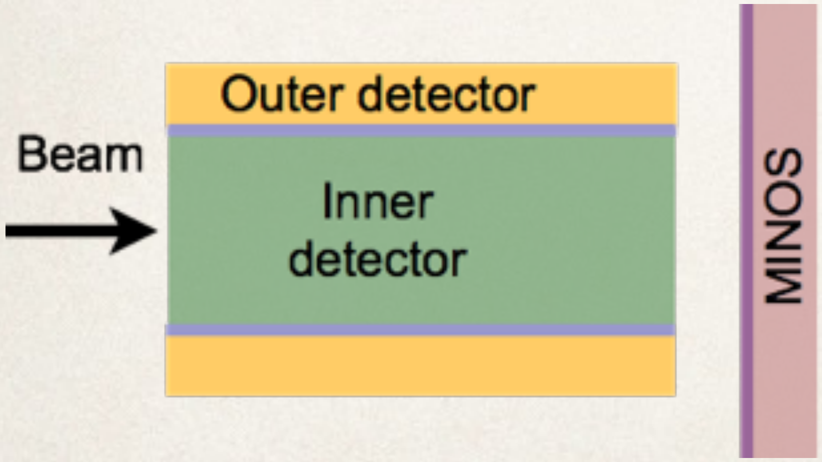

- We use simulation to correct for the fraction of events we fail to reconstruct due to
  - detector acceptance
  - reconstruction efficiency
- Our total acceptance x efficiency is **54%**

Neutrino flux

$$\left(\frac{d^2\sigma}{dx\,dy}\right)_{ij} = \frac{\sum_{\alpha\beta} U_{\alpha\beta ij}(N_{\mathrm{data},\alpha\beta} - N^{bkgd}_{\mathrm{data},\alpha\beta})}{\epsilon_{ij}(\Phi T)(\Delta x_i)(\Delta y_j)}$$

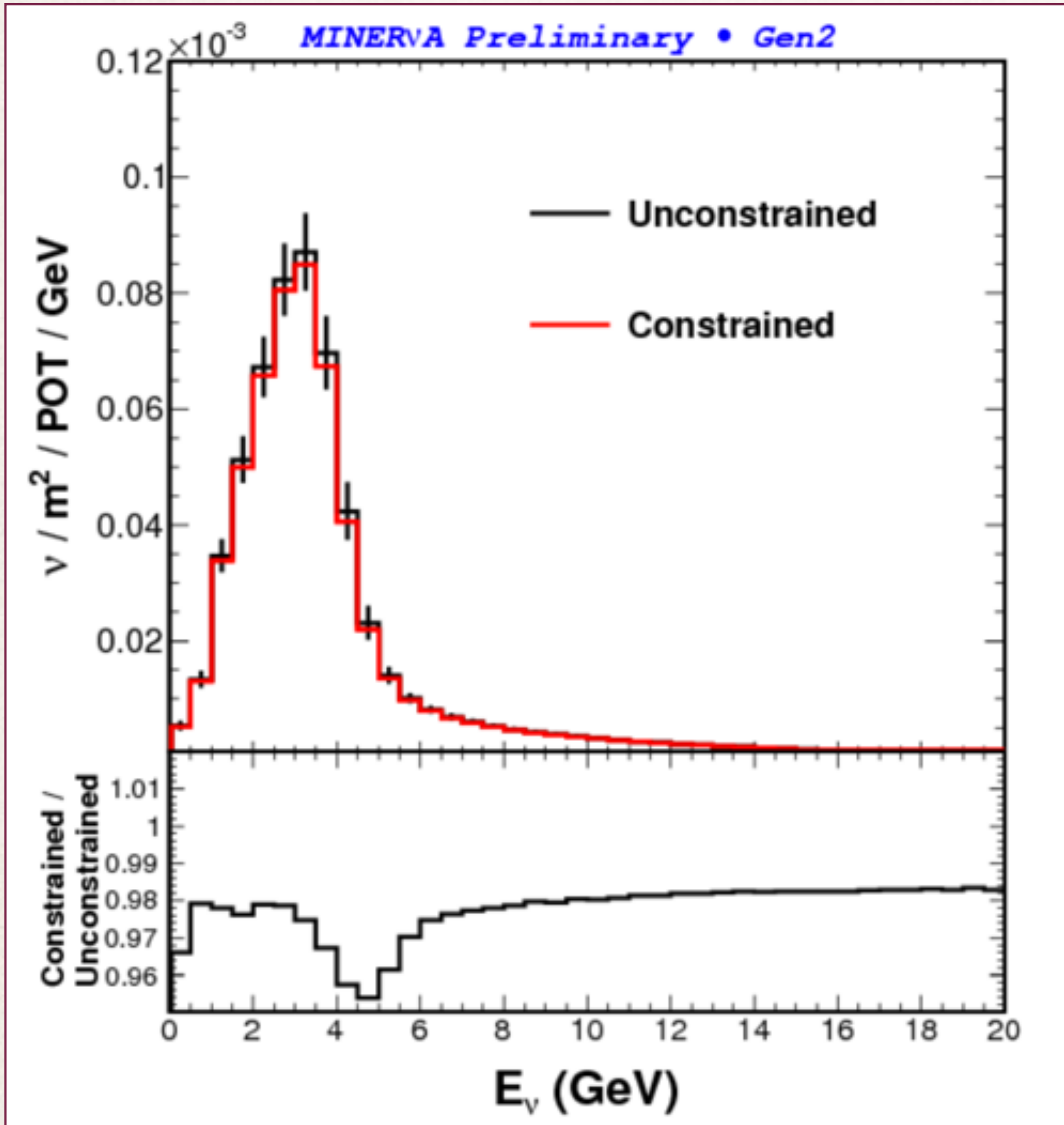

We divide by the **integrated** neutrino flux (0-100 GeV). We use the NuMI Gen2 PPFX flux, constrained by ν-e scattering measurements, as explained in the wine and cheese talk on Dec 18, 2015.

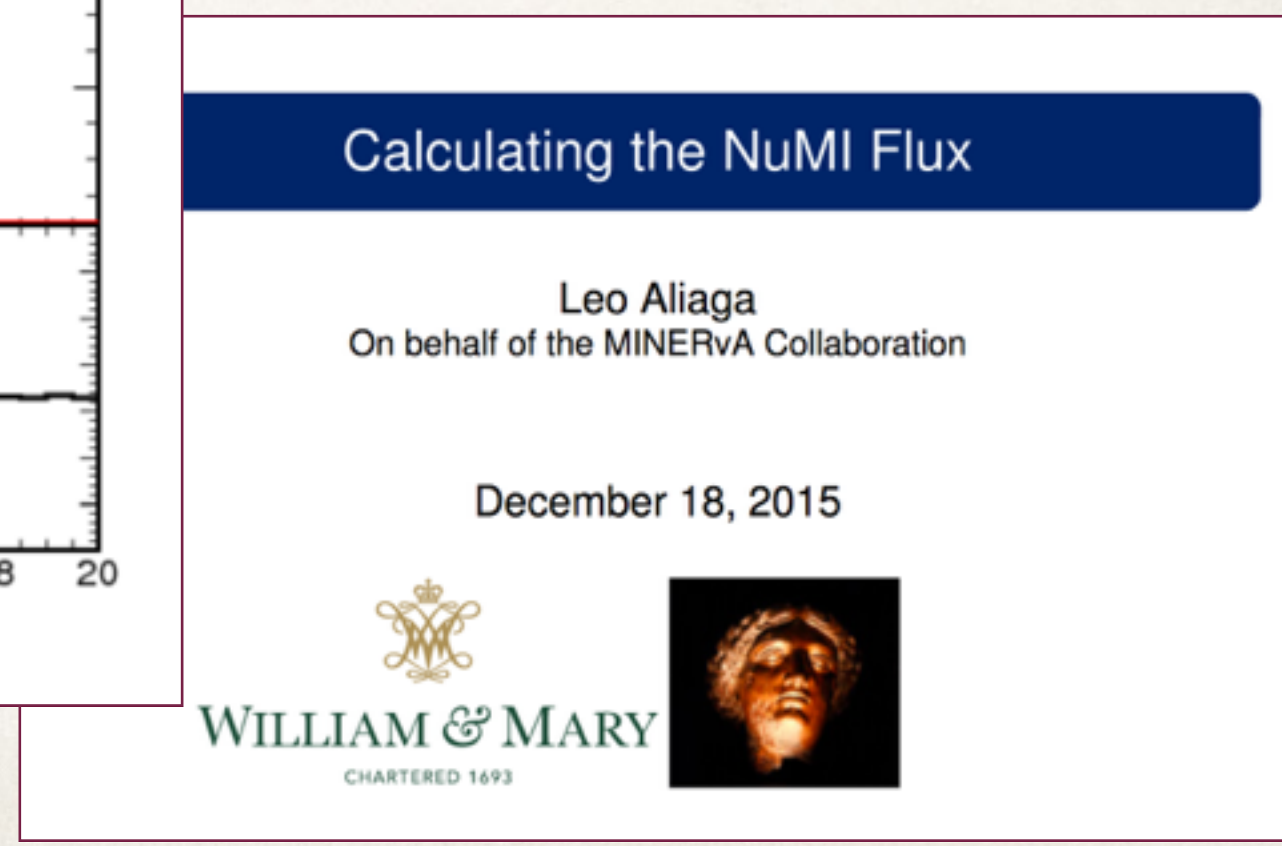

Protons on target

$$\left(\frac{d^2\sigma}{dx\,dy}\right)_{ij} = \frac{\sum_{\alpha\beta} U_{\alpha\beta ij}(N_{\mathrm{data},\alpha\beta} - N^{bkgd}_{\mathrm{data},\alpha\beta})}{\epsilon_{ij}(\Phi T)(\Delta x_i)(\Delta y_j)}$$

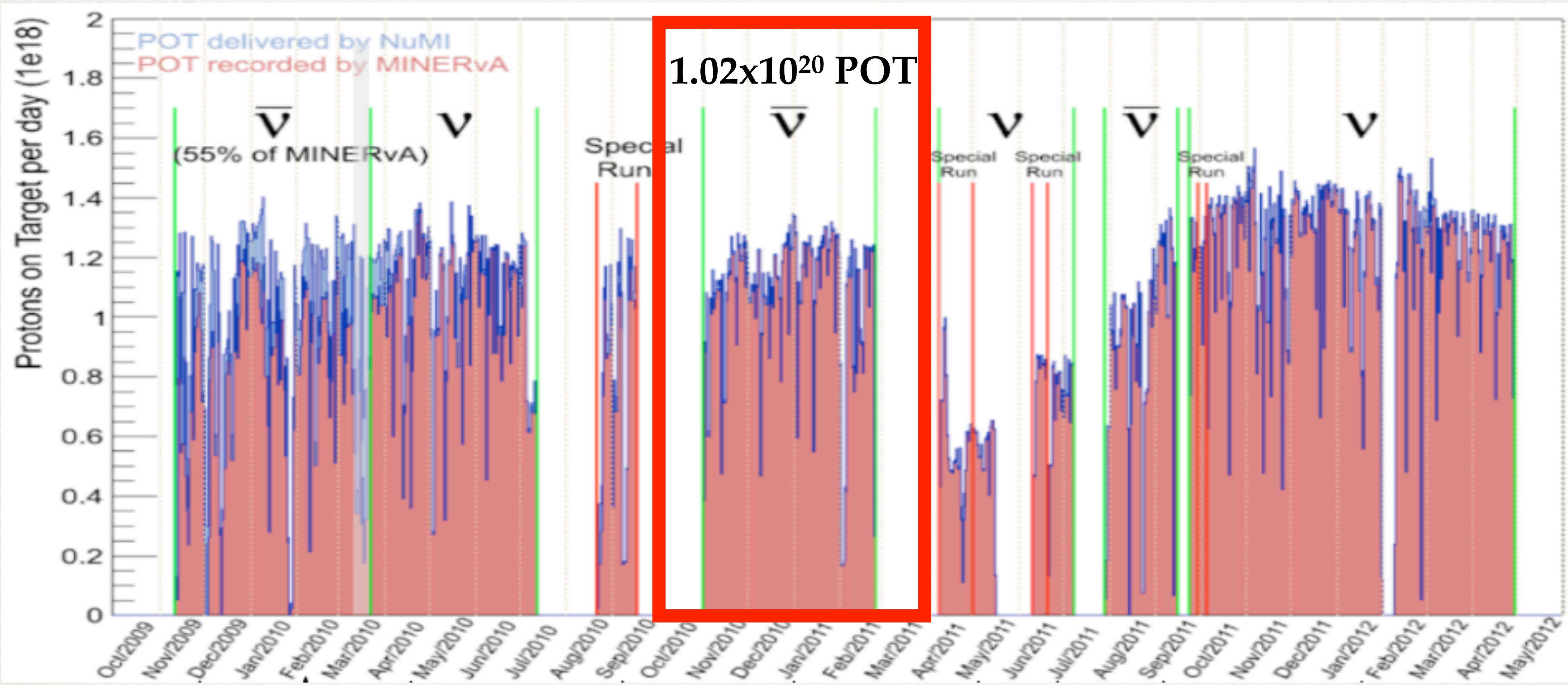

Thank you for the beam!

To get a total neutrino flux, we multiply the flux energy spectrum by the number of protons on target

Systematic uncertainties

Standard simulation

Perform analysis

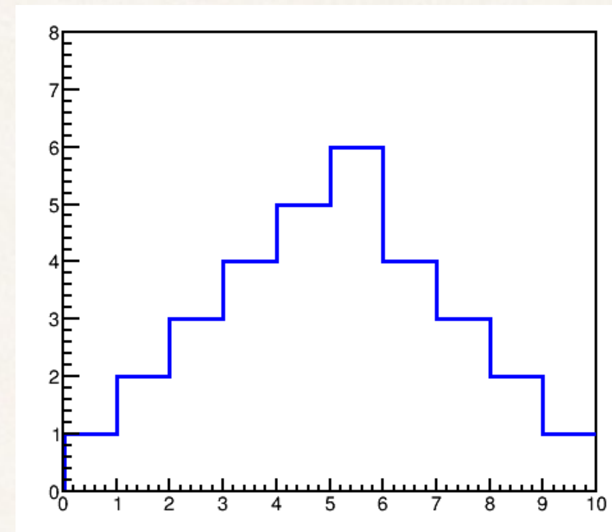

Adjust a parameter: once or many times

Uncertainty due to the shift is the difference between the distributions (or mean of them if there are many)

Simulation with one parameter adjusted

Perform analysis

Different events pass cuts?
Measured values shift?
Events are re-weighted?

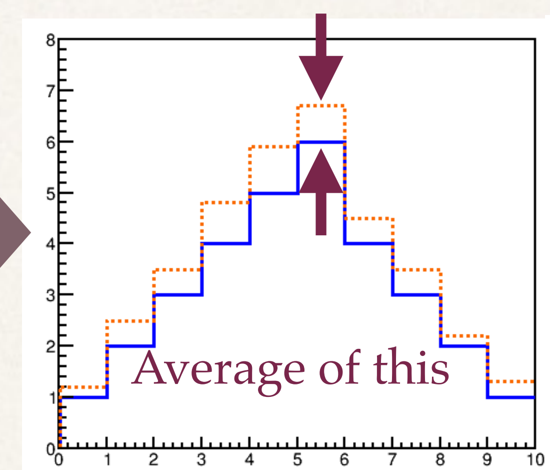

Shift quantity up

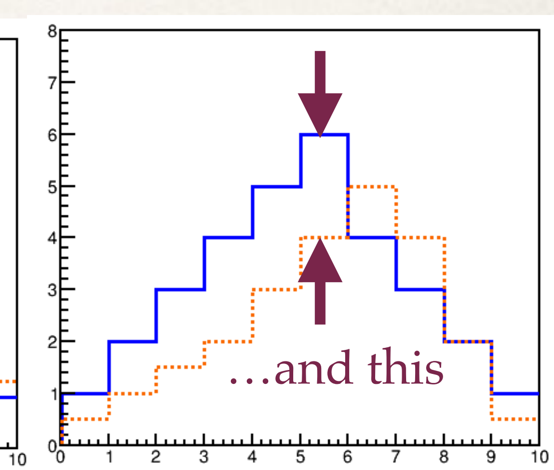

Shift quantity down

Examples: increase resonant cross section by 10%, smear muon angle by a random amount from a distribution, 100 “universes” of flux changes

Sources of systematic uncertainty

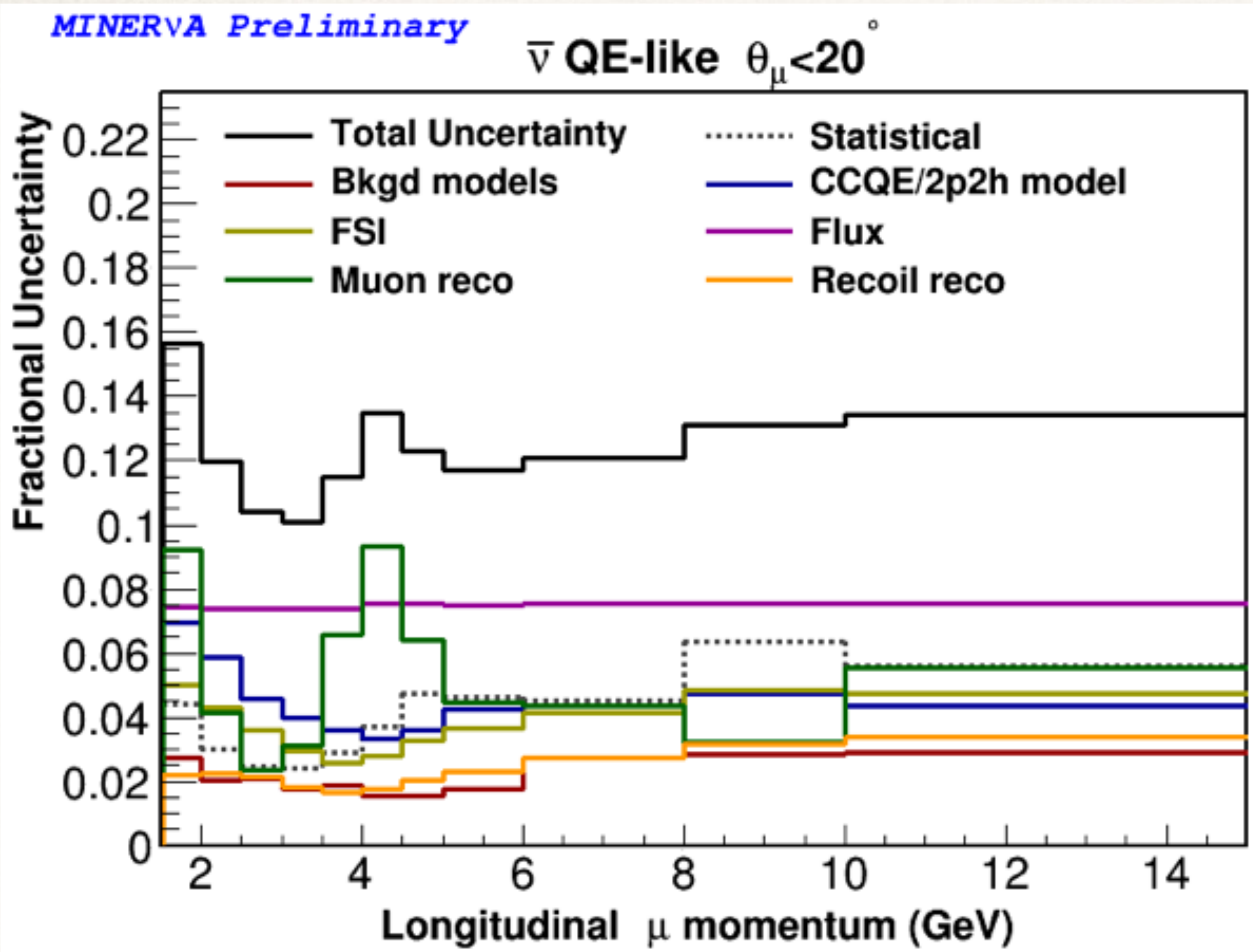

Uncertainties projected onto **longitudinal muon momentum**

- - - Statistical uncertainty

Background models

- **resonant** interactions affect background subtraction

CCQE / 2p2h model

- dominated by uncertainty in **correlation effect strength**

Final-state interactions

- **pion absorption** dominates

Flux

- beam focusing
- tertiary hadron production
- reweight to other experiments

Muon reconstruction

- **muon energy scale** dominates
- tracking efficiency
- muon angle and vertex position

Recoil reconstruction

- detector response to different particles - **neutron** dominates

Sources of systematic uncertainty

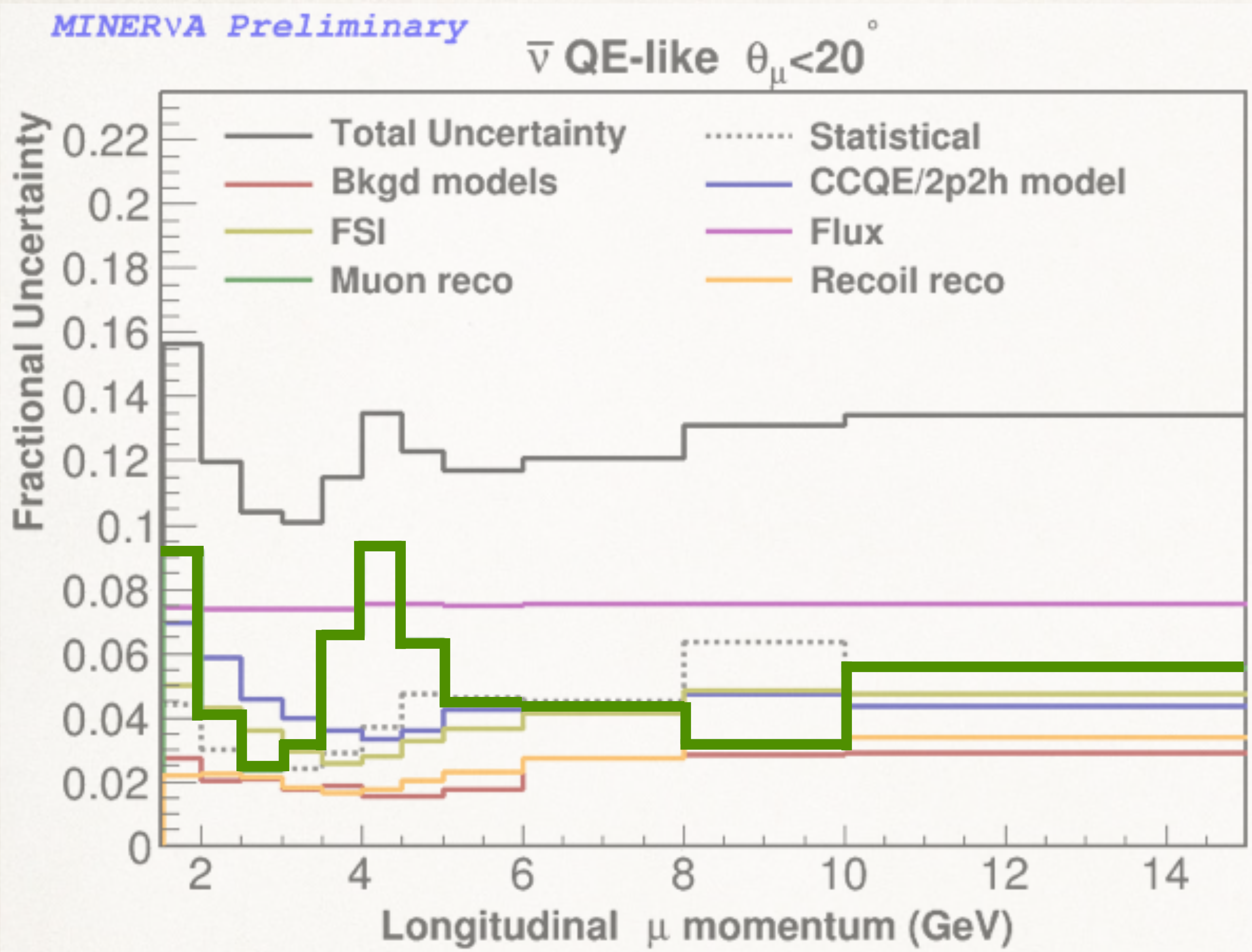

Why does the muon reconstruction uncertainty have this double-peaked shape?

- - - Statistical uncertainty

Background models

- **resonant** interactions affect background subtraction

CCQE / 2p2h model

- dominated by uncertainty in **correlation effect strength**

Final-state interactions

- **pion absorption** dominates

Flux

- beam focusing
- tertiary hadron production
- reweight to other experiments

Muon reconstruction

- **muon energy scale** dominates
- tracking efficiency
- muon angle and vertex position

Recoil reconstruction

- detector response to different particles - **neutron** dominates

Energy spectrum affects muon reconstruction

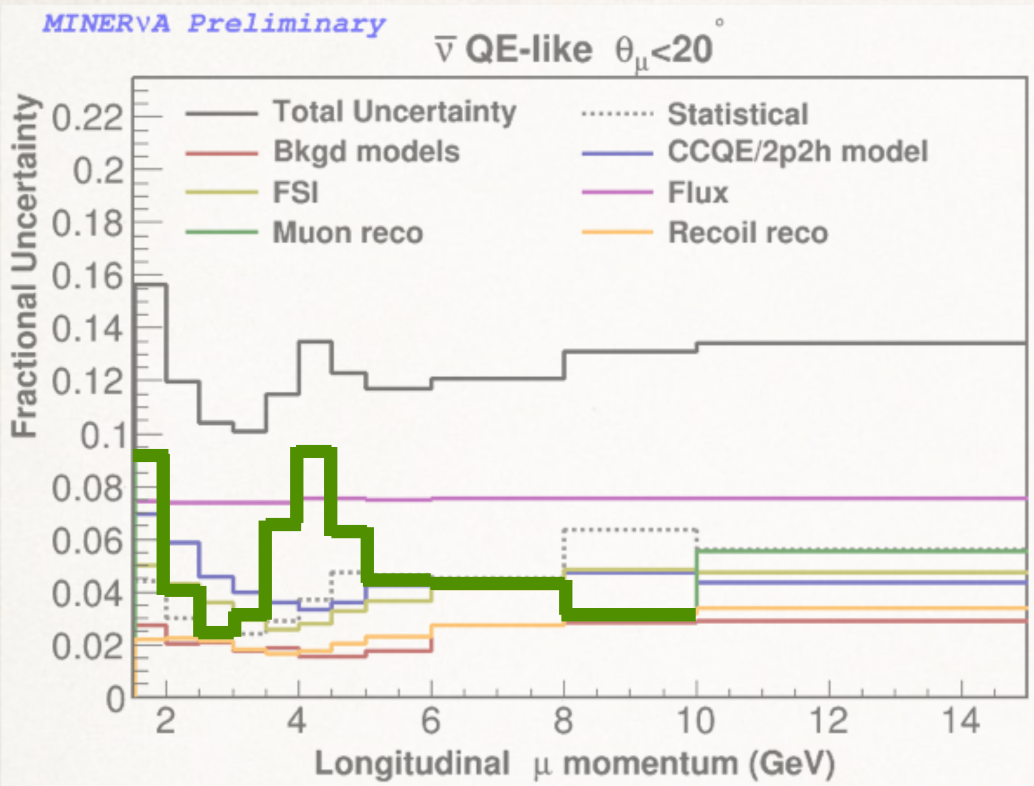

The muon energy scale uncertainty quantifies the effect of shifting the reconstructed muon energy by:

- 11 MeV (material assay)
- 30 MeV (energy deposition per cm)
- MINOS shift:
  - 2% for energy measured by range plus
  - 0.6 %(>1GeV) or 2.5% (<1GeV) for energy measured by curvature, added in quadrature

- The large muon reconstruction uncertainties correspond to the energies where the slope is steepest, and a small change in muon energy would lead to a large change in event count

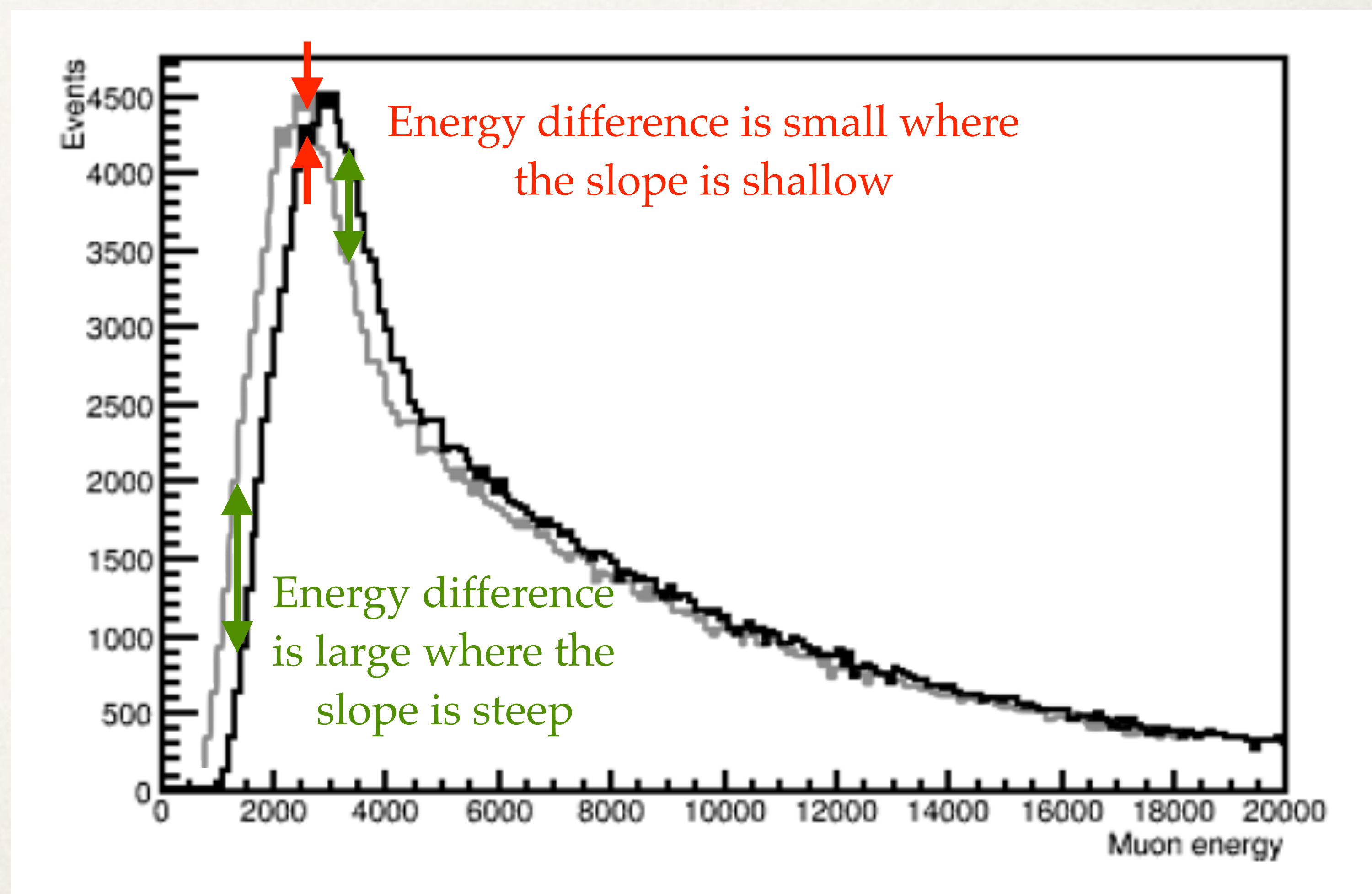

Sources of systematic uncertainty

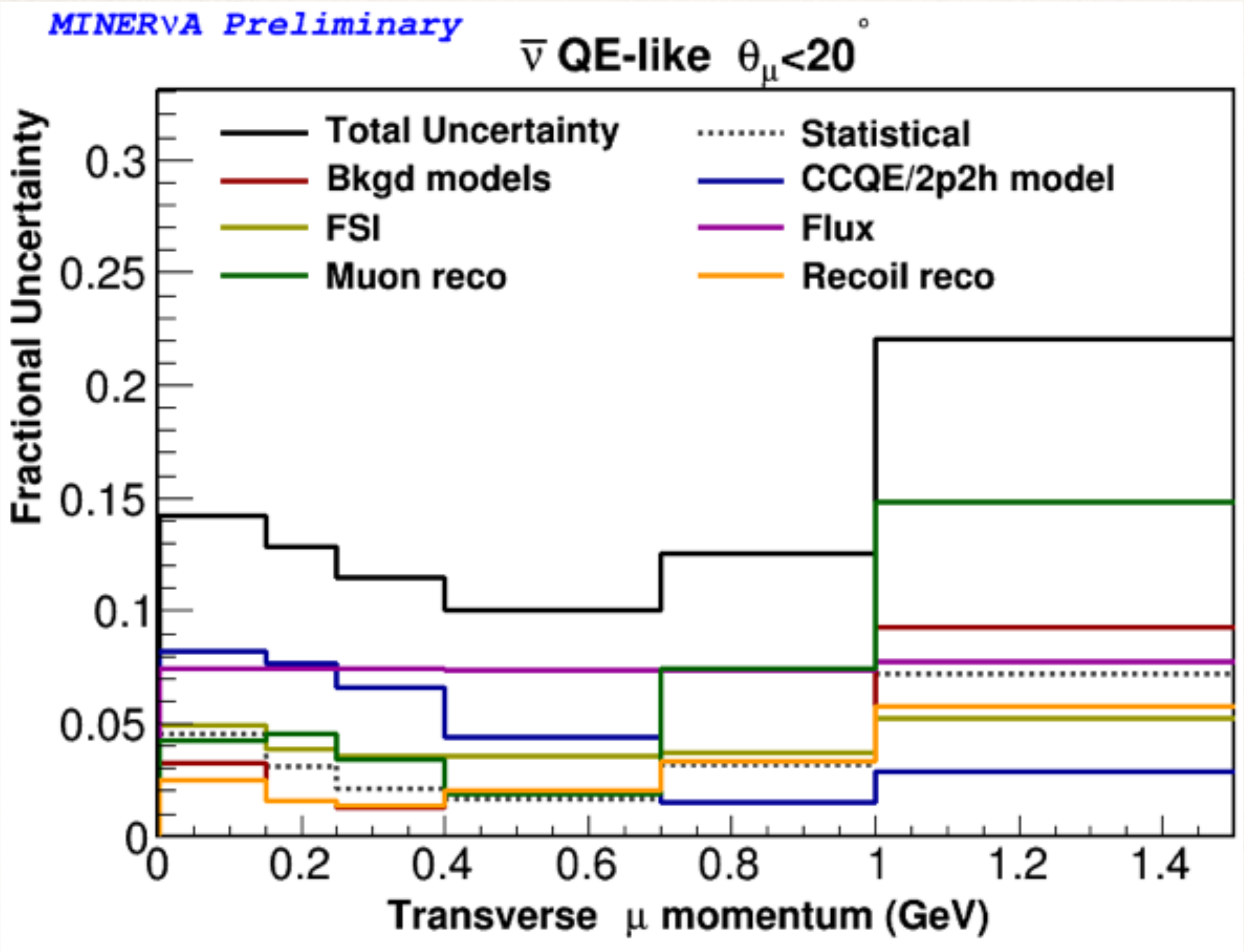

Summary of systematic uncertainties projected onto **transverse muon momentum**

- - - Statistical uncertainty

Background models

- **resonant** interactions affect background subtraction

CCQE / 2p2h model

- dominated by uncertainty in **correlation effect strength**

Final-state interactions

- **pion absorption** dominates

Flux

- beam focusing
- tertiary hadron production
- reweight to other experiments

Muon reconstruction

- **muon energy scale** dominates
- tracking efficiency
- muon angle and vertex position

Recoil reconstruction

- detector response to different particles - **neutron** dominates

Sources of systematic uncertainty

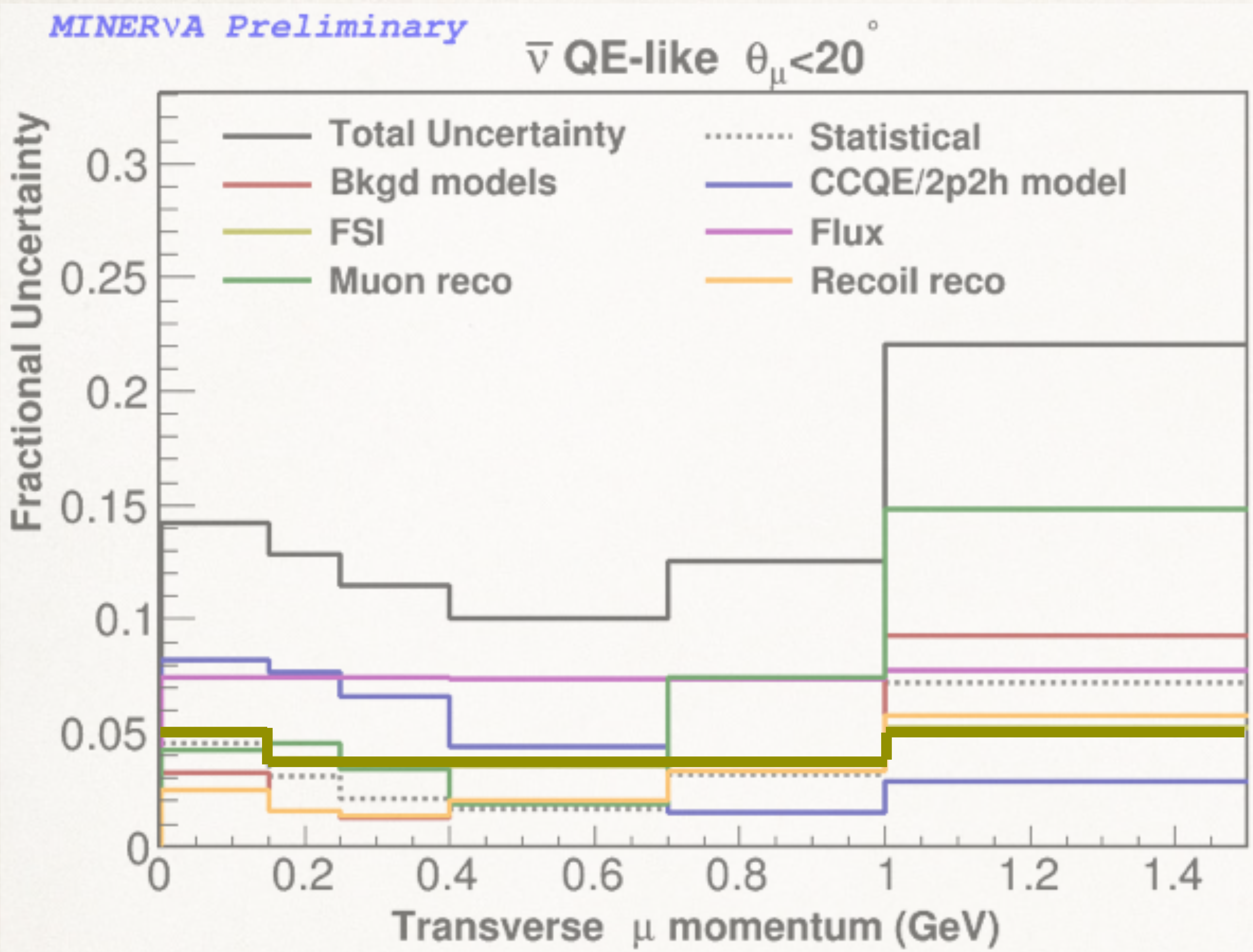

Dominated by pion absorption uncertainty: turns QE-like **background to signal**

- - - Statistical uncertainty

Background models

- **resonant** interactions affect background subtraction

CCQE / 2p2h model

- dominated by uncertainty in **correlation effect strength**

Final-state interactions

- **pion absorption** dominates

Flux

- beam focusing
- tertiary hadron production
- reweight to other experiments

Muon reconstruction

- **muon energy scale** dominates
- tracking efficiency
- muon angle and vertex position

Recoil reconstruction

- detector response to different particles - **neutron** dominates

CCQE signal model uncertainty

Remember our choice of signal definitions: QE-like vs. true CCQE.

QE-like	True CCQE
Final state with μ^+, neutrons and low-energy protons	Initial interaction is **CCQE** (including CCQE from a correlated pair)

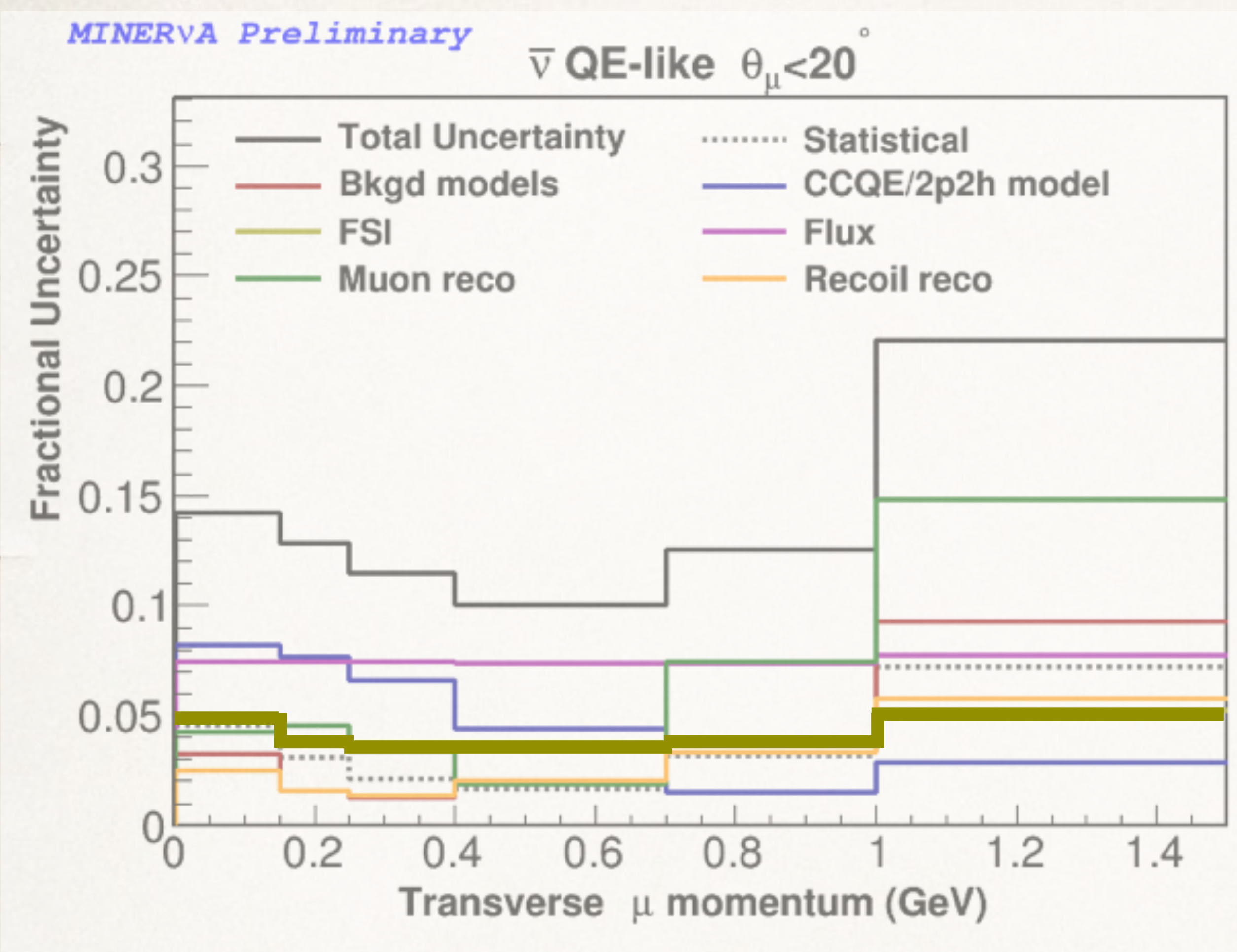

FSI moves background to signal

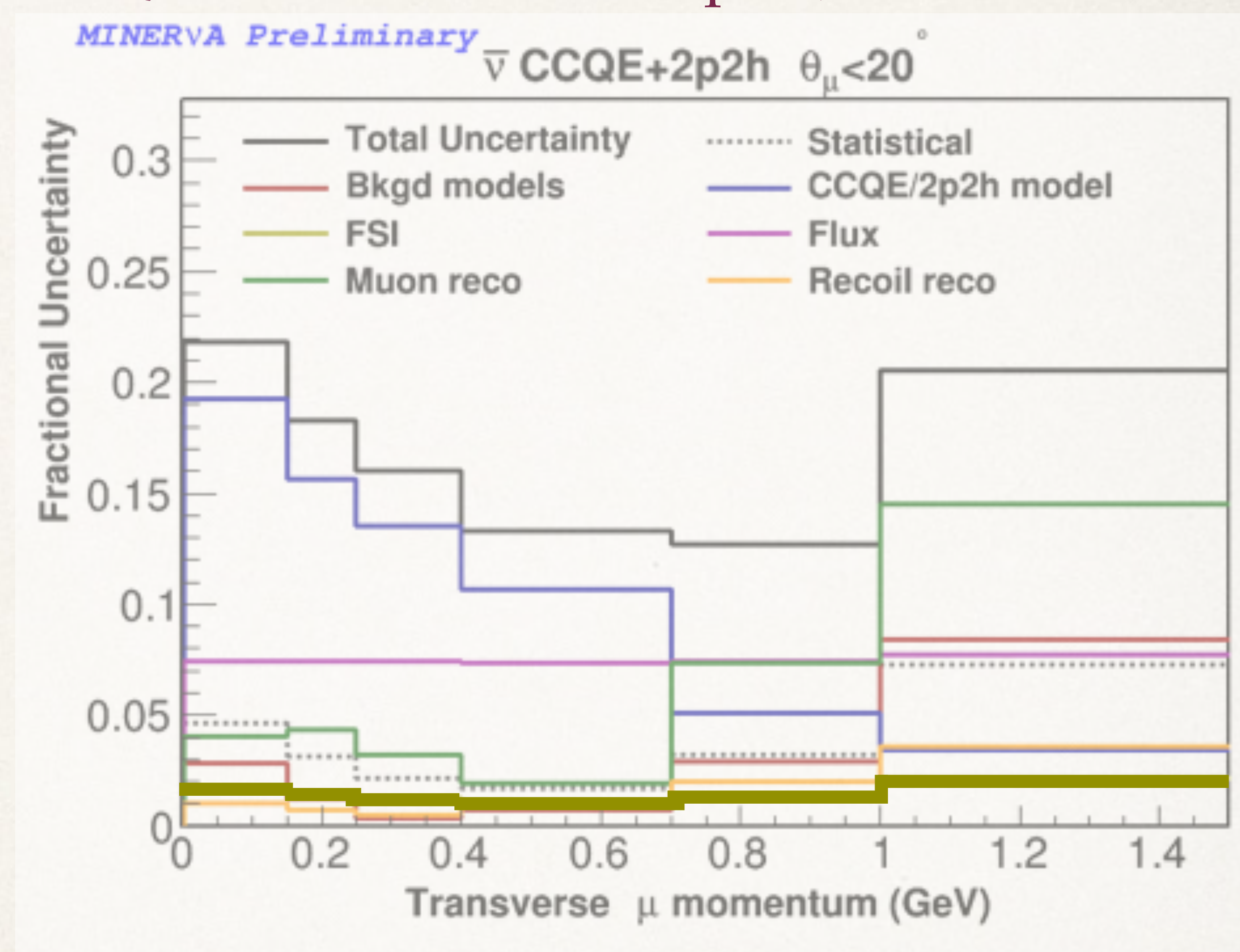

Signal definition depends on initial interaction - smaller FSI dependence

Sources of systematic uncertainty

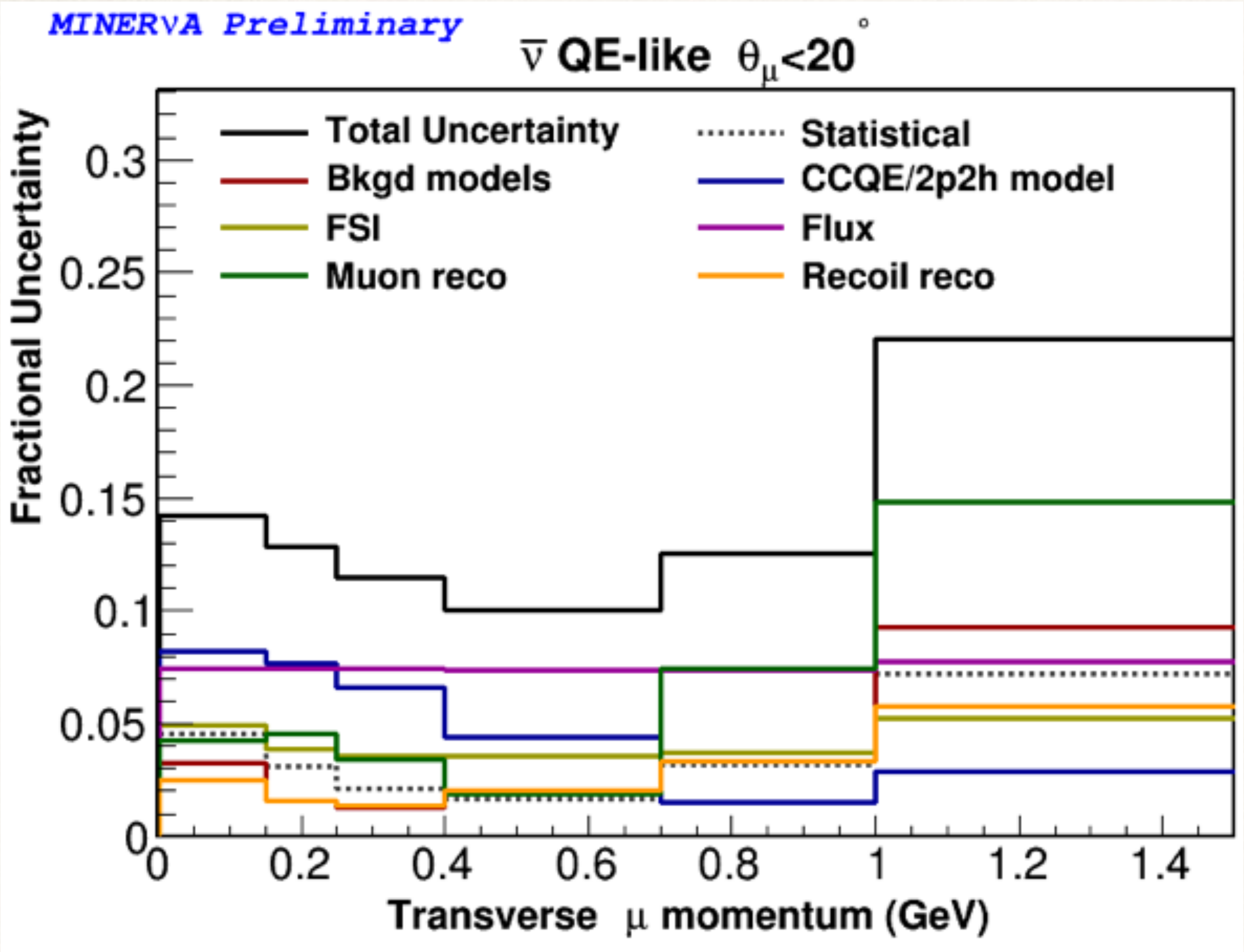

Summary of systematic uncertainties projected onto transverse muon momentum

- - - Statistical uncertainty

Background models

- **resonant** interactions affect background subtraction

CCQE / 2p2h model

- dominated by uncertainty in **correlation effect strength**

Final-state interactions

- **pion absorption** dominates

Flux

- beam focusing
- tertiary hadron production
- reweight to other experiments

Muon reconstruction

- **muon energy scale** dominates
- tracking efficiency
- muon angle and vertex position

Recoil reconstruction

- detector response to different particles - **neutron** dominates

Sources of systematic uncertainty

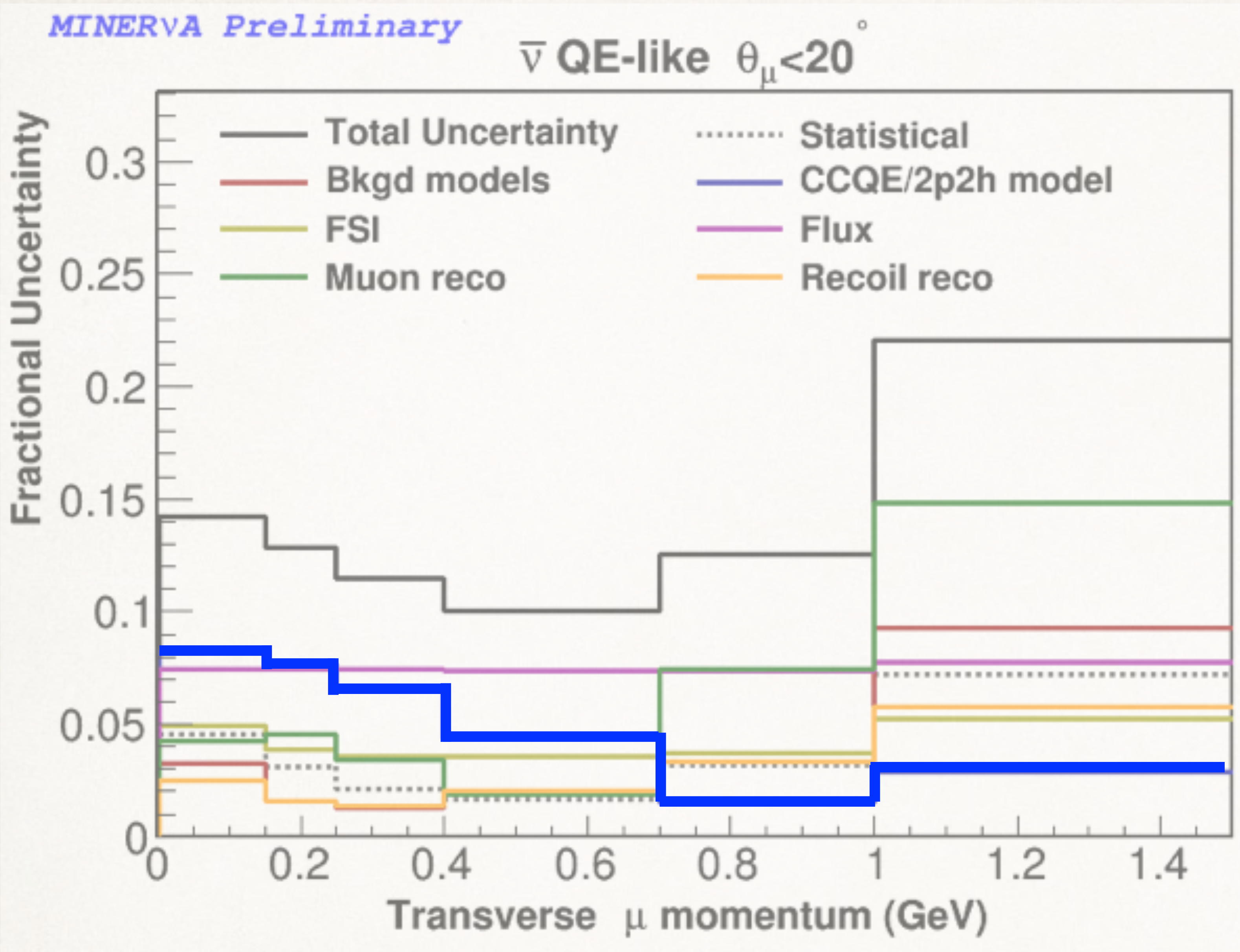

Why does our result depend on our signal model?

- - - Statistical uncertainty

Background models

- **resonant** interactions affect background subtraction

CCQE / 2p2h model

- dominated by uncertainty in **correlation effect strength**

Final-state interactions

- **pion absorption** dominates

Flux

- beam focusing
- tertiary hadron production
- reweight to other experiments

Muon reconstruction

- **muon energy scale** dominates
- tracking efficiency
- muon angle and vertex position

Recoil reconstruction

- detector response to different particles - **neutron** dominates

Challenge: signal model dependence

To test the signal model's effect on our data, we add 2p2h events (from the new Nieves MEC model, included in GENIE 2.10) to our simulation and see its effect on the data. We use **2p2h without RPA**, an extreme example (and not our best guess at the model)

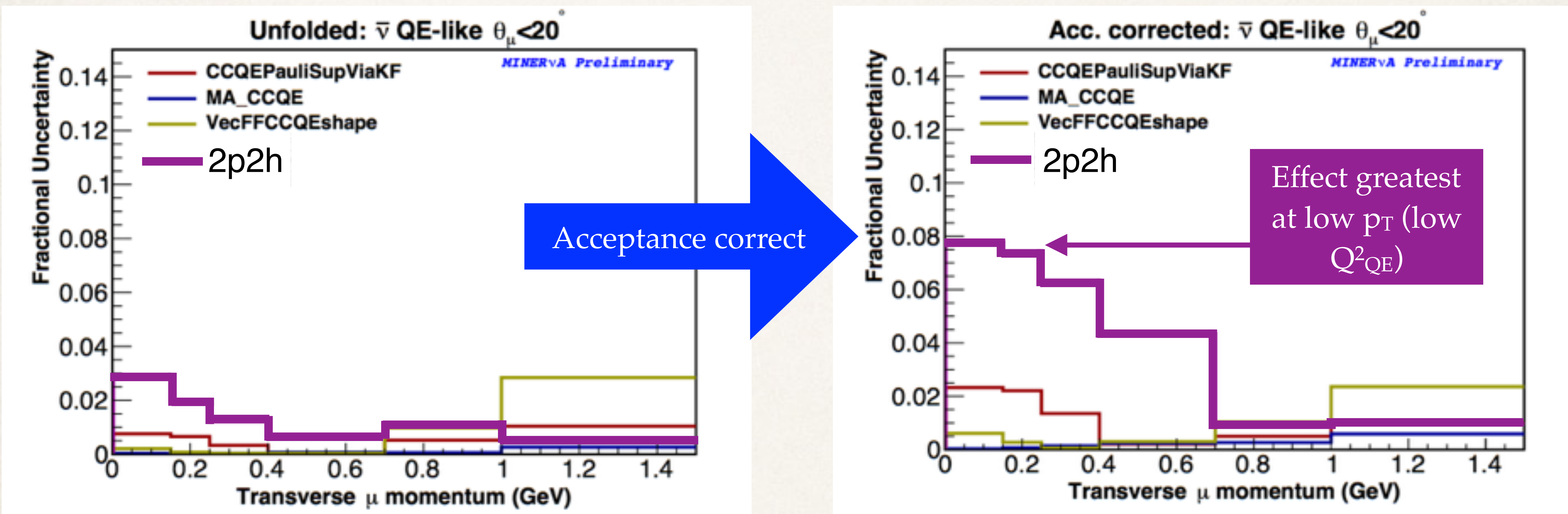

Background subtraction:
small uncertainty due to differing background fractions in the 2 samples

Acceptance correction:
large increase in uncertainty as acceptance is very different for 2p2h events

Reconstructed recoil distributions for QE-like events

Central QE-like simulation	QE-like 2p2h events
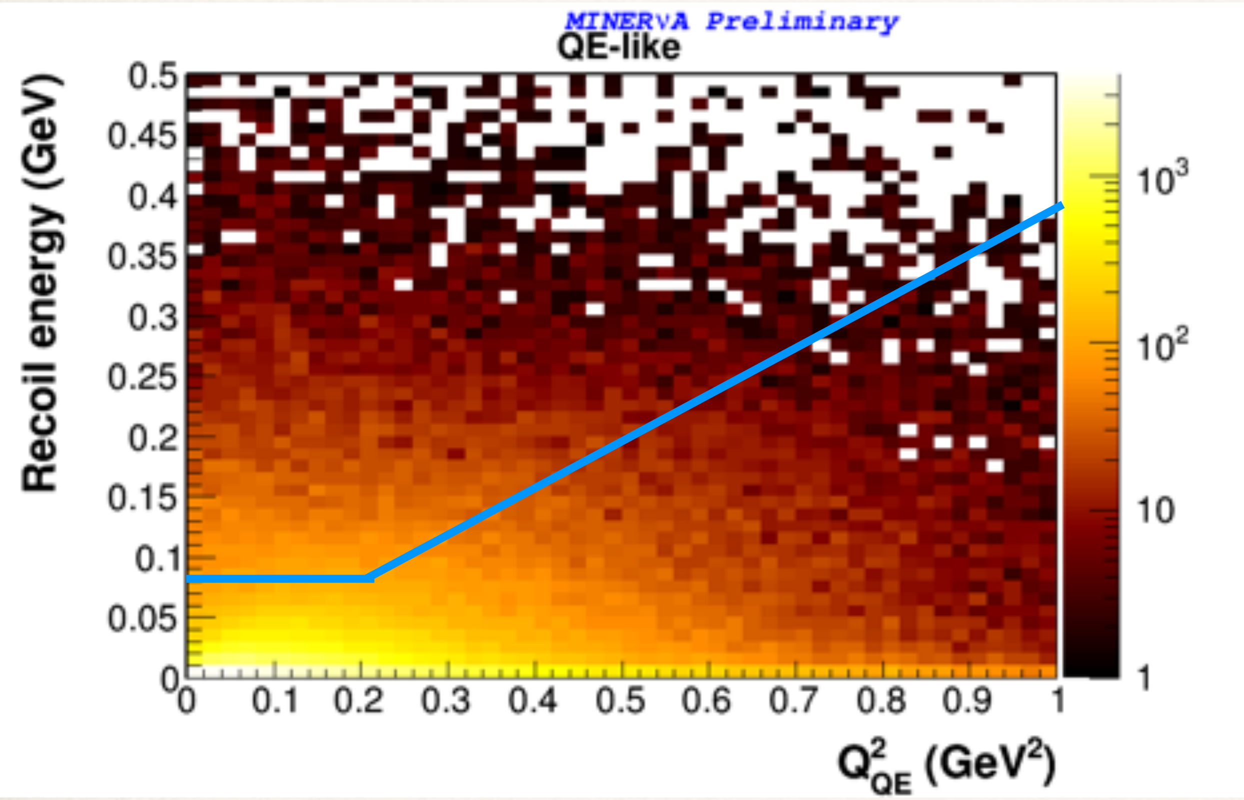	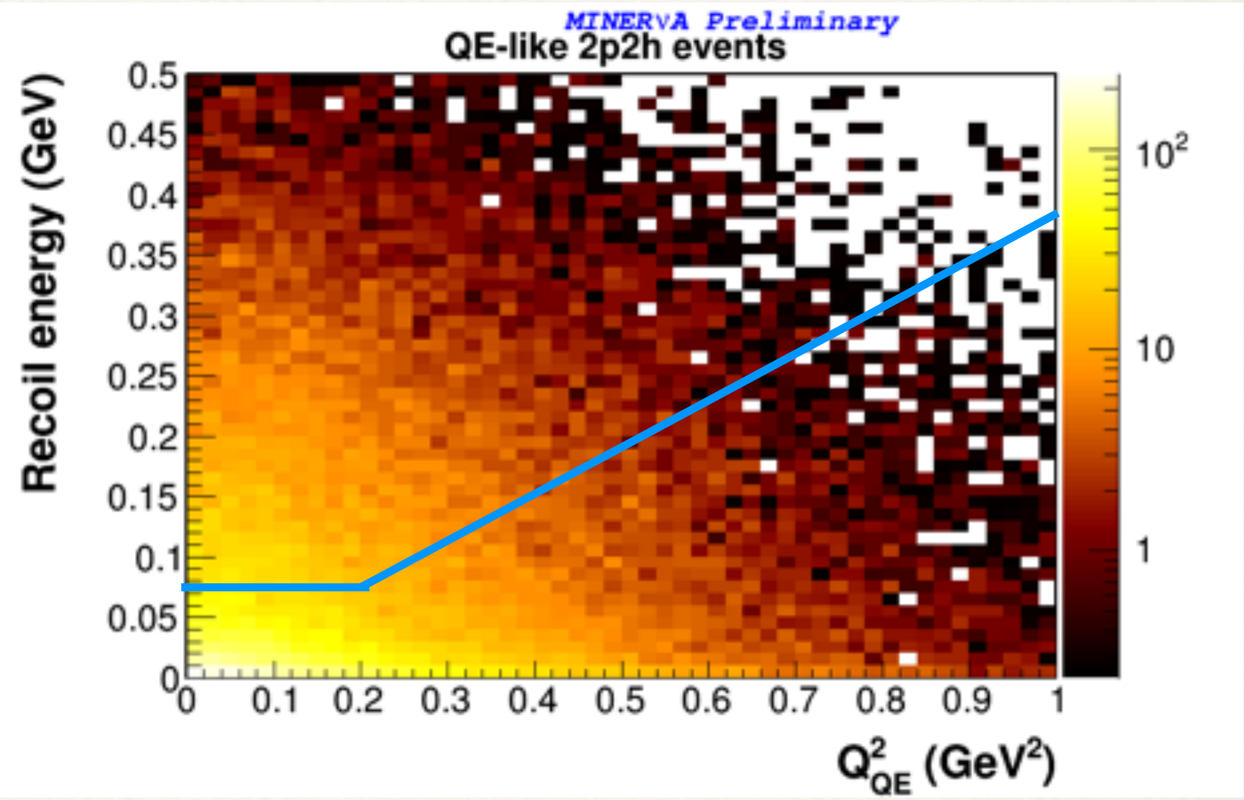
Acceptance: 54%	Acceptance: 43%

This additional recoil comes from second neutrons (**2-particle**-2-hole).
For QE-like, events with **any number of neutrons are signal**, if they have no pions or high-energy protons.

Uncertainty and signal definition

Remember our choice of signal definitions: QE-like vs. true CCQE.

QE-like

Final state with $\mu+$, neutrons and low-energy protons

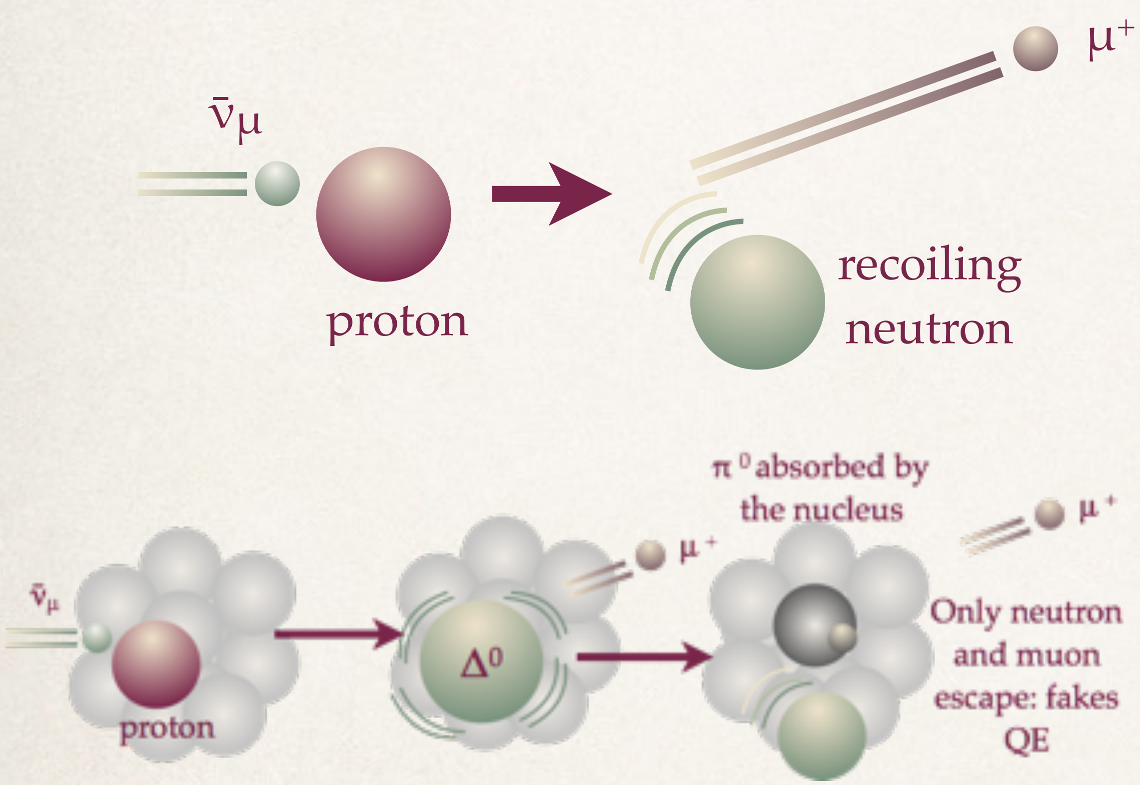

True CCQE

Initial interaction is CCQE **(including CCQE from a correlated pair)**

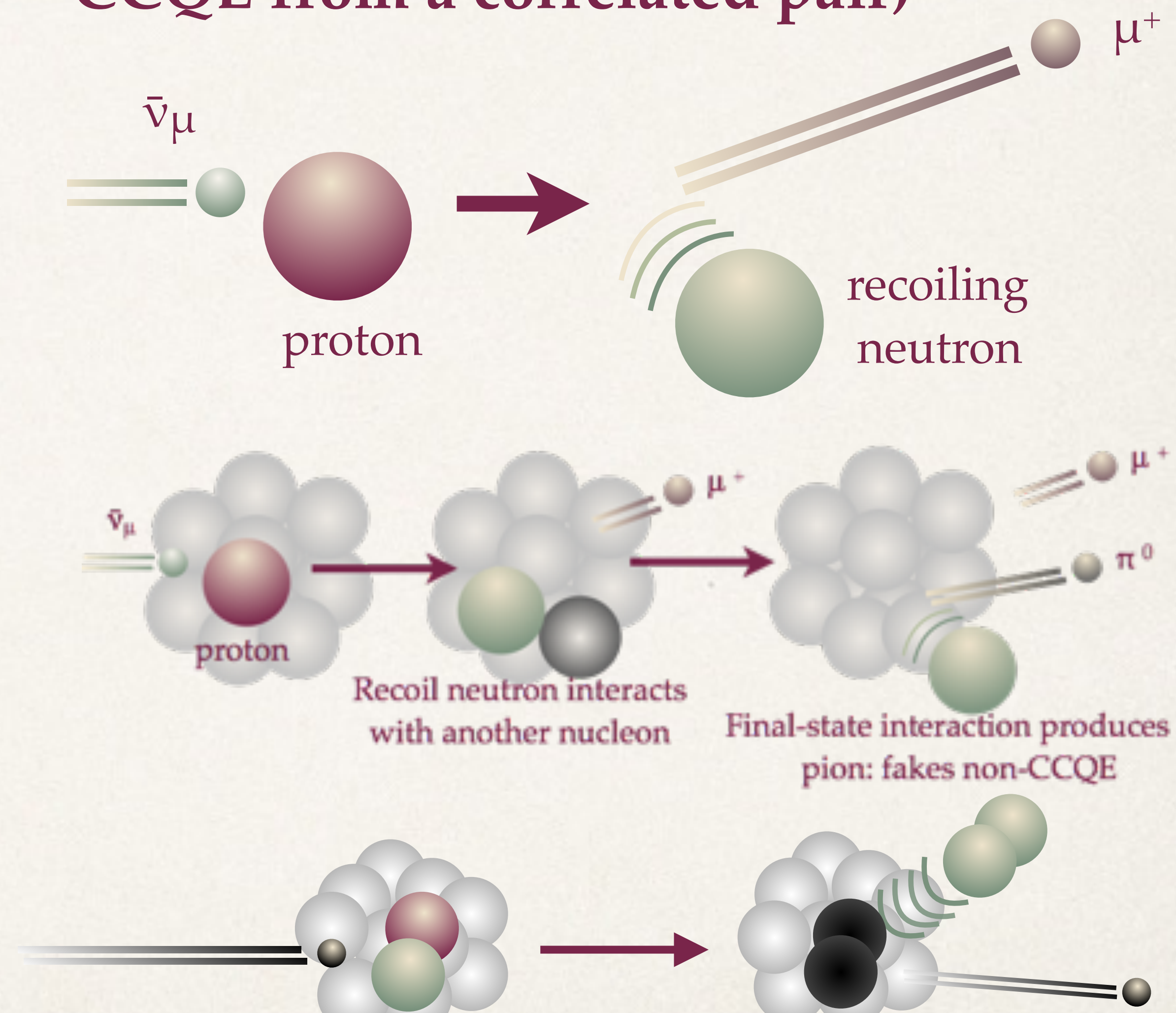

How would changing from QE-like to CCQE change the 2p2h uncertainty?

CCQE signal model uncertainty

Remember our choice of signal definitions: QE-like vs. true CCQE.

QE-like	True CCQE
Final state with $\mu+$, neutrons and low-energy protons	Initial interaction is CCQE **(including CCQE from a correlated pair)**

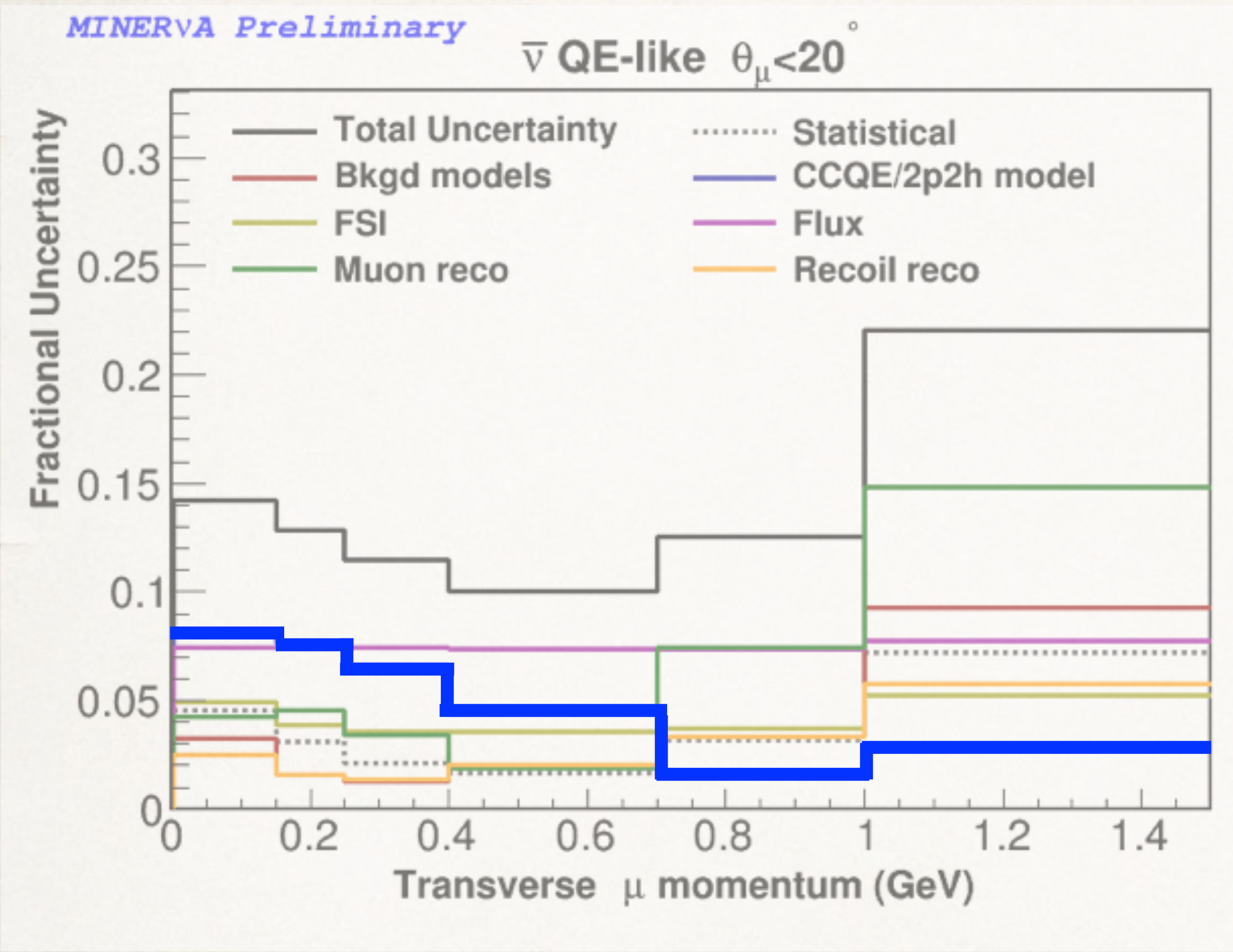

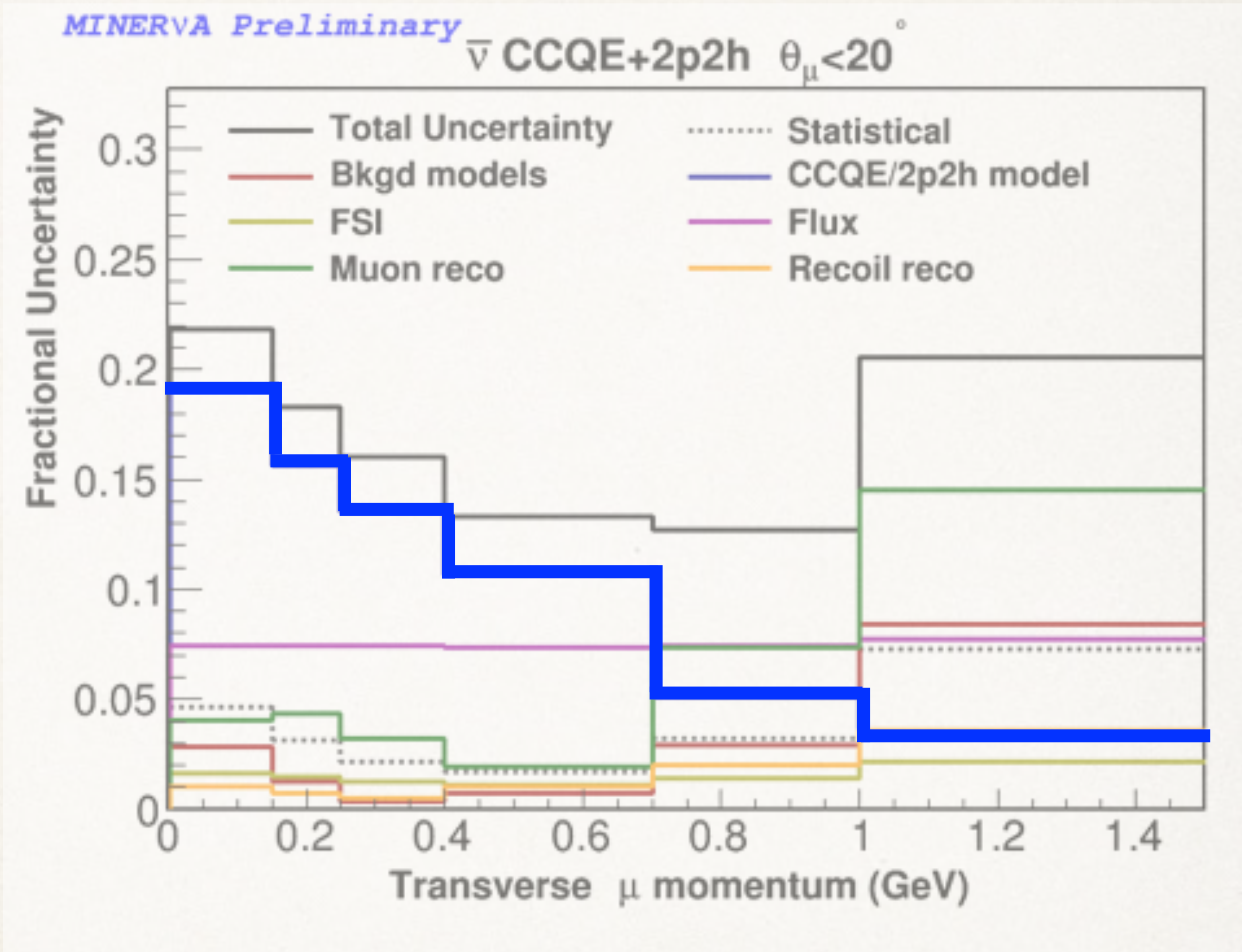

2p2h uncertainty is much higher for the true CCQE+2p2h definition - why?

CCQE reconstructed recoil

CCQE	2p2h (CCQE from correlated pair)

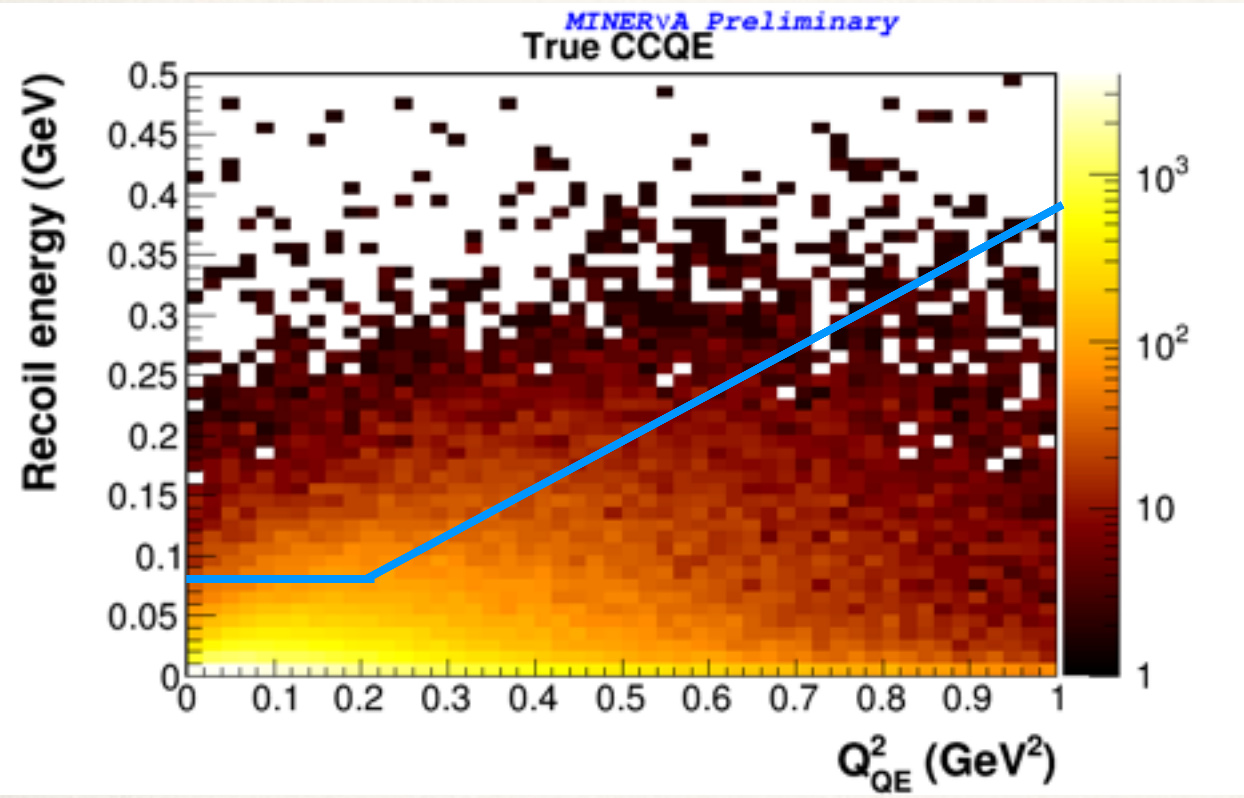

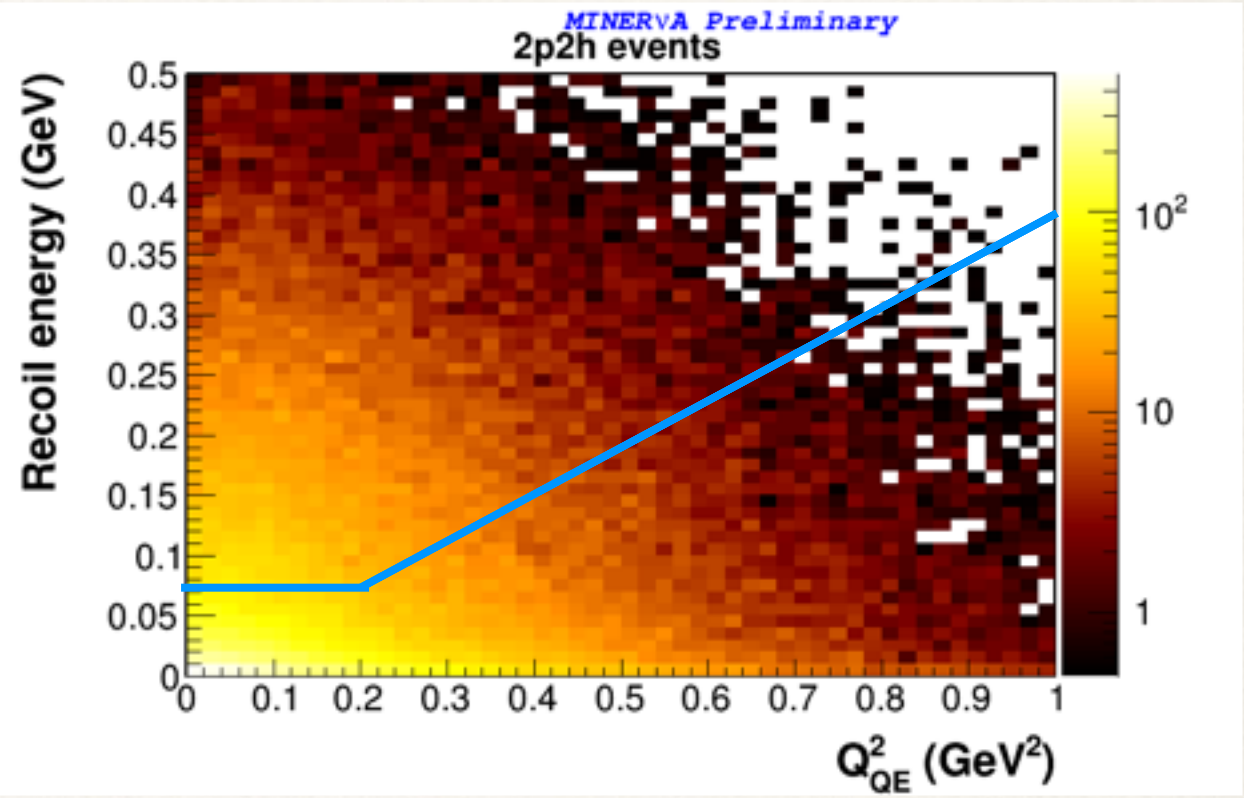

Acceptance: 58%
(QE-like: 54%)

Acceptance: 38%
(QE-like: 43%)

For this signal definition, our central value acceptance is larger than for QE-like, while for the 2p2h sample, it is smaller

2p2h fraction is higher for CCQE

QE-like: 16% is 2p2h

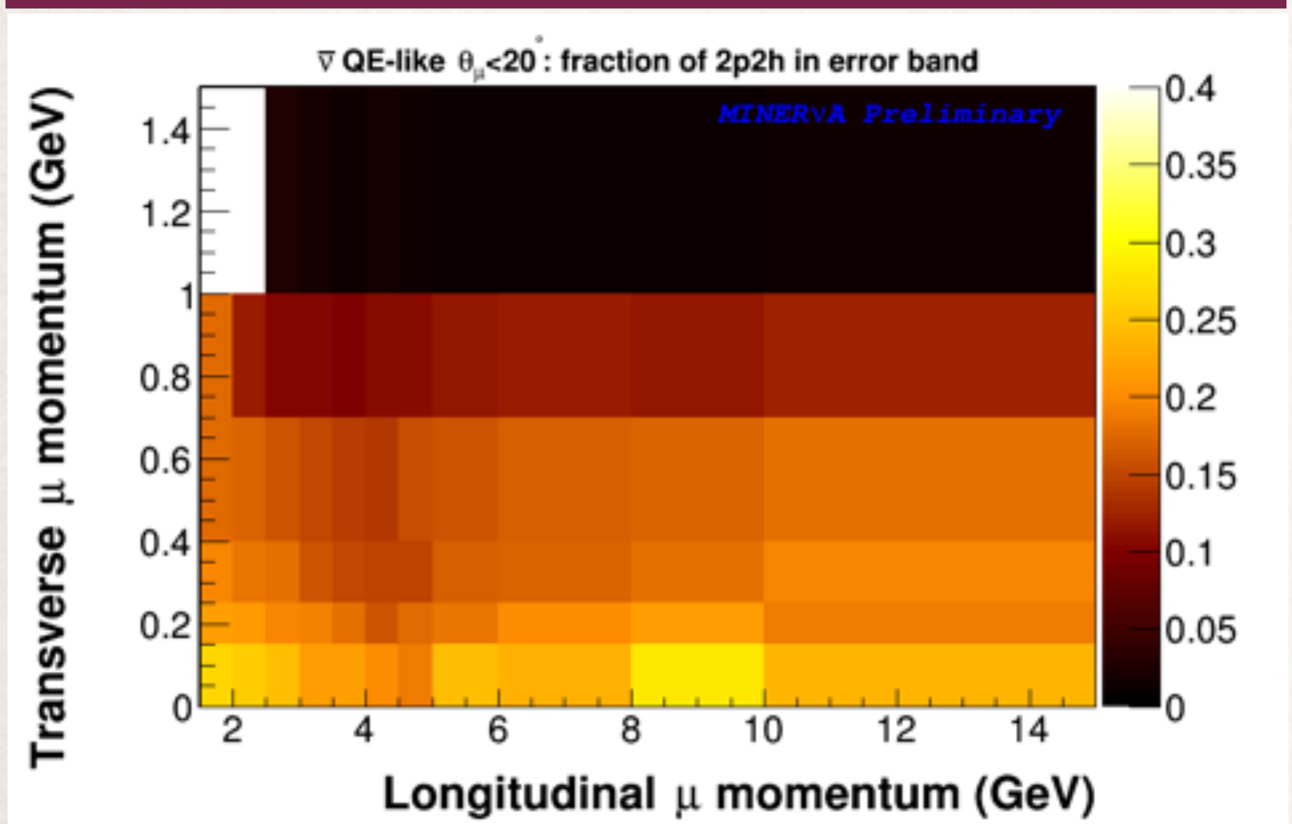

True CCQE: 21% is 2p2h

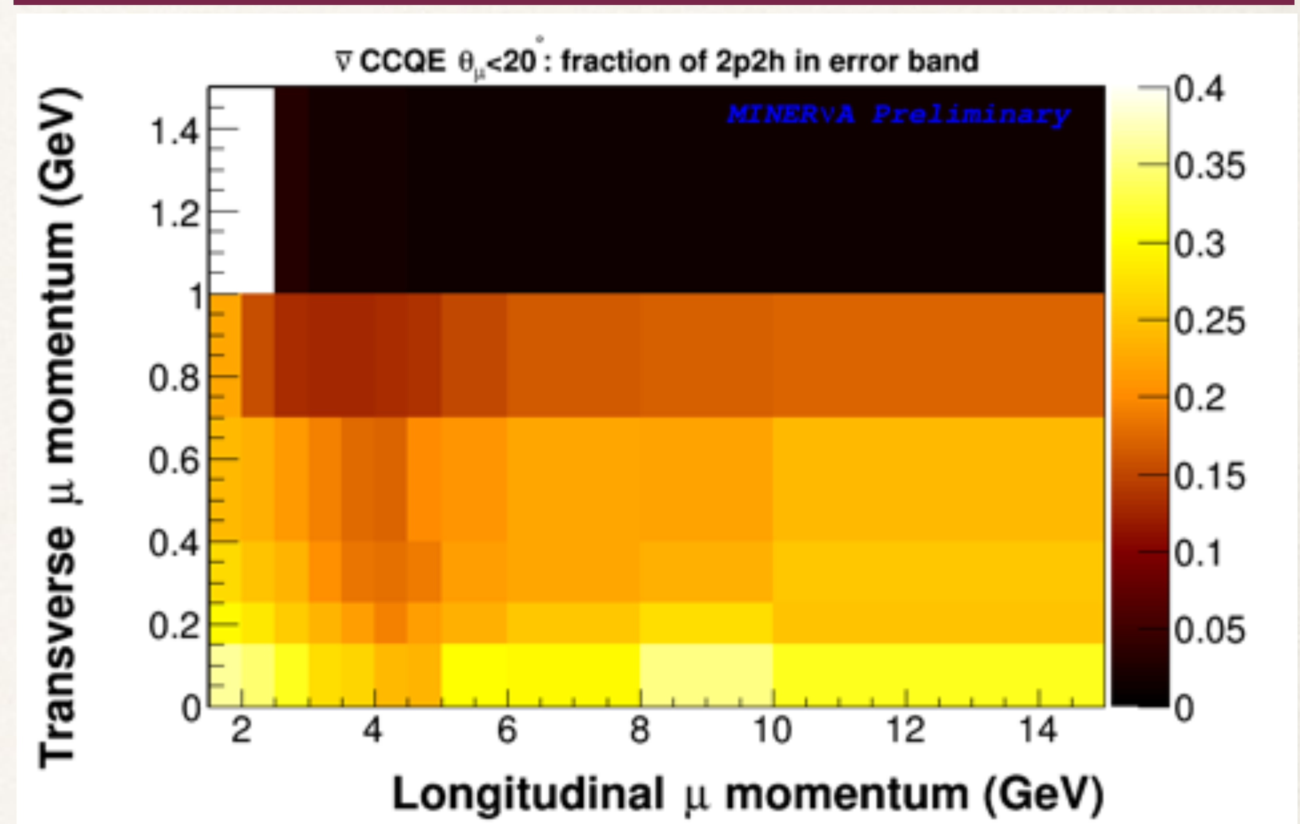

2p2h contribution used for the uncertainty calculation: compare with this paper "32% for antineutrino"

TABLE I. The 2p2h cross section in carbon vs. energy. The contribution saturates as a function of three-momentum transfer to a value that is 29% of the QE cross section for neutrino, 32% for antineutrino, an estimate for the nondelta component without the Δ absorption component is 15% and 17% of the QE cross section for neutrino and antineutrino.

	whole cross section (x 10^{-38} cm^2)			three-momentum transfer < 1.2 GeV		
Energy (GeV)	QE LFG+RPA	QE LFG noRPA	2p2h	2p2h no Δ	QE LFG+RPA	QE LFG noRPA
1 ν_μ	5.61	5.66	1.27	0.563	5.20	5.36
2	5.65	5.61	1.41	0.704	4.52	4.74
3	5.45	5.45	1.43	0.735	4.30	4.54
5	5.22	5.25	1.46	0.761	4.14	4.39
10	5.04	5.10	1.47	0.781	4.01	4.27
1 $\bar{\nu}_\mu$	1.56	1.96	0.459	0.306	1.56	1.95
2	2.68	3.03	0.887	0.520	2.52	2.89
3	3.26	3.55	1.07	0.609	2.93	3.27
5	3.83	4.05	1.24	0.686	3.29	3.61
10	4.31	4.47	1.38	0.749	3.58	3.88

Phys. Rev. D 88 (2013)

What we learned from this uncertainty

CCQE events,

2p2h events,

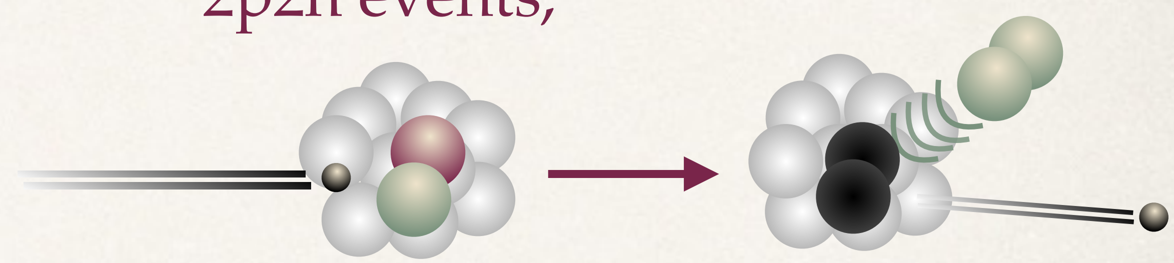

Non-CCQE events that are QE-like, and

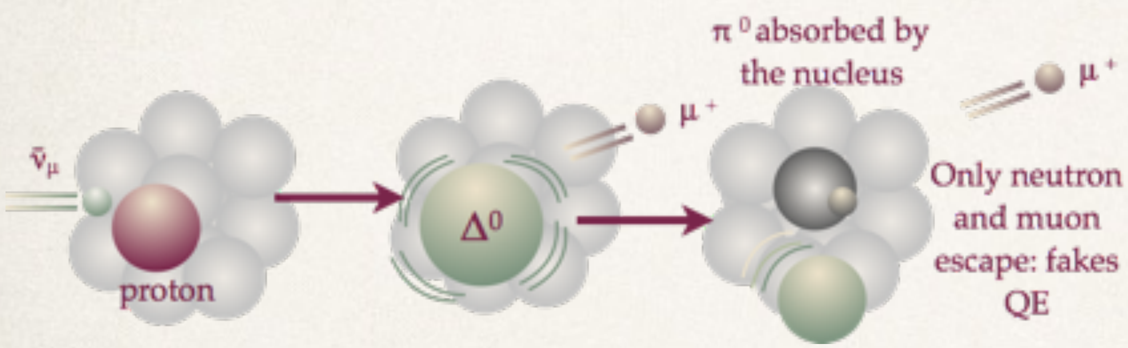

Background events with final-state pions

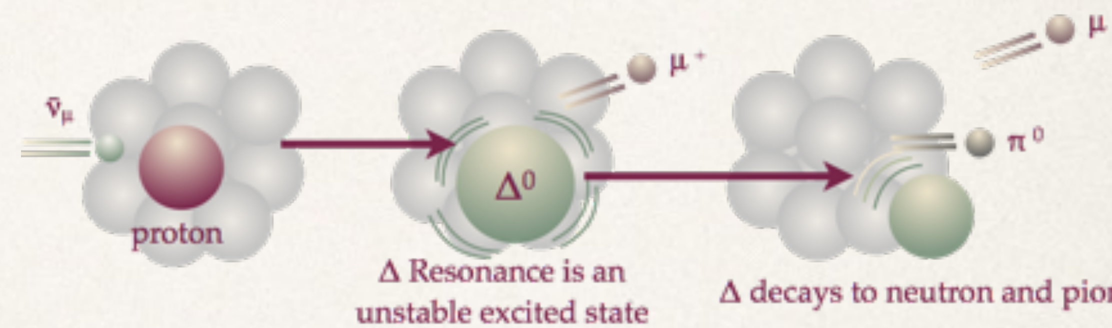

… each have their own recoil distributions. A recoil cut that gives high efficiency and purity when selecting or rejecting one category will do poorly at selecting or rejecting the others

Recoil distributions for interaction types

CCQE

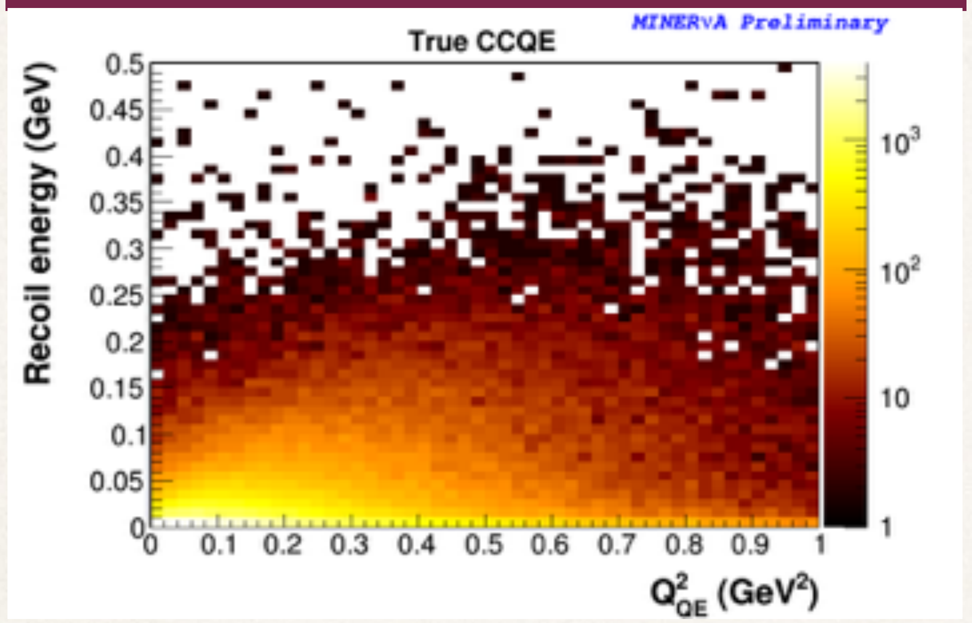

2p2h (CCQE from correlated pair)

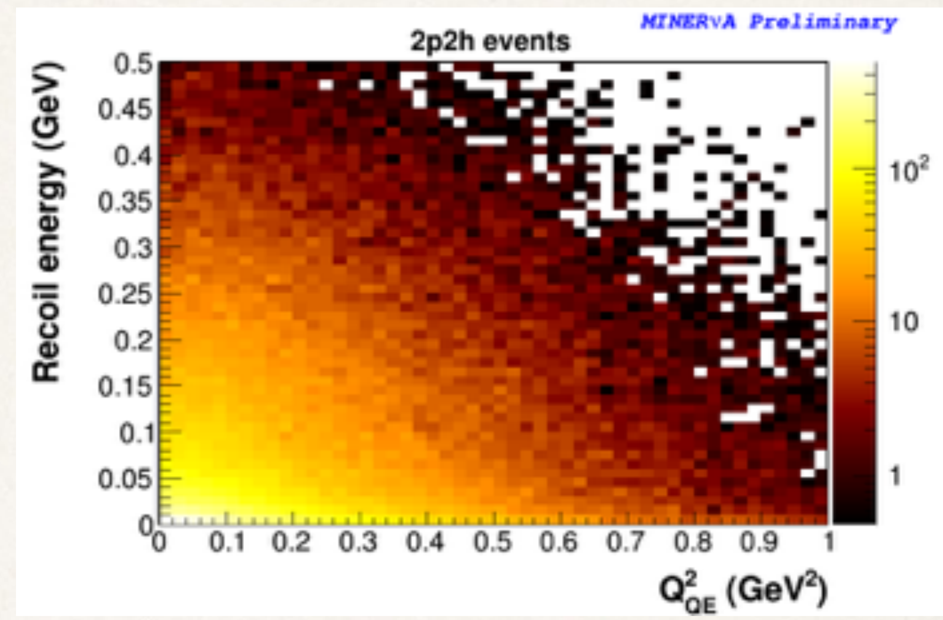

CCQE

QE-like

Non-CCQE QE-like

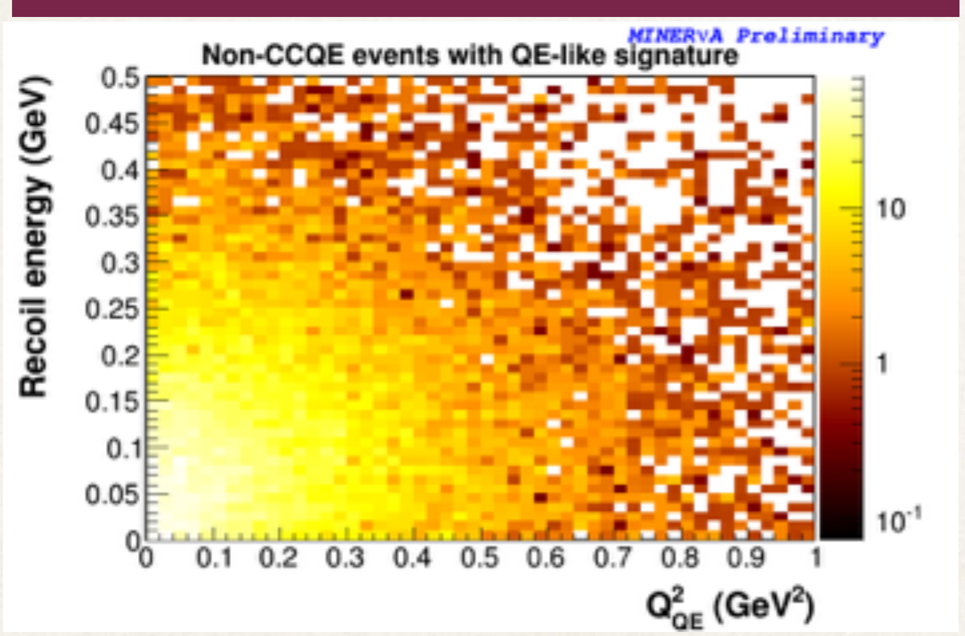

Backgrounds (pions or >120MeV protons)

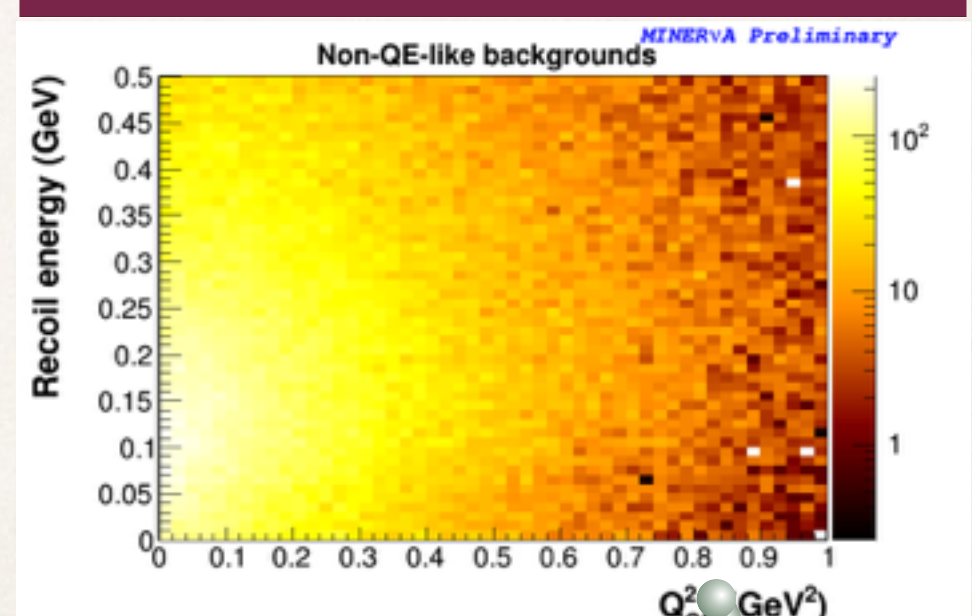

MINERvA's detector is so awesome, it can distinguish all these categories!

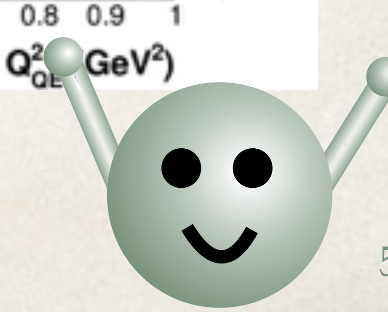

Recoil distributions for interaction types

CCQE

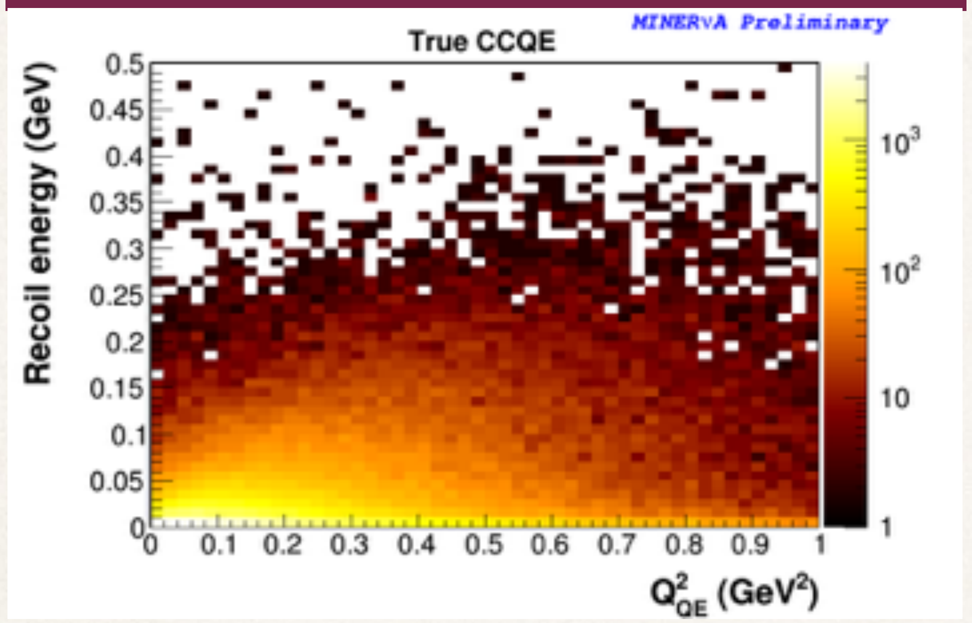

2p2h (CCQE from correlated pair)

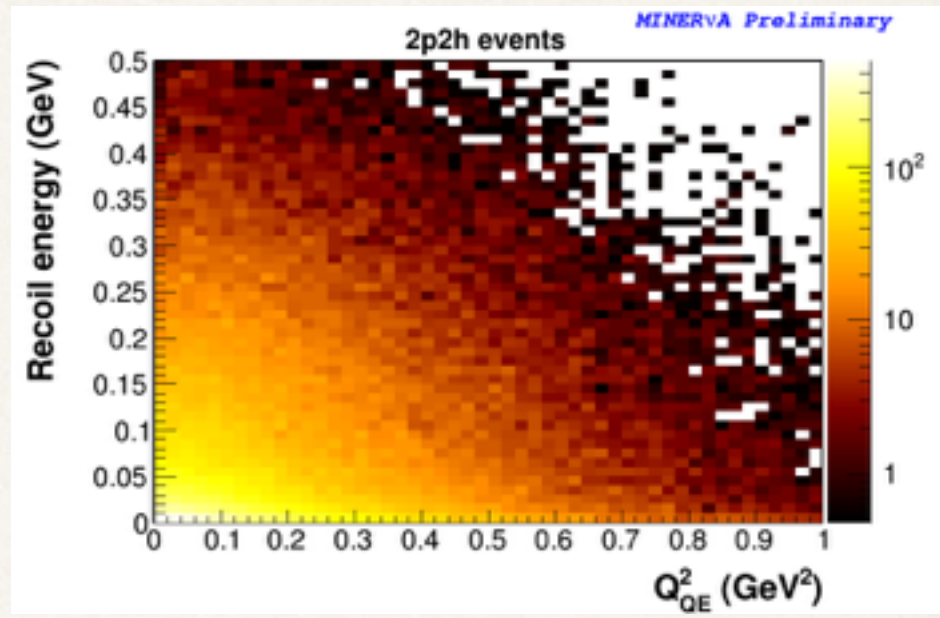

CCQE

QE-like

Non-CCQE QE-like

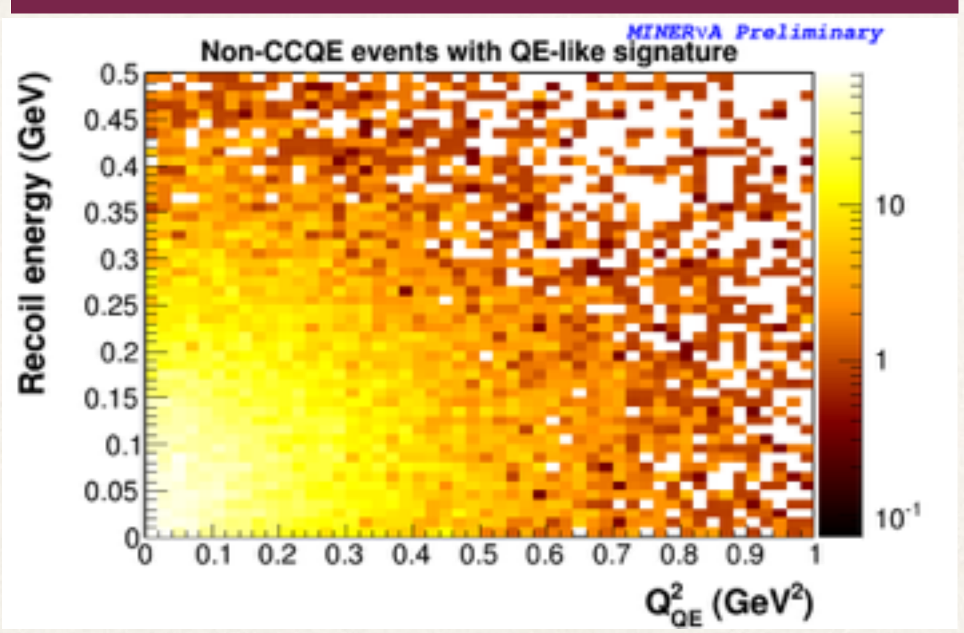

Backgrounds (pions or >120MeV protons)

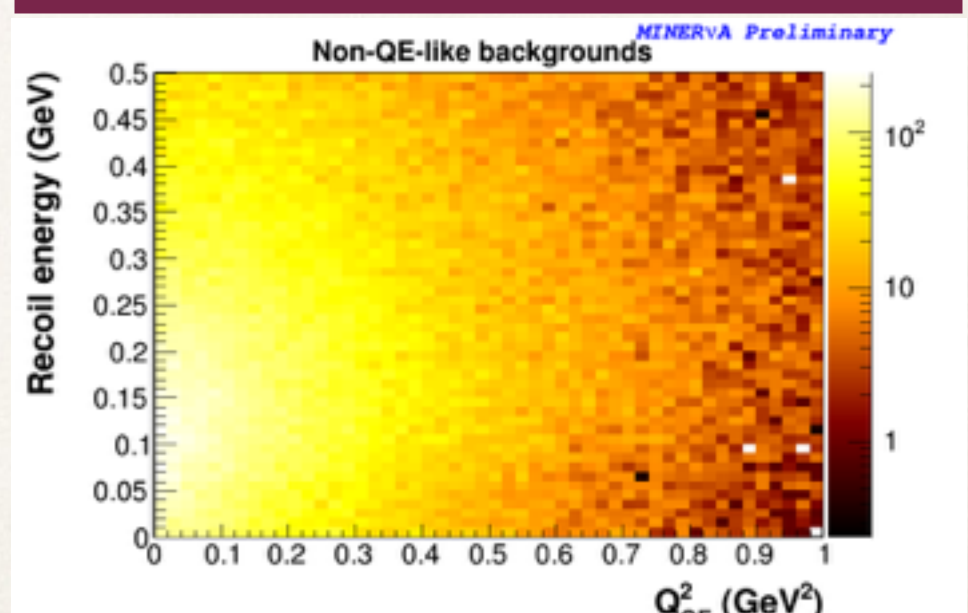

MINERvA's detector is so awesome, it can distinguish all these categories!

… but not optimally with today's cut-based analysis

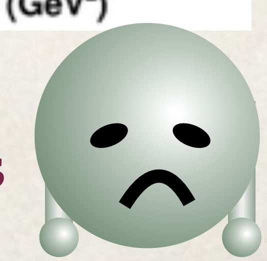

True "recoil" distributions

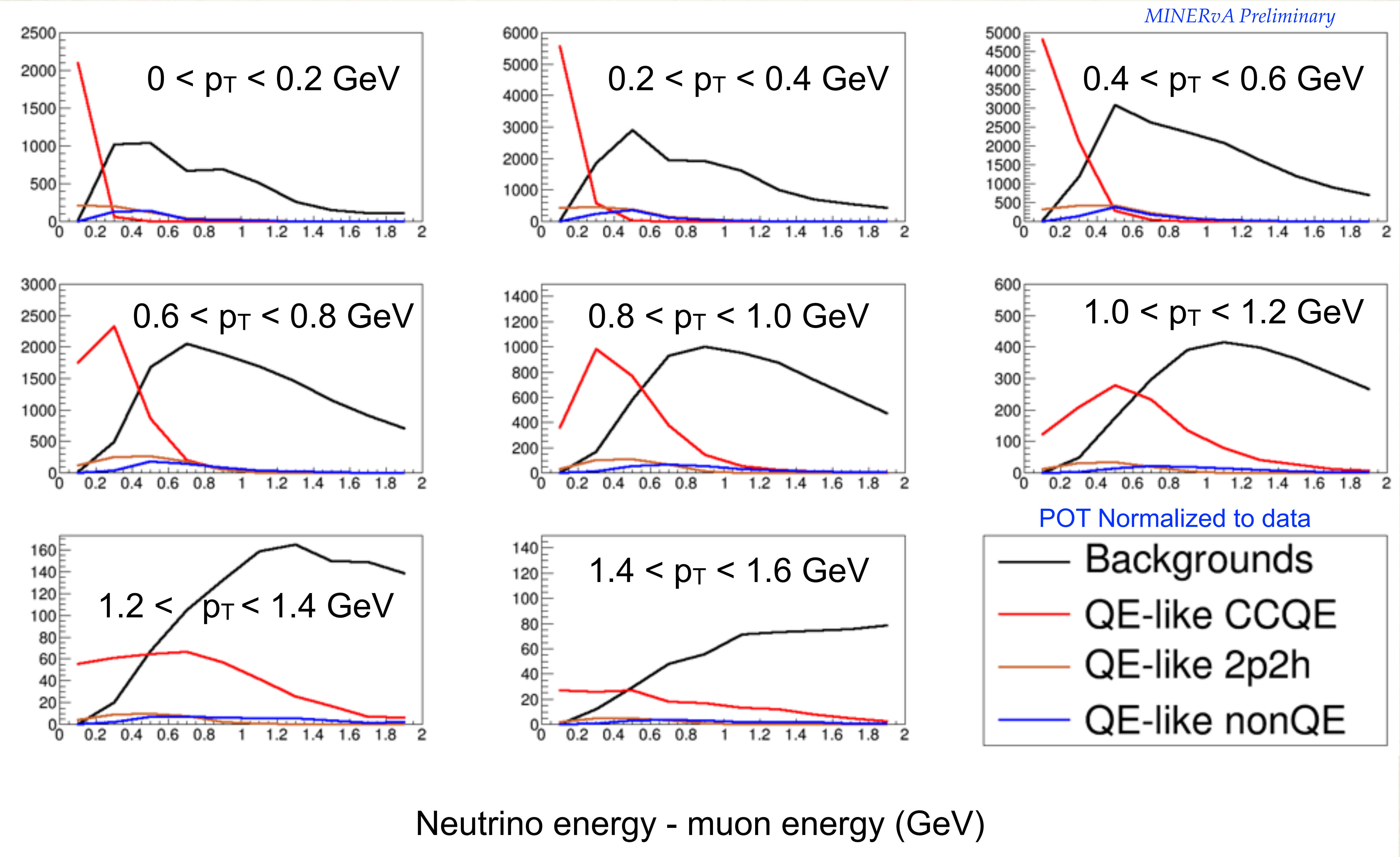

Learning from this uncertainty

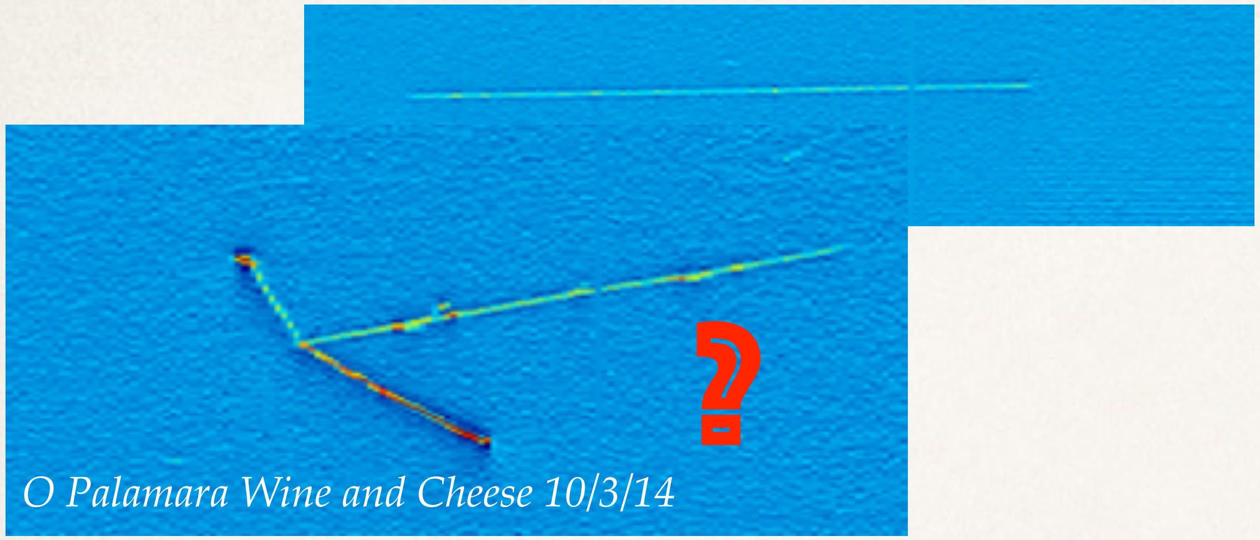

Experiments that can see nucleons must think hard about how to define "CCQE", and an observable to match

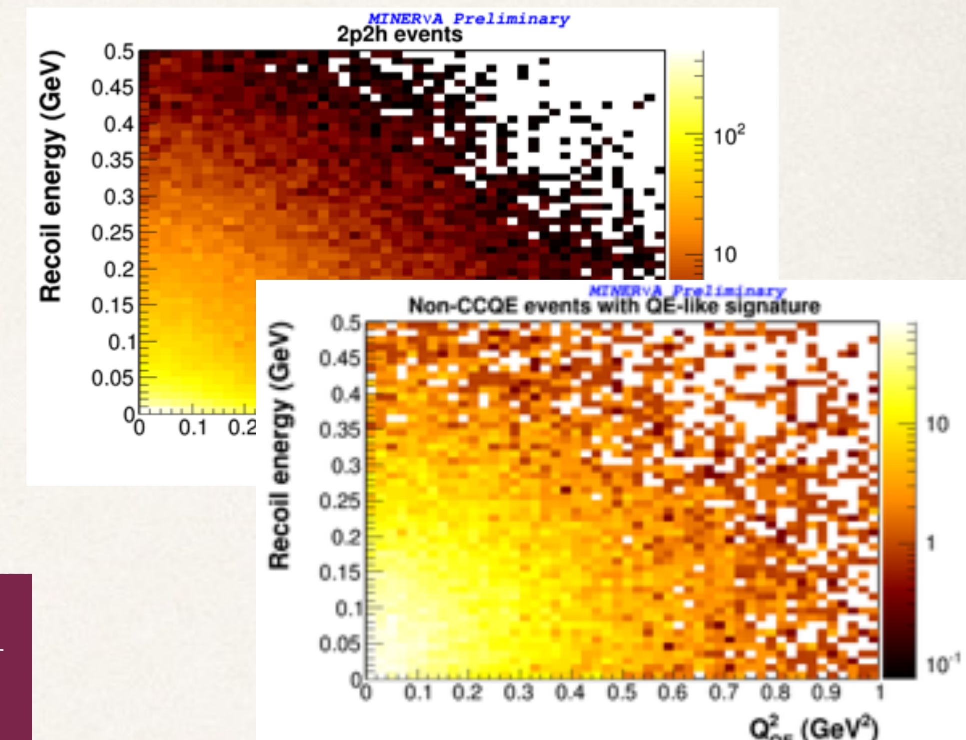

A simple calorimetric recoil cut can't select one category and reject others

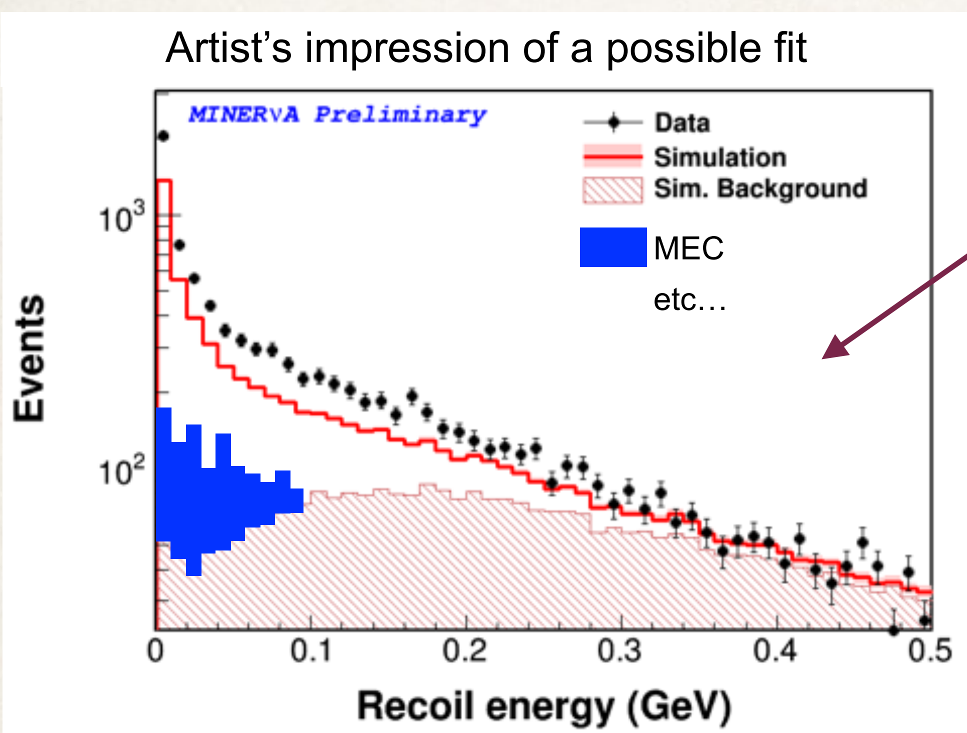

Artist's impression of a possible fit

Possible solution: replace recoil cut with a fraction fit to data of each component's simulated shape - an extended version of our background fit

This is a work in progress

QE-like cross section in muon kinematics

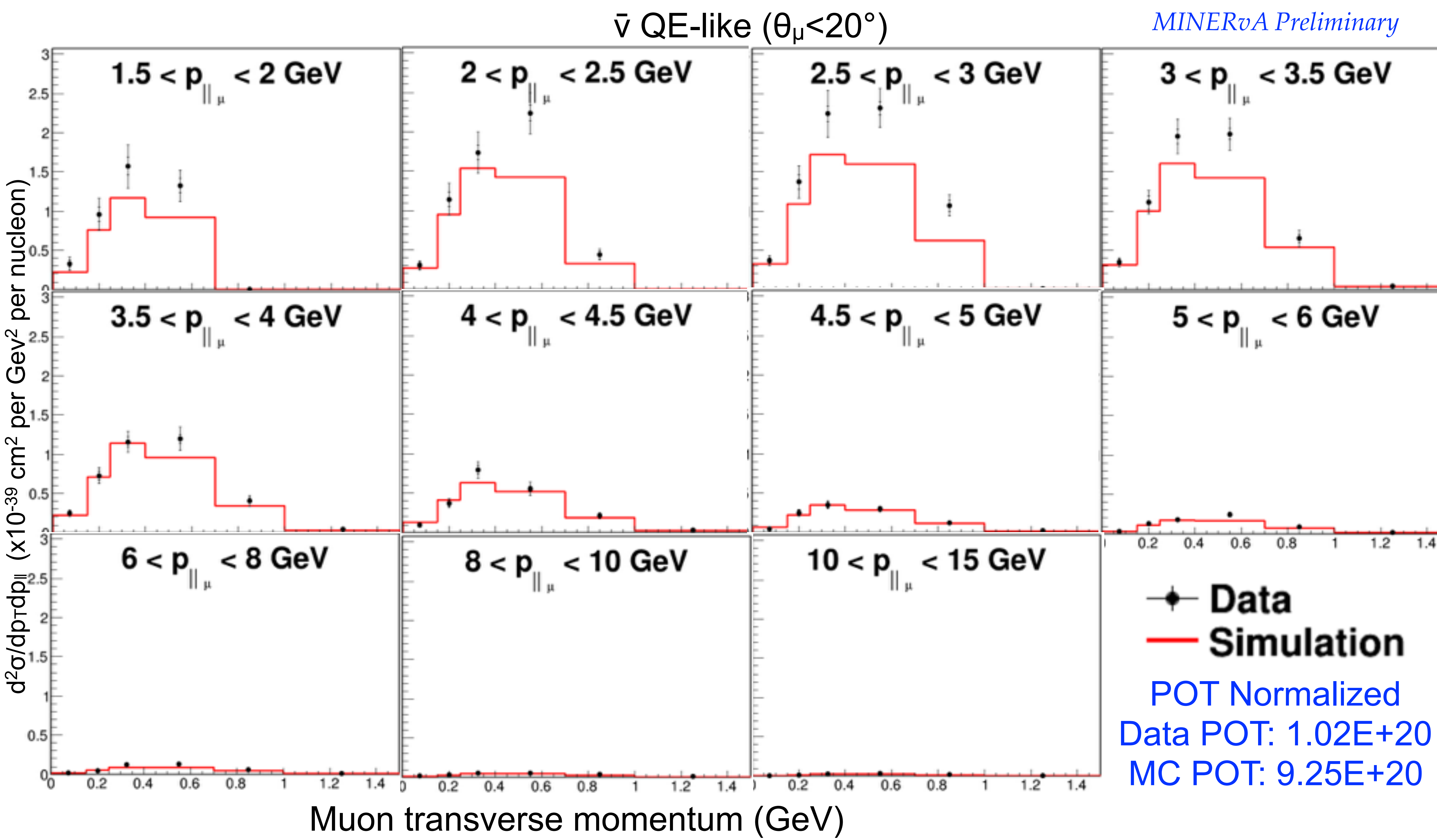

Zoom to see the shape: 1.5<p$_\parallel$<4.5 GeV

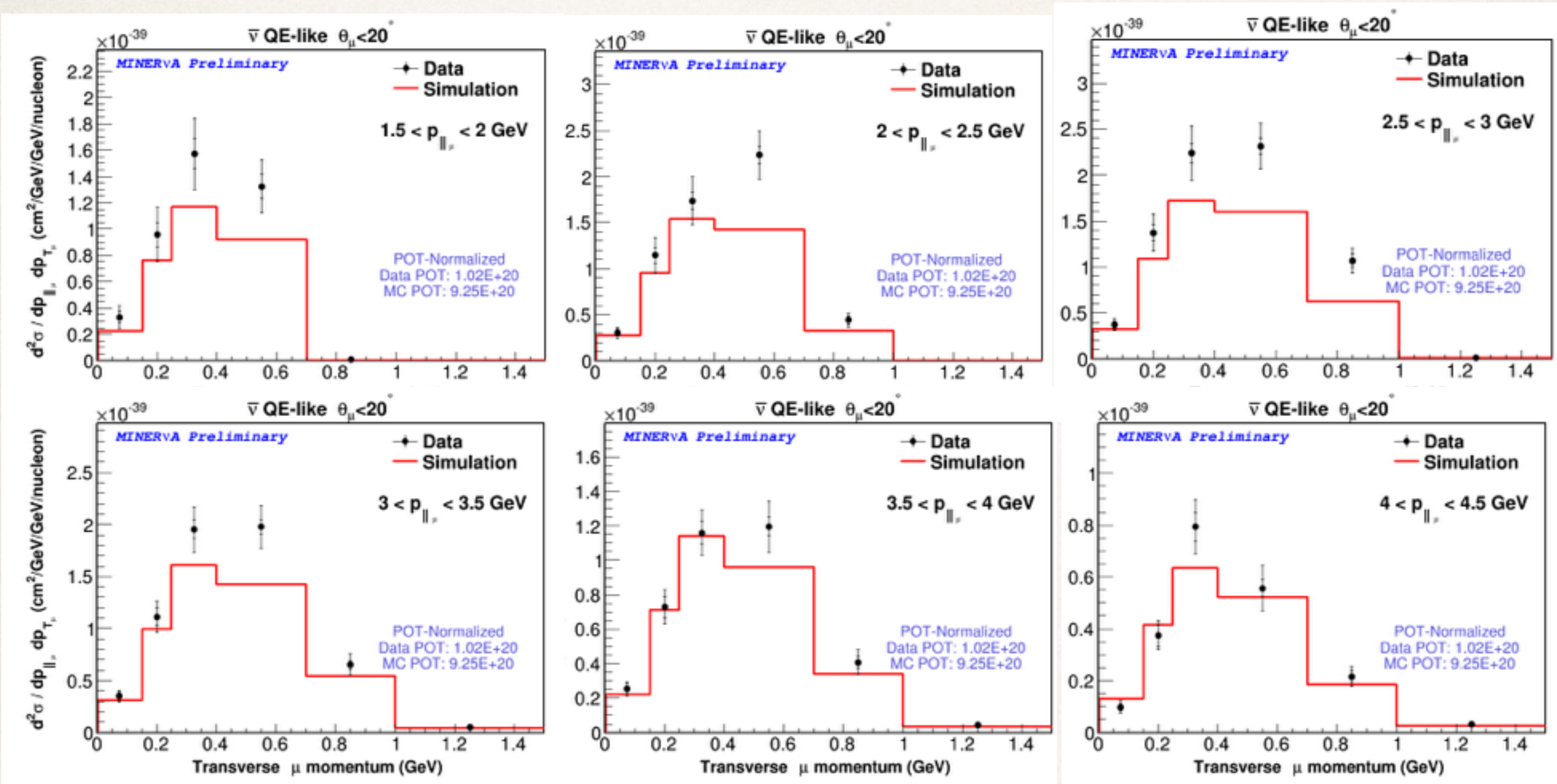

Zoom to see the shape: 1.5<$p_{\parallel}$<4.5 GeV

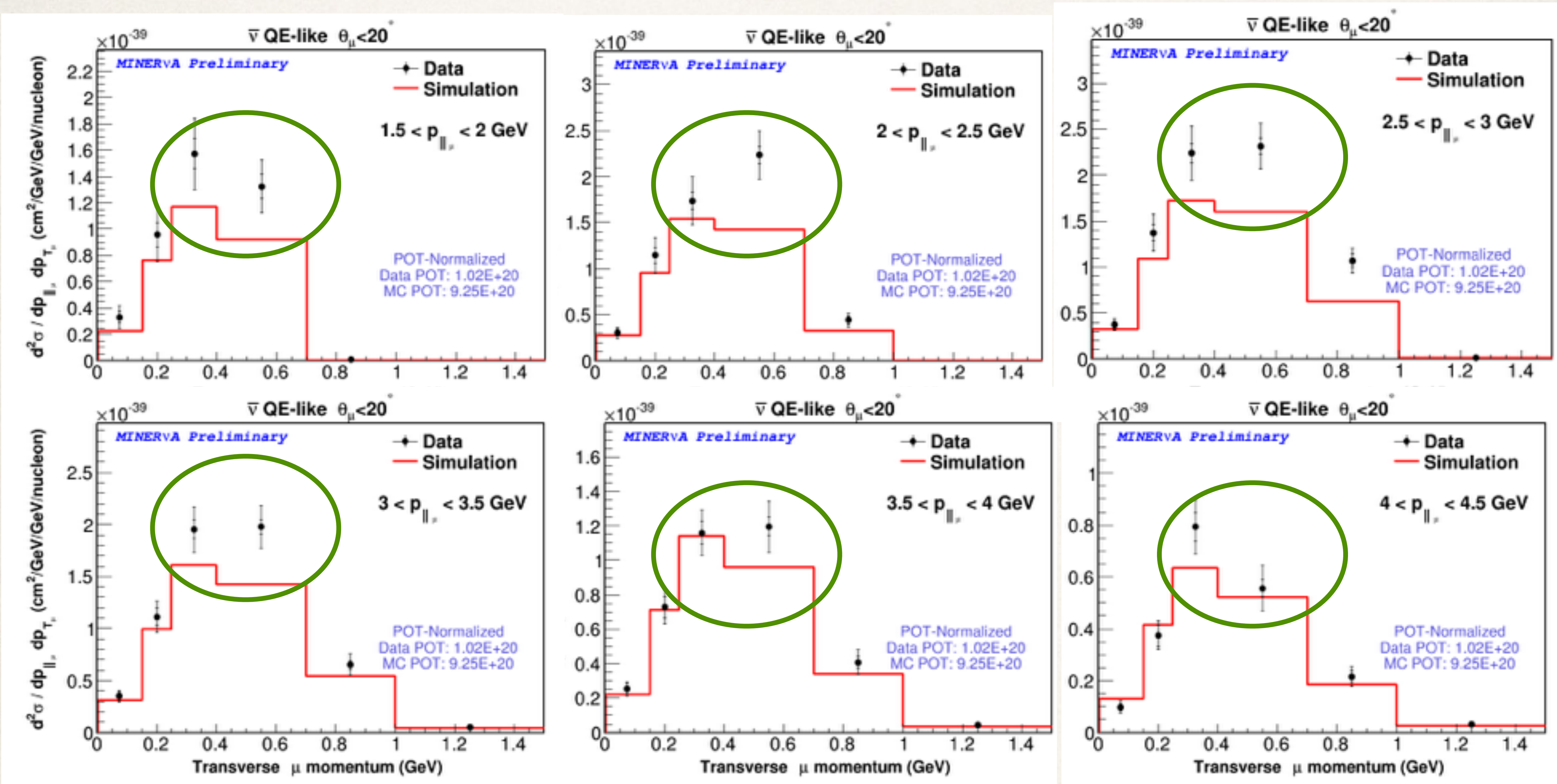

Zoom to see the shape: 4.5<p$_{\parallel}$<15 GeV

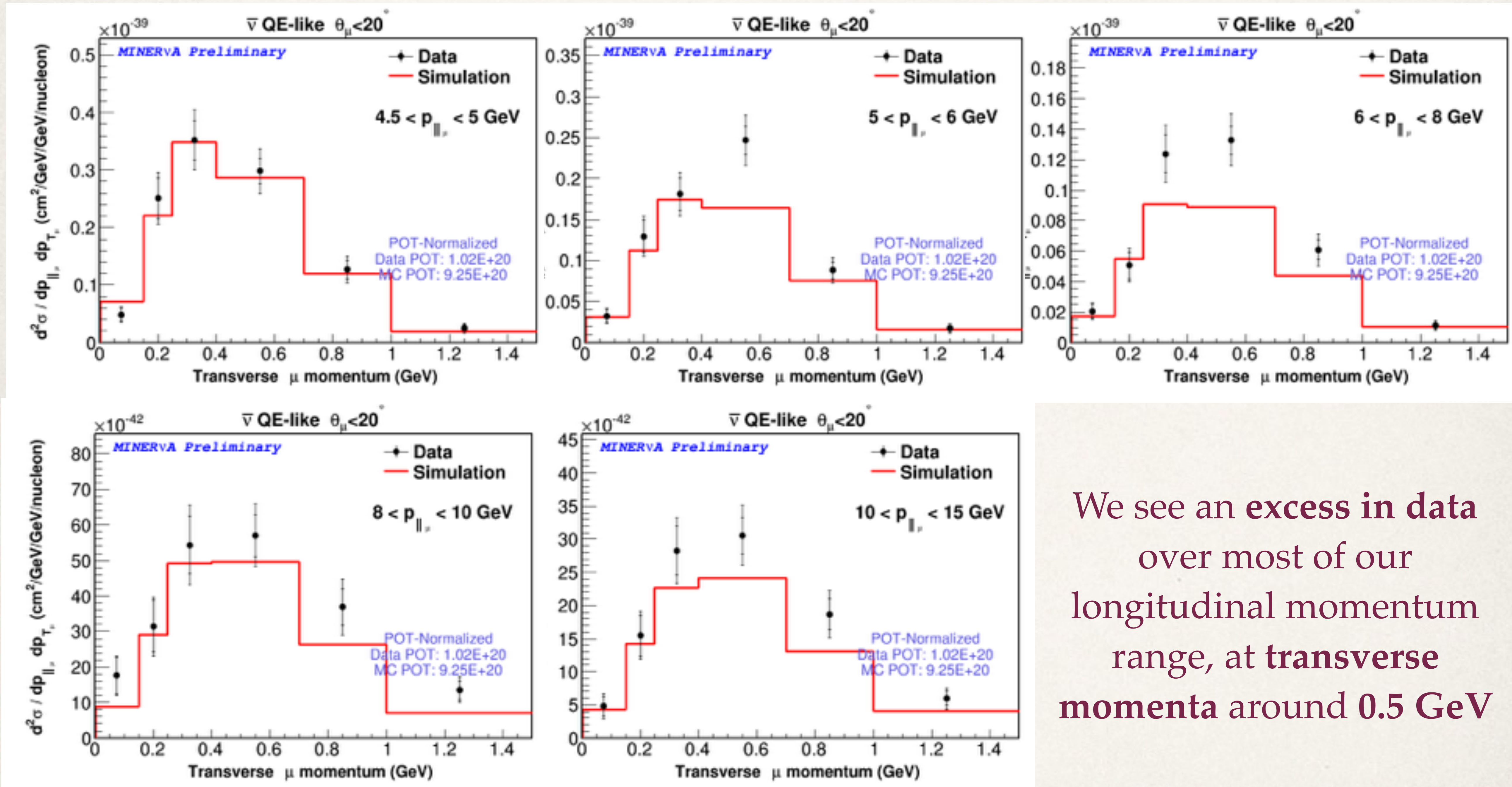

We see an **excess in data** over most of our longitudinal momentum range, at **transverse momenta** around **0.5 GeV**

Zoom to see the shape: $4.5<p_{\parallel}<15$ GeV

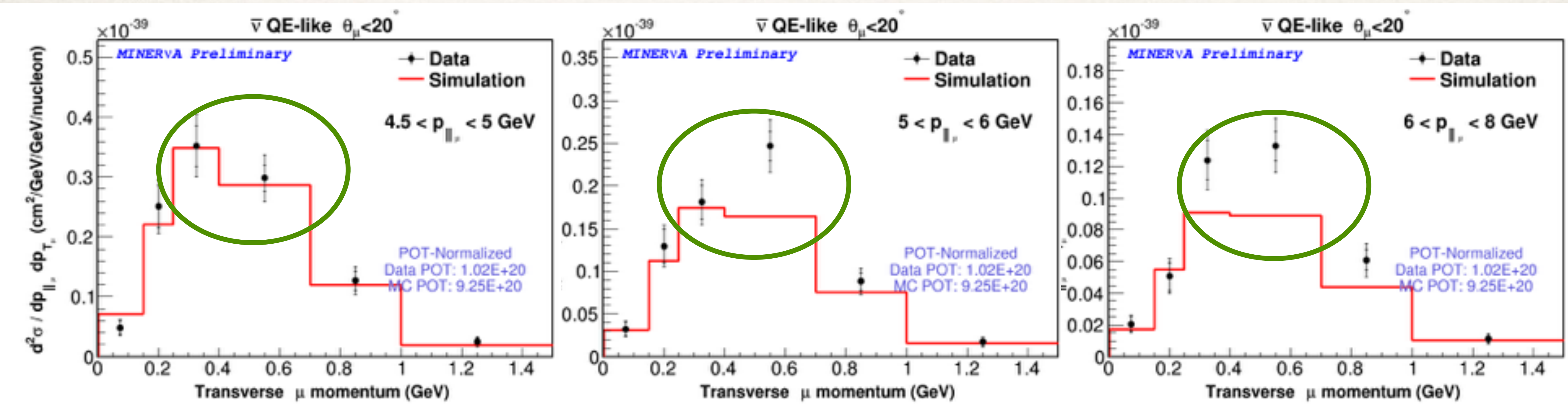

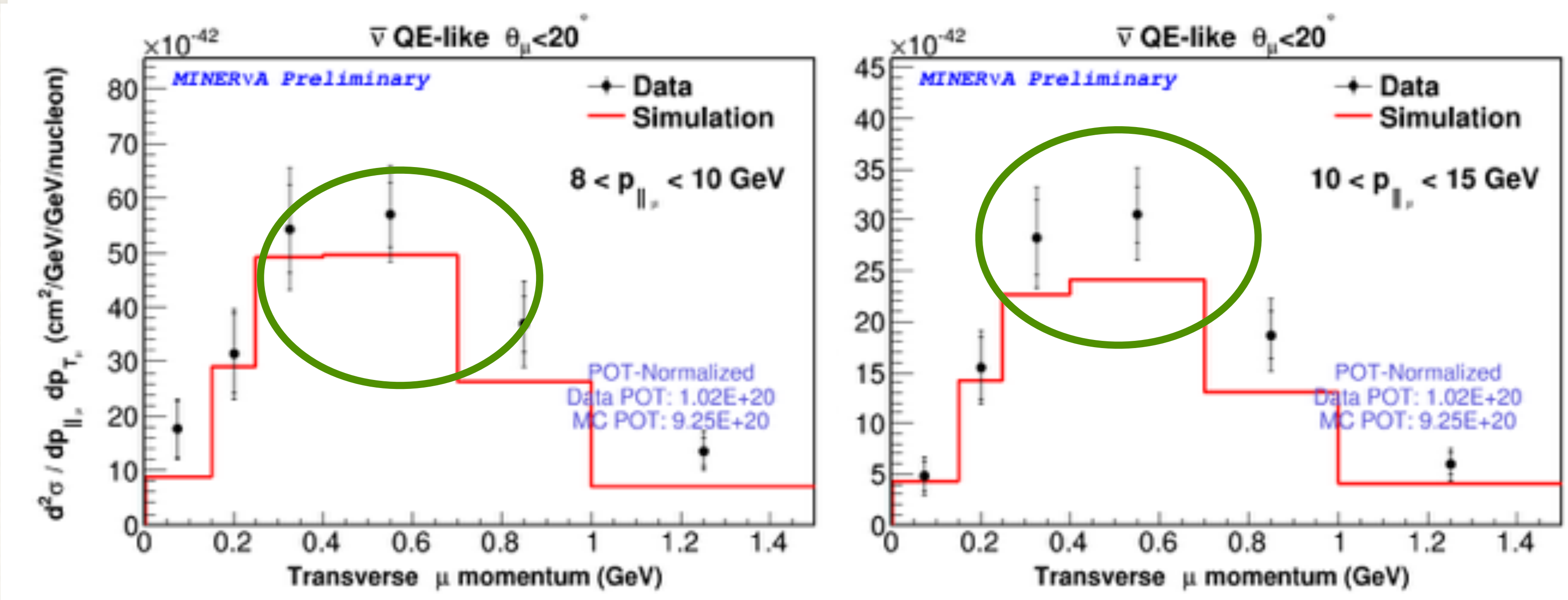

We see an **excess in data** over most of our longitudinal momentum range, at **transverse momenta** around **0.5 GeV**

Similar effects in neutrino-mode study

On December 11, 2015,Phil Rodrigues presented a similar excess in MINERvA's neutrino data at CCQE-dominated energies

While this analysis explored a different phase space, the regions with excess corresponded to a muon transverse momentum around 0.5 GeV

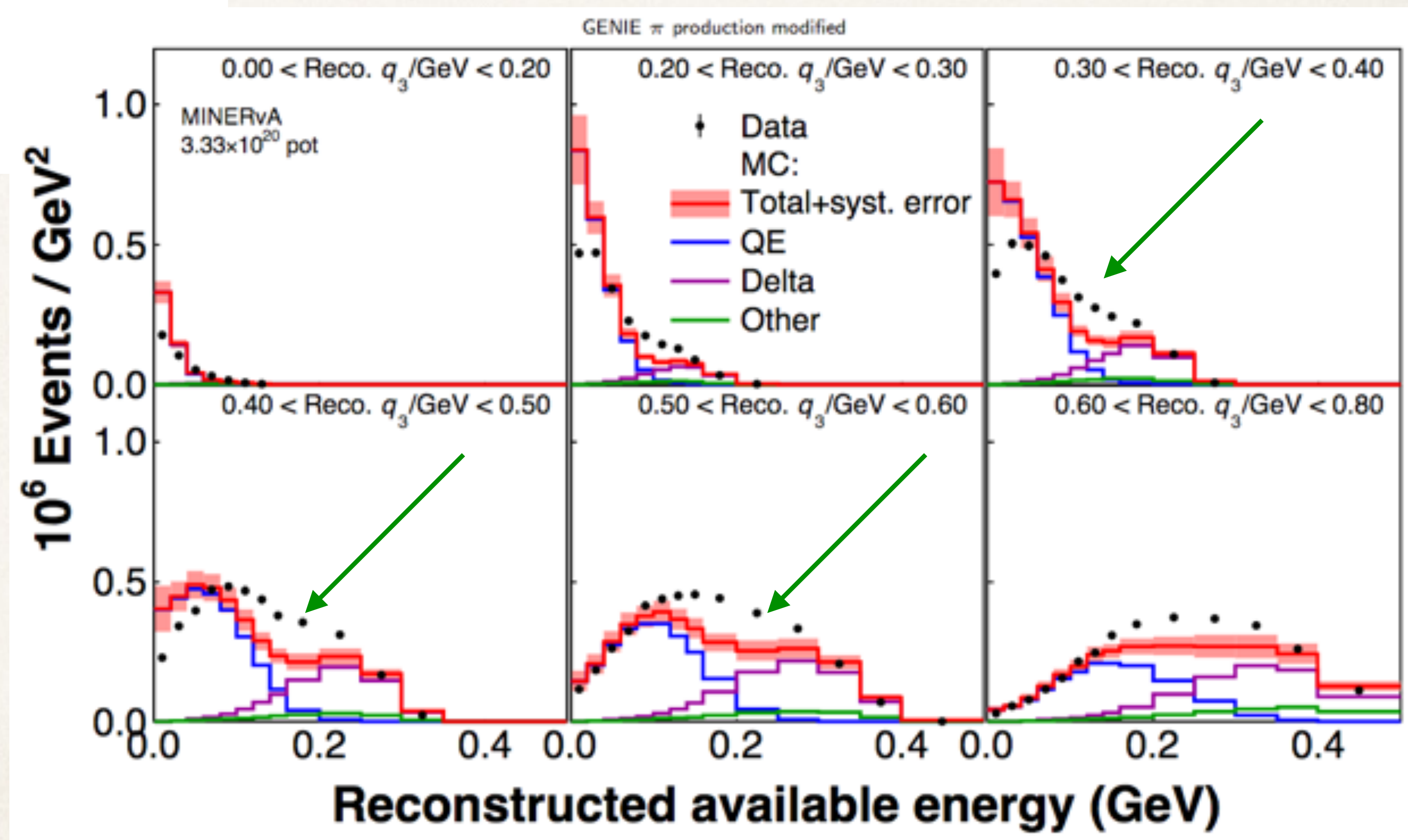

$d\sigma(E_\nu^{QE})/dQ^2_{QE}$ (flux weighted)

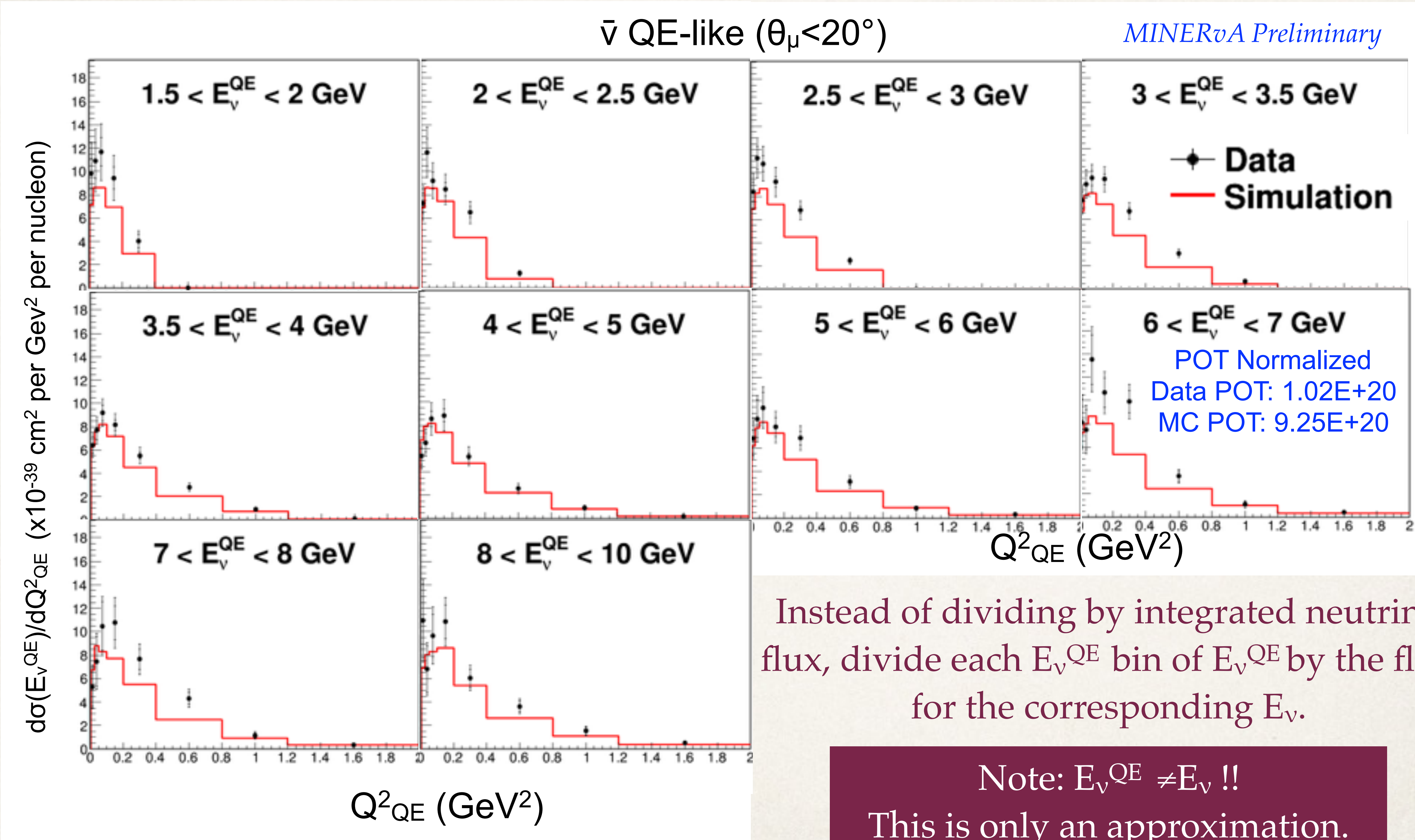

Instead of dividing by integrated neutrino flux, divide each E_ν^{QE} bin of E_ν^{QE} by the flux for the corresponding E_ν.

Note: $E_\nu^{QE} \neq E_\nu$!!
This is only an approximation.

Fiducial QE-like cross section $\sigma(E_\nu^{QE})$

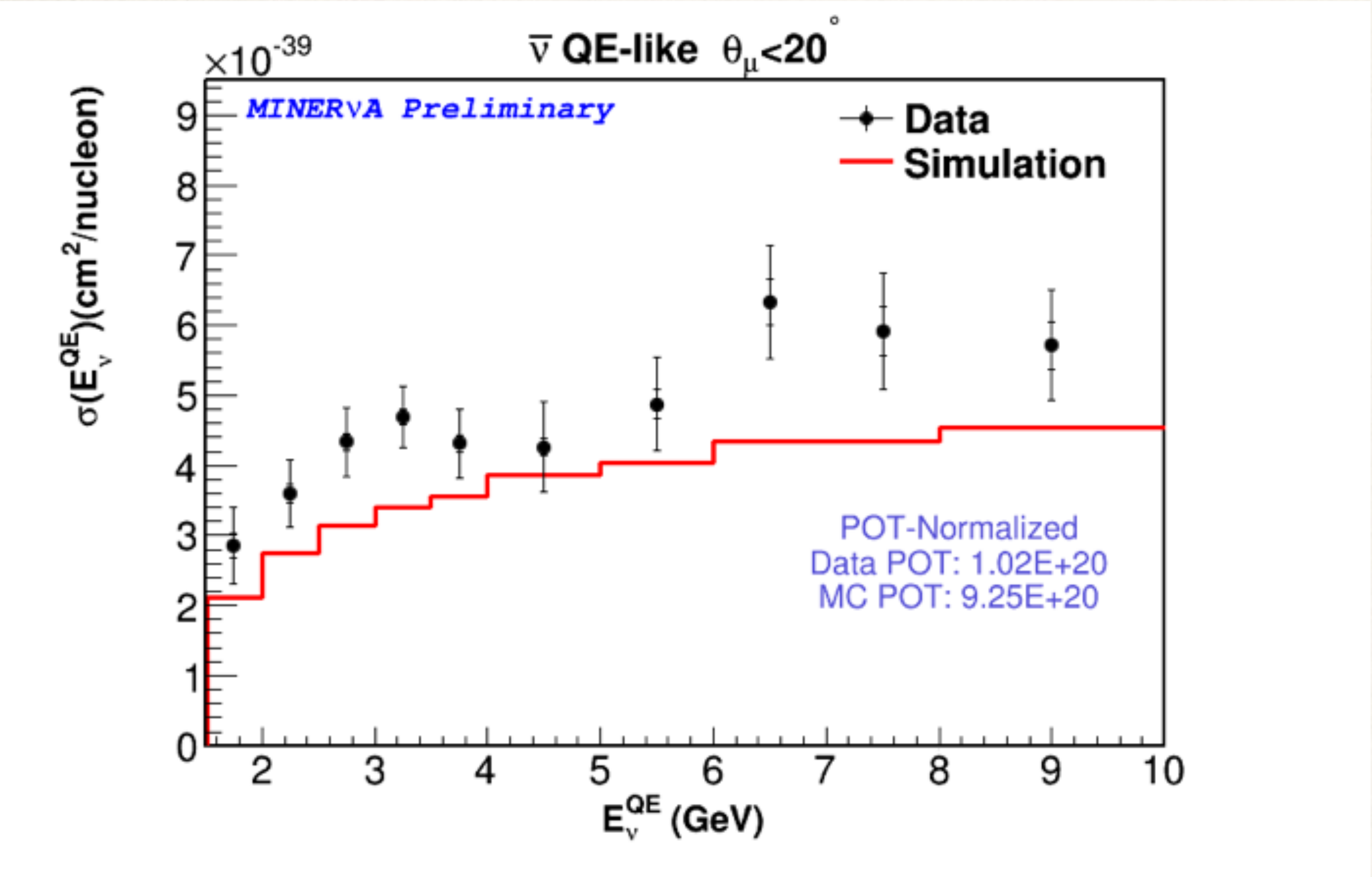

Again, using our flux profile in E_ν, we can generate an approximate total cross section vs. the neutrino energy E_ν^{QE} by scaling the event rate in each energy bin by that bin's total neutrino flux. Once more, note that this is **not exact** as $E_\nu^{QE} \neq E_\nu$

Compare with other experiments

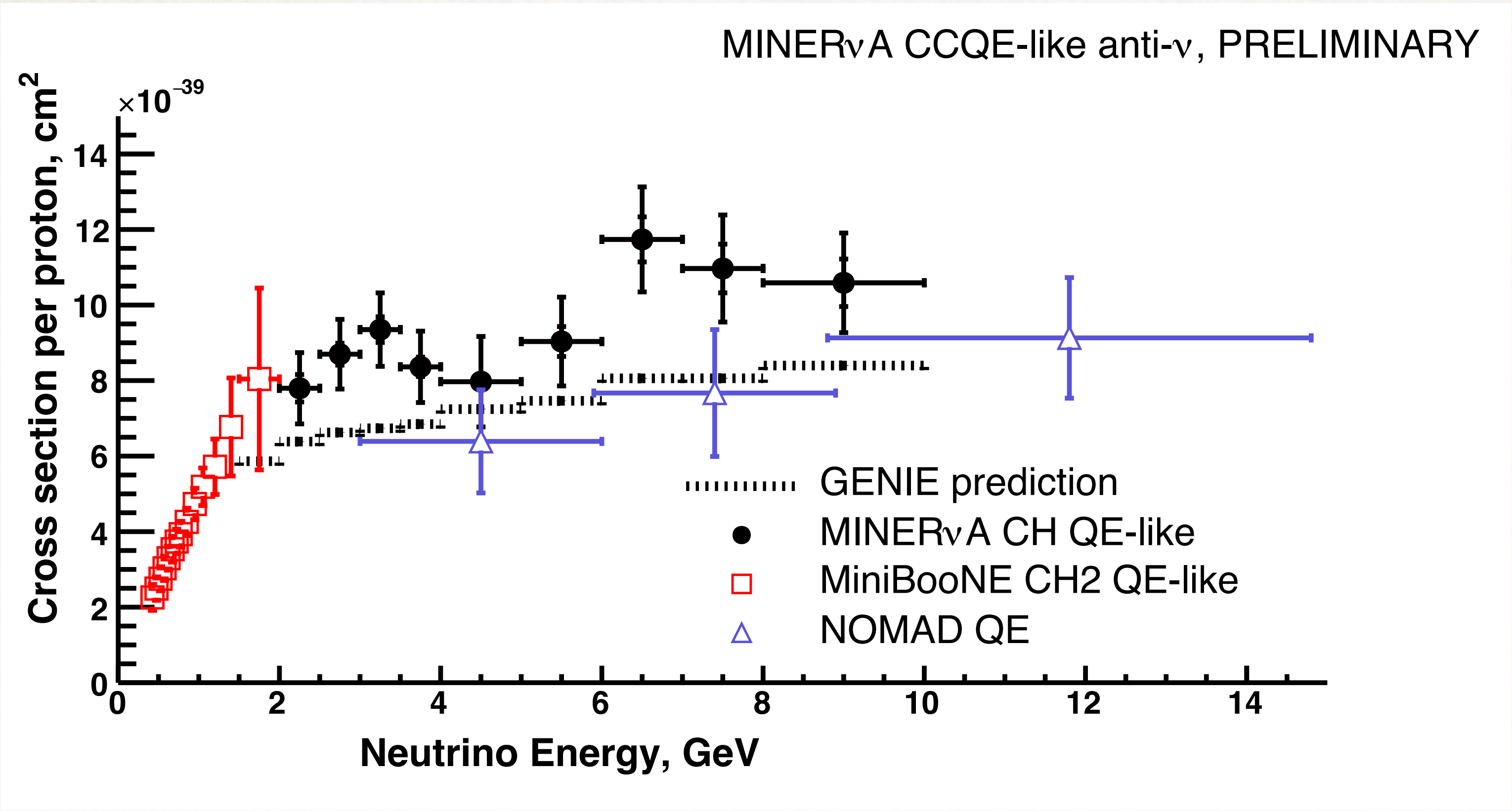

The first hints of problems with the Fermi gas model came from the disagreement between MiniBooNE and NOMAD results.We cautiously compare our QE-like cross section $\sigma(E_\nu^{QE})$ with those of the previous experiments, but remember…

NB: corrected to full acceptance (no angle restriction) for a more like-to-like comparison

- The three experiments use **different CCQE/CCQE-like signal definitions**
- Our "neutrino energy" is **not true neutrino energy**, but E_ν^{QE}. MiniBooNE, however, corrects its data to true E_ν.
- However, we divide by a flux that IS a function of true E_ν.
- MINERvA's cross section is on **scintillator** (CH), MiniBooNE's on **mineral oil** (CH_2)
- MINERvA appears to favor MiniBooNE's curve, but are we comparing like with like?

A.A. Aguilar-Arevalo et al. (MiniBooNE collaboration) Phys.Rev. D88 (2013) no.3, 032001 (2013)

V. Lyubushkin et al. (NOMAD collaboration) Eur. Phys. J. C 63, 355 (2009)

Muon-kinematics cross section vs. generators

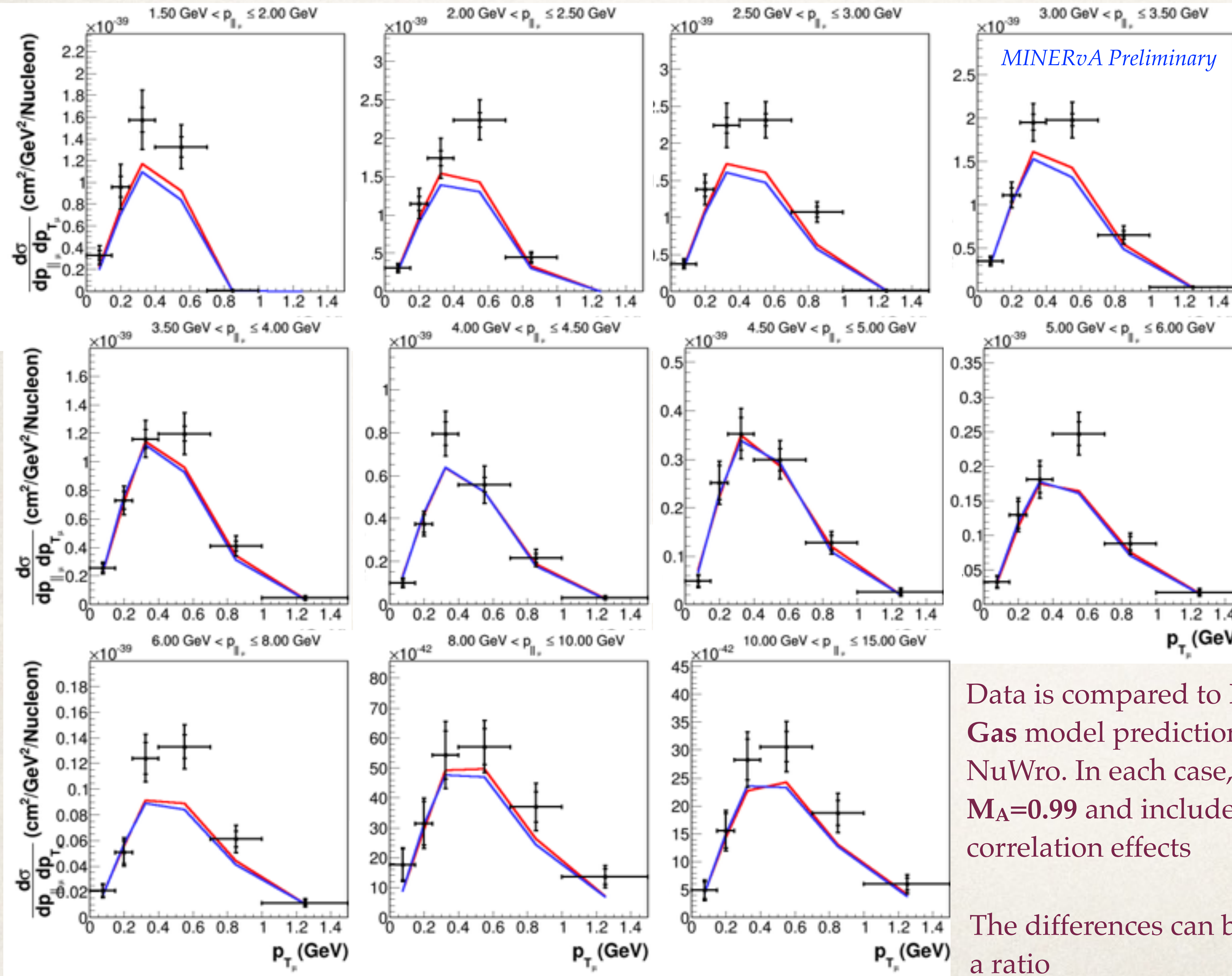

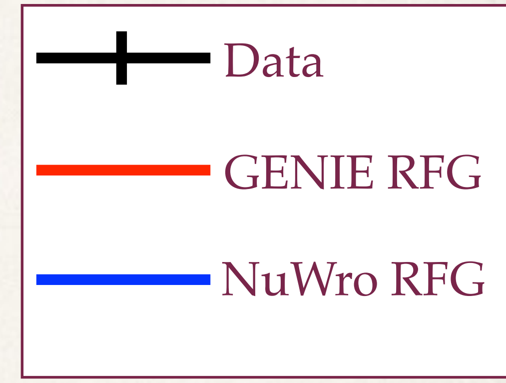

Data is compared to **Relativistic Fermi Gas** model predictions from GENIE and NuWro. In each case, the generators take **M_A=0.99** and include **no 2p2h or RPA** correlation effects

The differences can be seen more easily in a ratio

Comparisons with two generators

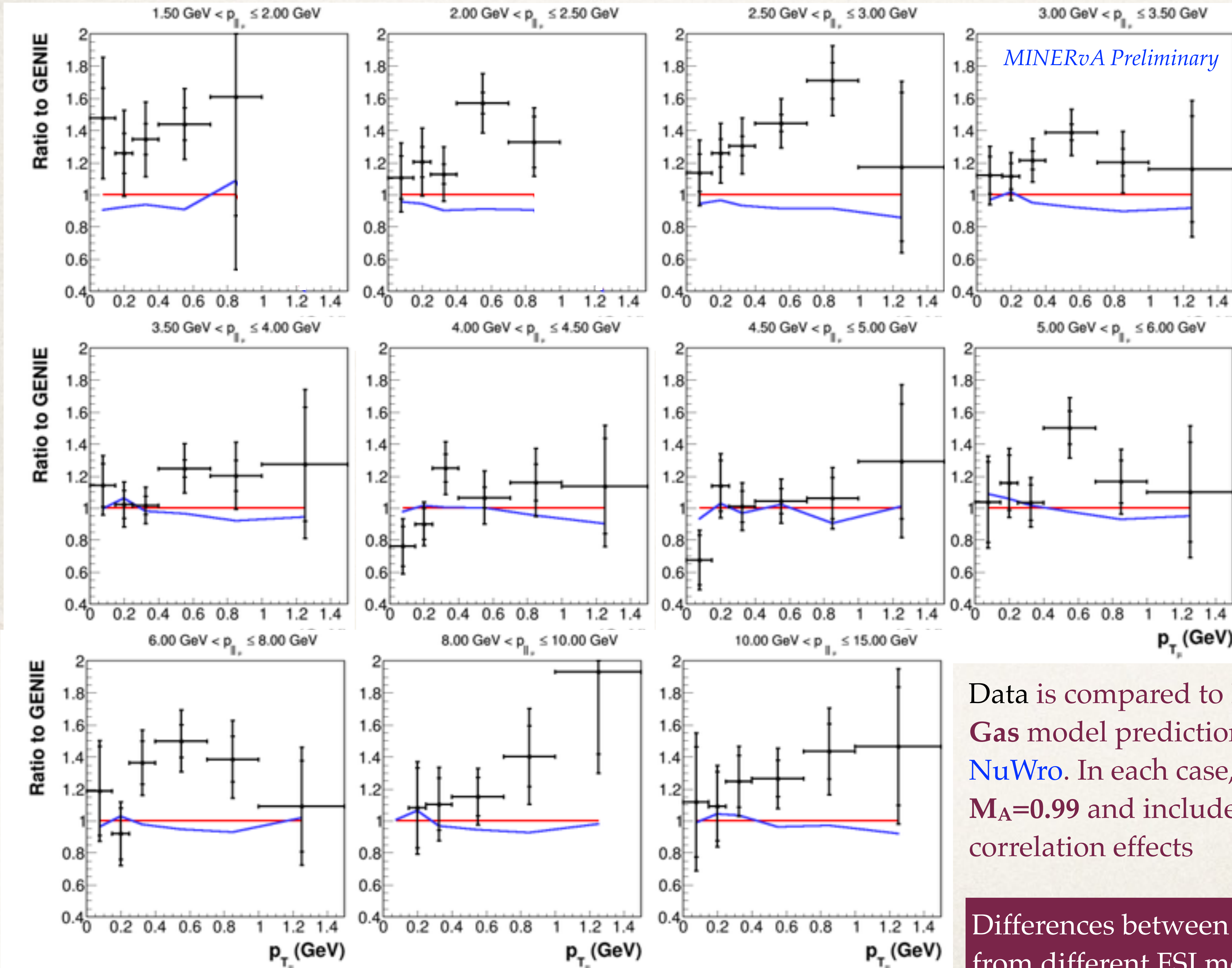

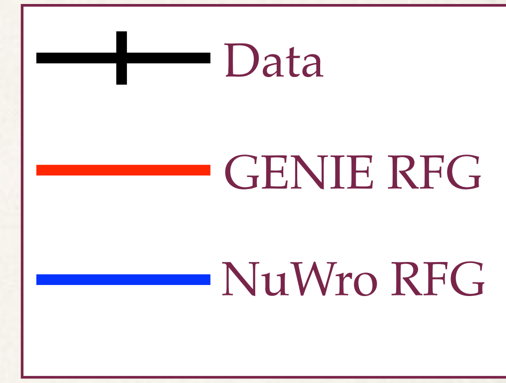

Data is compared to **Relativistic Fermi Gas** model predictions from GENIE and NuWro. In each case, the generators take **M_A=0.99** and include **no 2p2h or RPA** correlation effects

Differences between the generators stem from different FSI models.

Alternative nuclear models

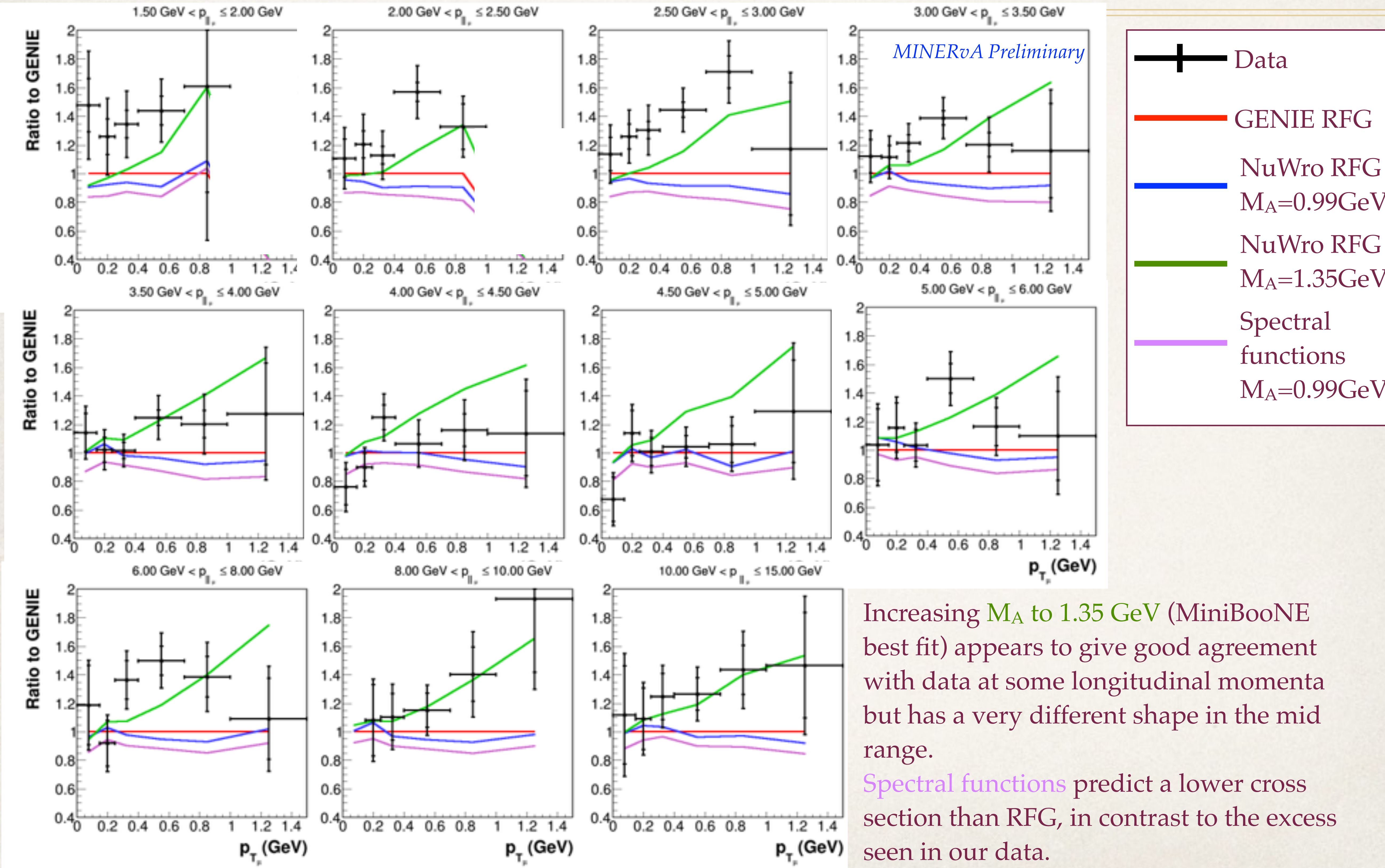

Increasing M_A to 1.35 GeV (MiniBooNE best fit) appears to give good agreement with data at some longitudinal momenta but has a very different shape in the mid range.

Spectral functions predict a lower cross section than RFG, in contrast to the excess seen in our data.

Adding 2p2h effects

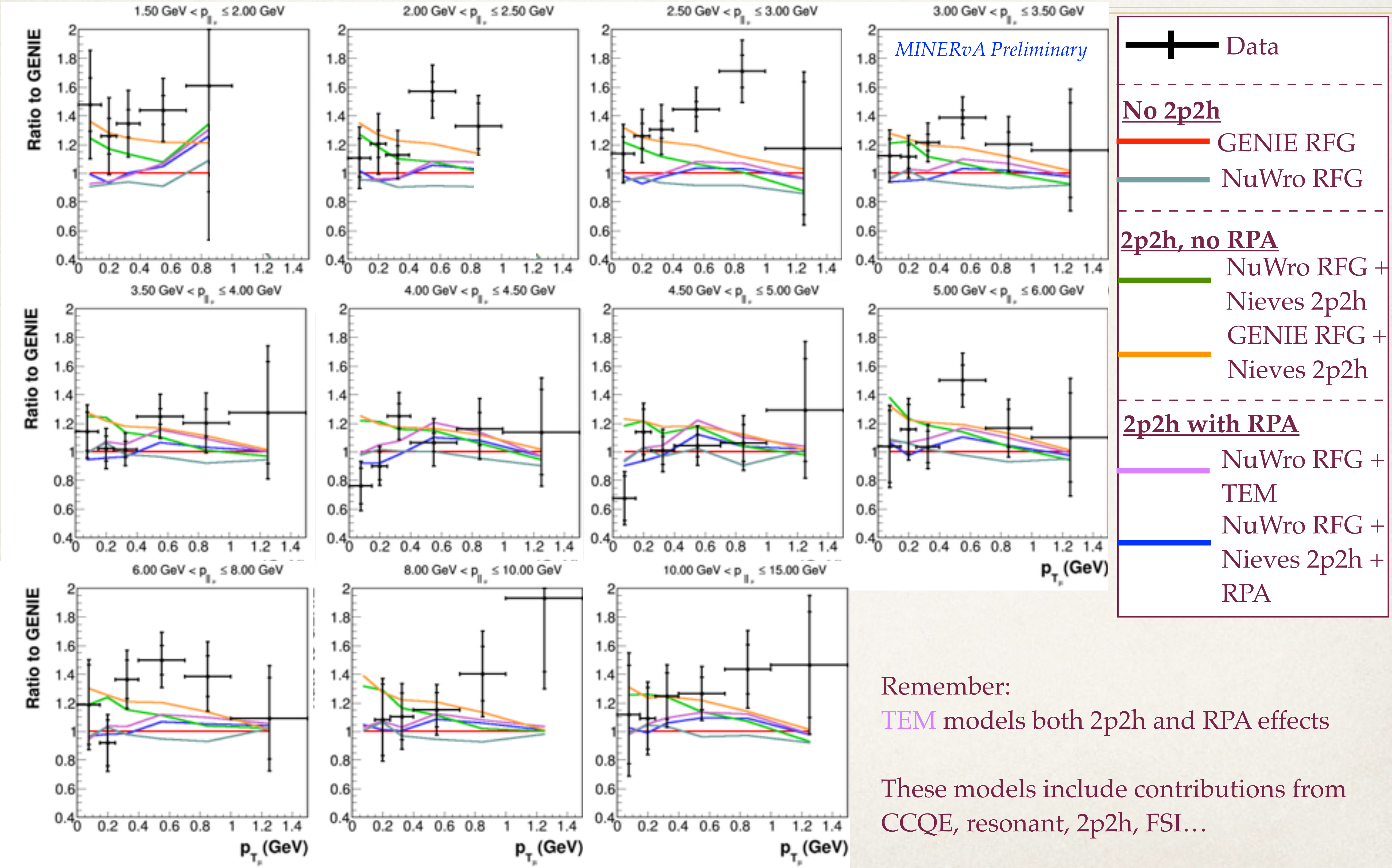

Remember:
TEM models both 2p2h and RPA effects

These models include contributions from CCQE, resonant, 2p2h, FSI…

χ^2 comparisons with models

Model	χ^2	/DOF (66)
1. RFG + Nieves + RPA	83.7	1.27
2. GENIE RFG	92.4	1.40
3. LFG + TEM	96.9	1.47
4. RFG + TEM	99.4	1.51
5. Spectral functions	100.3	1.52
6. NuWro RFG M_A = 1.35 GeV	109.3	1.66
7. NuWro RFG	114.1	1.73
8. GENIE+ Nieves, no RPA	129.5	1.96
9. RFG +Nieves, no RPA	157.5	2.39

χ^2 takes into account correlations between bins. To see greater differences between models, we should constrain systematics, especially the 2p2h

χ^2 comparisons with models

Model	χ^2	/DOF (66)
1. RFG + Nieves + RPA	83.7	1.27
2. GENIE RFG	92.4	1.40
3. LFG + TEM	96.9	1.47
4. RFG + TEM	99.4	1.51
5. Spectral functions	100.3	1.52
6. NuWro RFG M_A = 1.35 GeV	109.3	1.66
7. NuWro RFG	114.1	1.73
8. GENIE+ Nieves, no RPA	129.5	1.96
9. RFG +Nieves, no RPA	157.5	2.39

χ^2 takes into account correlations between bins. To see greater differences between models, we should constrain systematics, especially the 2p2h

- 2p2h models that include RPA are a better match to data than those that do not

χ^2 comparisons with models

Model	χ^2	/DOF (66)
1. RFG + Nieves + RPA	83.7	1.27
2. GENIE RFG	92.4	1.40
3. LFG + TEM	96.9	1.47
4. RFG + TEM	99.4	1.51
5. Spectral functions	100.3	1.52
6. NuWro RFG M_A = 1.35 GeV	109.3	1.66
7. NuWro RFG	114.1	1.73
8. GENIE+ Nieves, no RPA	129.5	1.96
9. RFG +Nieves, no RPA	157.5	2.39

χ^2 takes into account correlations between bins. To see greater differences between models, we should constrain systematics, especially the 2p2h

- 2p2h models that include RPA are a better match to data than those that do not
- GENIE and NuWro have differences in their modeling of the same processes: both RFG and RFG + Nieves 2p2h

Summary

- We have measured MINERvA's **first $\bar{\nu}$ double-differential cross sections**, for quasi-elastic-like scattering on plastic scintillator, in DUNE's energy range

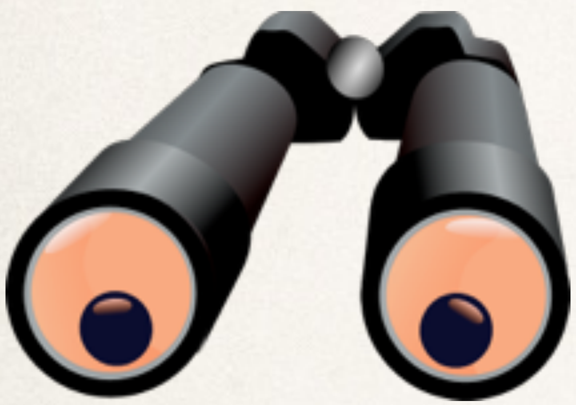

- We see an excess compatible with that seen by earlier neutrino mode analysis - look out for extra interactions when you run antineutrinos, NOvA!

- The complex spectrum of interactions in the CCQE regime presents a reconstruction challenge
  - we have some signal model dependency
  - but we are gaining new insights into these processes
  - oscillation experiments with different acceptances for these processes must be aware!

By J. Howard Miller, for Westinghouse, https://commons.wikimedia.org/w/index.php?curid=5249733

Backup slides

Alternatives to RFG model: Local Fermi Gas

- The "global" relativistic Fermi gas model treats nucleons as if they are in a constant potential well, as shown in the cartoon
- In the local Fermi gas model, this potential is modified based on position in the nucleus
- This is a 1-particle-1-hole effect - no pairs of nucleons

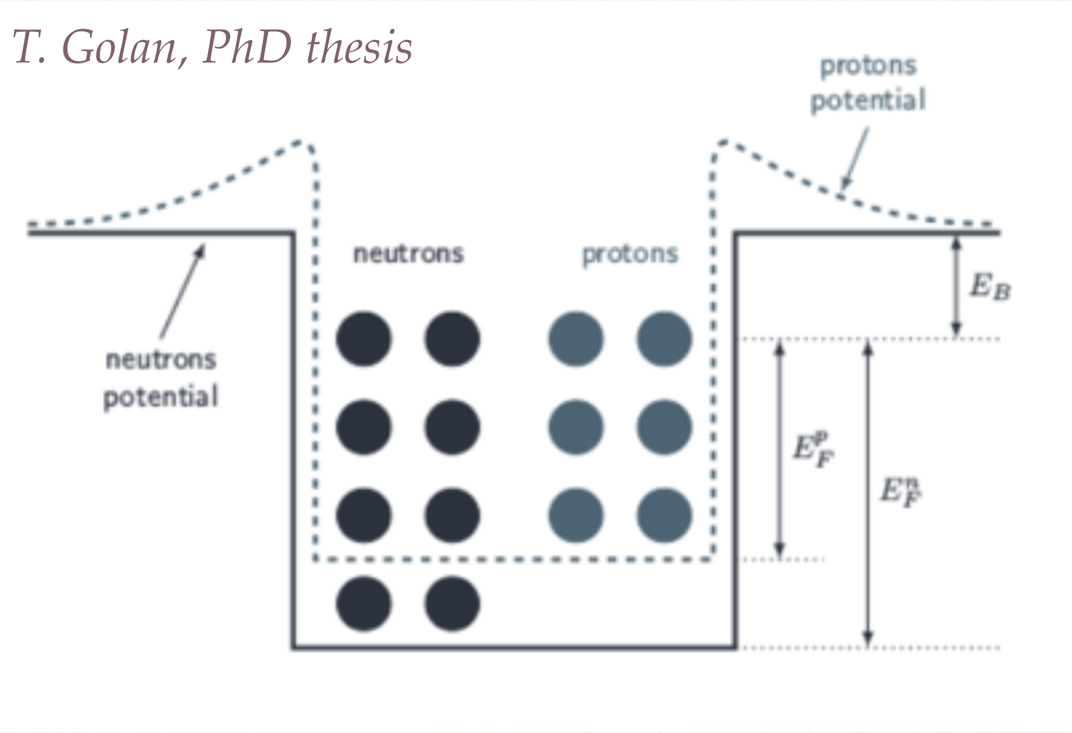

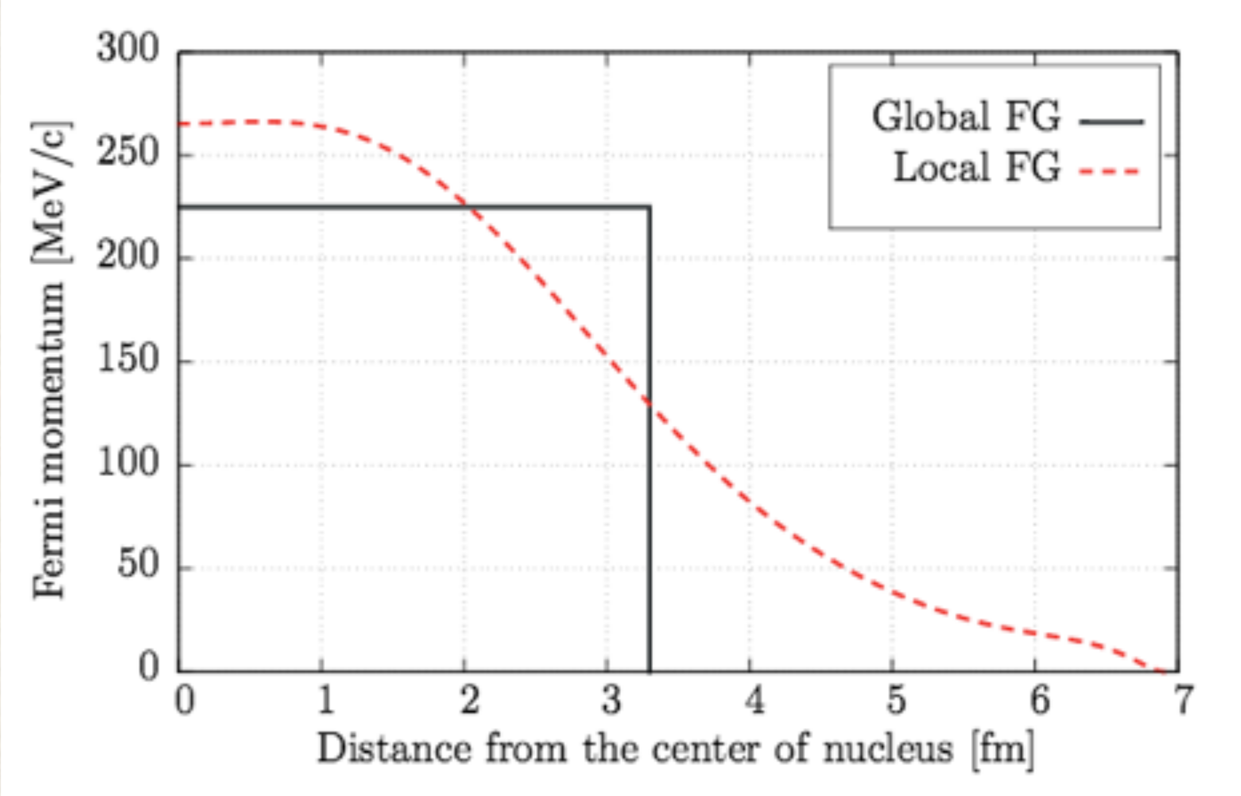

- The local Fermi gas model predicts a slightly higher cross section than the global relativistic Fermi gas

Improvements to RFG model: Spectral functions

- The spectral function describes the probability distribution for finding a particle with a given
  - momentum
  - removal energy
- It consists of a **single-particle** part and a **correlated-pair** part

T. Golan, PhD thesis

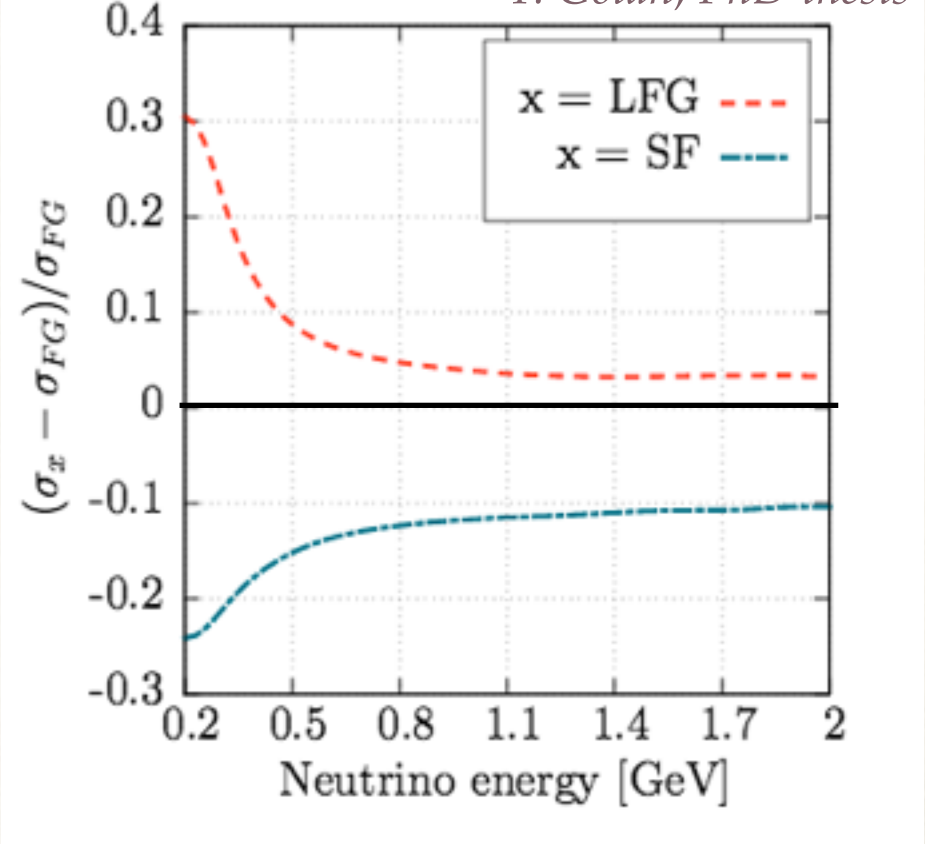

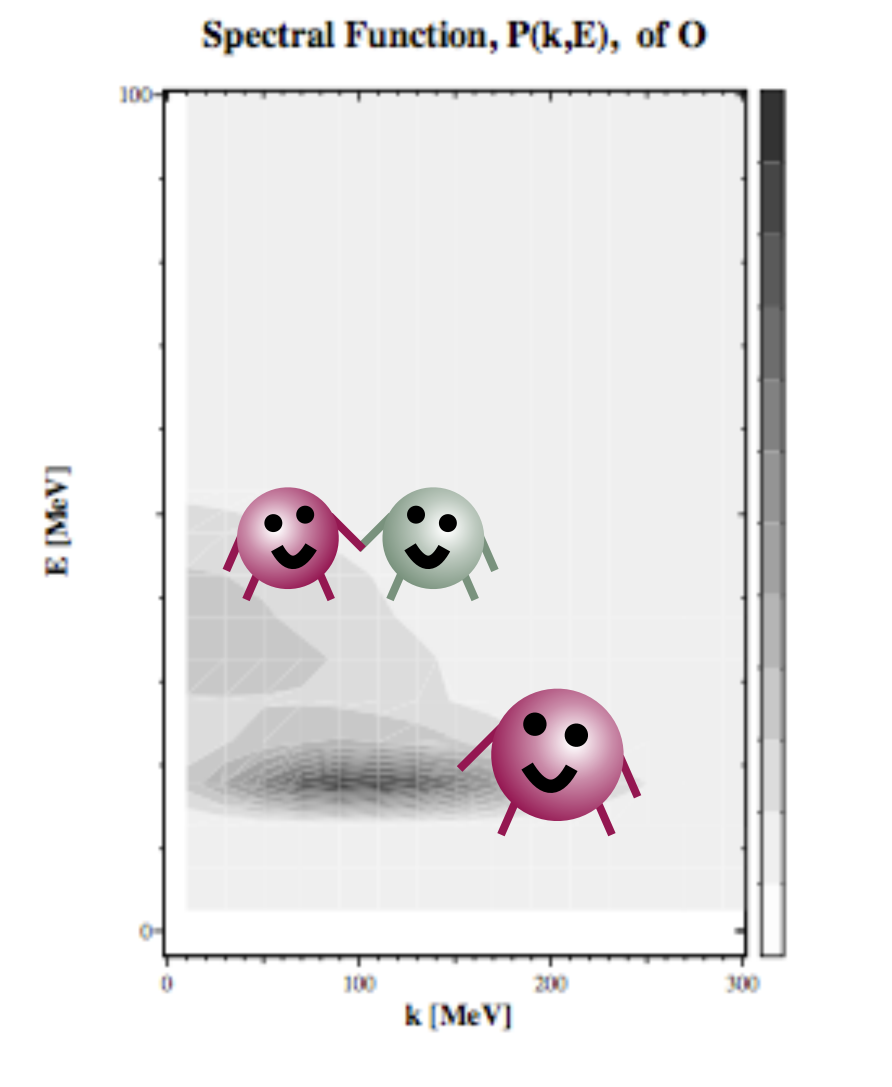

H. Nakamura & R.Seki, Nucl Phys B Proc. Supp 112, 1-3, 197-202 (2002)

- Spectral functions predict a slightly lower cross section than the global relativistic Fermi gas

Choosing a recoil cut for QE-like

Challenge: select a recoil cut for **maximum purity and efficiency** by varying the height of the **recoil cut shelf on the reconstructed data** and also varying the **threshold for the maximum proton kinetic energy** in the signal definition

Raising the **recoil shelf** decreases purity but increases acceptance for non-QE QE-like events

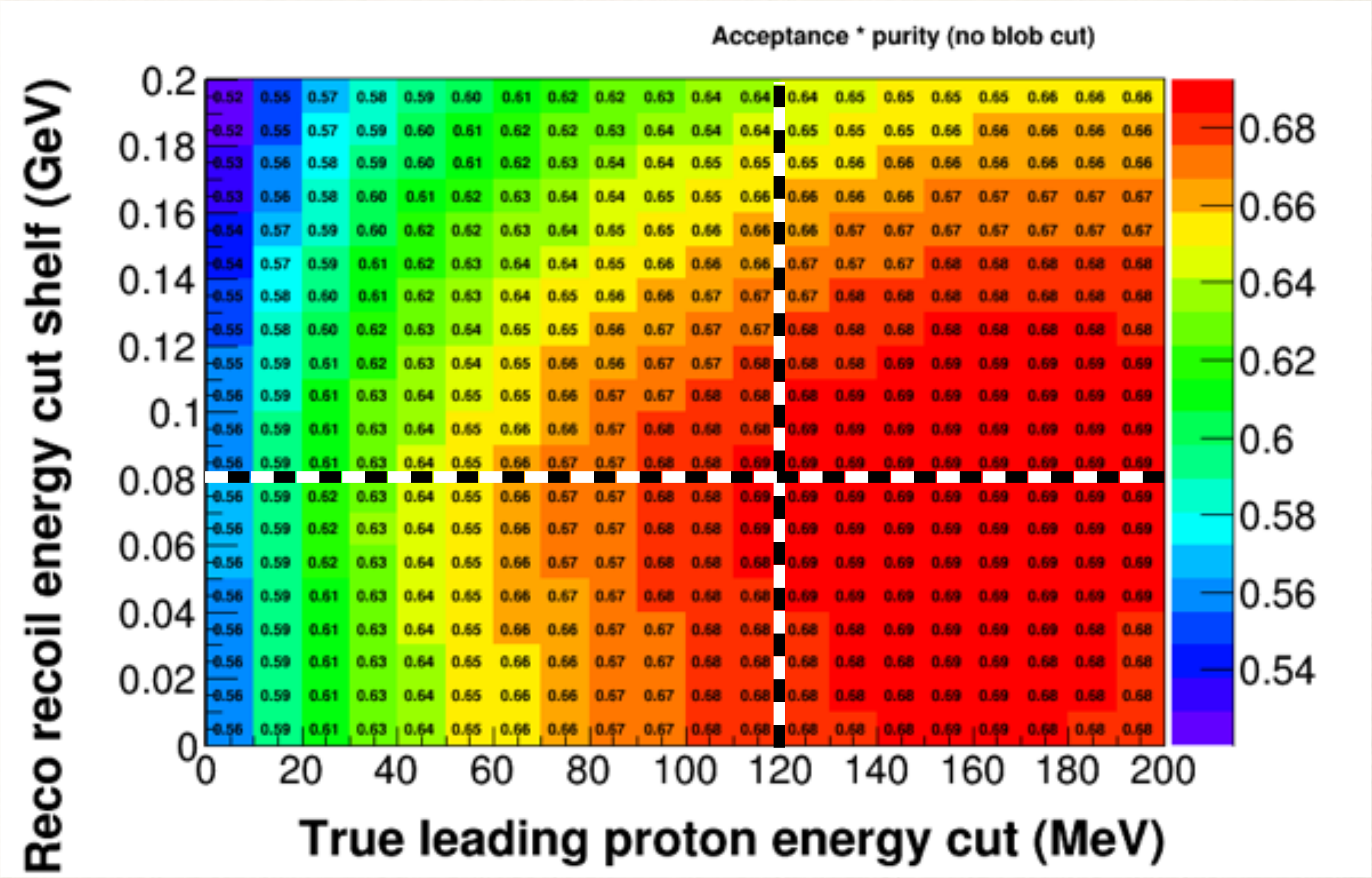

Lowering the cut threshold increases acceptance as events we cannot reconstruct become backgrounds

Selected values:
Shelf at 80 MeV
Proton kinetic energy threshold 120 MeV

Summary of reconstruction cuts

- Reconstructable event (no dead time during event, good MINOS and MINERvA data)
- Interaction vertex in the fiducial volume (tracker region of the detector)
- MINOS-matched μ^+
- No tracks other than the muon
- Recoil energy cut:
  - Reject if recoil > 0.45 GeV
  - Reject if recoil (GeV) > 0.03 + 0.3 Q^2_{QE} (GeV^2) except
  - Always accept if recoil < 0.08 GeV
- Muon longitudinal momentum < 15 GeV (the maximum on our histograms)
- Muon angle less than 20°

Systematic uncertainties from GENIE

CCQE model

Uncertainty	Default	Tweaked
MaCCQE	+25/ -15%	±3%
VecFF-CCQEShape	BBBA05 to Dipole	
CCQEPauli-SupViaKF	30%	

We also use a sample of CCQE plus an additional 23% Nieves 2p2h (no RPA) generated with GENIE 2.10 to evaluate an uncertainty for GENIE 2.8.4's non-modeling of 2p2h effects

Background model

Uncertainty	Default	Tweaked
MaNCEL	±25%	
EtaNCEL	±30%	
NormNCRES	±20%	
MaRES	±20%	
MvRES	±10%	±3%
NormDISCC		
Rvn1pi	±50%	±5%
Rvn2pi	±50%	
Rvp1pi	±50%	
Rvn2pi	±50%	
Rvp2pi	±50%	

FSI

Uncertainty	Default
MFP_N	±20%
MFP_Pi	±20%
FrElas_N	±30%
FrElas_Pi	±10%
FrInel_N	±40%
FrAbs_Pi	±20%
FrCEx_N	±50%
Theta Delta2Npi	Rein-Sehgal
FrCEx_Pi	±50%
FrAbs_N	±20%
FrPiProd_N	±20%
FrPiProd_Pi	±20%
AGKYxF1pi	±20%
RDecBR1gamma	±50%

Number of targets

$$\left(\frac{d^2\sigma}{dx\,dy}\right)_{ij} = \frac{\sum_{\alpha\beta} U_{\alpha\beta ij}(N_{\text{data},\alpha\beta} - N^{bkgd}_{\text{data},\alpha\beta})}{\epsilon_{ij}(\Phi T)(\Delta x_i)(\Delta y_j)}$$

CCQE targets: protons

$$\bar{\nu}_\mu + p \to \mu^+ + n$$

For a **CCQE** event on a single nucleon, the target is always a **proton**

Our fiducial volume contains **1.75 x 10^{30}** protons

QE-like targets: nucleons

$$\bar{\nu}_\mu + p \to \mu^+ + n$$
$$\bar{\nu}_\mu + p \to \mu^+ + \Delta^0 \to n + \pi^0(\text{absorbed})$$
$$\bar{\nu}_\mu + p \to \mu^+ + \Delta^0 \to p + \pi^-(\text{absorbed})$$
$$\bar{\nu}_\mu + n \to \mu^+ + \Delta^- \to n + \pi^-(\text{absorbed})$$

For the **CCQE-like** definition, both **protons and neutrons** are possible targets

Our fiducial volume contains **3.23 x 10^{30}** nucleons

As our plastic target composition is mostly CH, the nucleon/proton ratio is close to 13/7.

Excess in the different phase spaces

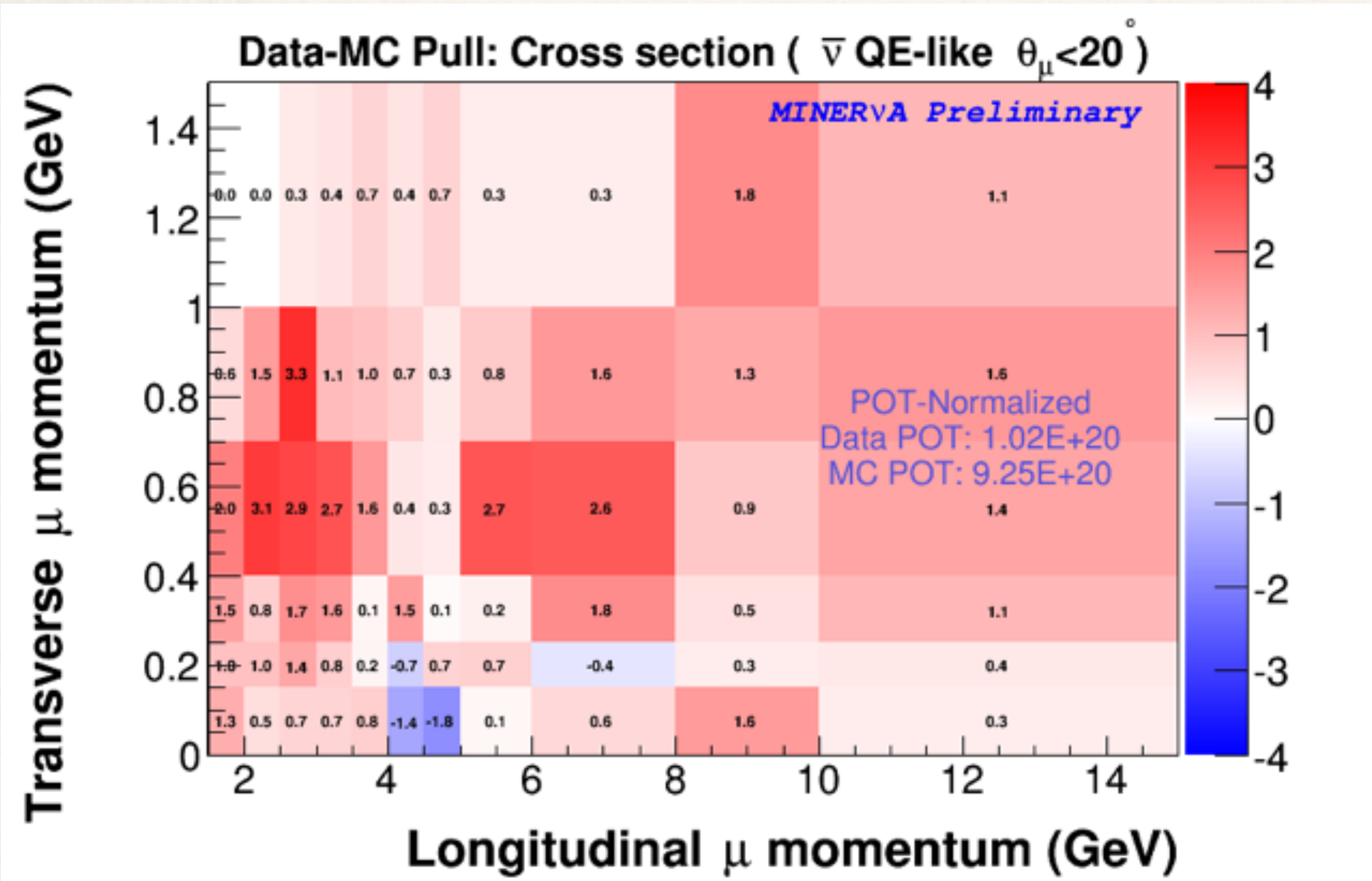

The excesses seen in the muon kinematic variables translate to the E_ν^{QE}/Q^2_{QE} phase space

Excess in the different phase spaces

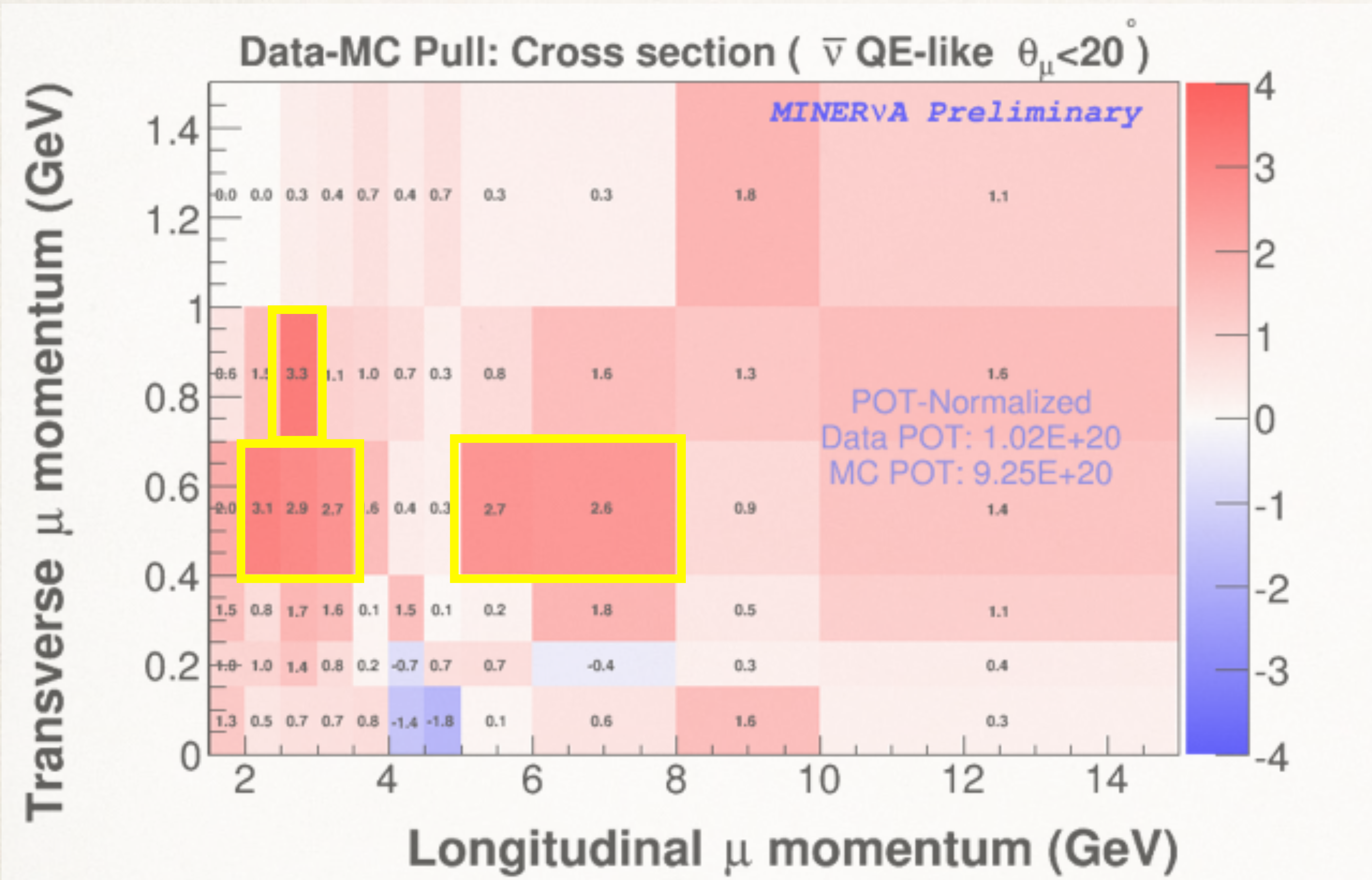

The excesses seen in the muon kinematic variables translate to the E_ν^{QE}/Q^2_{QE} phase space

Excess in the different phase spaces

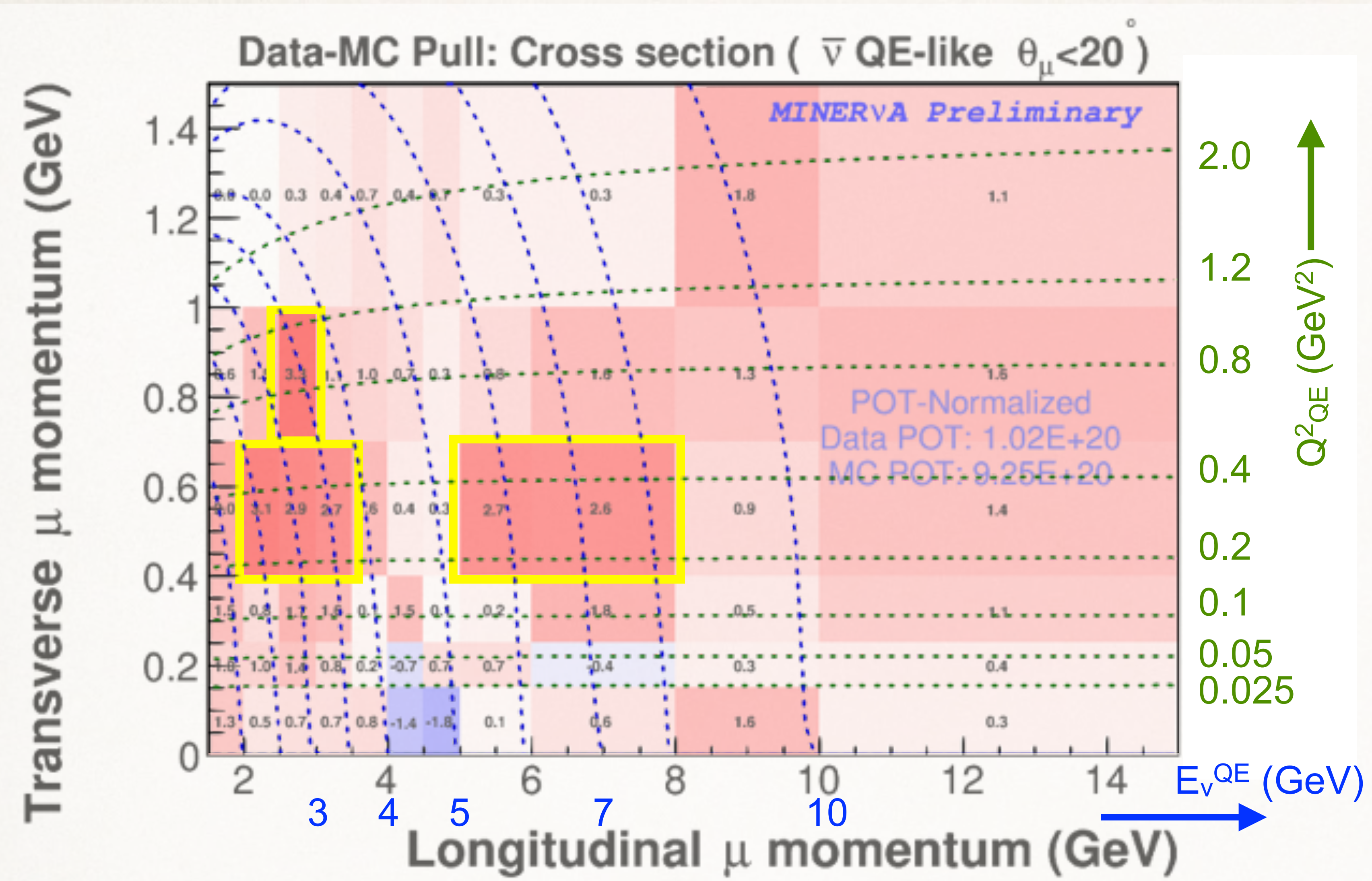

The excesses seen in the muon kinematic variables translate to the E_ν^{QE}/Q^2_{QE} phase space

Excess in the different phase spaces

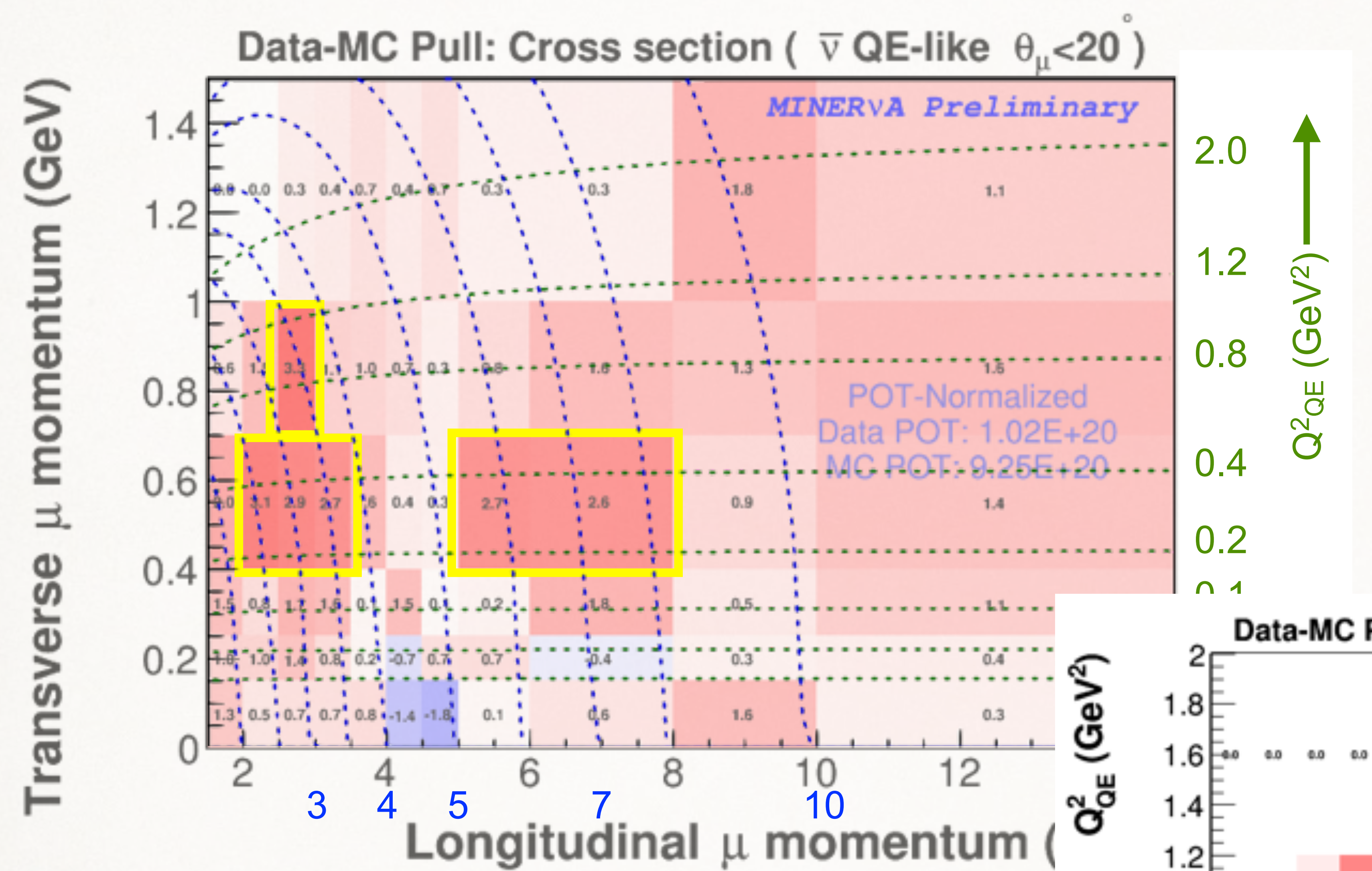

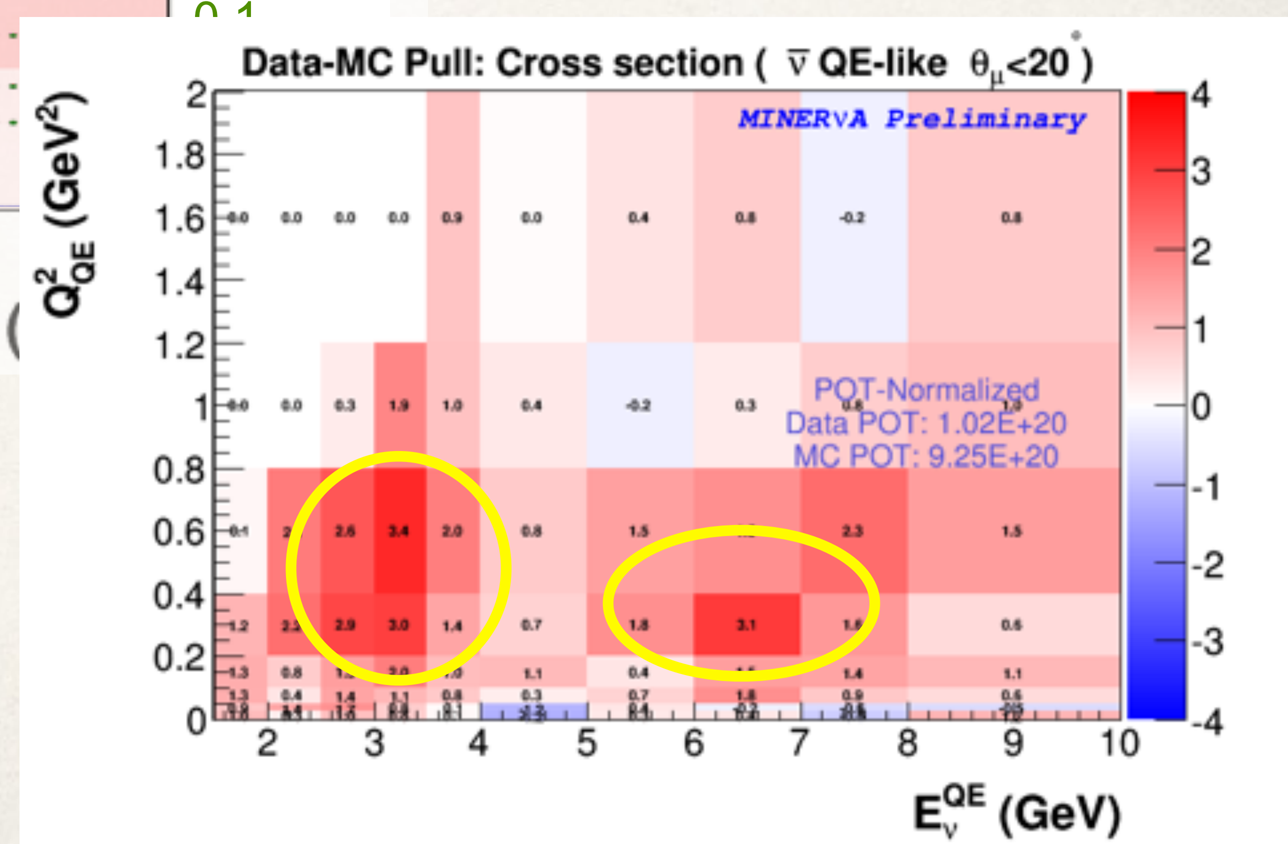

The excesses seen in the muon kinematic variables translate to the E_ν^{QE} / Q^2_{QE} phase space

Muon kinematic cross section, sliced the other way

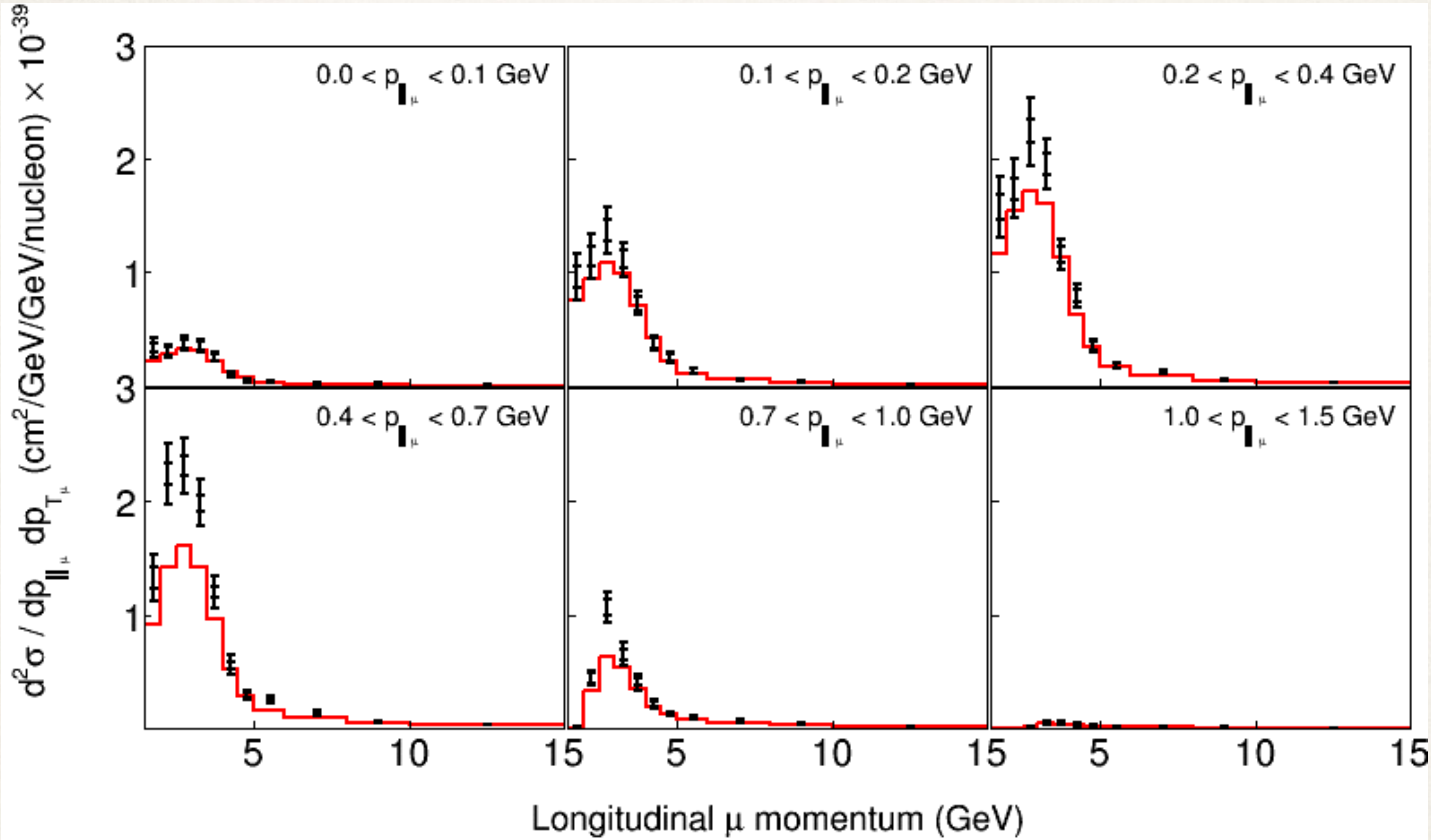

QE-like double differential cross section: flip book

QE-like double differential cross section: flip book

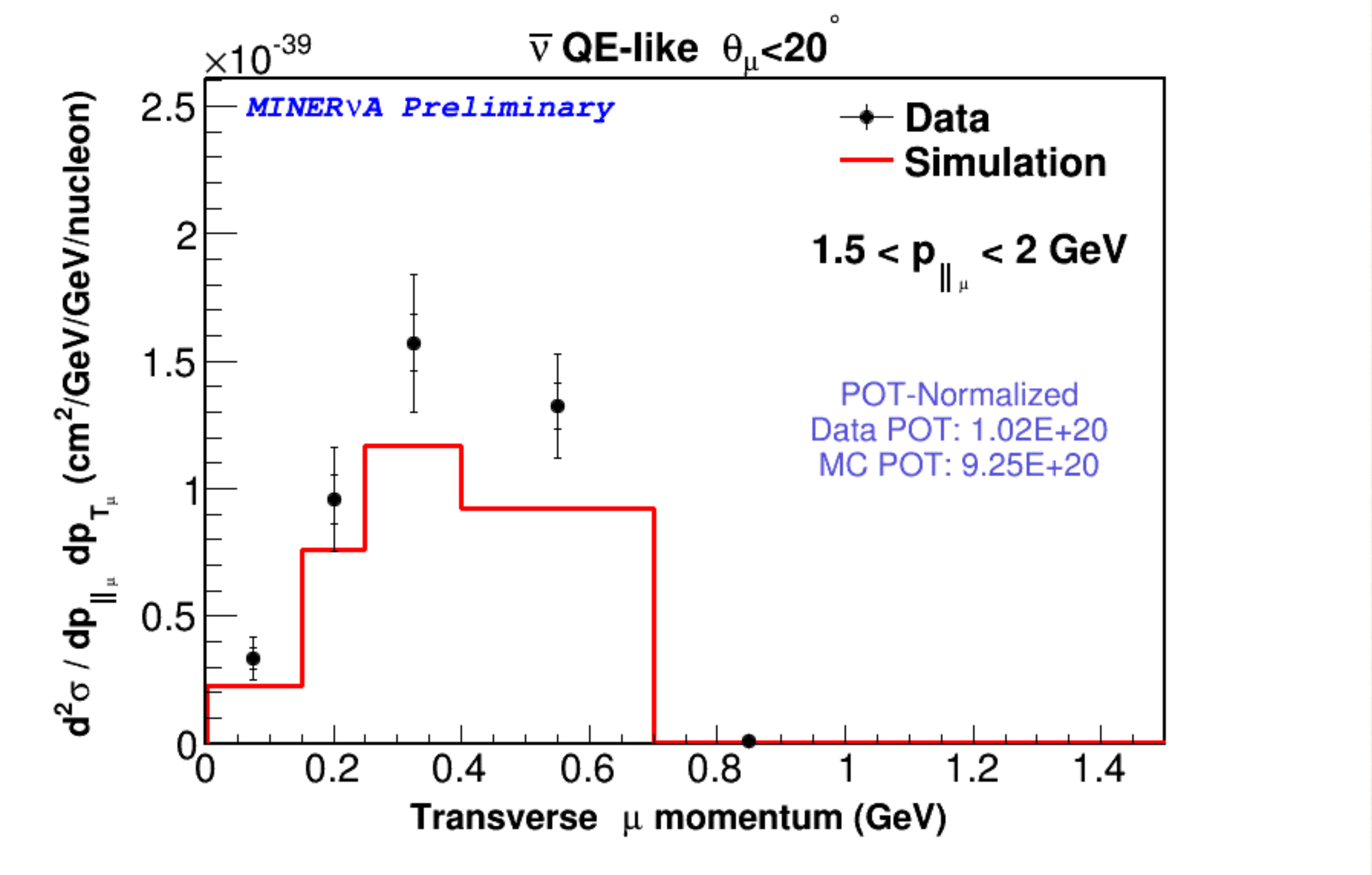

QE-like double differential cross section: flip book

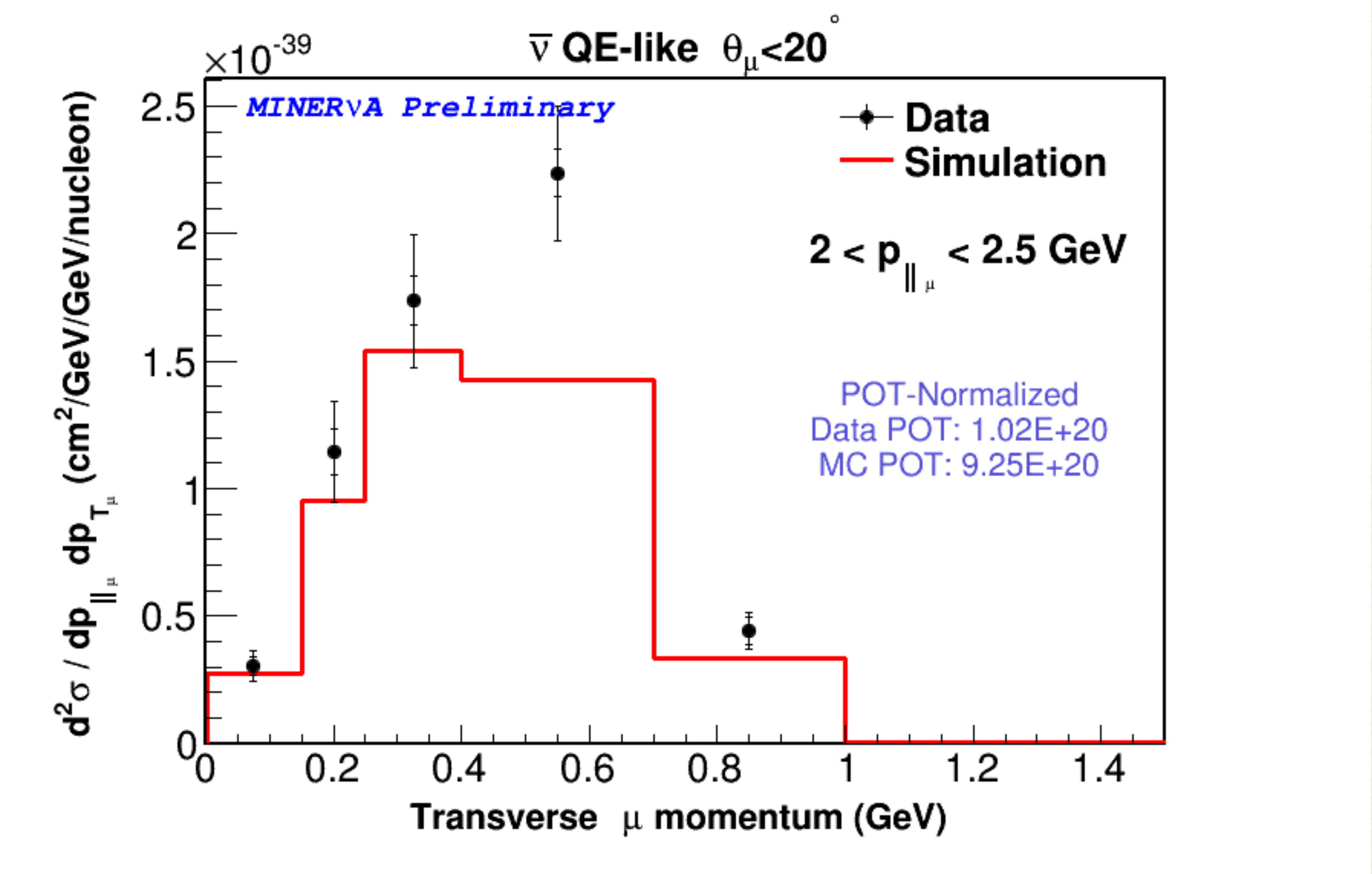

QE-like double differential cross section: flip book

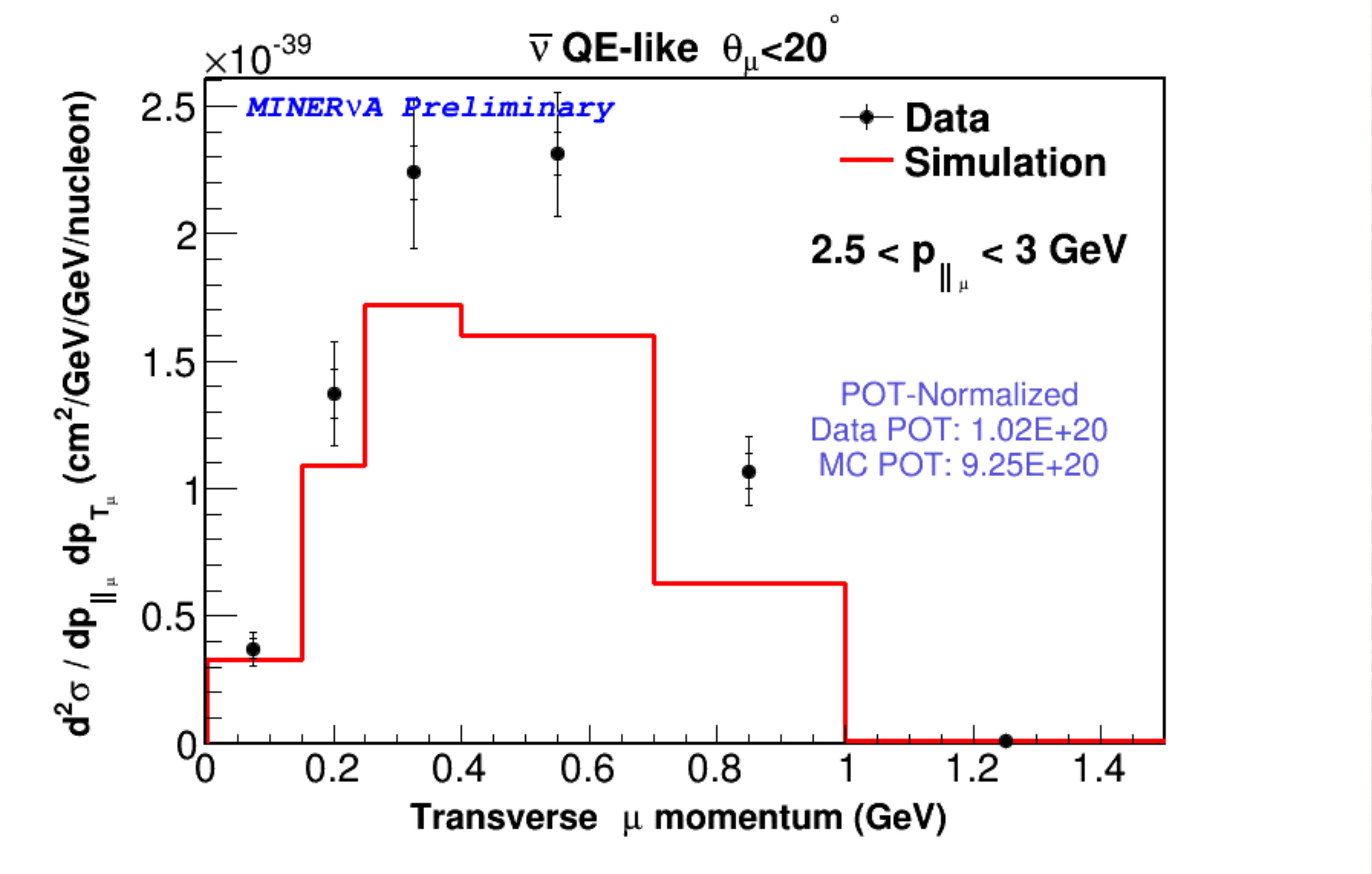

QE-like double differential cross section: flip book

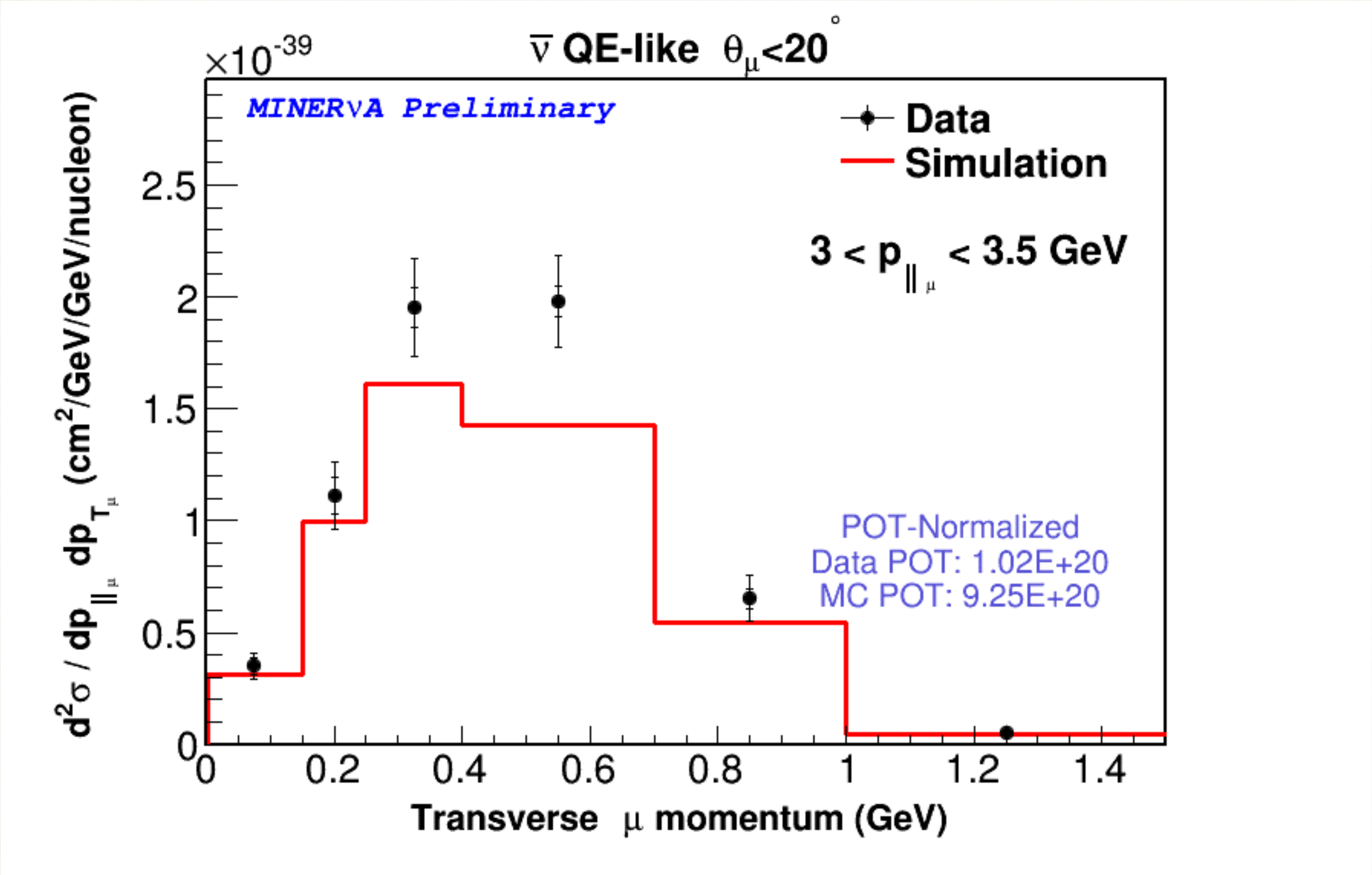

QE-like double differential cross section: flip book

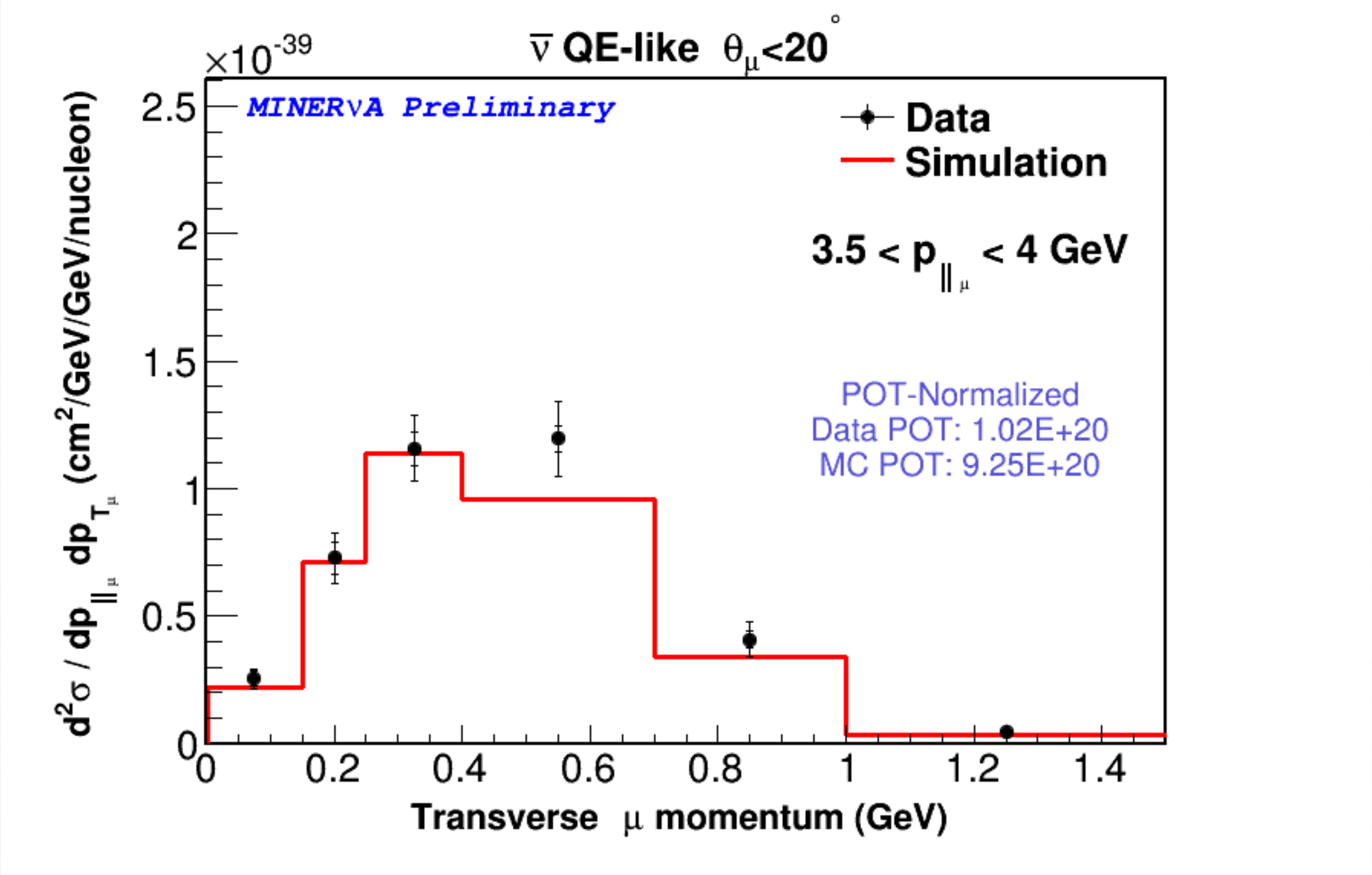

QE-like double differential cross section: flip book

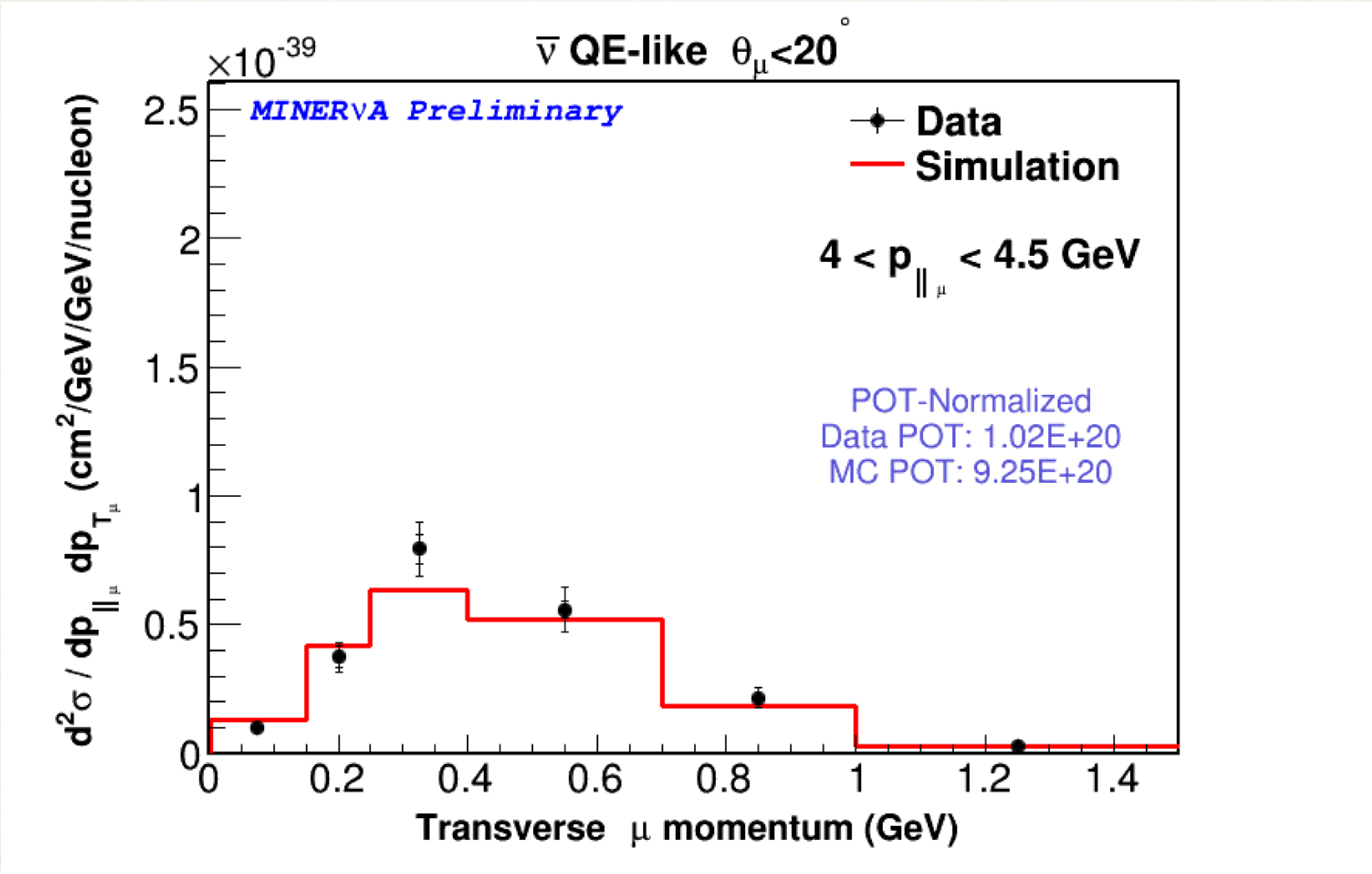

QE-like double differential cross section: flip book

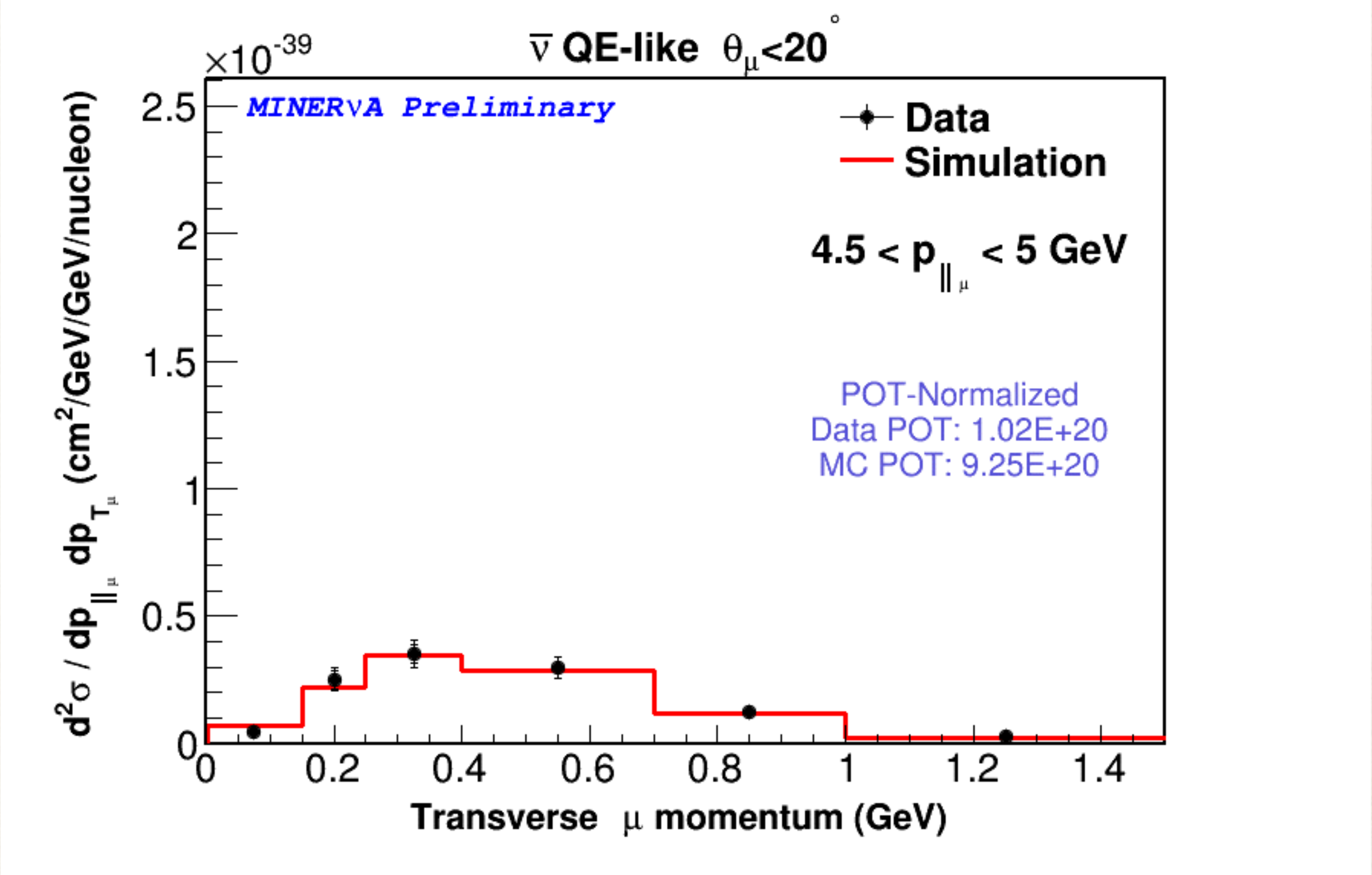

QE-like double differential cross section: flip book

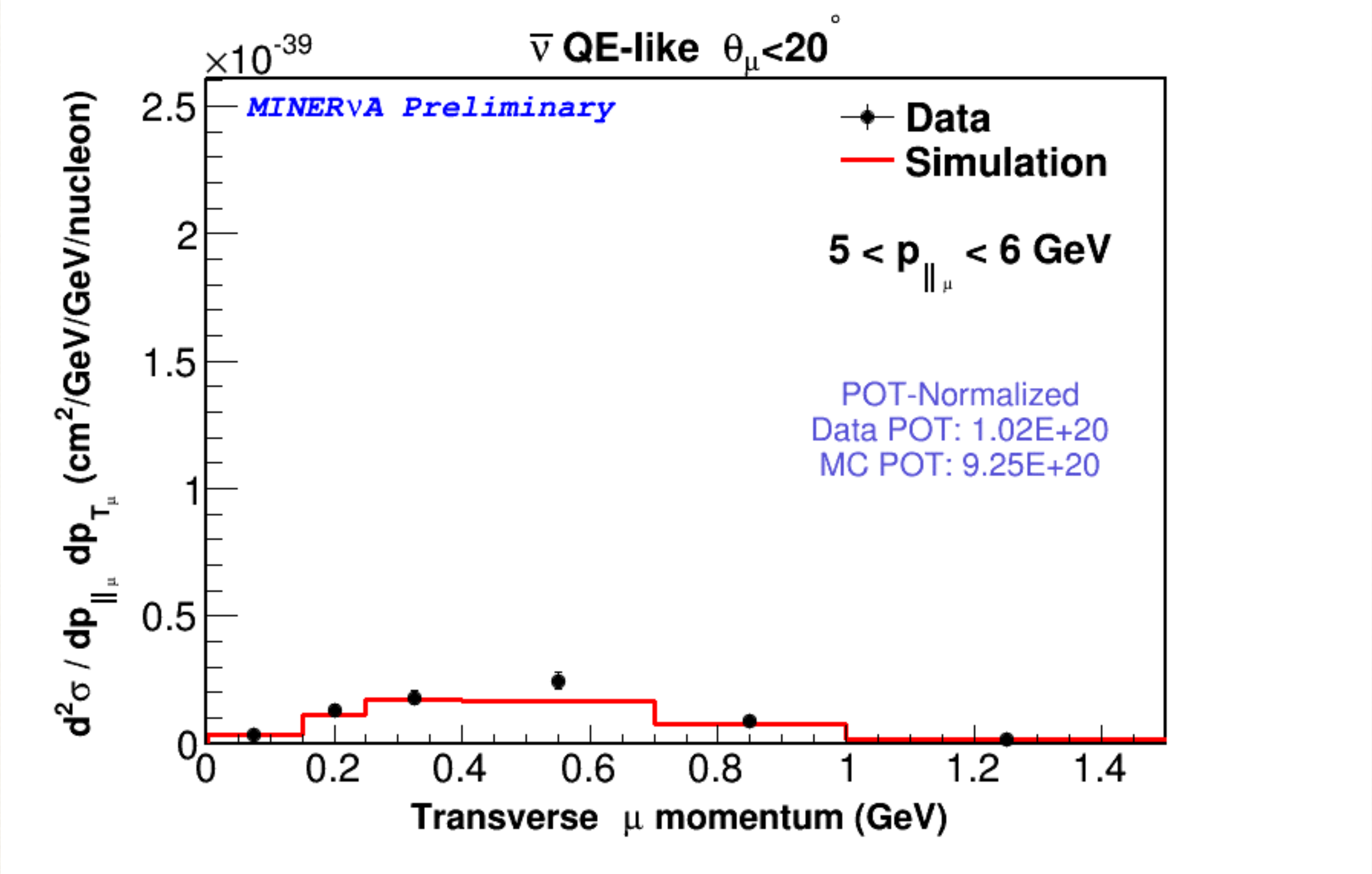

QE-like double differential cross section: flip book

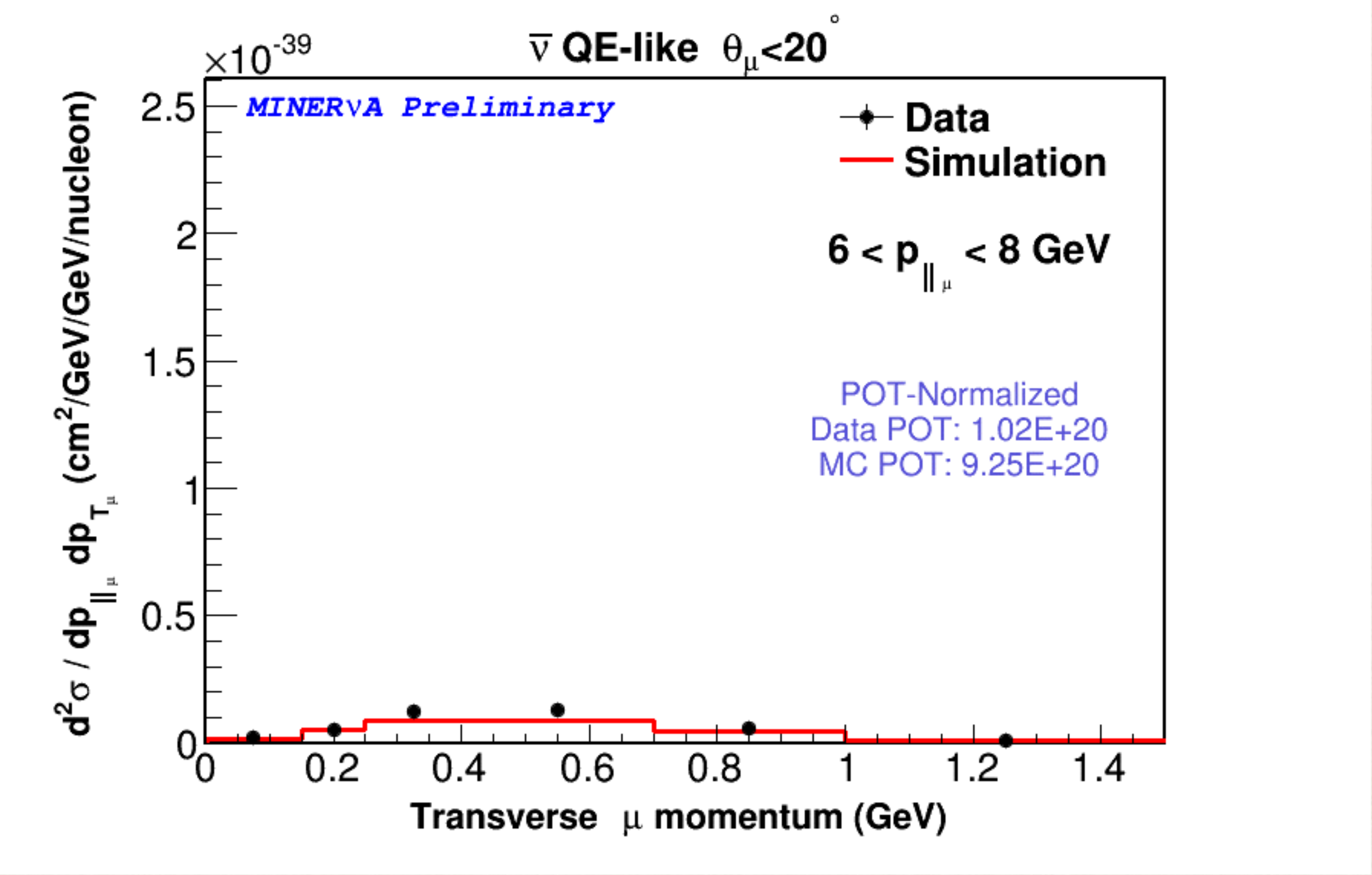

QE-like double differential cross section: flip book

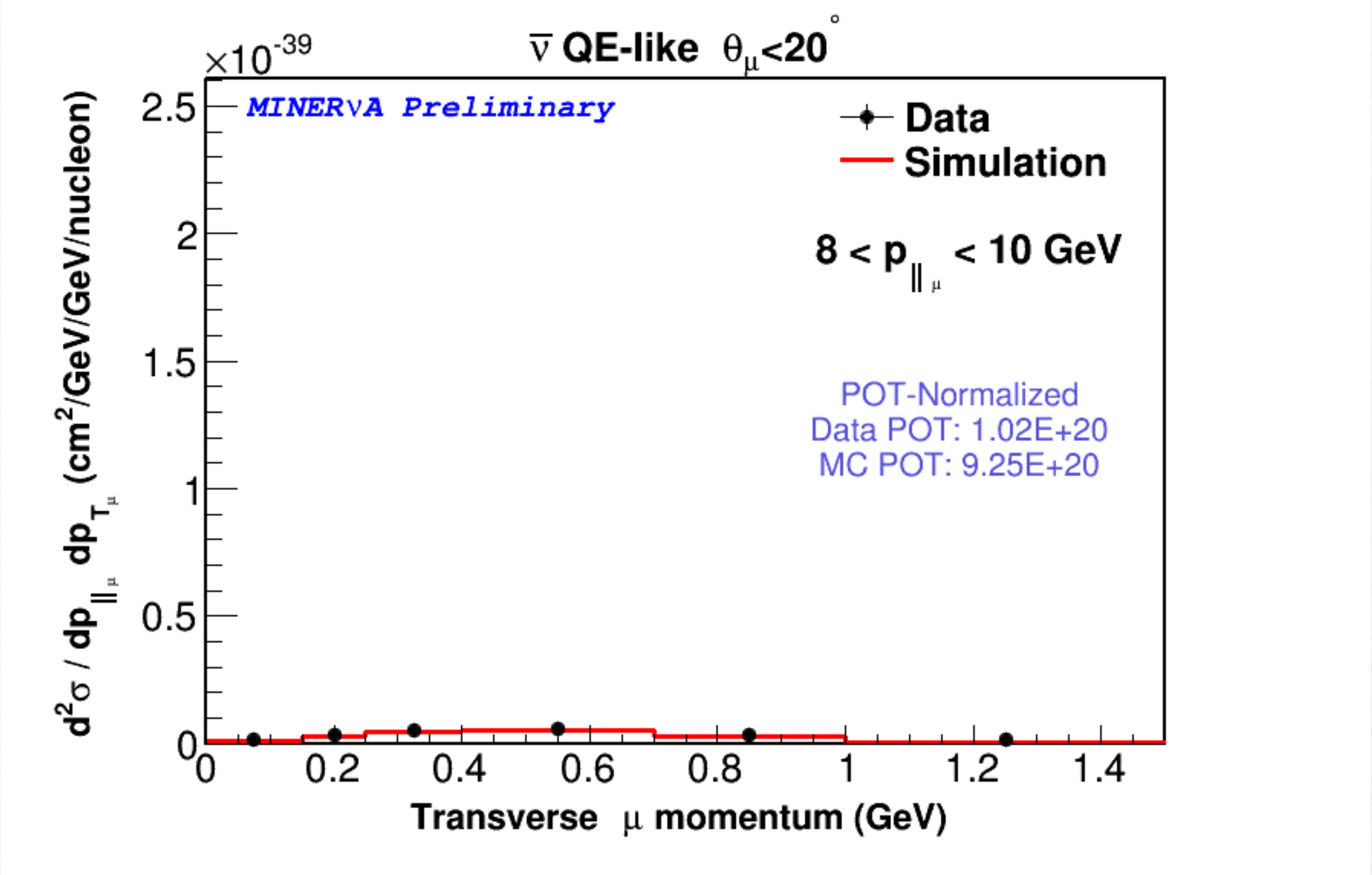

QE-like double differential cross section: flip book

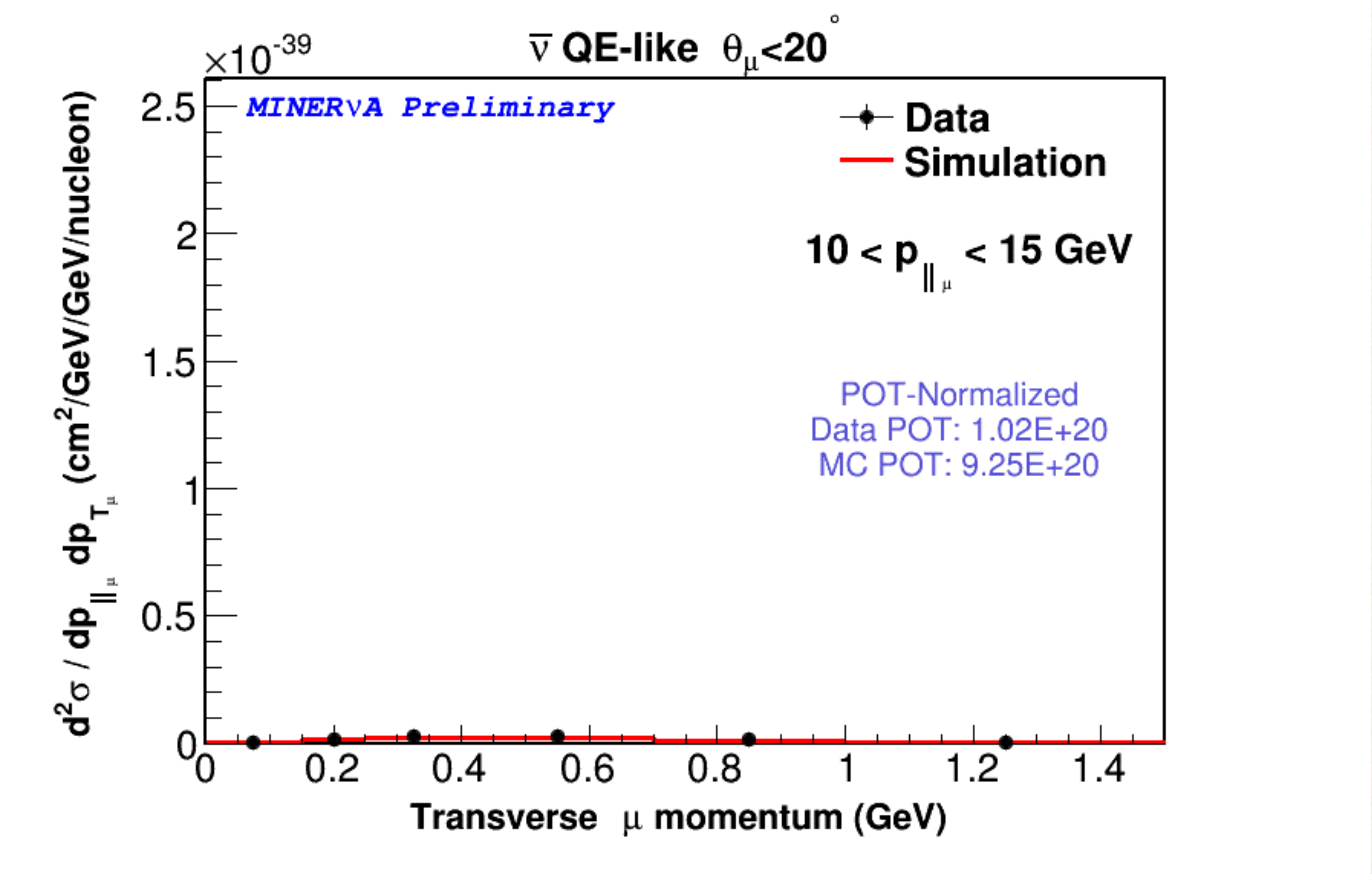

QE-like double differential cross section: flip book: each plot on its own scale

QE-like double differential cross section: own scales

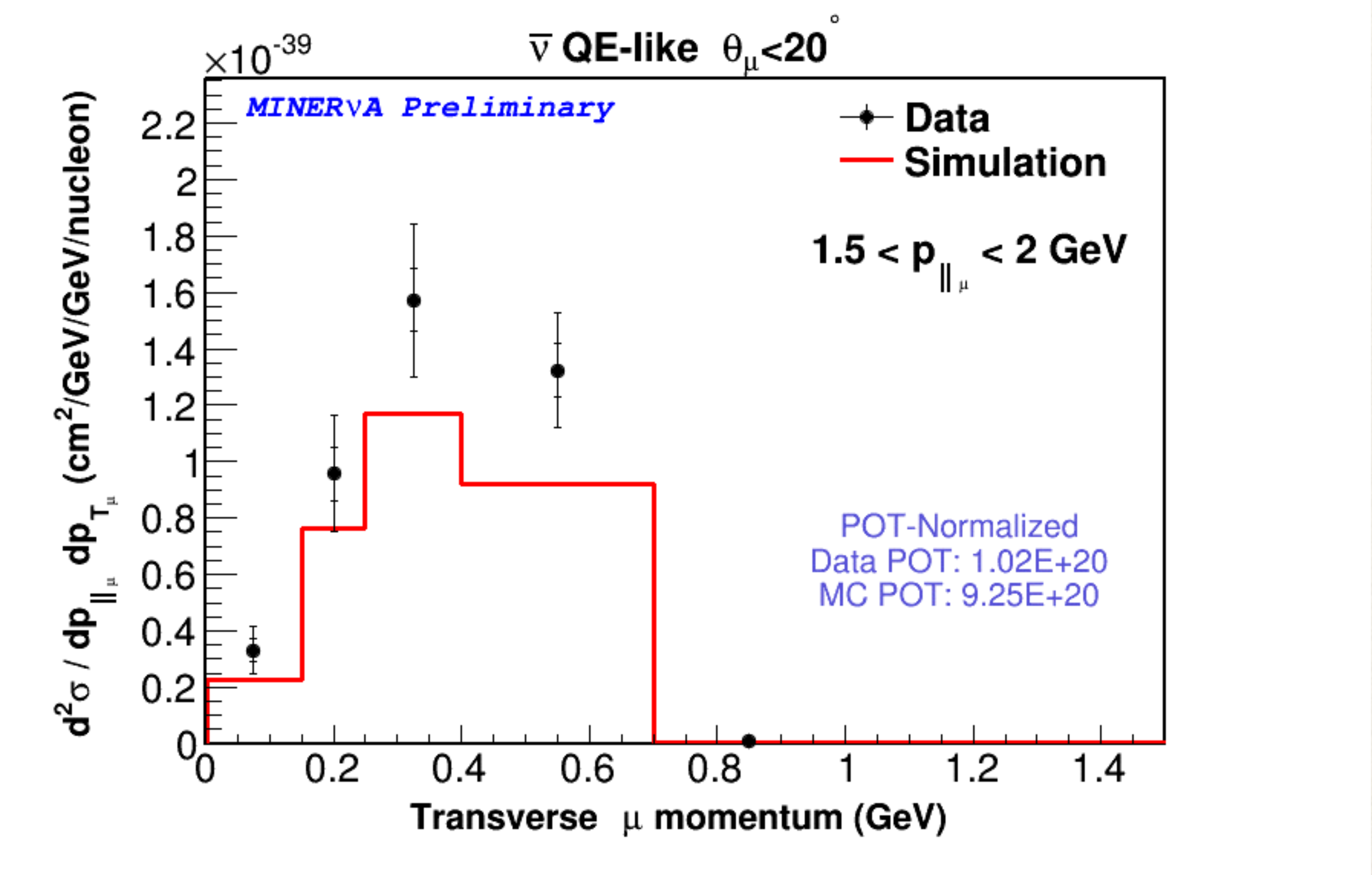

QE-like double differential cross section: own scales

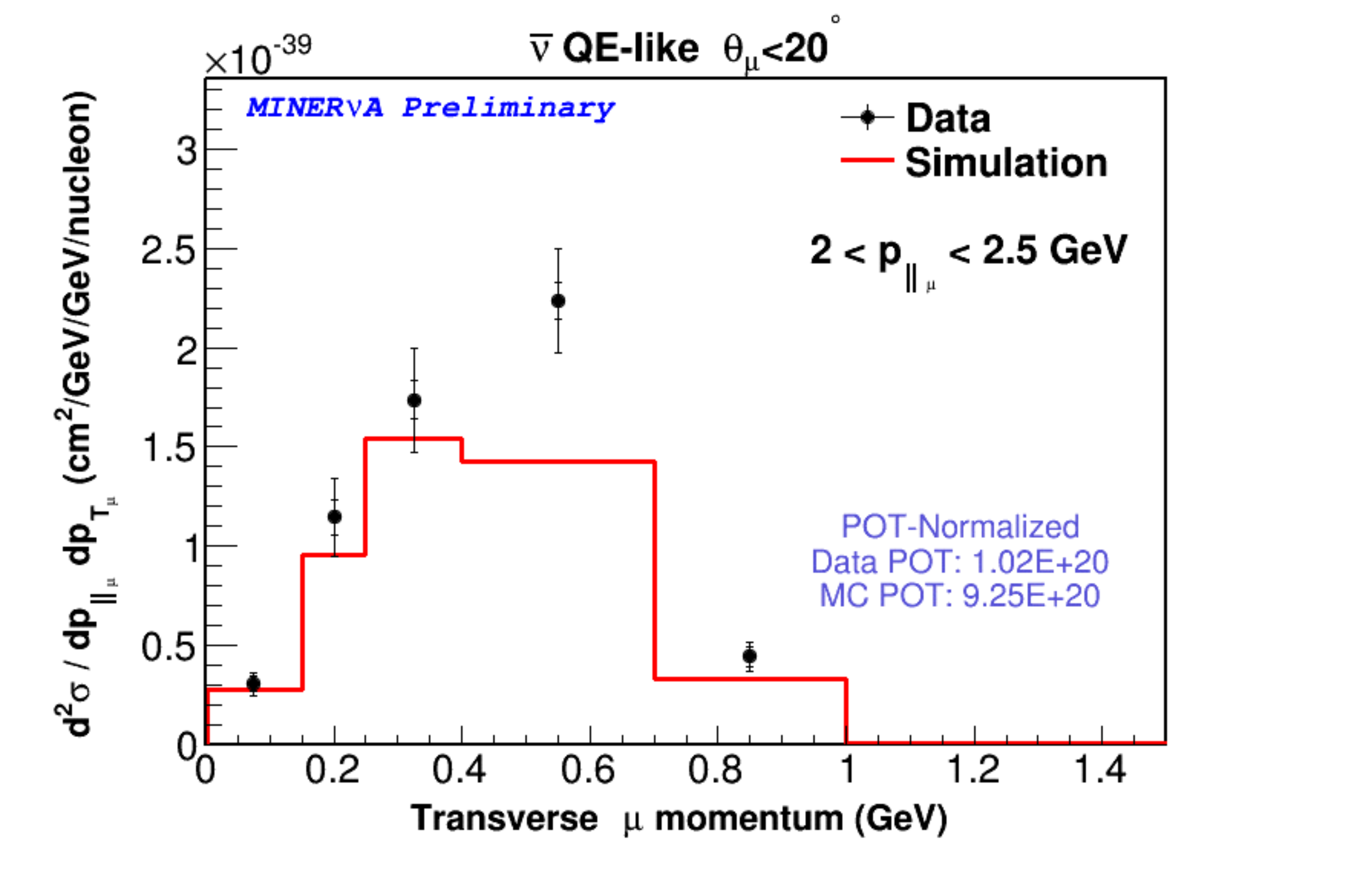

QE-like double differential cross section: own scales

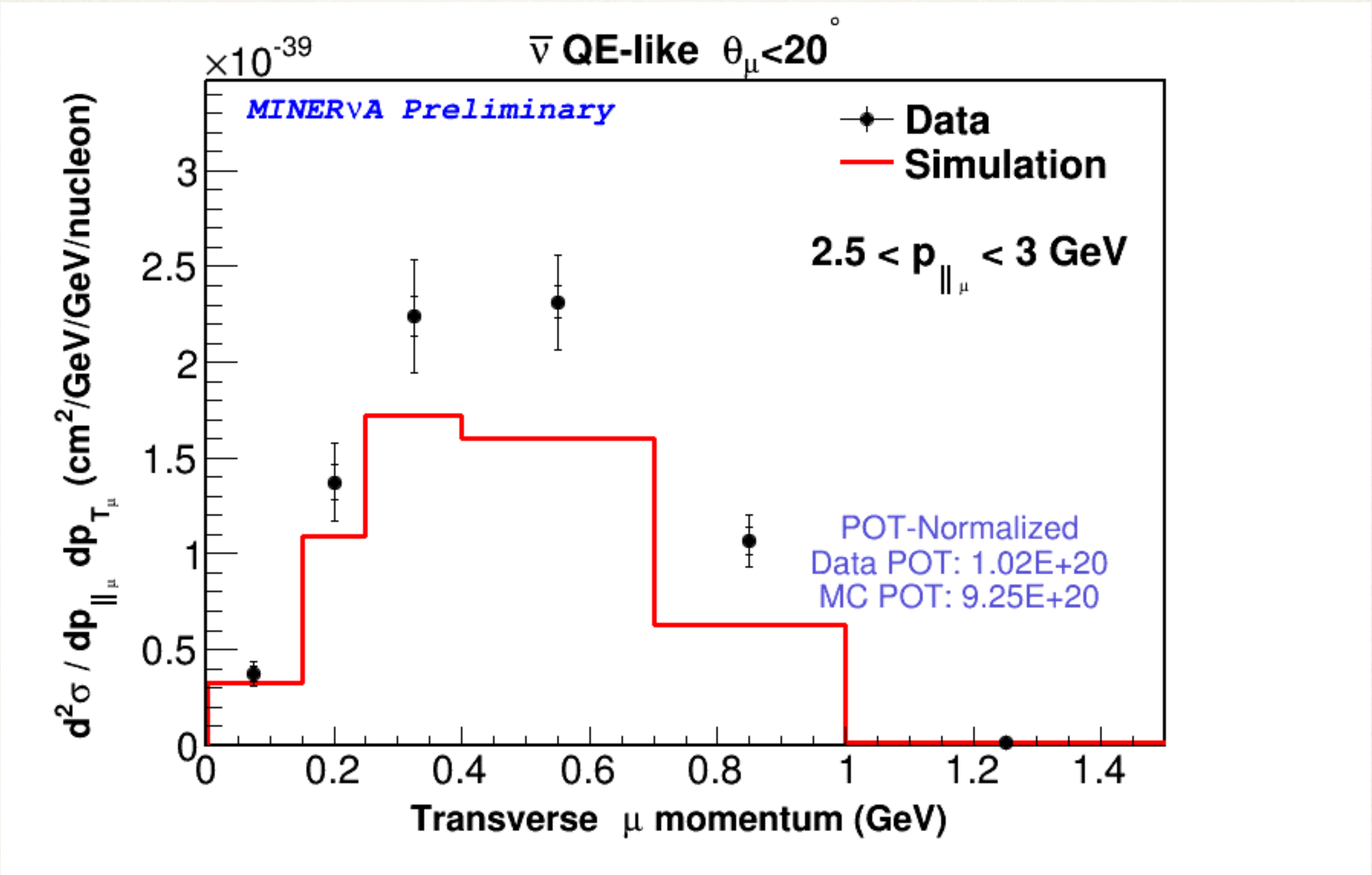

QE-like double differential cross section: own scales

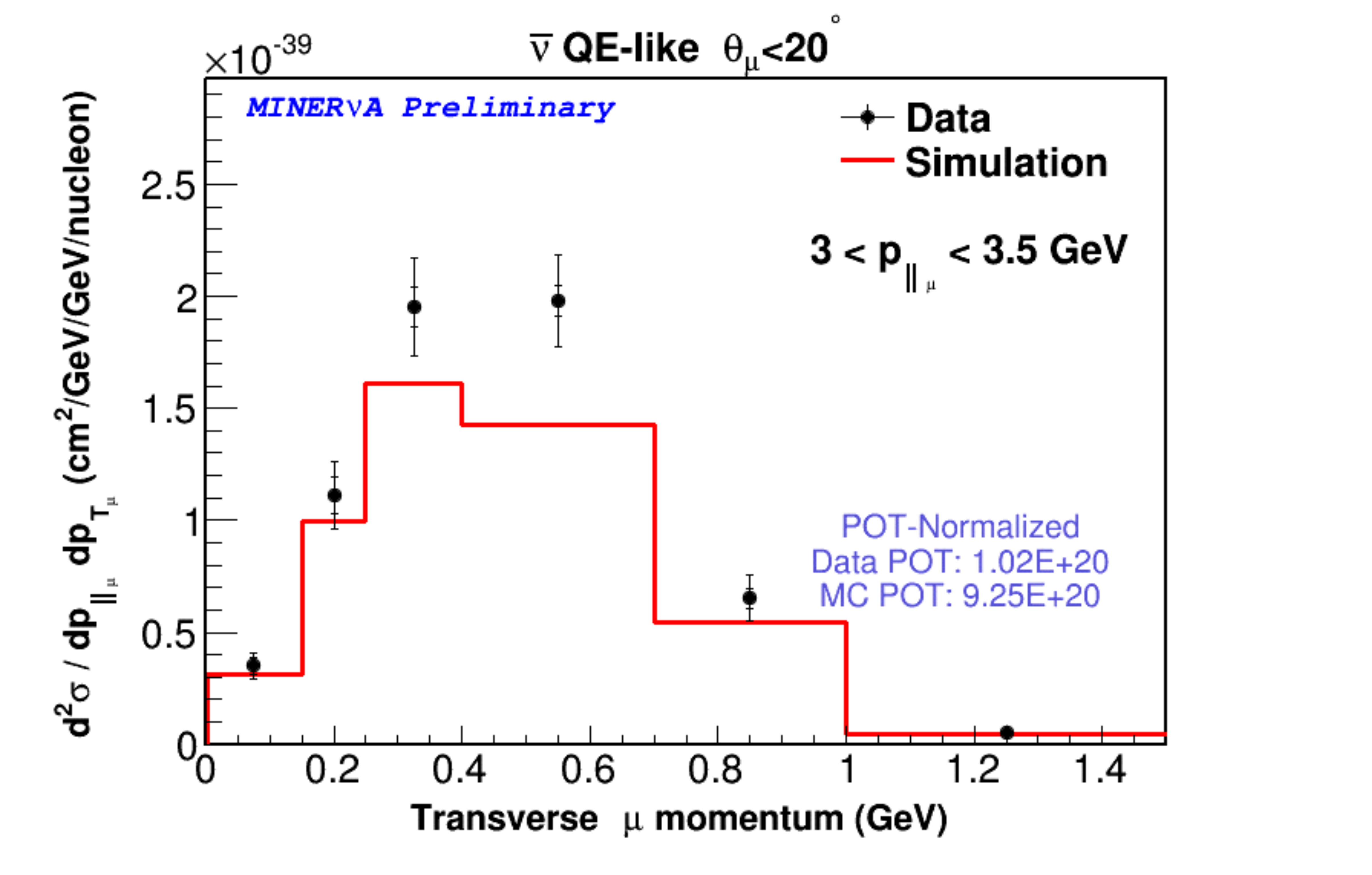

QE-like double differential cross section: own scales

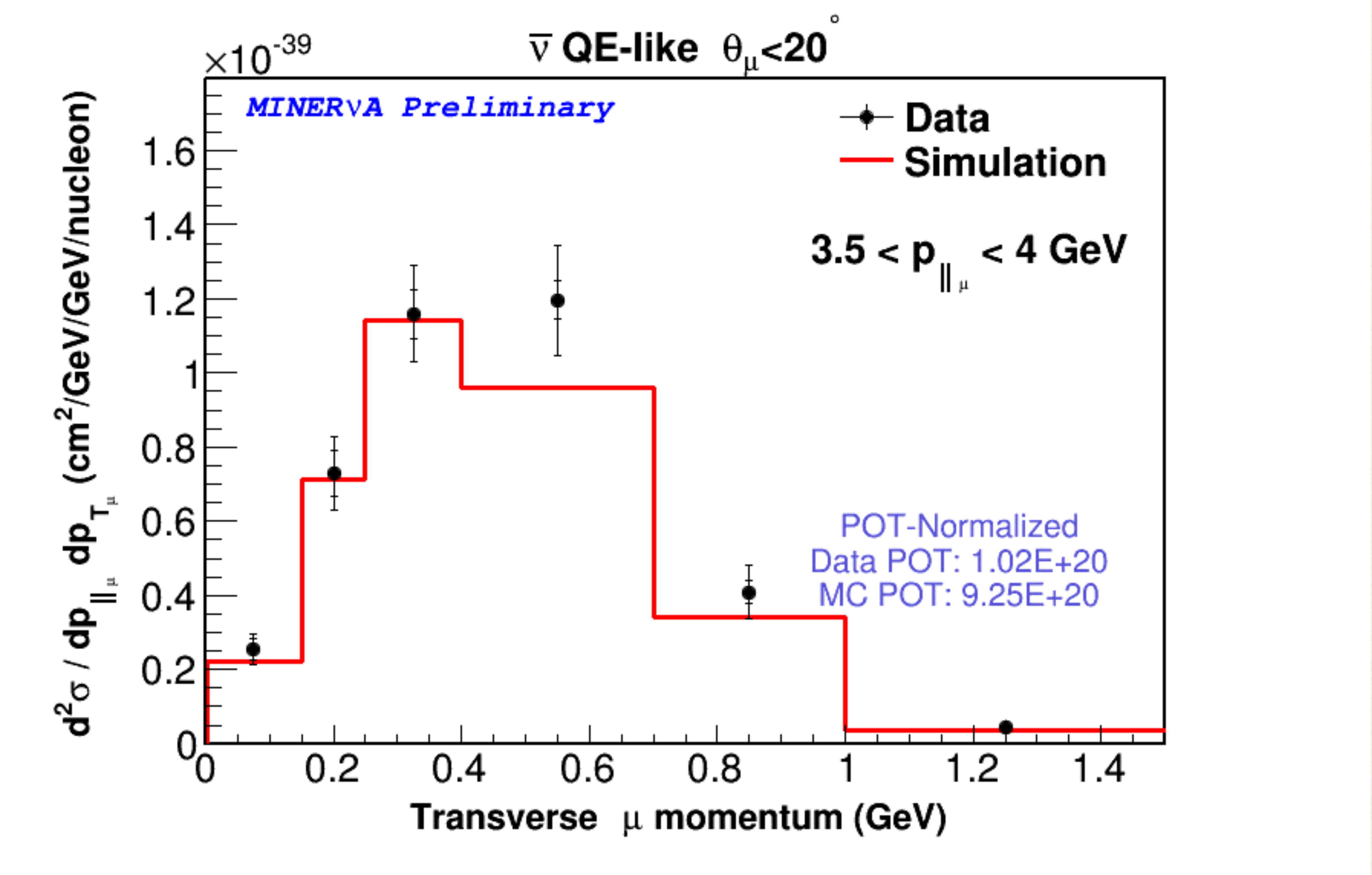

QE-like double differential cross section: own scales

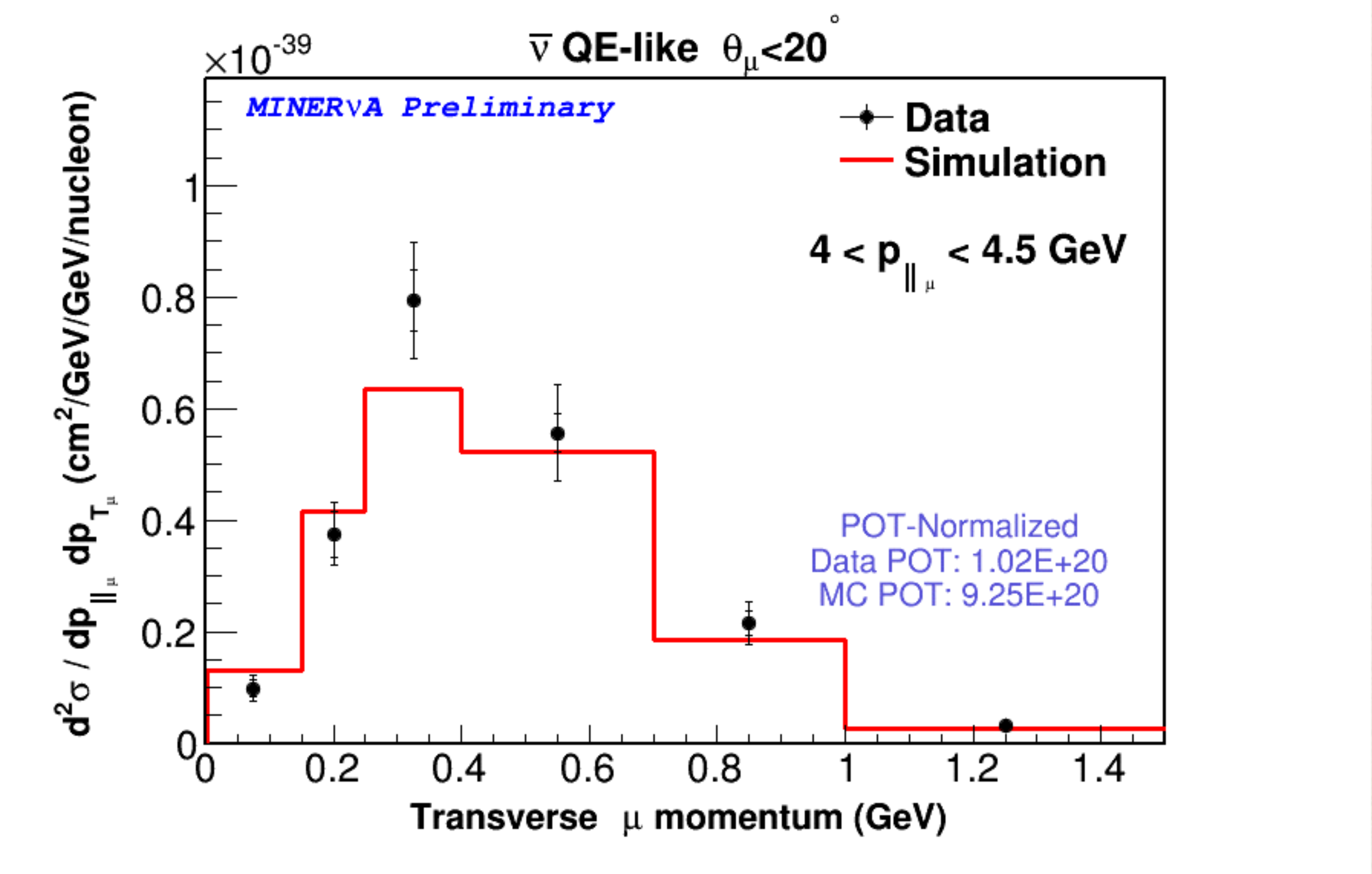

QE-like double differential cross section: own scales

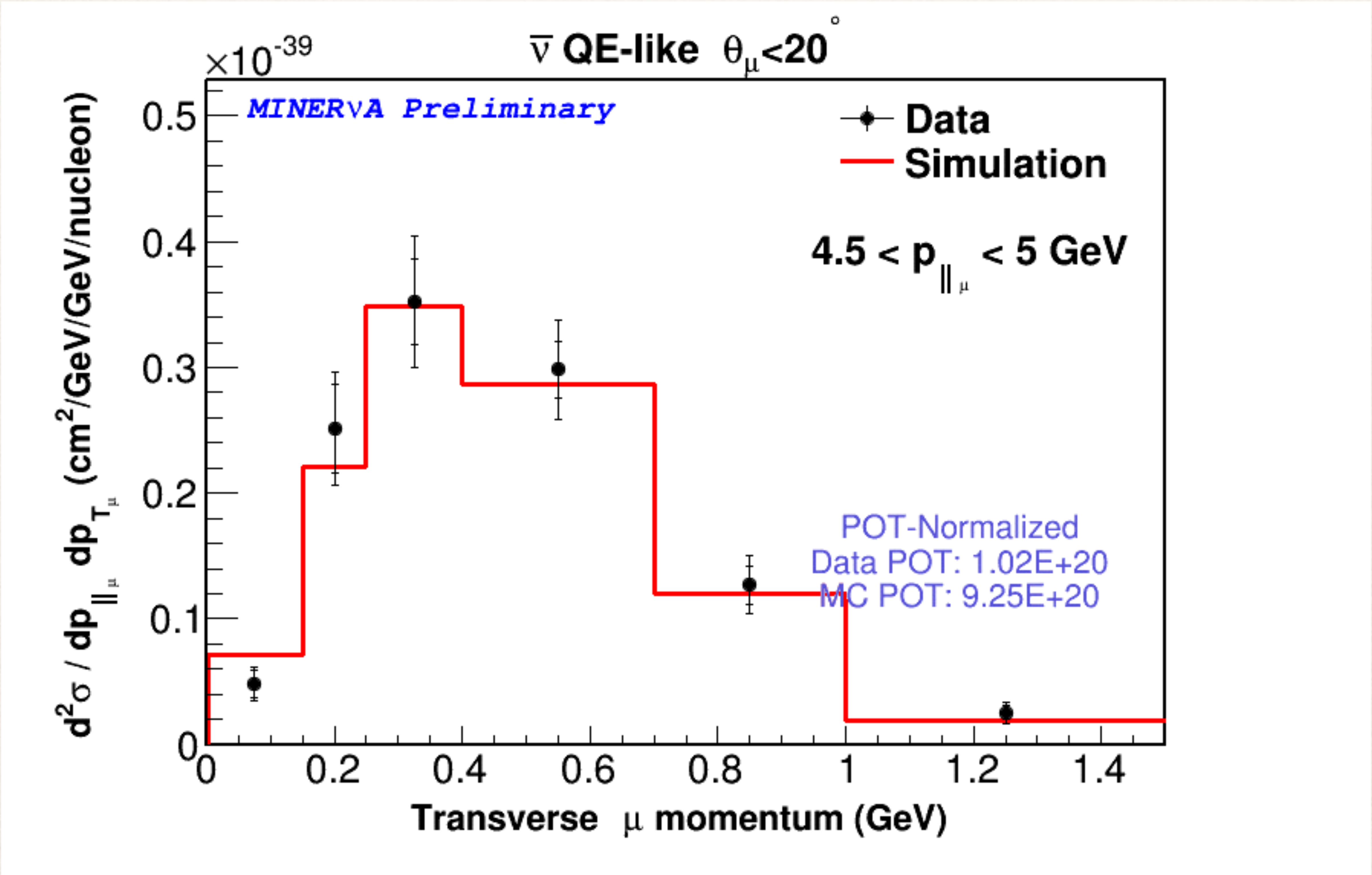

QE-like double differential cross section: own scales

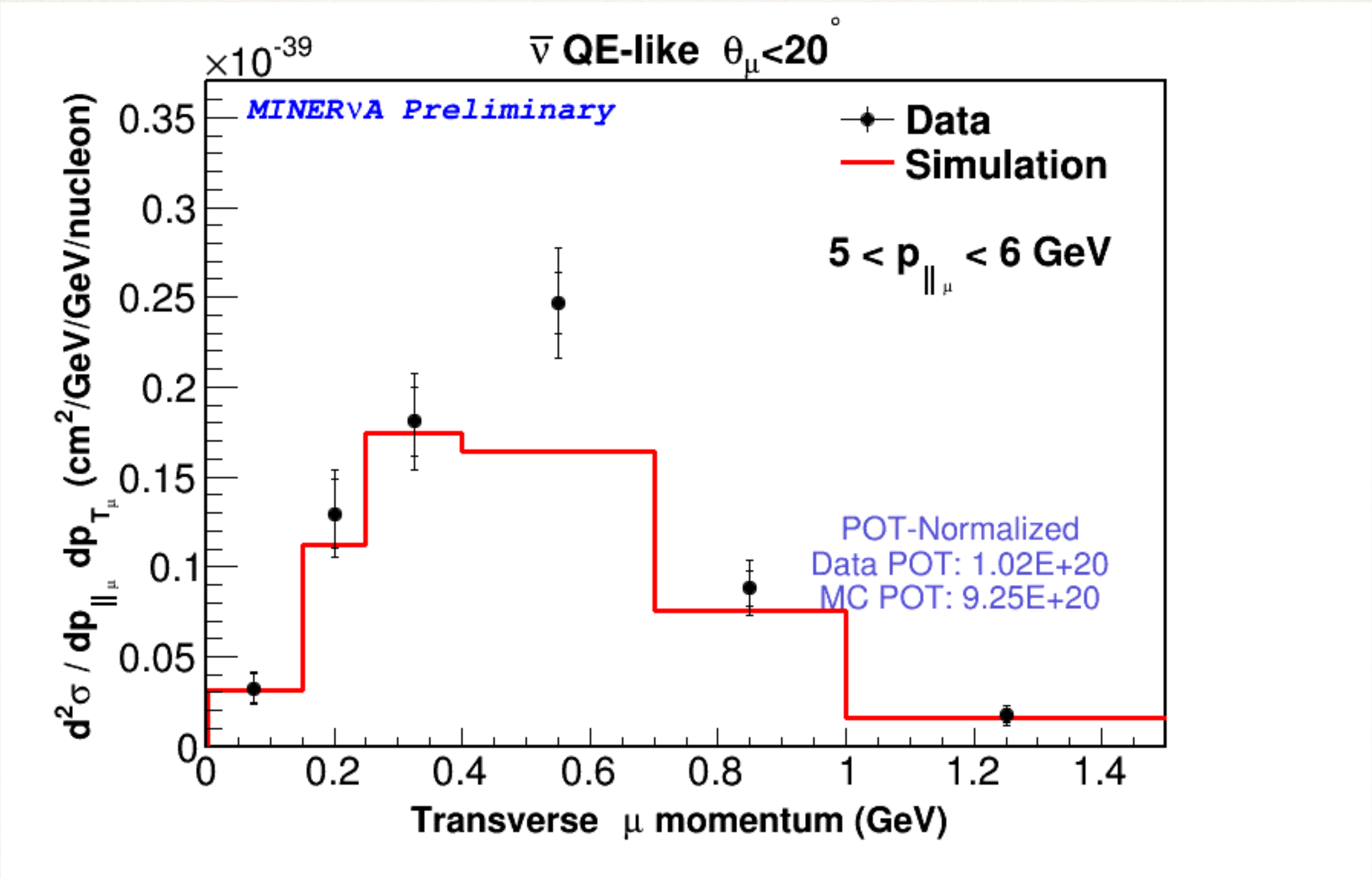

QE-like double differential cross section: own scales

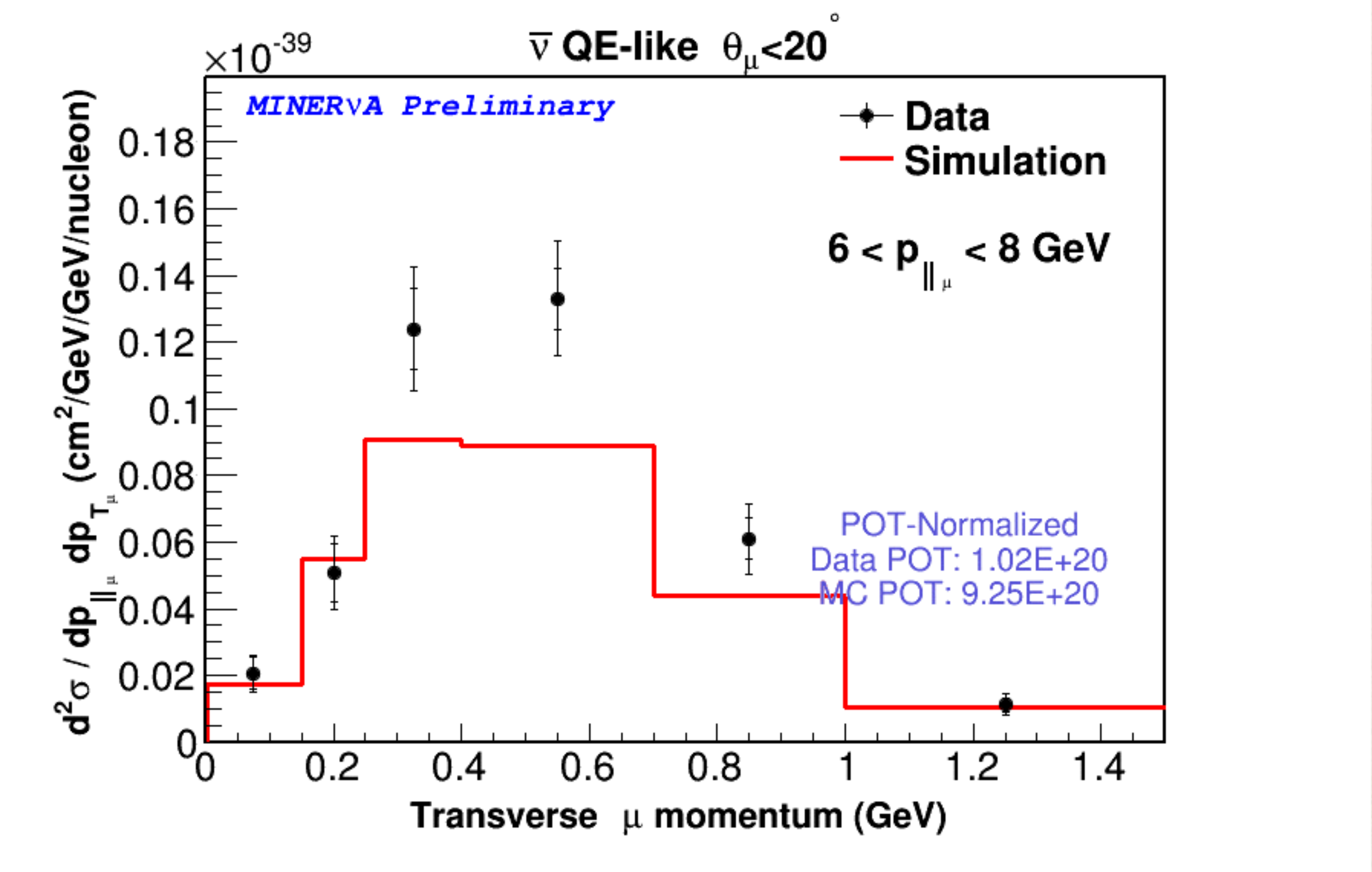

QE-like double differential cross section: own scales

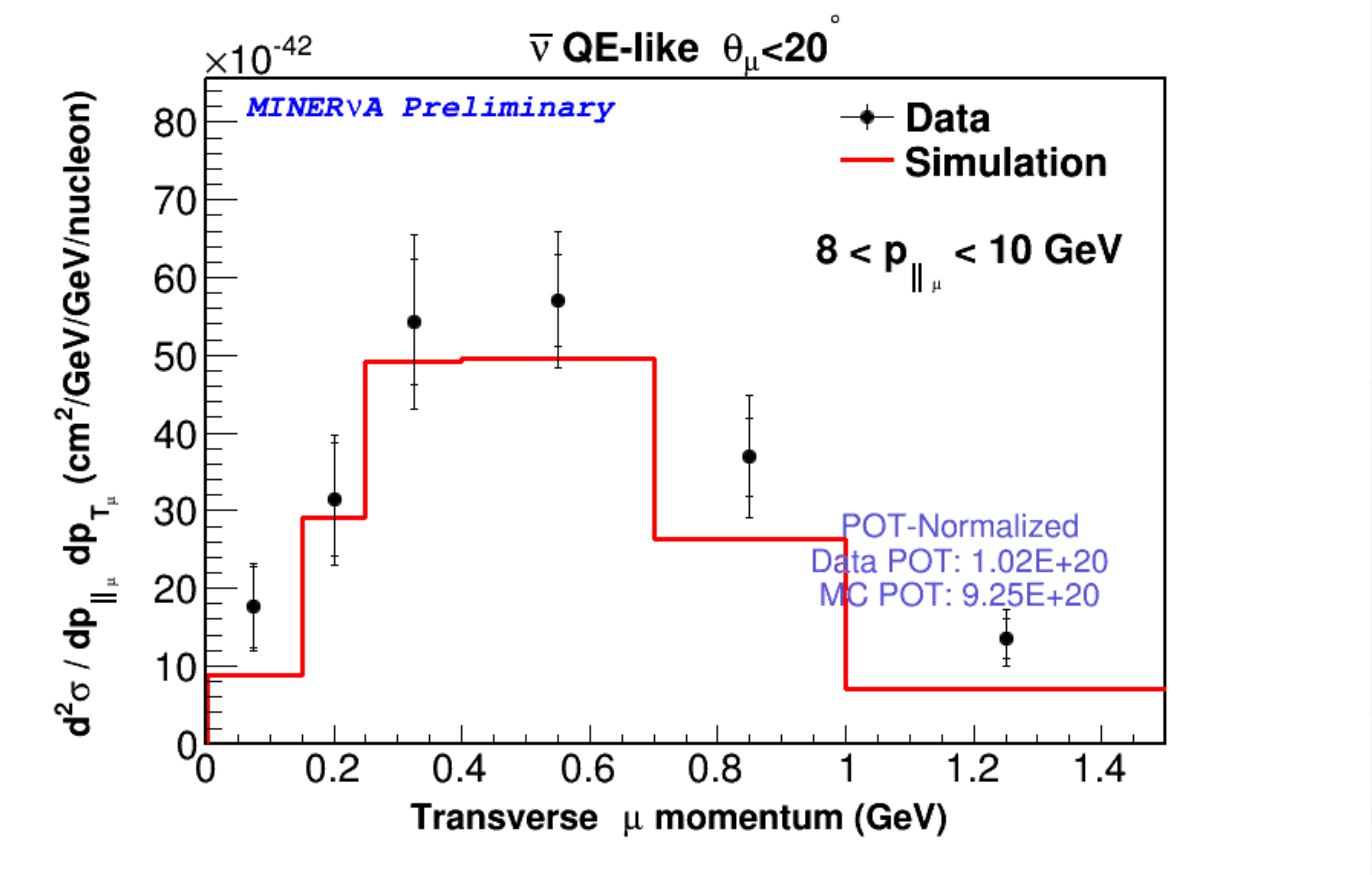

QE-like double differential cross section: own scales

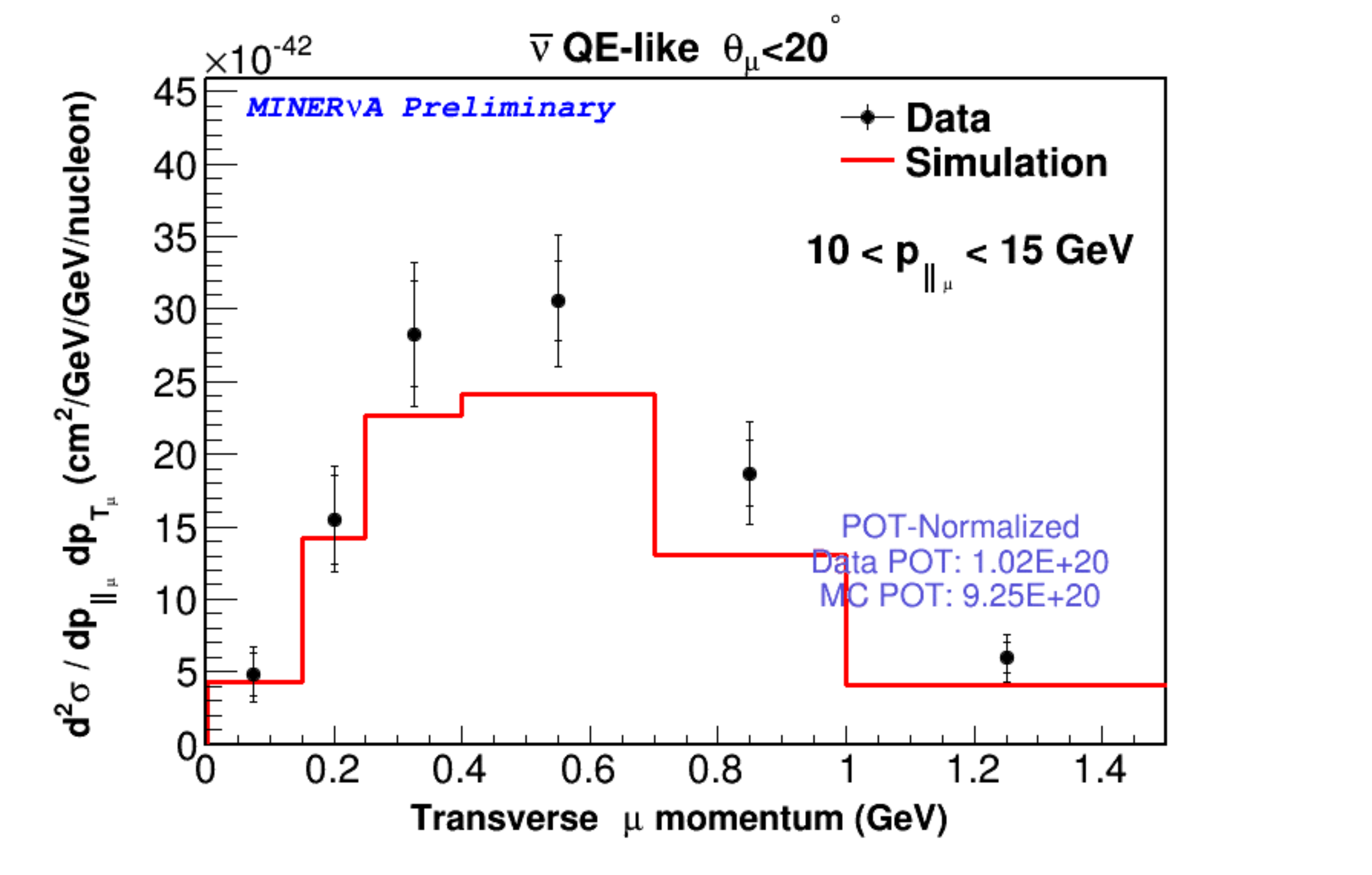

QE-like double differential cross section $d\sigma(E_\nu^{QE})/dQ^2_{QE}$

$d\sigma(E_\nu^{QE})/dQ^2_{QE}$ - fixed scale

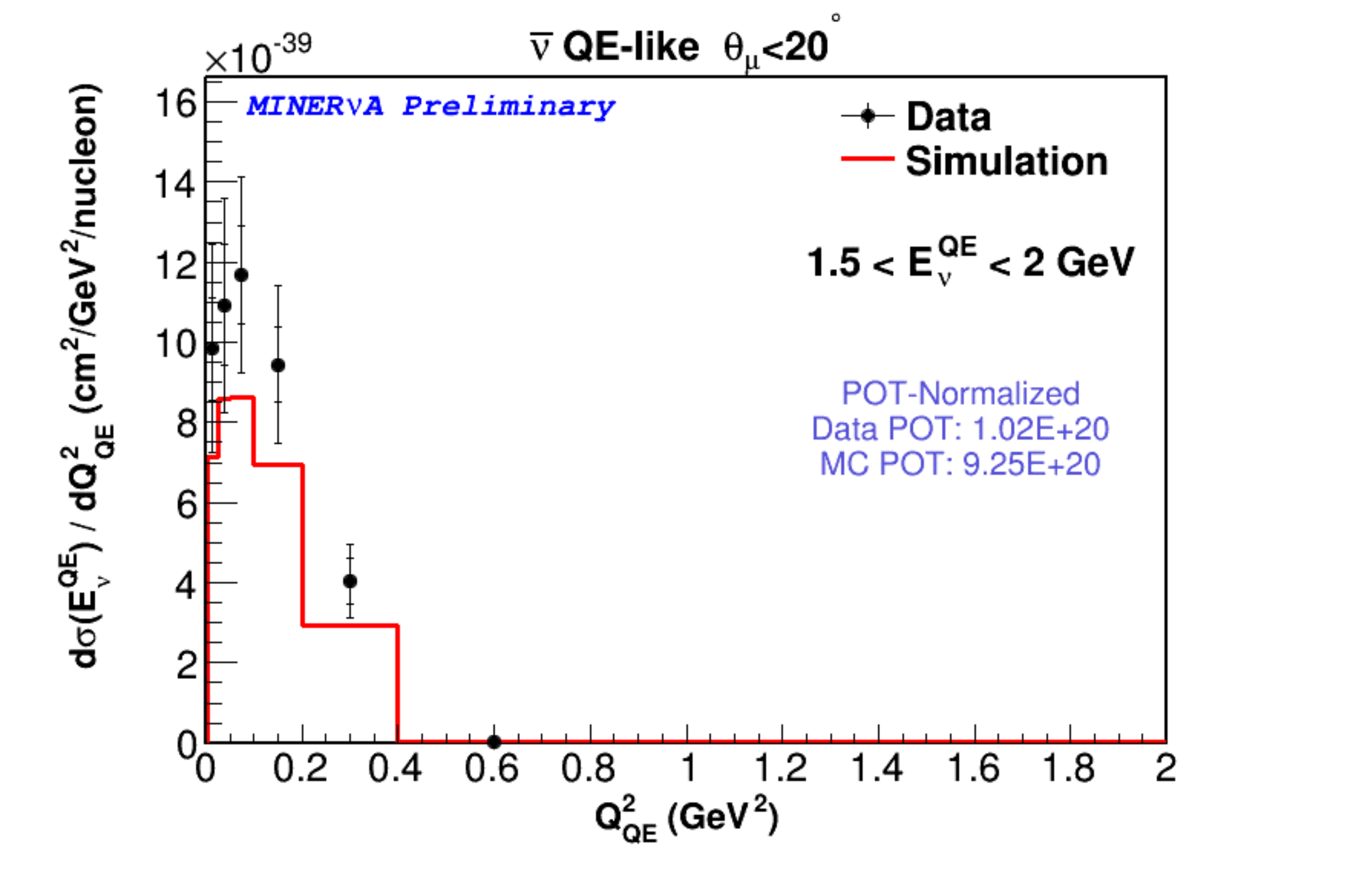

$d\sigma(E_\nu^{QE})/dQ^2_{QE}$ - fixed scale

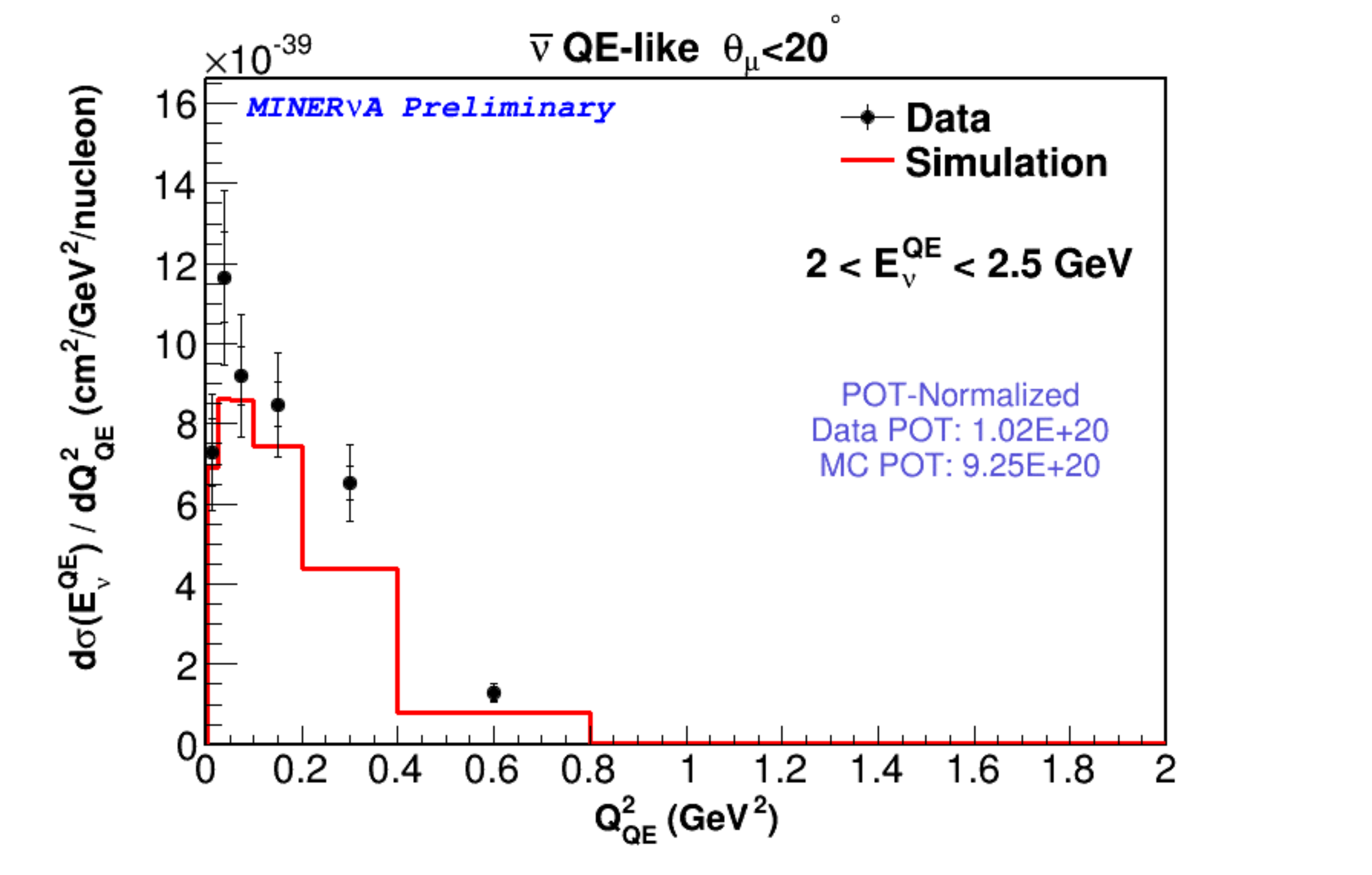

$d\sigma(E_\nu^{QE})/dQ^2_{QE}$ - fixed scale

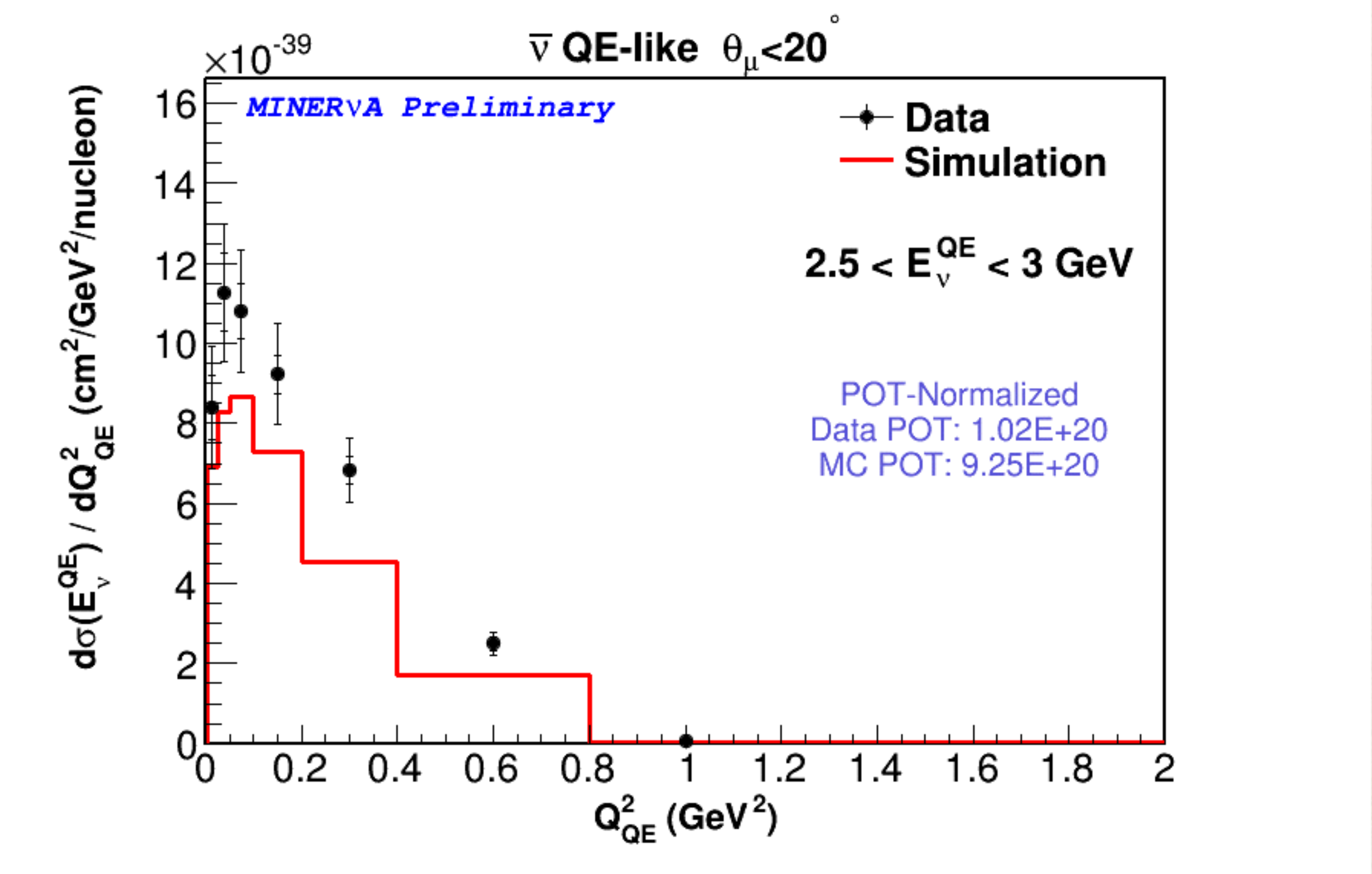

$d\sigma(E_\nu^{QE})/dQ^2_{QE}$ - fixed scale

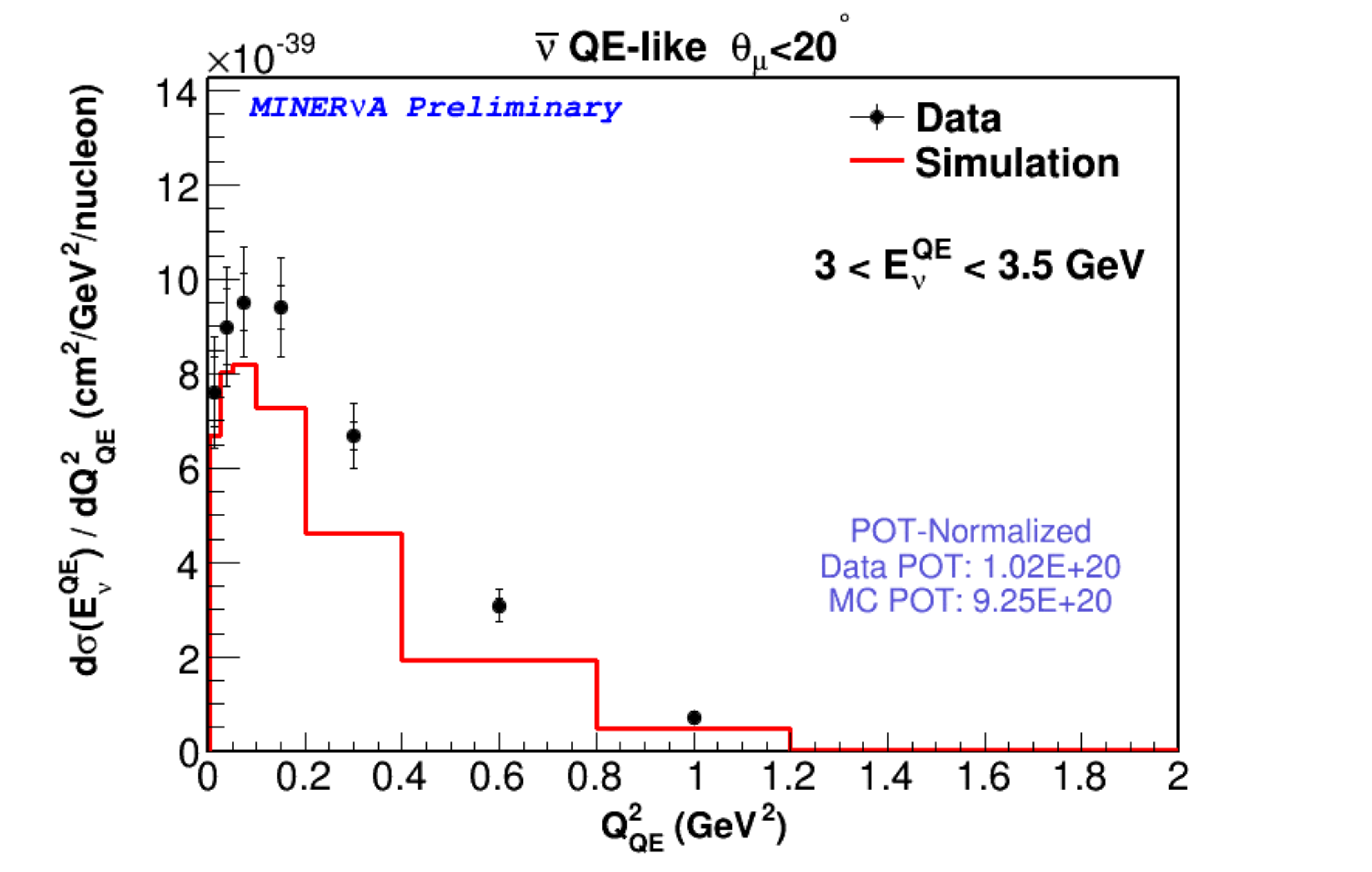

$d\sigma(E_\nu^{QE})/dQ^2_{QE}$ - fixed scale

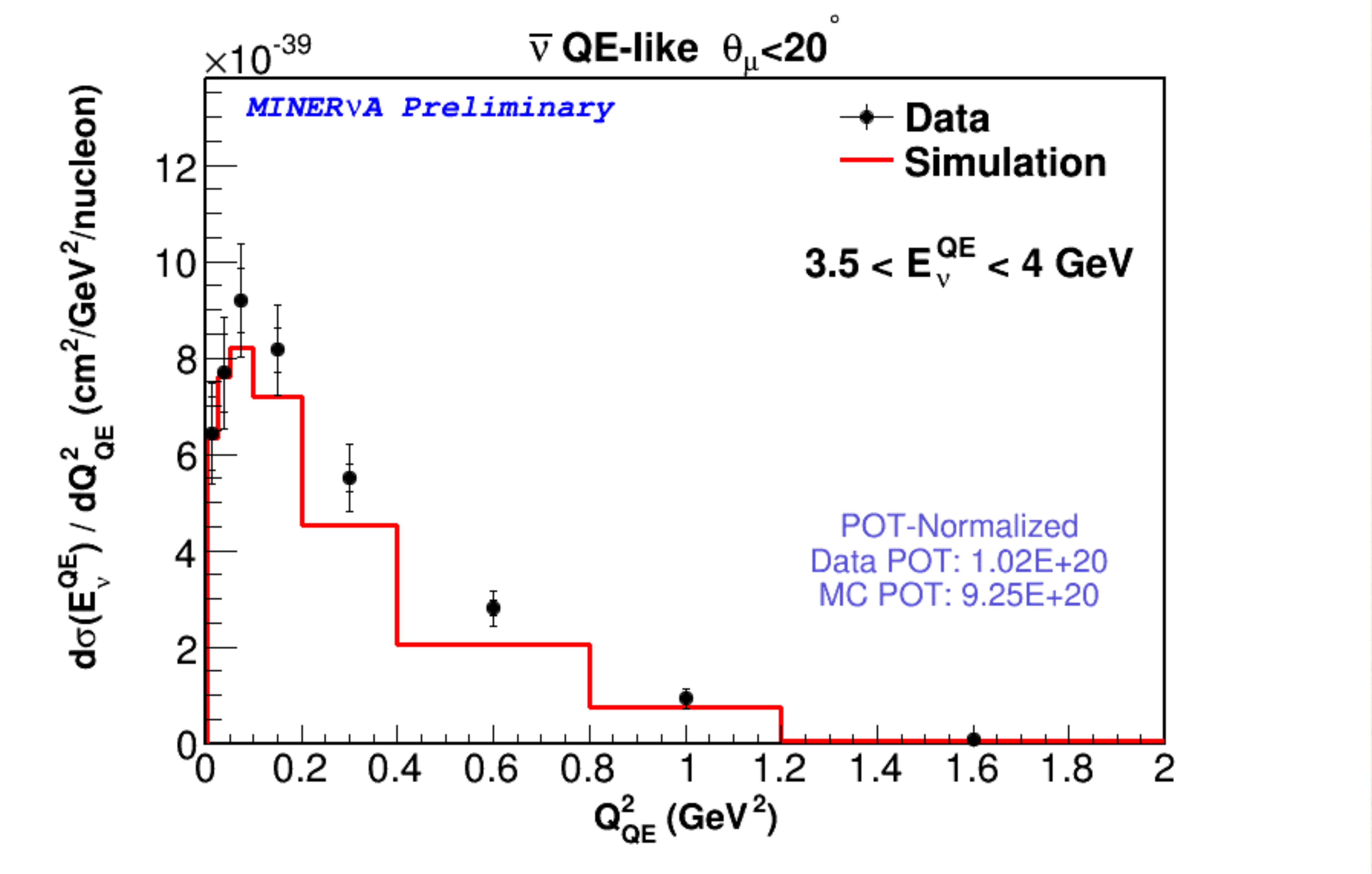

$d\sigma(E_\nu^{QE})/dQ^2_{QE}$ - fixed scale

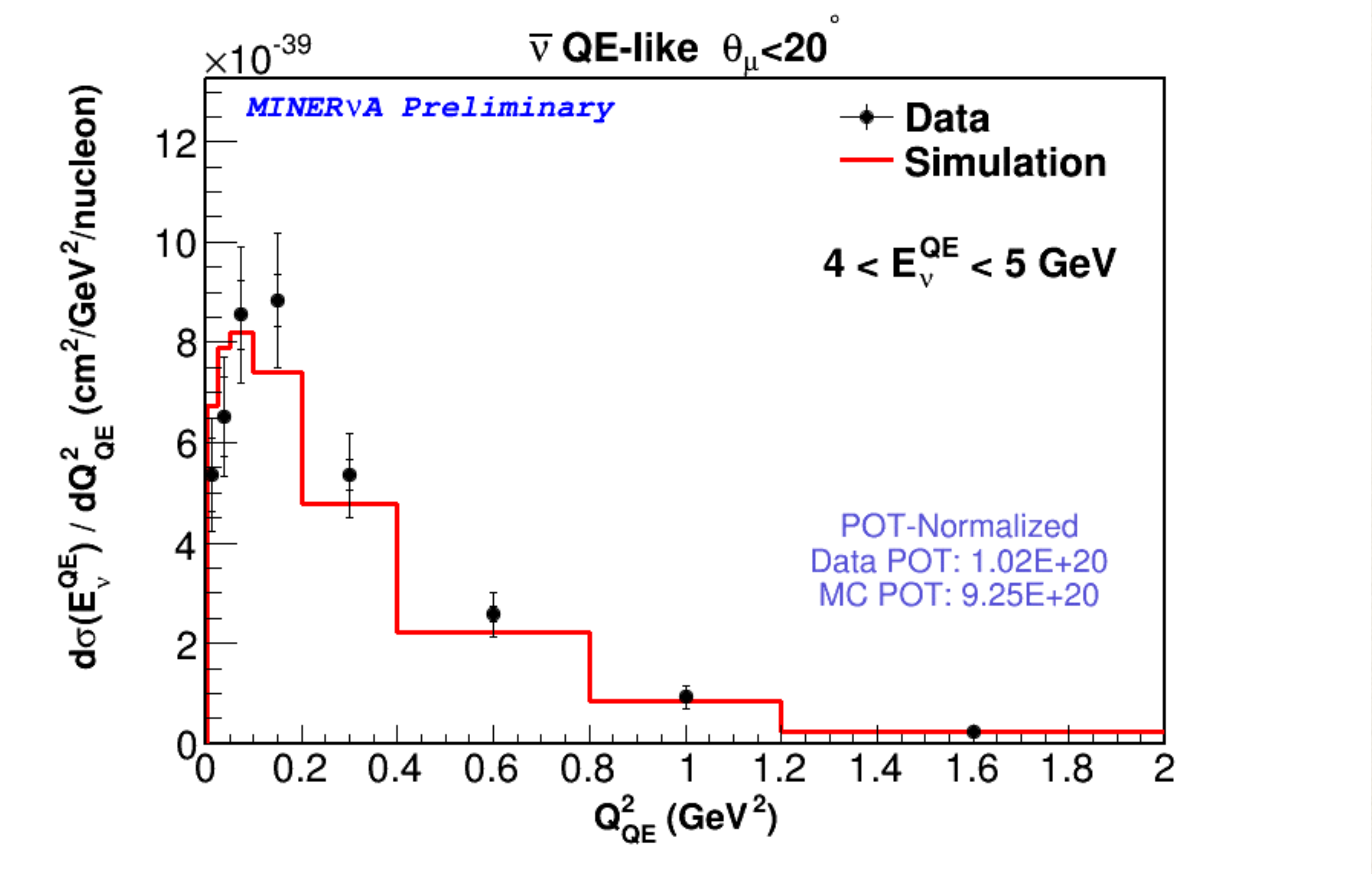

$d\sigma(E_\nu^{QE})/dQ^2_{QE}$ - fixed scale

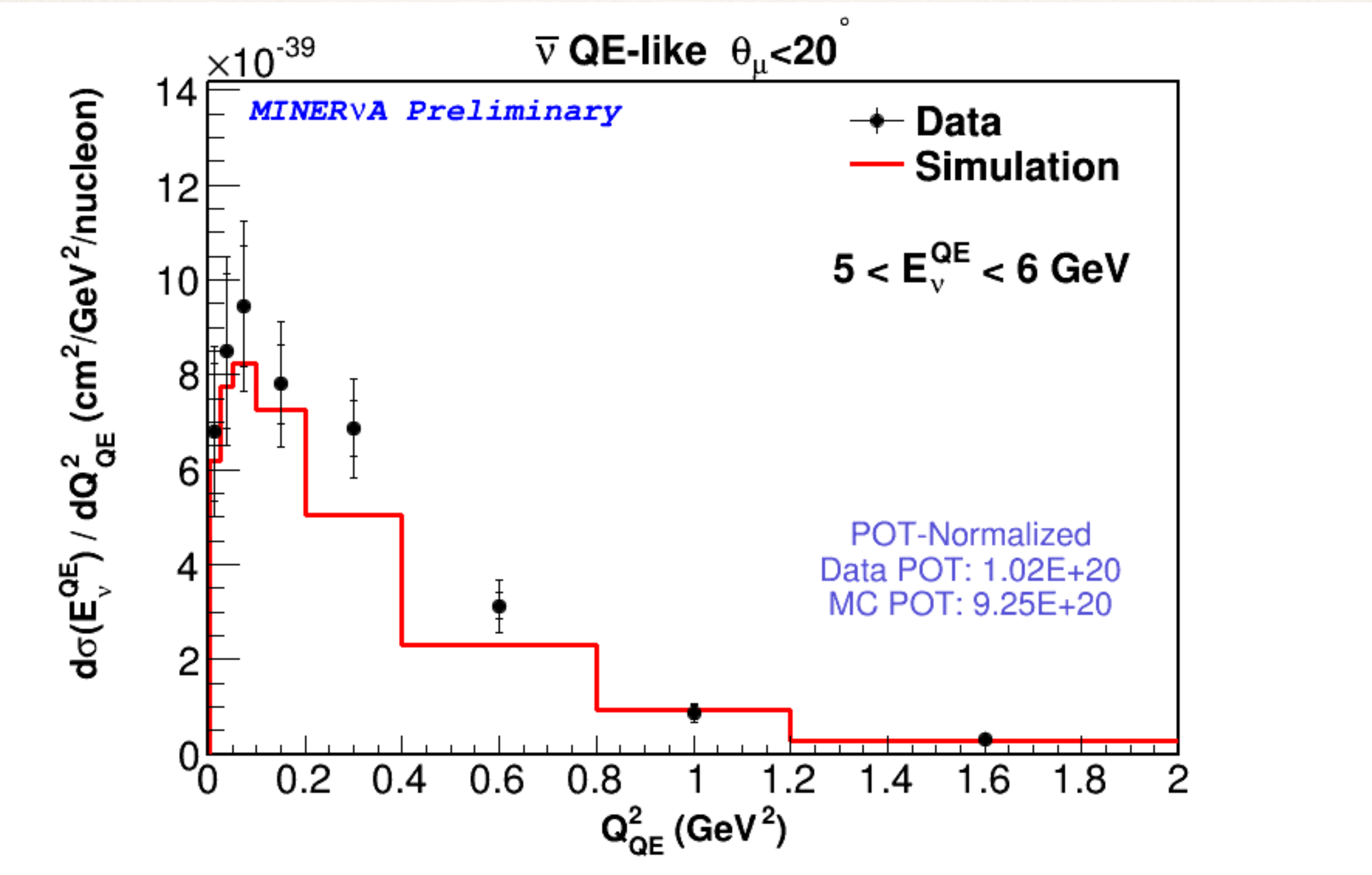

$d\sigma(E_\nu^{QE})/dQ^2_{QE}$ - fixed scale

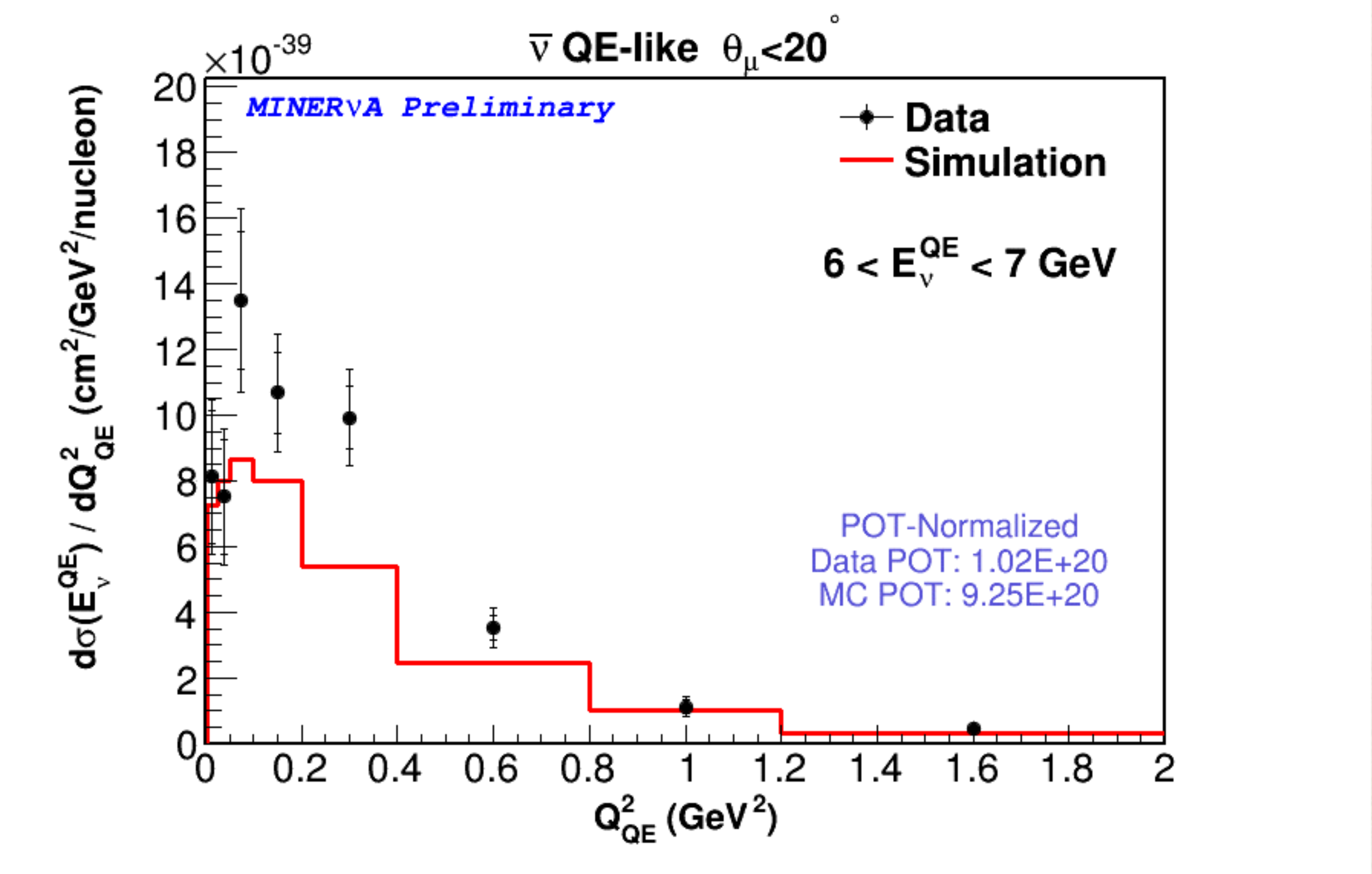

$d\sigma(E_\nu^{QE})/dQ^2_{QE}$ - fixed scale

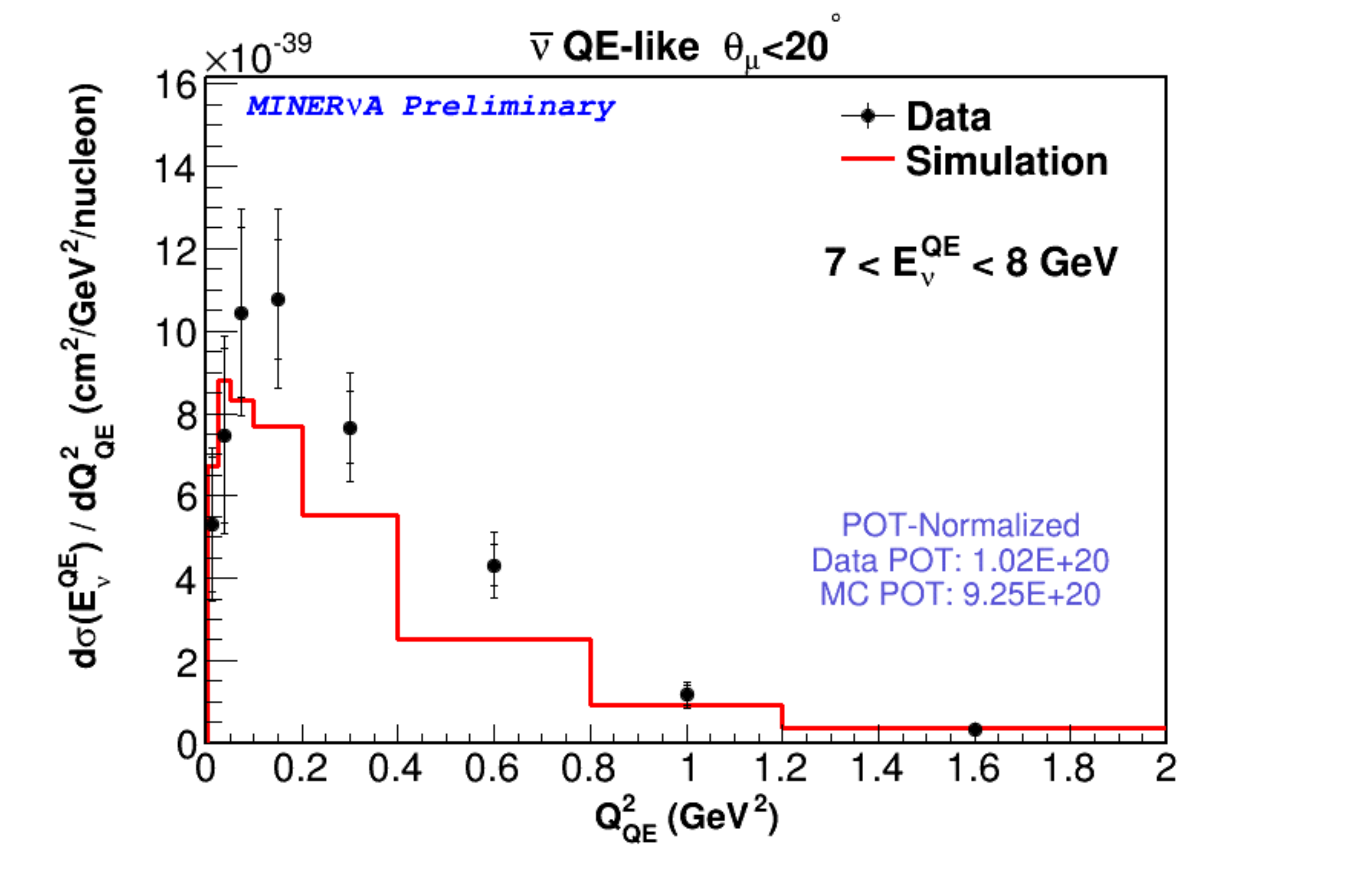

$d\sigma(E_\nu^{QE})/dQ^2_{QE}$ - fixed scale

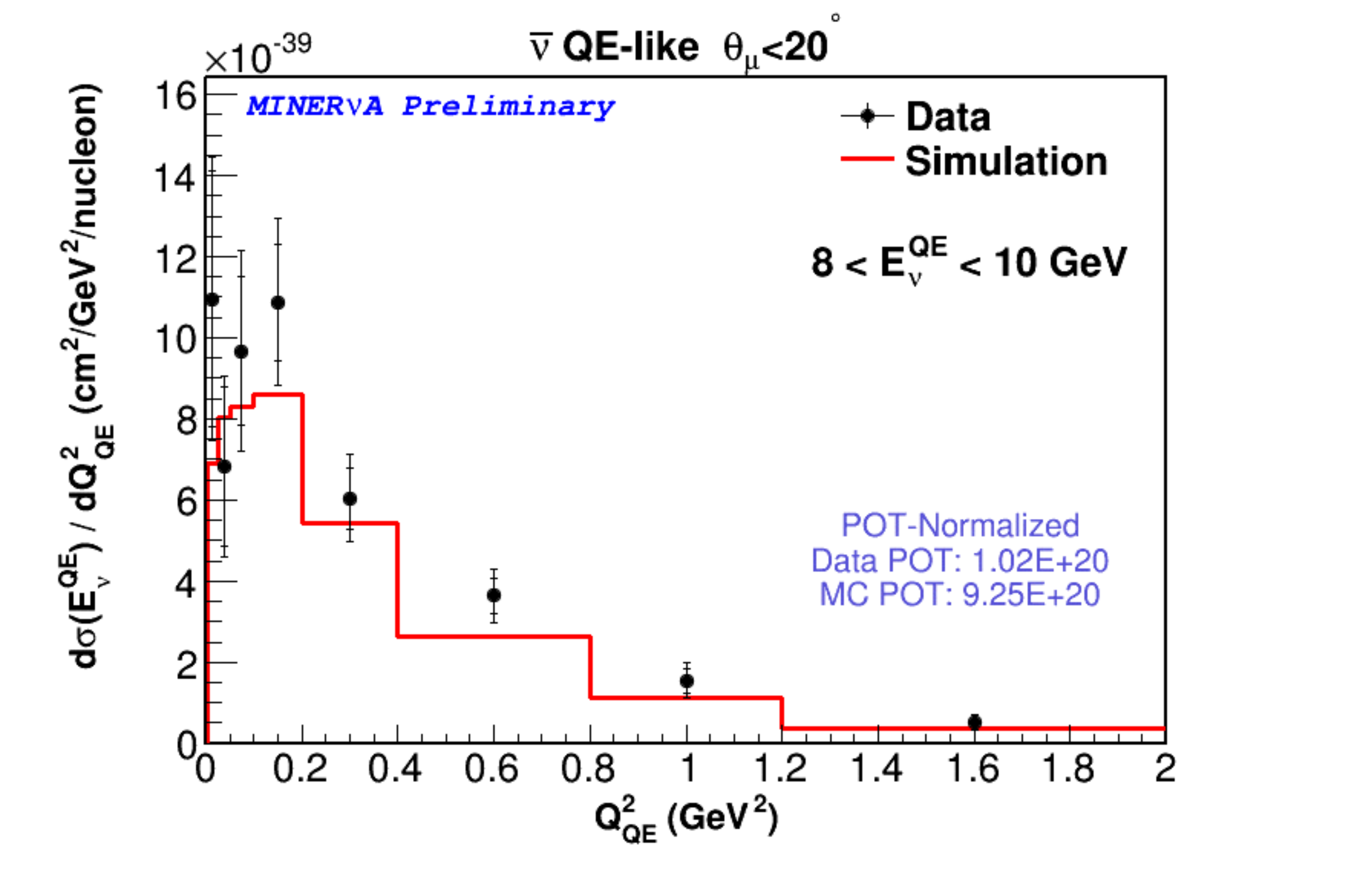

E_ν plot shape

Cross section in E_ν^{QE} has a dip in the falling edge of the flux peak. How significant is it?
To check: fit data/MC with a constant, excluding 3.5–6 GeV. Make a modified data histogram with 3.5–6 GeV bins moved so their data/MC ratio is the average. Compare data/MC χ^2 for original and modified data histograms

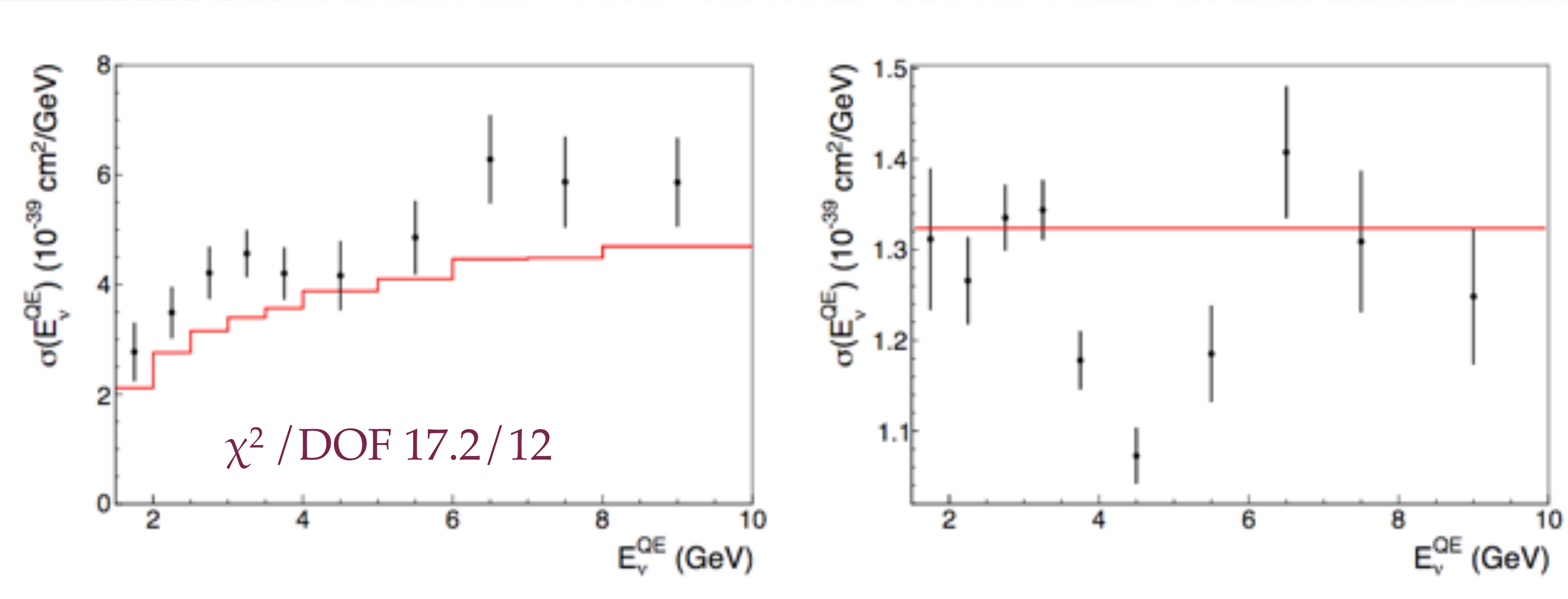

Best fit data/MC ratio 1.32

With those bins set to MC * 1.32 →

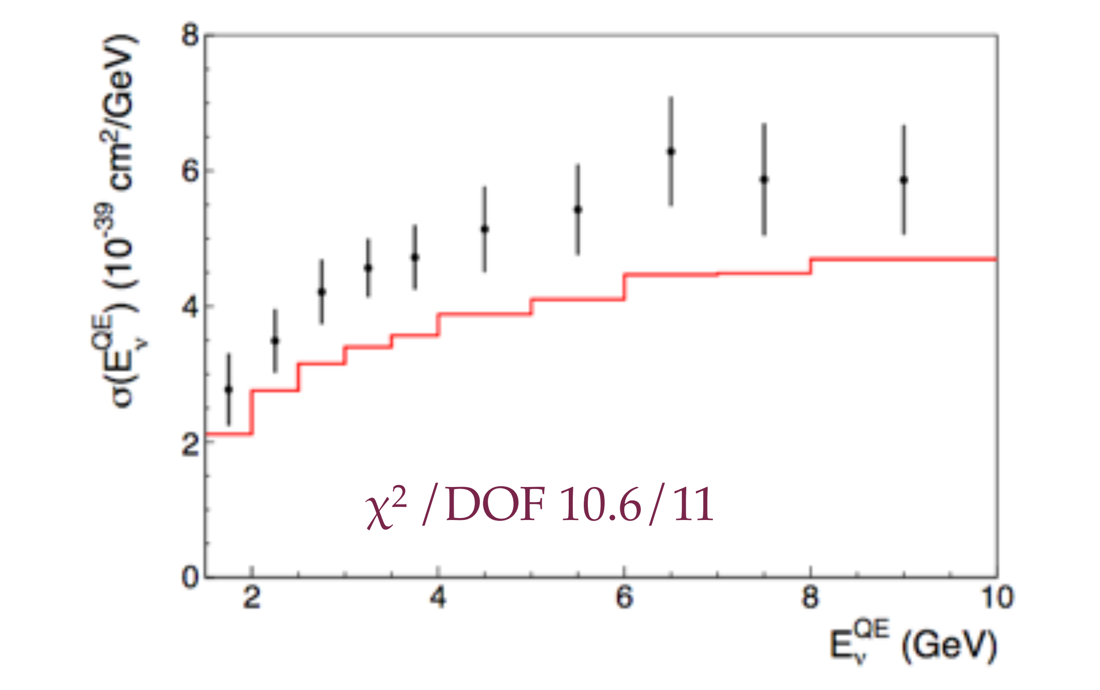

χ^2 changes from 17.2/12 to 10.6/11

This corresponds to falling flux edge

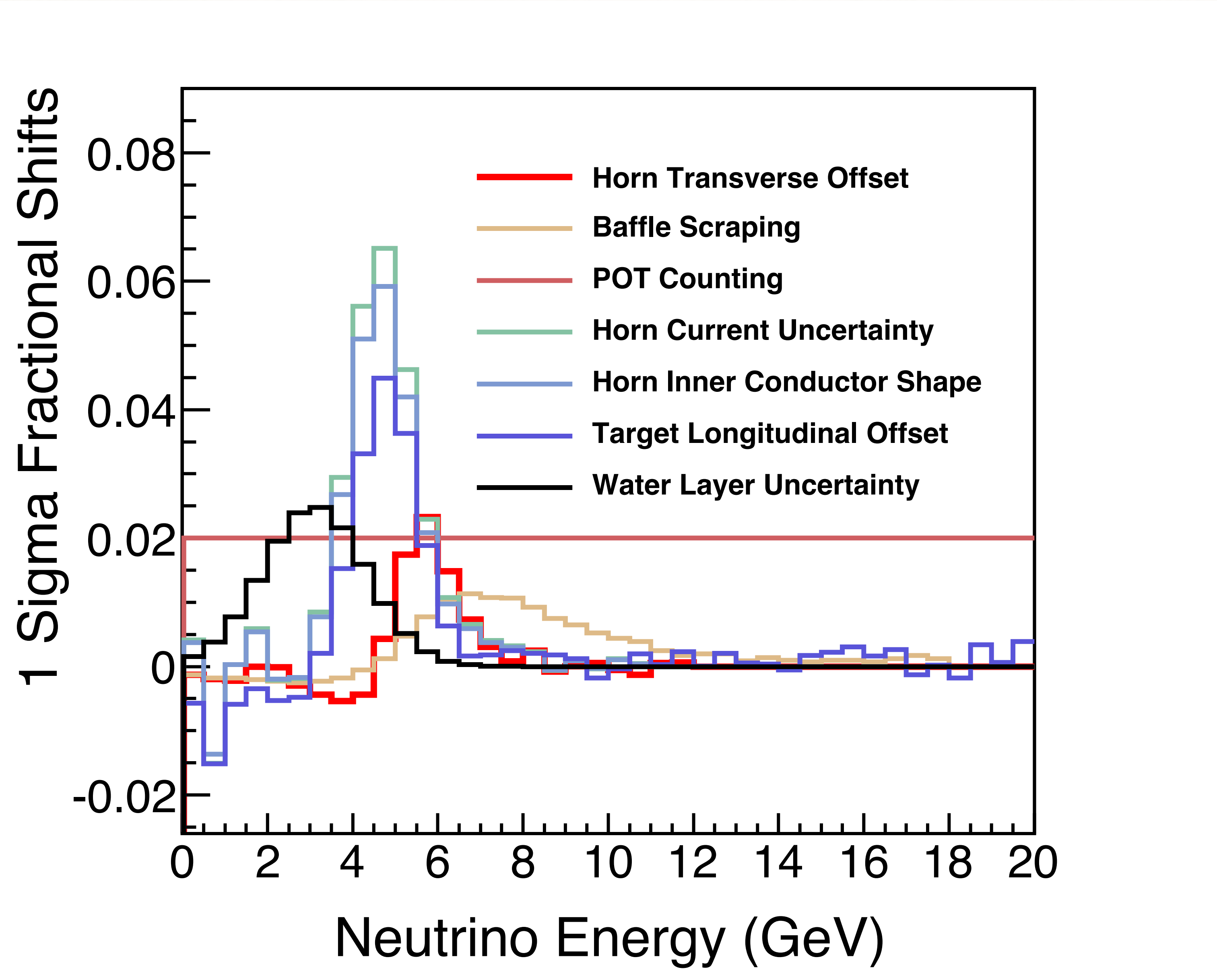

There are beam focusing uncertainties here

Comparison with others CCQE

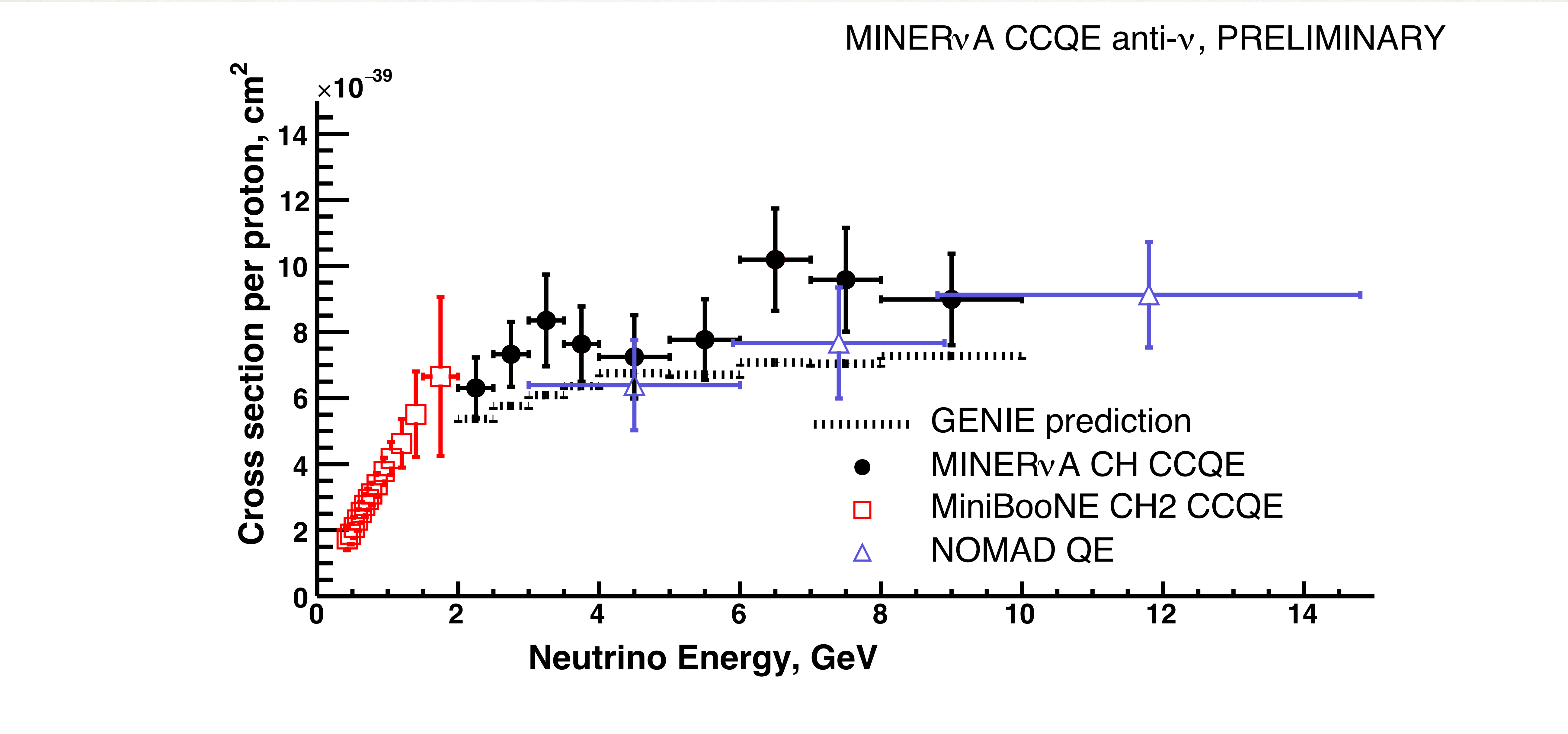

Our Monte Carlo: GENIE 2.8.4

Interaction models	**CCQE: axial form-factor**	Dipole with axial mass 0.99 GeV
	CCQE:Vector form-factors	BBBA05
	CCQE: Pseudoscalar form-factors	PCAC/Goldberger-Treiman
	Resonance and coherent	Rein-Seghal
	DIS	GRV94/GRV98 with Bodek-Yang
	DIS and QEL charm	*Kovalenko, Sov.J.Nucl.Phys.52:934 (1990)*
Nuclear effects	**Nuclear model**	RFG, Fermi momentum=225MeV, Pauli blocking, Bodek-Ritchie tail
	FSI modeling	INTRANUKE-hA *(S. Dytman, AIP Conf Proc, 896, pp. 178-184 (2007))*
	Hadronization model	AGKY – transitions between KNO-based and JETSET *T. Yang, AIP Conf. Proc.967:269-275 (2007)*
	Formation zone	SKAT

C. Andreopoulos, et al., NIM 288A, 614, 87 (2010)

Vertex resolution < 5mm

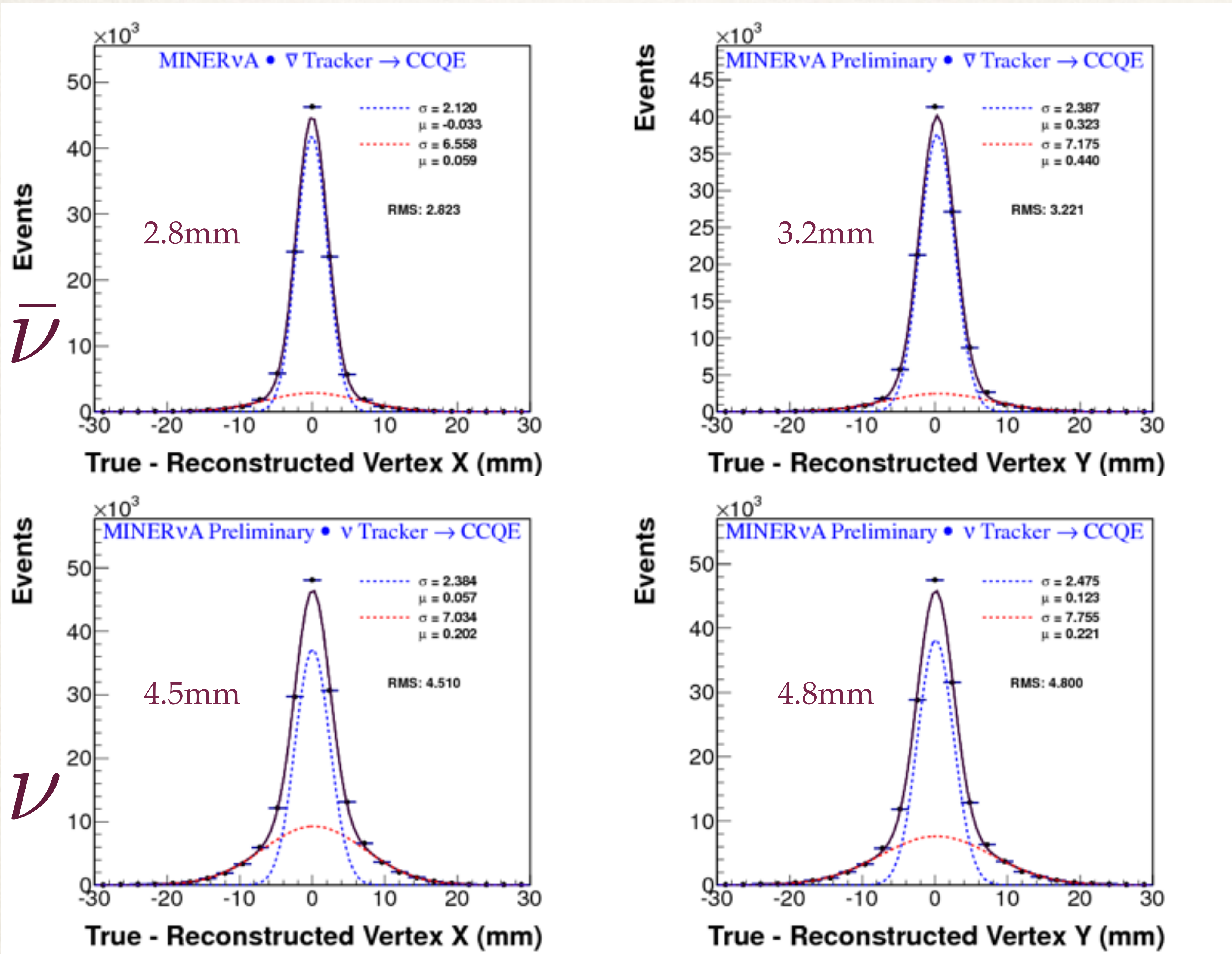

Q^2_{QE} resolution ~ $Q^2_{QE}/4$

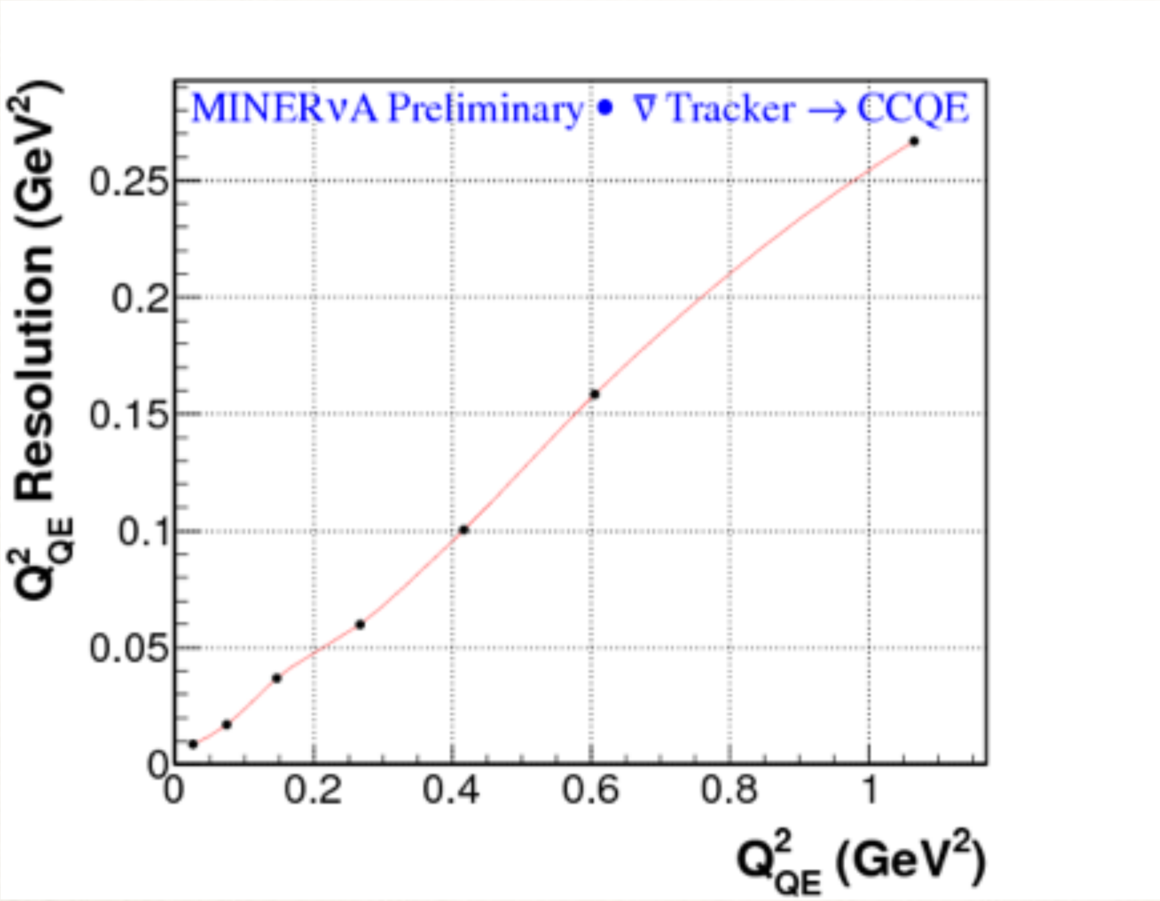

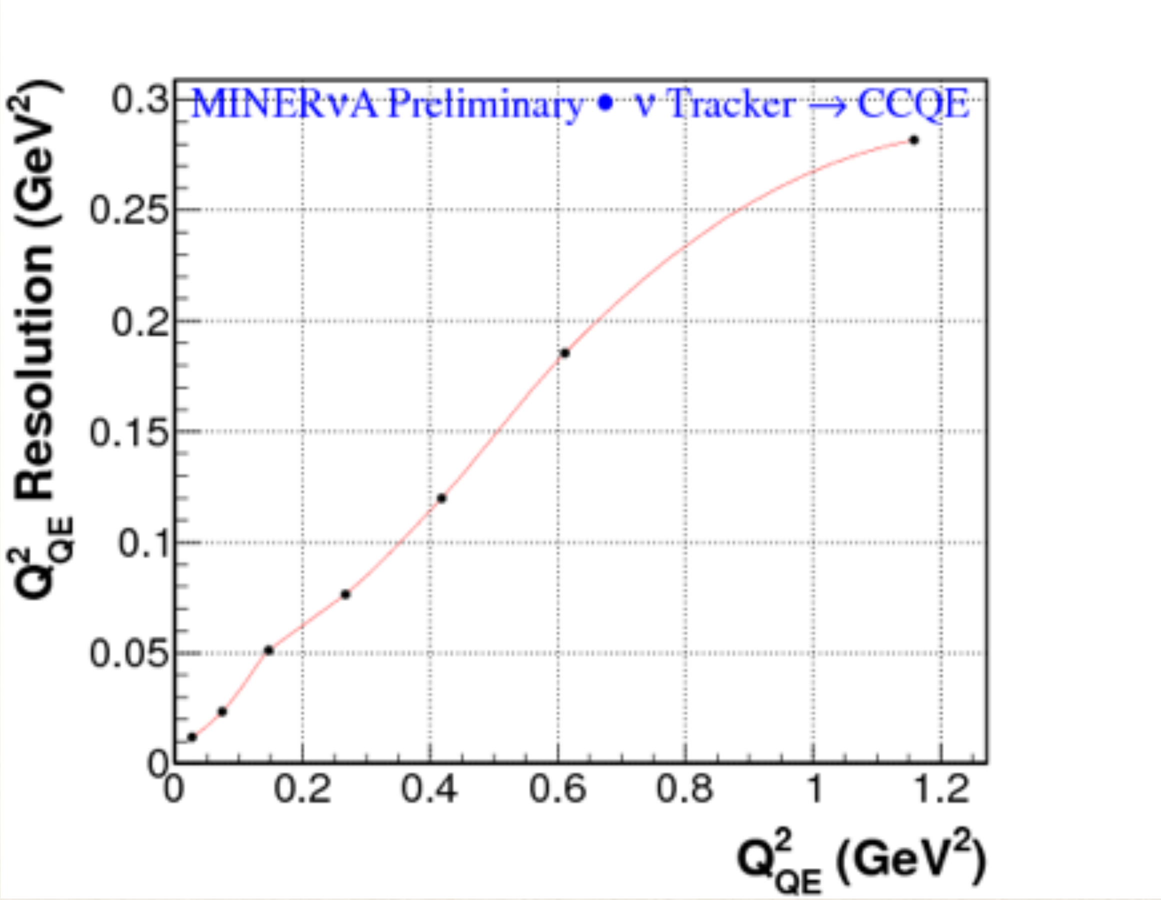

Angular resolution: x-z plane, $\bar{\nu}$

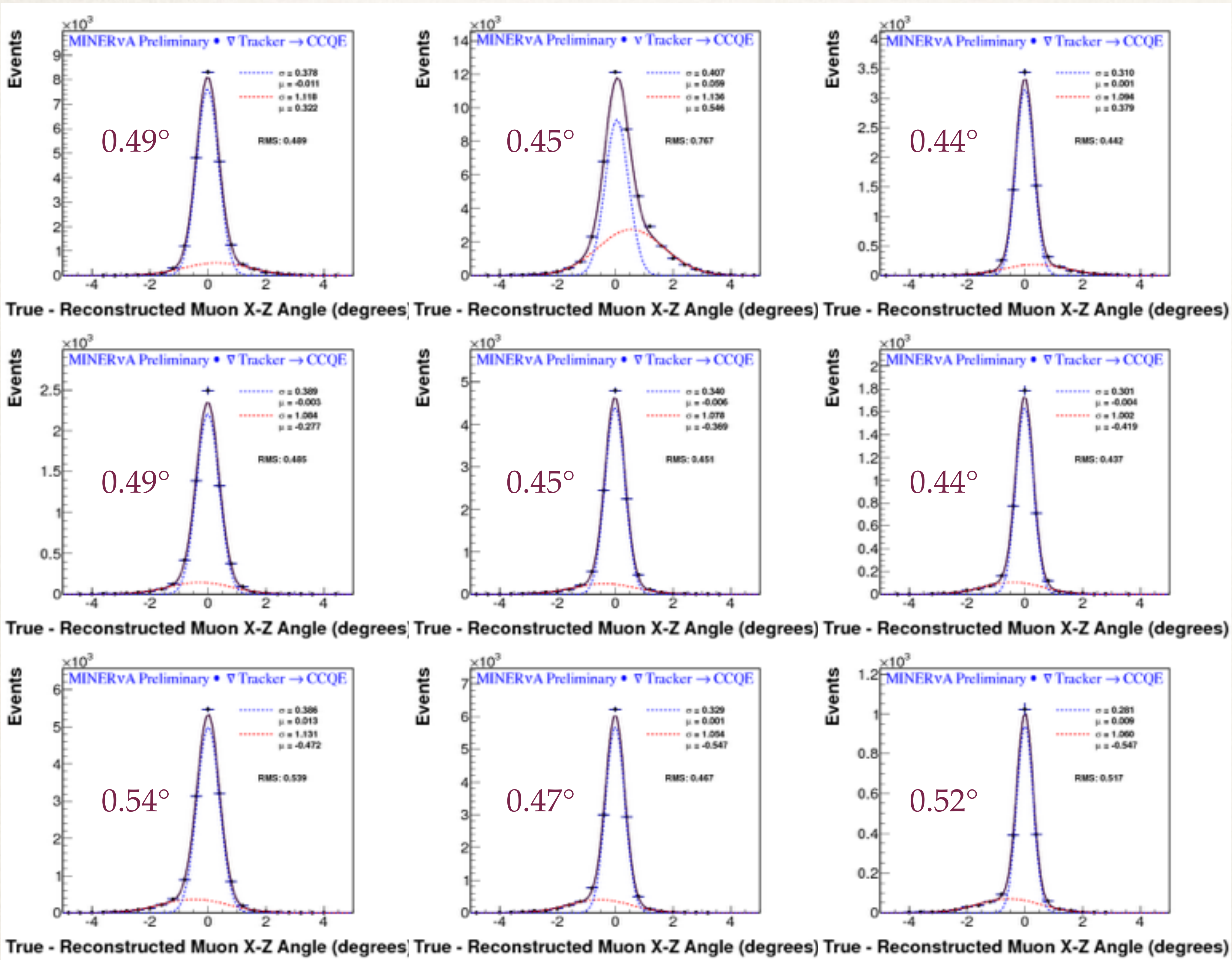

$E_\mu < 3$GeV,
3 - 5 GeV,
> 5GeV

$\theta_{\mu,x} < 1°$,
1 - 4°,
$> 4°$

Angular resolution: x-z plane, ν

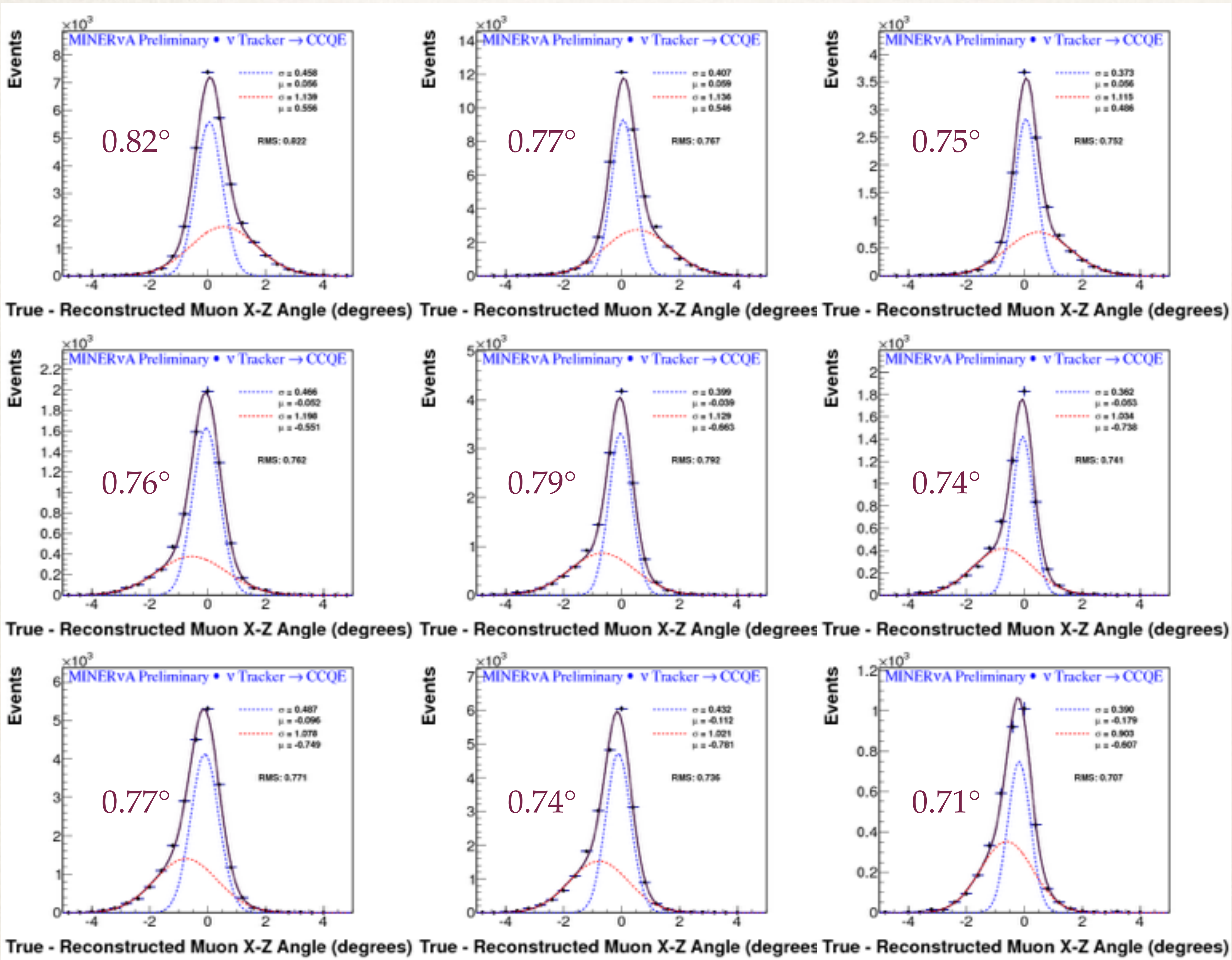

$E_{\mu} < 3$GeV,
3 - 5 GeV,
> 5GeV

$\theta_{\mu,x} < 1°$,
1 - 4°,
$> 4°$

Angular resolution: y-z plane, $\bar{\nu}$

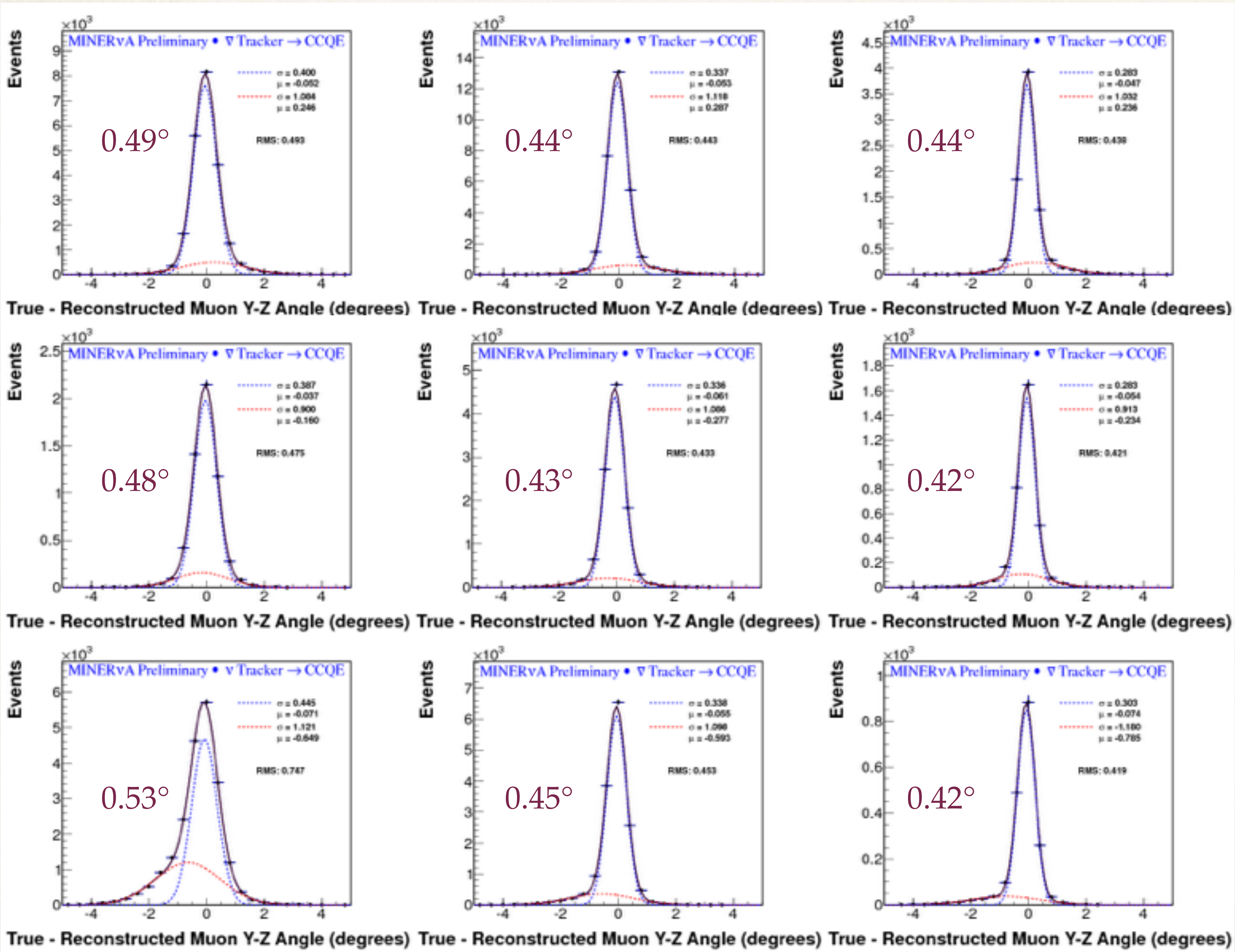

$E_{\mu} < 3$GeV,
3 - 5 GeV,
> 5GeV

$\theta_{\mu,y} < 1°$,
1 - 4°,
$> 4°$

Note: the beam is in the y-z plane, slightly misaligned from the z axis

Angular resolution: y-z plane, ν

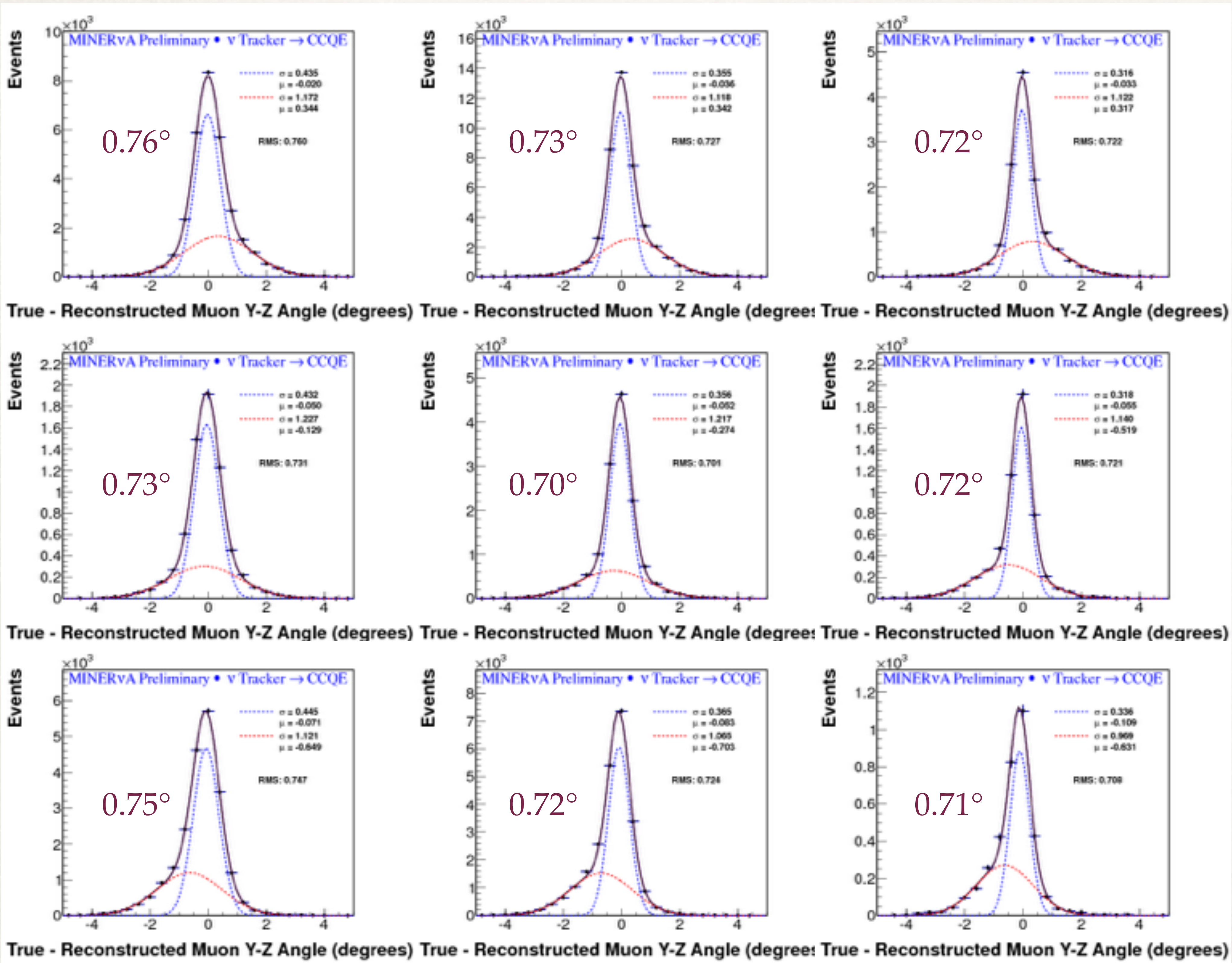

$E_\mu < 3$GeV,
3 - 5 GeV,
> 5GeV

$\theta_{\mu,y} < 1°$,
1 - 4°,
> 4°

Note: the beam is in the y-z plane, slightly misaligned from the z axis

Muon energy resolution, $\bar{\nu}$

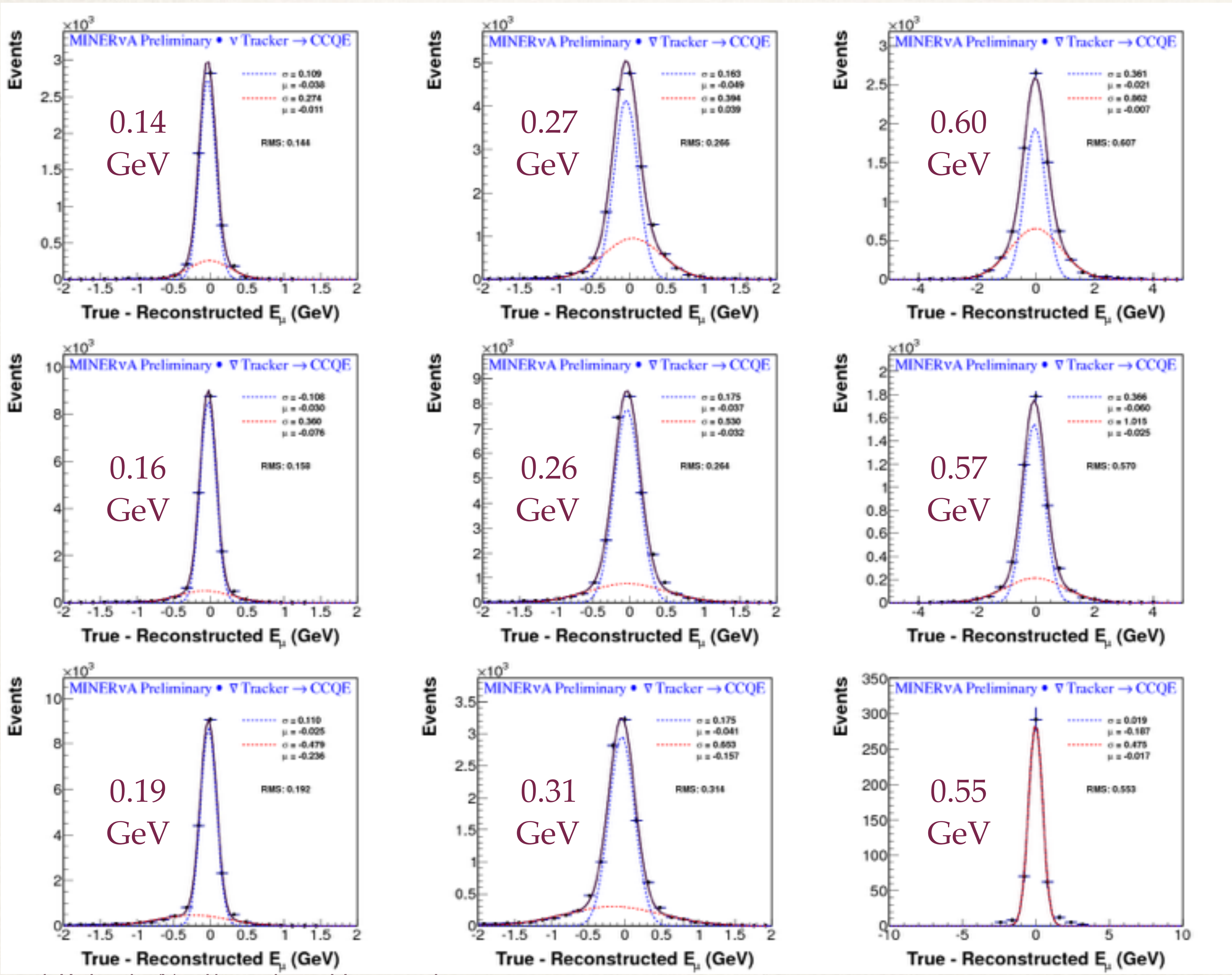

$E_\mu < 3$GeV,
3 - 5 GeV,
$>$ 5GeV

$\theta_\mu < 5°$,
5-10°,
$> 10°$

Muon energy resolution, ν

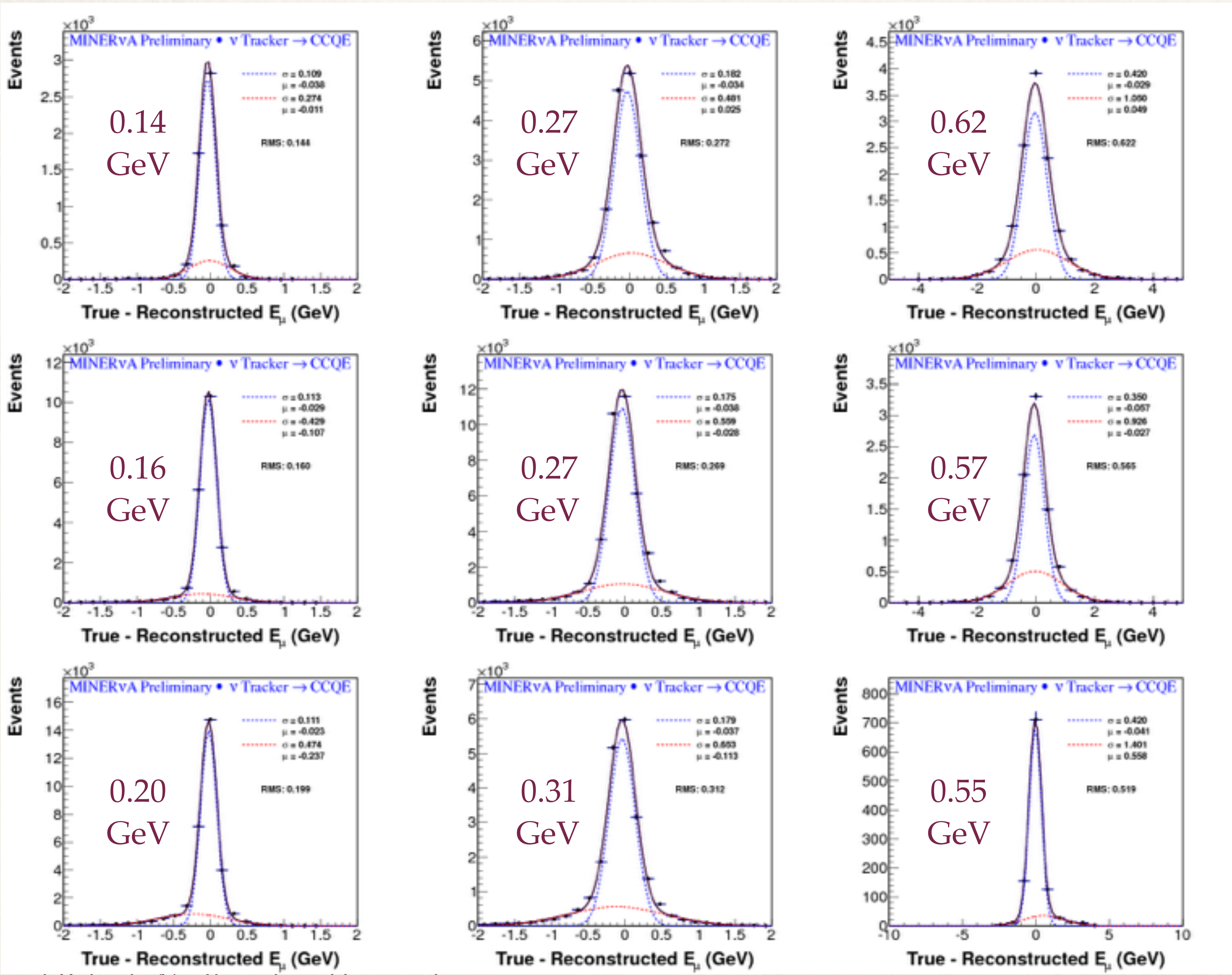

$E_\mu < 3$GeV, 3 - 5 GeV, > 5GeV

$\theta_\mu < 5°$, 5-10°, > 10°

Varying nuclear model with 2p2h

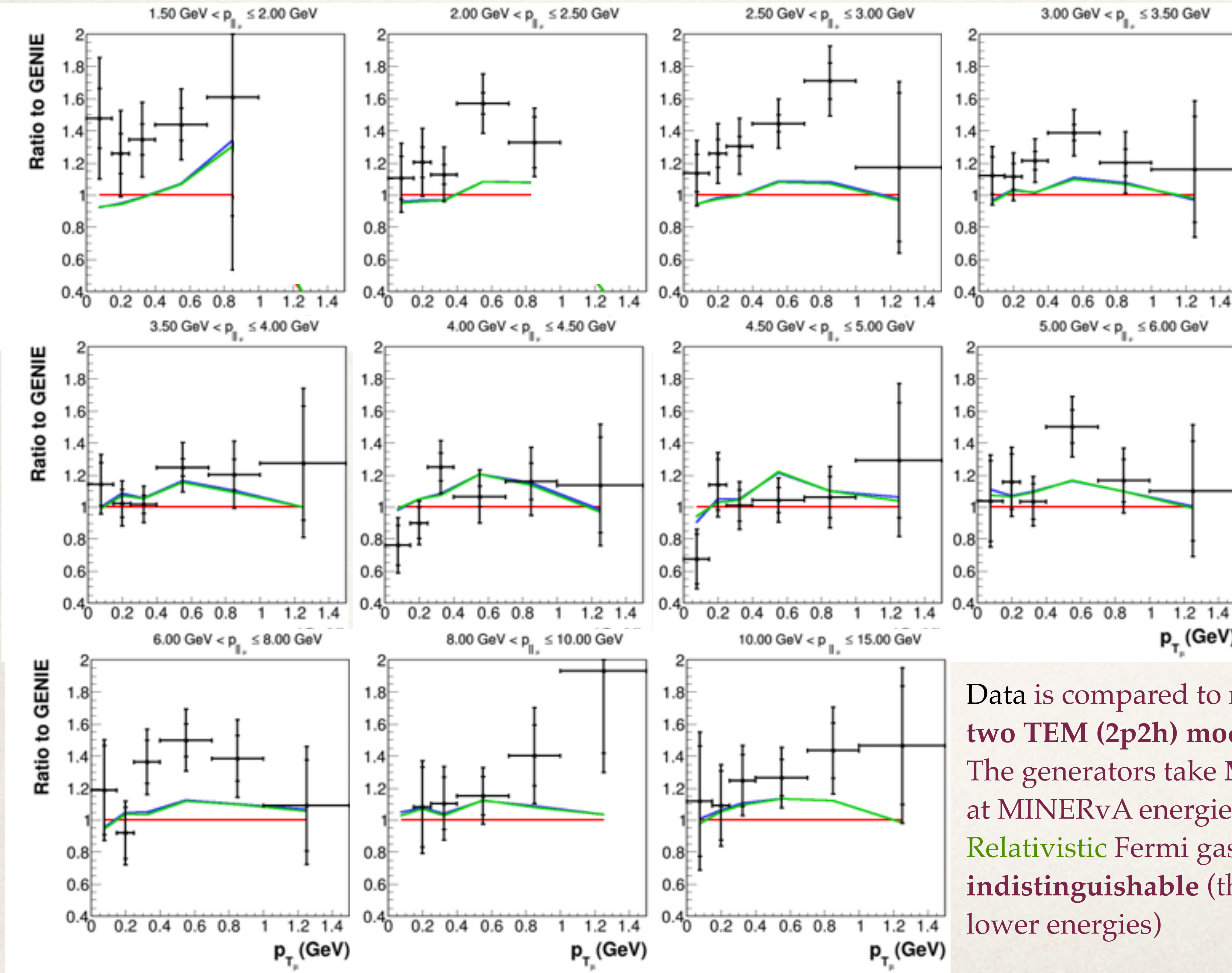

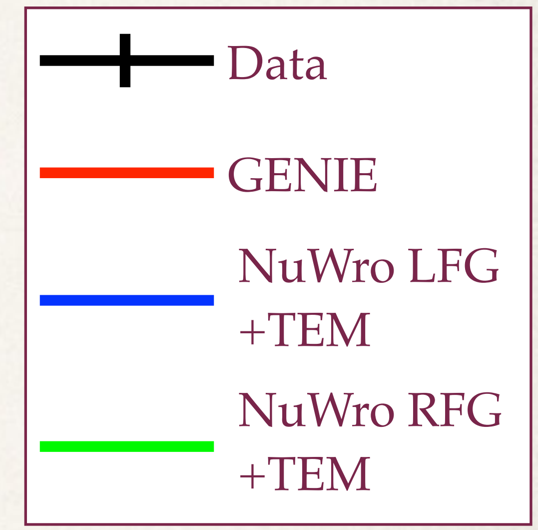

Data is compared to nominal GENIE and **two TEM (2p2h) models** from NuWro. The generators take **M_A=0.99.** We see that at MINERvA energies, the Local and Relativistic Fermi gas models are almost **indistinguishable** (the differences are at lower energies)